



UNIVERSITAT AUTÒNOMA DE BARCELONA

Departament d'Enginyeria Química

Escola d'Enginyeria

**STUDIES ON THE OXIDATIVE ABILITY OF
HORSE LIVER ALCOHOL DEHYDROGENASE
AND ITS COFACTOR REGENERATION**

Rossmery Anaid Rodríguez Hinestroza

Bellaterra, May 2014

Title of the thesis: Studies on the oxidative ability of horse liver alcohol dehydrogenase and its cofactor regeneration

Accomplish by: Rossmery Anaid Rodríguez Hinestroza

Directed by: Maria Dolors Benaiges Massa
Carmen López Díaz
Josep López Santín

Doctoral studies in Biotechnology
Departament d'Enginyeria Química
Escola d'Enginyeria
Universitat Autònoma de Barcelona

MARIA DOLORS BENAIGES MASSA, profesora titular del Departament d'Enginyeria Química de la Universitat Autònoma de Barcelona, CARMEN LÓPEZ DÍAZ, Investigadora postdoctoral del Departament d'Enginyeria Química de la Universitat Autònoma de Barcelona y JOSEP LÓPEZ SANTÍN, Catedrático del Departament d'Enginyeria Química de la Universitat Autònoma de Barcelona.

CERTIFICAMOS:


Que la Ingeniera Química ROSSMERY ANAID RODRÍGUEZ HINESTROZA ha realizado bajo nuestra dirección el trabajo titulado: "STUDIES ON THE OXIDATIVE ABILITY OF HORSE LIVER ALCOHOL DEHYDROGENASE AND ITS COFACTOR REGENERATION", el cual se presenta en esta memoria y que constituye su Tesis para optar al Grado de Doctor por la Universitat Autònoma de Barcelona.

Y para que conste a los efectos oportunos, presentamos en la Escola d' Enginyeria de la Universitat Autònoma de Barcelona, la mencionada Tesis, firmando el presente certificado en

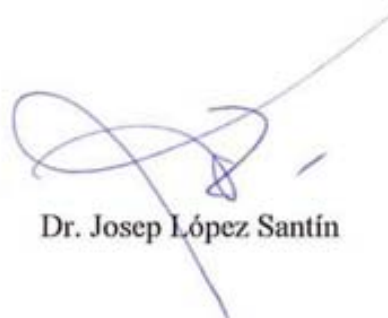
Bellaterra (Cerdanyola del Vallès), 12 de mayo de 2014



Dra. Maria Dolors Benaiges Massa



Dra. Carmen López Díaz



Dr. Josep López Santín

*To my parents, grandparents,
my brother and my niece
You are the most important for me in this world*

ACKNOWLEDGEMENTS

Now, it is time to look back and remember the experiences, tears, laughs and all that I have learned during my PhD experiments and writing the thesis. But, I was not alone, there were a lot of people that encouraged me and I have to say “thank you very much”.

First of all, to my supervisors Dolors, Carmen y Josep, for your support, guidance, availability, patience, understanding and help in everything I needed. Also, to Théo, for the opportunity to work in his research group in Toulouse, for his guidance, aid and treated me as other of his PhD students. As well to the rest of the aldolases group Gloria C, Goyo, Gloria G and Carles. To Pierre Aimar, my first contact in the Laboratoire de Génie Chimique.

To Milja and Max for all the good times at the lab, for helping me with my experiments and always supporting me. I'll never forget when we took a break while we were waiting the results of the HPLC, looking for funny things like “la tigresa”. To Inés, for her availability and kindness every time. To Gerard, which arrived to the lab in the last year, but it was there to support me as well. To Yolanda who aided me with the potentiostat experiments. To all the guys from the aldolases group: Jordi, Alfred, Martina, Marcel·la, Dani, Nataša and especially to Juanmi who was my classmate when I was studying Chemical Engineering in Venezuela, thank you for let me now this PhD opportunity, for your help and advices.

To my dear friends here in “la ETSE”: Angélica, Mariángel, Andrea, Laura, Nelsy, Mabel, Lorena, Andreia, Cynthia and Margot for being there, listening me, encouraging me and cheering me up all the time. To Luis, Tercia, Rebeca, Lucía, Gaby, Pedro, Susan, Cindy, Ahmad for bringing the good mood to the office, for the laughs and relaxing moments. To the rest of the chemical engineering department, specially to the secretaries Montse, Nati, Rosa and Míriam.

To all the staff of the Laboratoire of Génie Chimique: Dang Chen, Raluca, Yves, Willian, Guillaume, Teddy and Fabian for all your help and good moments at the lab.

To Mailhyn, my best friend and sister for being there for me all the time and everywhere, for always having time to support me and hold me when I need it (te quiero ami). To

Eliana, my good friend and second sister, she is always there, we don't need to talk everyday and say so much, I always can count on her. To my beloved friends Johan, Nadja, Diana, Felipe some of you are so far away but you are still being good friends. To my other friends from here and from there, I'll never forget you.

To my parents who are unconditional, no matter the distance, there are always for me and they will do anything for me and me for them, I love you!. To my brother sapa, we don't talk so much, only to say child things to each other, but that's our way to say we care about. To my niece Nitol, my little angel that I love as my own child, she always makes me happy.

To all the people that made it possible thank you! After all I finally finished my thesis!

ABSTRACT

The study of the use of enzymes as industrial biocatalysts has been increased in the last decades, since they offer several advantages as their ability to accept a wide range of substrates, high specificity and selectivity, allowing mild reaction conditions. One of the most promising fields of their application is the production of compounds with biological activity for therapeutical purposes.

This doctoral thesis is a contribution to the research of horse liver alcohol dehydrogenase (HLADH) as biocatalyst, particularly its ability to oxidize Cbz-amino alcohols to obtain valuable compounds as Cbz-amino aldehydes to produce Cbz-aminopolyols, and Cbz- β -aminoacids. Therefore, Cbz-ethanolamine and Cbz- β -amino propanol were selected as model compounds.

First, alcohol dehydrogenases from different origins as yeast and horse liver (commercial and in house) were tested for the oxidation of Cbz-ethanolamine. In house HLADH was selected as the best biocatalyst, in terms of specific activity and kinetic parameters. Moreover, HLADH catalyzed oxidation of Cbz-ethanolamine was performed and the direct formation of the acid, Cbz-glycine, was observed. Several methods were tested to promote the production of the intermediate product (aldehyde, Cbz-glycinal), but only the use of semicarbazide hydrochloride allowed obtaining Cbz-glycinal by its capture as Cbz-glycinal semicarbazone, yielding up to 84% with less than 12% Cbz-glycine yield. Cbz-glycinal semicarbazone acid hydrolysis with formaldehyde provided 48.5% of Cbz-glycinal recovery. Nevertheless, the amount of impurities, mostly formaldehyde, made it not such a good substrate for a further aldol addition to dihydroxyacetone phosphate (DHAP) catalyzed by aldolases in order to obtain aminopolyols (*chapter 4*).

On the other hand, coupling the oxidation of Cbz-ethanolamine by HLADH and the aldol addition of DHAP catalyzed with RhuA with DHAP pulses addition did not produce Cbz-aminopolyols, forming only 64.1% yield of Cbz-glycine (*chapter 5*).

Next, the high oxidative ability of HLADH was also exploited to produce Cbz- β -alanine from Cbz- β -amino propanol; a complete conversion was obtained at 72 h in a batch mode. In order to enhance the productivity, a fed-batch operation was proposed

providing 88.4% Cbz- β -alanine yield at 96 h with 2.3-fold improved productivity compared to the batch operation (*chapter 6*).

Finally, the study of NAD⁺ cofactor regeneration was carried out by enzymatic and electrochemical methods. Enzymatic substrate-coupled regeneration of NAD⁺ was studied using acetaldehyde as second substrate with an almost complete conversion to Cbz- β -alanine in the first 2 h of reaction in a batch operation. However, fed-bach mode was not so efficient (65% conversion at 2 h, only one pulse addition of substrate), and the reaction was stopped at 2 h (*chapter 6*). Direct electrochemical regeneration of NAD⁺ using a filter-press microreactor was performed by coupling it with the HLADH catalyzed oxidation of Cbz- β -amino propanol for the production of Cbz- β -alanine. Employing a batch operation 77.1% Cbz- β -amino propanol conversion and a complete regeneration was obtained at 24 h. Meanwhile, the fed-bach operation increased production maintaining 80.0% conversion and one half of complete cofactor regeneration conversion at 51 h (*chapter 7*).

TABLE OF CONTENTS

ACKNOWLEDGEMENTS	i
ABSTRACT	iii
TABLE OF CONTENTS	v
LIST OF TABLES.....	xi
LIST OF FIGURES.....	xiii
1. INTRODUCTION	3
1.1 Biotransformation	3
1.2 Enzymes	4
1.3 Oxidoreductases.....	6
1.3.1 Dehydrogenases	7
1.4 Horse liver alcohol dehydrogenase (HLADH)	9
1.4.1 Structure	9
1.4.2 Mechanism	11
1.4.3 Applications.....	12
1.5 Regeneration of the cofactor NAD⁺	12
1.5.1 Chemical regeneration.....	13
1.5.2 Photochemical regeneration	14
1.5.3 Enzymatic regeneration of NAD ⁺	14
1.5.4 Electrochemical regeneration	16
1.5.4.1 Direct anodic regeneration of NAD(P) ⁺	17
1.5.4.2 Mediated electrochemical regeneration of NAD(P) ⁺	19
1.5.4.3 Electroenzymatic regeneration of NAD(P) ⁺	21
1.5.4.4 Microreactors	21
1.6 Engineering of the reaction media and enzymatic reactors	24

1.7	Synthesis of aminopolyols	27
1.7.1	Aldolases	28
1.7.1.1	DHAP-dependent aldolases	29
1.8	Oxidation of β-amino alcohols to β-amino acids.....	32
2.	OBJECTIVES.....	37
3.	GENERAL MATERIALS AND METHODS	41
3.1	Materials.....	41
3.2	Obtention of enzymes	41
3.2.1	Purification of Horse liver alcohol dehydrogenase	41
3.2.2	Purification of rhamnulose-1-phosphate aldolase (RhuA) on immobilized metal-chelate affinity chromatography (IMAC)	42
3.3	Synthesis of L-rhamnulose-1-phosphate	43
3.4	Analytical methods	46
3.4.1	Horse liver alcohol dehydrogenase enzymatic activity assay	46
3.4.2	RhuA enzymatic activity assay	46
3.4.3	Determination of protein concentration	47
3.4.4	DHAP concentration assay.....	48
3.4.5	Quantification of substrates and products	48
3.4.5.1	Concentration of L-lactaldehyde and L-rhamnulose-1-phosphate	48
3.4.5.2	Concentration of carboxybenzyl (Cbz) compounds	49
4.	OXIDATION OF CBZ-AMINO ALCOHOLS CATALYZED BY HORSE LIVER ALCOHOL DEHYDROGENASE	53
4.1	Introduction	53
4.2	Methods	56
4.2.1	Comparison of different types of ADH and feasibility of the oxidation of Cbz-ethanolamine	56

4.2.2 Oxidation of Cbz-ethanolamine catalyzed by HLADH using semicarbazide hydrochloride.....	57
4.2.3 Preparation of the support glyoxal-agarose and MANA-agarose	59
4.2.4 Immobilization of HLADH.....	60
4.2.5 Oxidation of Cbz-ethanolamine catalyzed by HLADH	61
4.2.6 Oxidation of Cbz-ethanolamine to Cbz-glycinal using immobilized HLADH..	61
4.3 Results and discussion.....	62
4.3.1 Selection of the biocatalyst and feasibility of the oxidation of Cbz-ethanolamine by ADH.....	62
4.3.2 HLADH catalyzed oxidation of Cbz-ethanolamine	65
4.3.2.1 Oxidation of Cbz-ethanolamine catalyzed by HLADH in aqueous medium using semicarbazide hydrochloride for aldehyde entrapment .	65
i. Effect of the pH.....	68
ii. Cbz-glycinal semicarbazone formation at higher enzymatic activity.....	69
iii. Cbz-glycinal recovery from Cbz-glycinal semicarbazone.....	73
4.3.2.2 Evaluation of the support MANA-agarose for aldehyde entrapment .	75
4.3.2.3 Oxidation of Cbz-ethanolamine in aqueous medium with cosolvents.	77
4.3.2.4 Use of immobilized HLADH for the oxidation of Cbz-ethanolamine ...	79
i. Immobilization of HLADH in glyoxal-agarose.....	79
ii. Immobilized-HLADH catalyzed oxidation of Cbz-ethanolamine in aqueous medium	81
iii. Immobilized-HLADH catalyzed oxidation of Cbz-ethanolamine in biphasic medium	82
4.4 Conclusions	83
5. COUPLING OF THE HLADH CATALYZED OXIDATION OF CBZ-AMINO ALCOHOLS AND ALDOL ADDITION FOR THE PRODUCTION OF CBZ-AMINOPOLYOLS	87
5.1 Introduction	87

5.2	Methods	89
5.2.1	Coupled oxidation of Cbz-ethanolamine by HLADH and aldol addition catalyzed by RhuA	89
5.2.2	Study of DHAP degradation.....	89
5.2.3	Coupled Cbz-ethanolamine oxidation and aldol addition with DHAP pulses	89
5.2.4	Analysis of coupled reaction product by LC-MS.....	90
5.3	Results and discussion.....	91
5.3.1	Preliminary studies of the coupled oxidation of Cbz-ethanolamine by HLADH and DHAP aldol addition catalyzed by RhuA.....	91
5.3.1.1	Selection of the coupled reaction conditions	91
5.3.1.2	DHAP degradation.....	93
5.3.2	Coupled enzymatic reaction for the synthesis of Cbz-aminopolyol with DHAP pulses addition.....	94
5.4	Conclusions	97
6.	HORSE LIVER ALCOHOL DEYDROGENASE CATALYZED OXIDATION OF CBZ-β-AMINO ALCOHOLS TO CBZ-β-AMINO ACIDS....	101
6.1	Introduction	101
6.2	Methods	104
6.2.1	Batch oxidation of Cbz- β -amino propanol catalyzed by HLADH.....	104
6.2.2	Fed-batch oxidation of Cbz- β -amino propanol	105
6.2.3	Oxidation coupled to enzymatic cofactor regeneration.....	105
6.3	Results and discussion.....	106
6.3.1	Preliminary studies of batch oxidation of Cbz- β -amino propanol catalyzed by HLADH	106
6.3.2	Batch oxidation of Cbz- β -amino propanol for the synthesis of Cbz- β -alanine catalyzed by HLADH.....	110
6.3.3	Fed-batch oxidation of Cbz- β -amino propanol to Cbz- β -alanine catalyzed by HLADH.....	112
6.3.4	Enzymatic substrate-coupled regeneration of NAD ⁺	114

6.3.4.1 Batch oxidation of Cbz- β -amino propanol and enzymatic regeneration of NAD ⁺	114
6.3.4.2 Fed-batch oxidation of Cbz- β -amino propanol and enzymatic regeneration of NAD ⁺	116
6.4 Conclusions	119
7. HLADH-CATALYZED OXIDATION OF CBZ-AMINO ALCOHOLS USING ELECTROREGENERATED NAD⁺ IN A FILTER-PRESS MICROREACTOR.....	123
7.1 Introduction	123
7.2 Materials and methods.....	125
7.2.1 Electrokinetic studies	125
7.2.2 Preparative electrolysis.....	127
7.2.3 Quantification of NADH and NAD ⁺	130
7.2.4 Quantification of substrate and products by HPLC.....	131
7.2.5 Electrochemical behavior of the compounds involved in the NADH oxidation.....	131
7.2.6 Electrochemical oxidation of NADH and systematic study of several physicochemical parameters.....	131
7.2.7 Enzymatic oxidation catalyzed by HLADH coupled with electrochemical regeneration of NAD ⁺	132
7.3 Results and discussion.....	133
7.3.1 Direct electrochemical regeneration of NAD ⁺ in a three-electrode classical electrochemical cell.....	133
7.3.1.1 Current potential curves for NADH oxidation.....	134
i. On platinum anode.....	134
ii. On gold anode.....	135
7.3.1.2 Effect of the substrate Cbz- β -amino propanol and the product Cbz- β -alanine on the shape of the current potential curves obtained for NADH oxidation... ..	137

7.3.1.3 Effect of the potential scan rate on the NADH electrochemical oxidation.....	139
7.3.2 Oxidation of NADH in a filter-press microreactor at the steady state	141
7.3.3 Coupled oxidation of Cbz-ethanolamine and electrochemical regeneration of NAD ⁺	143
7.3.4 Effect of physicochemical parameters on the electrochemical oxidation of NADH	145
7.3.5 Coupled oxidation of Cbz-β-amino propanol and electrochemical regeneration of NAD ⁺	150
7.3.6 Coupled fed-batch oxidation of Cbz-β-amino propanol and electrochemical regeneration of NAD ⁺	153
7.4 Conclusions	156
GENERAL CONCLUSIONS	161
REFERENCES	165
ANNEXES	193
Annex 1. Platinum electrode studies	193
i. Buffer.....	193
ii. Buffer with 20 mM Cbz-ethanolamine	194
iii. Buffer with 20 mM NADH	194
Annex 2. Gold electrode studies	195
i. Buffer.....	195
ii. Buffer with 20 mM Cbz-ethanolamine	195
iii. Buffer with 20 mM NADH	196
iv. Preparative electrolysis.....	196
v. Coupled HLADH catalyzed Cbz-amino propanol oxidation and electroregeneration of NAD ⁺	201

LIST OF TABLES

Table 1.2.1 Summary of the enzymes classification based on the International Union of Biochemistry and Molecular Biology (IUBMB) guidelines. Adapted from Buchholz and coworkers (Buchholz, Kasche et al. 2005).....	5
Table 1.2.2 Industrial enzymes applications (Gavrilescu and Chisti 2005).....	6
Table 4.3.1 Enzymatic activity of ADH from different sources	62
Table 4.3.2 Kinetic parameters of Cbz-ethanolamine oxidation catalyzed by ADH from different sources. The reactions were performed with 5 mM Cbz-ethanolamine in 50 mM sodium pyrophosphate buffer pH 8.7, 5 mM NAD ⁺ and a final enzymatic activity of 20 U/mL in house HLADH, 1.44 U/mL commercial HLADH and 0.042 U/mL YADH in a final volume of 5 mL.....	63
Table 4.3.3 Summary of HLADH catalyzed oxidation of Cbz-ethanolamine using semicarbazide hydrochloride to obtain Cbz-glycinal semicarbazone. The reactions were performed with 20 mM Cbz-ethanolamine in 50 mM sodium pyrophosphate buffer pH 8.7, 20 mM NAD ⁺ , 300 mM and 600 mM semicarbazide concentration, and HLADH activity of 80 U/mL at room temperature (20-22°C) in a final volume of 5 mL for 151 h.....	72
Table 6.3.1 Effect of the temperature in the preliminary batch oxidation of Cbz-β-amino propanol to Cbz-β-alanine catalyzed by HLADH after 50 h of reaction. The reactions were performed with 10 mM Cbz-β-amino propanol in 100 mM sodium pyrophosphate buffer pH 8.7, 10 mM NAD ⁺ and 100 U/mL HLADH at 25°C.....	108
Table 6.3.2 Summary of the results for the oxidation of Cbz-β-amino propanol to Cbz-β-alanine catalyzed by HLADH. 18.7 mM Cbz-β-amino propanol, 100 U/mL HLADH , pH 8.7 and 25°C were used for all the cases.	118
Table 7.3.1 Molar extinction coefficients of NADH and NAD ⁺ in 100 mM sodium pyrophosphate buffer pH 8.7 at room temperature.	141

LIST OF FIGURES

Figure 1.2.1 Classical vs present development of enzymes (Kirk et al., 2002).	4
Figure 1.3.1 Reaction of the dehydrogenation of ethanol by alcohol dehydrogenase.	8
Figure 1.4.1 Structure of horse liver alcohol dehydrogenase-ternary complex of ADH with NAD ⁺ and difluorobenzyl alcohol. Dimeric structure showing the overall chain fold for the subunits: NAD ⁺ (black), difluorobenzyl alcohol (pink) and two Zn ⁺² ions (red) per monomer. (Frey A. and Hageman D. 2007)	10
Figure 1.5.1 Enzymatic regeneration of cofactors. For substrate-coupled regeneration, the two enzymes are the same, E1=E2; for enzyme coupled regeneration, E1 and E2 represent two different enzymes (Liu and Wang 2007).	15
Figure 1.5.2 NAD(P) ⁺ -dependent oxidation reactions: (A) direct electrochemical regeneration, (B) indirect electrochemical regeneration, (C) enzyme-coupled electrochemical regeneration.	17
Figure 1.5.3 Internal distribution of a filter press microreactor used for the electrochemical regeneration of NADH.	23
Figure 1.7.1 Aldol addition of DHAP to Cbz-amino aldehyde catalyzed by a DHAP dependent aldolase	27
Figure 1.7.2 Obtention of iminocyclitols from aminopolyols.	27
Figure 1.7.3 Reaction of L-rhamnulose-1-phosphate decomposition catalyzed by RhuA.	30
Figure 1.7.4 Structure of the C ₄ -symmetric RhuA with its molecular fourfold axis (Grueninger and Schulz 2008).	31
Figure 1.7.5 Oxidation of Cbz-amino alcohols by horse liver alcohol dehydrogenase.	32
Figure 1.8.1 Oxidation of Cbz-β-amino alcohols by horse liver alcohol dehydrogenase.	34
Figure 3.3.1 Enzymatic synthesis scheme of L-rhamnulose-1-phosphate catalyzed by rhamnulose-1-phosphate aldolase (RhuA).	43
Figure 3.3.2 Reaction of oxidative decarboxilation of D-threonine by ninhydrin for the synthesis of L-lactaldehyde.	44
Figure 3.4.1 Reaction scheme for the determination of the enzymatic activity of horse liver alcohol dehydrogenase (HLADH).	46
Figure 3.4.2 Reaction scheme for the determination of the enzymatic activity of rhamnulose-1-phosphate aldolase (RhuA).	47
Figure 4.1.1 Oxidation of Cbz-ethanolamine by horse liver alcohol dehydrogenase.	54
Figure 4.1.2 Schiff base formed by semicarbazide hydrochloride and Cbz-glycinal.	54
Figure 4.2.1 Scheme of the work up of Cbz-glycinal semicarbazone to obtain Cbz-glycinal. Adapted from Andersson and Wolfenden (Andersson and Wolfenden 1982).	58

Figure 4.3.1 Time course of the preliminary batch oxidation of Cbz-ethanolamine. Cbz-ethanolamine (●), Cbz-glycine (○), HLADH (▲). The reaction was performed with 5 mM Cbz-ethanolamine in 50 mM sodium pyrophosphate buffer pH 8.7, 5 mM NAD⁺, 20 U/mL HLADH enzymatic activity at room temperature (20-22°C) in a final volume of 5 mL for 48 h. 64

Figure 4.3.2 Influence of the concentration of semicarbazide hydrochloride in the yield of Cbz-glycinal semicarbazone (black bars) and Cbz-glycine (gray bars) and conversion of Cbz-ethanolamine (white bars). The reactions were performed with 5 mM Cbz-ethanolamine in 50 mM sodium pyrophosphate buffer pH 8.7, 5 mM NAD⁺ and HLADH activity of 16 U/mL at room temperature (20-22°C) in a final volume of 5 mL for 24 h. 66

Figure 4.3.3 Influence of the concentration of semicarbazide hydrochloride in the yield of Cbz-glycinal semicarbazone (black bars) and Cbz-glycine (gray bars) and Cbz-ethanolamine conversion (white bars). The reactions were performed with 20 mM Cbz-ethanolamine in 50 mM sodium pyrophosphate buffer pH 8.7, 20 mM NAD⁺ and HLADH activity of 16 U/mL at room temperature (20-22°C) in a final volume of 5 mL for 48 h. 67

Figure 4.3.4 Effect of the pH in the yield of Cbz-glycinal semicarbazone (black bars) and Cbz-glycine (gray bars) and Cbz-ethanolamine conversion (white bars). The reactions were performed with 20 mM Cbz-ethanolamine, 600 mM semicarbazide hydrochloride, 20 mM NAD⁺ and HLADH activity of 16 U/mL at room temperature (20-22°C) in a final volume of 5 mL for 72 h. 68

Figure 4.3.5 Concentration profile of Cbz-ethanolamine oxidation using semicarbazide hydrochloride 300 mM (A) and 600 mM (B). The reactions were performed with 20 mM Cbz-ethanolamine in 50 mM sodium pyrophosphate buffer pH 8.7, 20 mM NAD⁺ and HLADH activity of 80 U/mL at room temperature (20-22°C) for 151 h. Cbz-ethanolamine (●), Cbz-glycine (○), Cbz-glycinal semicarbazone (■), HLADH (▲). 70

Figure 4.3.6 Elution of Cbz-glycinal semicarbazone in the CM Sephadex ion exchange chromatography. The resin was previously equilibrated with 5 mM triethylammonium bicarbonate pH 7.2 and the elution was performed by applying a linear gradient of 5 to 400 mM triethylammonium bicarbonate pH 7.2 at room temperature (20-22°C) and a flow rate of 0.1 mL/min. Cbz-ethanolamine (white), Cbz-glycinal semicarbazone (black) and Cbz-glycine (gray). 73

Figure 4.3.7 Study of the use of MANA-agarose gel in the oxidation of Cbz-ethanolamine. The reactions were performed with 20 mM Cbz-ethanolamine in 50 mM sodium pyrophosphate buffer pH 8.7, 20 mM NAD⁺ and HLADH activity of 20 U/mL at 25°C for 72 h using MANA-agarose:reaction medium (v/v) (1:10 and 1:1). Cbz-ethanolamine conversion (white bars), Cbz-glycine yield (gray bars) and HLADH remaining activity (dark gray bars). 76

Figure 4.3.8 Stability of HLADH in presence of 75 mM sodium pyrophosphate buffer pH 8.7 and 4% v/v DMF during 24 h. 77

Figure 4.3.9 Time course of the Cbz-ethanolamine oxidation catalyzed by HLADH in presence of 4% (v/v) DMF. The reaction was performed with 20 mM Cbz-ethanolamine in 75 mM sodium pyrophosphate buffer pH 8.7, 4% v/v DMF, 20 mM NAD⁺ and 20 U/mL HLADH at 25°C. Cbz-ethanolamine (●), Cbz-glycine (○), HLADH (▲). 78

Figure 4.3.10 Time course of HLADH immobilization on glyoxal-agarose. The immobilization was performed with 1 g agarose in 10 mL of 100 mM sodium bicarbonate buffer pH 10.0 at room temperature (20-22°C). The immobilization was carried out using low (A) and high (B) load of enzyme. Measured activities in supernatant (▼), suspension (x) and blank (◆). 80

Figure 4.3.11 Time course of the Cbz-ethanolamine oxidation catalyzed by immobilized HLADH on glyoxal-agarose in aqueous medium. The reaction was performed with 20 mM Cbz-ethanolamine in 75 mM sodium pyrophosphate buffer pH 8.7, 20 mM NAD ⁺ , 2 g of 50 U/mL support immobilized HLADH at 37°C in a final volume of 7 mL. Cbz-ethanolamine (●), Cbz-glycine (○), HLADH (▲).....	81
Figure 4.3.12 Time course of the Cbz-ethanolamine oxidation catalyzed by immobilized HLADH on glyoxal-agarose in biphasic medium. The reaction was performed with 20 mM Cbz-ethanolamine in 75 mM sodium pyrophosphate buffer pH 8.7, 20 mM NAD ⁺ , 2 g of 50 U/mL support immobilized HLADH at 37°C in reaction medium: ethyl acetate (1:1) for a final volume of 7 mL. Cbz-ethanolamine (●), aqueous phase (solid line), organic phase (dotted line), HLADH (▲).....	82
Figure 5.1.1 Coupled oxidation of Cbz-ethanolamine by HLADH and aldol addition catalyzed by RhuA	88
Figure 5.3.1 Effect of the pH in the coupled oxidation of Cbz-ethanolamine by HLADH and the aldol addition catalyzed by RhuA. The reactions were performed using 20 mM Cbz-ethanolamine with 20 mM NAD ⁺ and 40 mM DHAP, adding HLADH and RhuA to reach 20 and 60 U/mL, respectively, in a final volume of 5 mL at pH 7 and 8 at room temperature (20-22°C) in 48 h reaction time. Coupled reaction product (black bars) and Cbz-glycine (gray bars).	92
Figure 5.3.2 Enzymatic DHAP degradation at pH 8 and 4°C. The medium consisted of 20 mM Cbz-ethanolamine, 40 mM DHAP, HLADH and RhuA in final enzymatic activities of 20 and 30 U/mL, respectively in a volume of 5 mL.	93
Figure 5.3.3 Time course of coupled Cbz-ethanolamine oxidation by HLADH and DHAP aldol addition catalyzed by RhuA at 4°C (A) and 25°C (B). The reactions were performed using 20 mM Cbz-ethanolamine with 20 mM NAD ⁺ and 40 mM DHAP, adding HLADH and RhuA to reach 450 and 80 U/mL, respectively, in a final volume of 5 mL at pH 8 with 40 mM DHAP pulses every 2 h during the first 6 h and then every 24 h during 52 h of reaction. Cbz-ethanolamine (●), Cbz-glycine (○), coupled reaction product (■), HLADH (▲), RhuA (▼).	95
Figure 6.1.1 Oxidation of Cbz-β-amino propanol by horse liver alcohol dehydrogenase.	102
Figure 6.1.2 Oxidation of Cbz-β-amino propanol catalyzed by HLADH coupled with the enzymatic regeneration of NAD ⁺ using acetaldehyde as cosubstrate.	103
Figure 6.3.1 Time course of the preliminary batch oxidation of Cbz-β-amino propanol. The reaction was performed with 10 mM Cbz-β-amino propanol in 100 mM sodium pyrophosphate buffer pH 8.7, 10 mM NAD ⁺ and 100 U/mL HLADH in a final volume of 5 mL at 25°C for 72 h. Cbz-β-amino propanol (●), Cbz-β-alanine (○), HLADH enzymatic activity (▲).....	107
Figure 6.3.2 Reaction of Cbz-β-alanine using NAD ⁺ :NADH (1:1) at several temperatures. The reactions were performed with 10 mM Cbz-β-alanine in 100 mM sodium pyrophosphate buffer pH 8.7, 5 mM NAD ⁺ :NADH (1:1) and 100 U/mL HLADH in a final volume of 5 mL at 25°C for 72 h. Cbz-β-alanine: 25°C (●), 40°C (○); HLADH enzymatic activity : 25°C (▲), 40°C (Δ).	109
Figure 6.3.3 Time course of the batch oxidation of Cbz-β-amino propanol to Cbz-β-alanine. The reaction was performed with 18.7 mM Cbz-β-amino propanol in 100 mM sodium pyrophosphate buffer pH 8.7, 37.4 mM NAD ⁺ and 100 U/mL HLADH in a final volume of 5 mL at 25°C for 72 h. Cbz-β-amino propanol (●), Cbz-β-alanine (○), HLADH enzymatic activity (▲).	111

Figure 6.3.4 Time course of the fed-batch oxidation of Cbz- β -amino propanol to Cbz- β -alanine. The reaction was performed with 18.7 mM Cbz- β -amino propanol in 100 mM sodium pyrophosphate buffer pH 8.7, 112.2 mM NAD⁺ and 100 U/mL HLADH in a final volume of 5 mL at 25°C for 96 h. 5 mM Cbz- β -amino propanol pulses were added at 3, 25.5 and 45.5 h. Cbz- β -amino propanol (●), Cbz- β -alanine (○), HLADH enzymatic activity (▲). 113

Figure 6.3.5 Time course of the batch synthesis of Cbz- β -alanine using the enzyme substrate-coupled regeneration system acetaldehyde/HLADH. The reaction was performed with 18.7 mM Cbz- β -amino propanol in 100 mM sodium pyrophosphate buffer pH 8.7, 37.4 mM NAD⁺, 200 mM acetaldehyde and 100 U/mL HLADH at 25°C for 2 h. Cbz- β -amino propanol (●), Cbz- β -alanine (○), HLADH enzymatic activity (▲). 115

Figure 6.3.6 Time course of the fed-batch synthesis of Cbz- β -alanine using the substrate-coupled regeneration system acetaldehyde/HLADH. The reaction was performed with 18.7 mM Cbz- β -amino propanol in 100 mM sodium pyrophosphate buffer pH 8.7, 18.7 mM NAD⁺, 200 mM acetaldehyde and 100 U/mL HLADH in a final volume of 5 mL at 25°C for 96 h. 5 mM Cbz- β -amino propanol pulses were added at 0.5, 2.5, 4 and 6 h. Cbz- β -amino propanol (●), Cbz- β -alanine (○), HL-ADH enzymatic activity (▲). 117

Figure 7.1.1 Scheme of the chemical oxidation of Cbz-ethanolamine and direct electrochemical regeneration of NAD⁺..... 124

Figure 7.1.2 Scheme of the chemical oxidation of Cbz- β -amino propanol and direct electrochemical regeneration of NAD⁺..... 124

Figure 7.2.1 Apparatus used to carry out electrokinetic studies (1). Insets: (2) Reduced volume (20 mL) Metrohm cell; (3) Cell with electrodes; (4) Working electrode=rotating disc of platinum or gold; (5) Platinum counter electrode; (6) Saturated calomel used as reference electrode. 125

Figure 7.2.2 Schematic representation (A) and pictures (B) of the experimental set-up used to carry out preparative electrolysis. (A) Scheme: (1) Filter-press microreactor; (2, 2a/2b/2c zoom of the microchannels: (i) inlet face, (ii) outlet face, (iii) membrane face, (iv) electrode face) Microstructured anode; (3) Microstructured cathode; (4) 'pseudo-reference' electrodes (Pt wire); (5) Nafion cationic membrane; (6) Peristaltic pumps; (7) Anolyte feed storage tank; (8) Catholyte feed storage tank. (B) Pictures: (9) Overall apparatus used; (10) Filter-press microreactor system and feed tanks for anolyte (covered by aluminum foil) and for catholyte; (11 and 12) dismantled microreactor shown micro-grooved anode (gold) and cathode (platinum). 128

Figure 7.3.1 Current potential curves obtained on a platinum disc anode (S=3.14 mm²) at room temperature. (A): transient state without convection/ $\omega=0$; r=100 mV/s; (B): steady state on a rotating disc $\omega=1000$ rpm, r=5 mV/s. 1: residual current (75 mM sodium pyrophosphate buffer pH 8.7); 2: (1) + 20 mM Cbz-ethanolamine; 3: (1) + 20 mM NADH. 134

Figure 7.3.2 Current potential curves obtained on a gold disc anode (S=3.14 mm²) at room temperature. (A): transient state without convection/ $\omega=0$; r=100 mV/s; (B): steady state on a rotating disc $\omega=1000$ rpm, r=5 mV/s. 1: residual current (75 mM sodium pyrophosphate buffer pH 8.7); 2: (1) + 20 mM Cbz-ethanolamine; 3: (1) + 20 mM NADH. 136

Figure 7.3.3 Current potential curves obtained at the steady state on a rotating disc $\omega=1000$ rpm, r=5 mV/s; room temperature. (A): platinum disc anode (S=3.14 mm²); (B): gold disc anode (S= 3.14 mm²) 1: residual current (100 mM sodium pyrophosphate buffer pH 8.7); 2: (1) + 15 mM Cbz- β -alanine; 3: (1) + 5mM NADH; 4: (3) + 15 mM Cbz- β -amino propanol; 5: (3) + 15 mM Cbz- β -alanine 137

Figure 7.3.4 Current potential curves obtained on a gold disc anode ($S=3.14 \text{ mm}^2$) at transient state and at room temperature. $\omega=0 \text{ rpm}$, $r=100 \text{ mV/s}$. 1: residual current (75 mM sodium pyrophosphate buffer pH 8.7); 2: 1+300 mM semicarbazide hydrochloride; 3: 1+ 20 mM NADH.	139
Figure 7.3.5 Current potential curves obtained on a gold disc anode ($S=3.14 \text{ mm}^2$) at room temperature and transient state without convection/ $\omega=0$. Electrolyte: 100 mM sodium pyrophosphate buffer pH 8.7. (1) Residual current (100 mV/s); (2), (3) and (4): 15 mM NADH, at 50, 100 and 200 mV/s respectively	140
Figure 7.3.6 Applied potential dependence of the conversion of NADH, obtained during preparative electrolysis achieved using a filter press microreactor on a microstructured gold made anode $S=18 \text{ cm}^2$. Anolyte: 20 mM of NADH in 75 mM sodium pyrophosphate buffer pH 8.7. Catholyte: 75 mM sodium pyrophosphate buffer pH 8.7. $T=40^\circ\text{C}$; $Q_{\text{anolyte}}=Q_{\text{catholyte}}=50 \text{ }\mu\text{L/min}$	143
Figure 7.3.7 Oxidation of 20 mM Cbz-ethanolamine with 20 mM NAD^+ at pH 8.7. HLADH was added to reach 500 U/mL in a final volume of 10 mL at 40°C coupled with 2.2 h of NAD^+ electroregeneration. Cbz-ethanolamine (●) and HLADH (▲)	144
Figure 7.3.8 Flow rate (A), temperature (B) and applied potential (C) dependences of the conversion of NADH, obtained during preparative electrolysis achieved using a filter press microreactor on a microstructured gold made anode $S=18 \text{ cm}^2$. Anolyte: 20 mM NADH, 20 mM Cbz-ethanolamine and 20 U/mL HLADH in 75 mM sodium pyrophosphate buffer pH 8.7. Catholyte: 75 mM sodium pyrophosphate buffer pH 8.7. Electrolysis duration: 2 min. (A): $T=40^\circ\text{C}$; $E_{\text{applied}}=1 \text{ V/Pt wire}$; (B): Flow rate 50 $\mu\text{L/min}$; $E_{\text{applied}}=1 \text{ V/Pt wire}$; (C) $T=40^\circ\text{C}$; Flow rate 50 $\mu\text{L/min}$	146
Figure 7.3.9 Effect of the NADH concentration dependence in the conversion of NADH at the steady state, obtained during preparative electrolysis achieved using a filter press microreactor on a microstructured gold made anode $S=18 \text{ cm}^2$. Anolyte: 20 mM NADH, 20 mM Cbz-ethanolamine and 20 U/mL HLADH in 75 mM sodium pyrophosphate buffer pH 8.7. Catholyte: 75 mM sodium pyrophosphate buffer pH 8.7. Electrolysis time: 2 min at 1 V. $T=40^\circ\text{C}$; $Q_{\text{anolyte}}=Q_{\text{catholyte}}=50 \text{ }\mu\text{L/min}$	148
Figure 7.3.10 Comparison of the conversion of 20 mM NADH in reaction medium applying current (0.8- I_{max}) and potential (1 V) at the steady state during preparative electrolysis achieved using a filter press microreactor on a microstructured gold made anode $S=18 \text{ cm}^2$. Anolyte: 20 mM of NADH, 20 mM Cbz-ethanolamine and 20 U/mL HLADH in 75 mM sodium pyrophosphate buffer pH 8.7. Catholyte: 75 mM sodium pyrophosphate buffer pH 8.7. Electrolysis time: 2 min at 1 V. $T=40^\circ\text{C}$; $Q_{\text{anolyte}}=Q_{\text{catholyte}}=50 \text{ }\mu\text{L/min}$	150
Figure 7.3.11 Time course of the batch coupled oxidation of Cbz- β -amino propanol to Cbz- β -alanine and electrochemical regeneration of NAD^+ in a filter-press microreactor. The reaction was performed with 18.7 mM Cbz- β -amino propanol in 100 mM sodium pyrophosphate buffer pH 8.7, 37.4 mM NAD^+ and 100 U/mL HLADH in a final volume of 10 mL at 25°C for 24 h (Anolyte). Catholyte: 100 mM sodium pyrophosphate buffer pH 8.7. Electrolysis time: 2 min at 0.5 mA. $T=40^\circ\text{C}$; $Q_{\text{anolyte}}=Q_{\text{catholyte}}=1 \text{ mL/min}$. Cbz- β -amino propanol (●), Cbz- β -alanine (○), NAD^+ (■) and NADH (□).	151
Figure 7.3.12 Comparison of the substrate conversion and HLADH enzymatic activity for the oxidation of Cbz- β -amino propanol. The conversion of Cbz- β -amino propanol (●) and the HLADH enzymatic activity (▲) for the reaction with no regeneration is represented with a solid line and the coupled oxidation with electrochemical regeneration of NAD^+ with a dotted line.	152

Figure 7.3.13 Time course of the fed-batch coupled oxidation of Cbz- β -amino propanol to Cbz- β -alanine and electrochemical regeneration of NAD⁺ in a filter-press microreactor. The reaction was performed with 18.7 mM Cbz- β -amino propanol in 100 mM sodium pyrophosphate buffer pH 8.7, 37.4 mM NAD⁺ and 100 U/mL HLADH in a final volume of 10 mL at 25°C for 50 h. 5 mM Cbz- β -amino propanol pulses were added at 4 and 26 h (Anolyte). Catholyte: 100 mM sodium pyrophosphate buffer pH 8.7. Electrolysis time: 48 h at 0.5 mA. T=40°C; Q_{anolyte} = Q_{catholyte} = 1 mL/min. Cbz- β -amino propanol quantity (●), Cbz- β -amino propanol conversion (◆), NAD⁺ (■) and NADH (□)..... 154

Figure 7.3.14 HLADH enzymatic activity profile for the fed-batch coupled oxidation of Cbz- β -amino propanol and electrochemical regeneration of NAD⁺ in a filter-press microreactor. 155

Figure A.1.1 Current potential curves obtained on a platinum disc anode (S=3.14 mm²) at room temperature. Residual current of 75 mM sodium pyrophosphate buffer pH 8.7. (A) Transient state without convection/ $\omega=0$ and several scan rates (r); (1) 20 mV/s, (2) 50 mV/s, (3) 100 mV/s, (4) 200 mV/s; (B) Steady state on a rotating disc r=5 mV/s and several angular velocities (ω); (1) 500 rpm, (2) 1000 rpm, (3) 2000 rpm, (4) 5000 rpm..... 193

Figure A.1.2 Current potential curves obtained on a platinum disc anode (S=3.14 mm²) at room temperature. Residual current of 75 mM sodium pyrophosphate buffer pH 8.7 with 20 mM Cbz-ethanolamine (A) Transient state without convection/ $\omega=0$ and several scan rates (r); (1) 20 mV/s, (2) 50 mV/s, (3) 100 mV/s, (4) 200 mV/s; (B) Steady state on a rotating disc r=5 mV/s and several angular velocities (ω); (1) 500 rpm, (2) 1000 rpm, (3) 2000 rpm, (4) 5000 rpm. 194

Figure A.1.3 Current potential curves obtained on a platinum disc anode (S=3.14 mm²) at room temperature. Residual current of 75 mM sodium pyrophosphate buffer pH 8.7 with 20 mM NADH. (A) Transient state without convection/ $\omega=0$ and several scan rates (r); (1) 20 mV/s, (2) 50 mV/s, (3) 100 mV/s, (4) 200 mV/s; (B) Steady state on a rotating disc r= 5 mV/s and several angular velocities (ω); (1) 500 rpm, (2) 1000 rpm, (3) 2000 rpm, (4) 5000 rpm..... 194

Figure A.2.1 Current potential curves obtained on a gold disc anode (S=3.14 mm²) at room temperature. Residual current of 75 mM sodium pyrophosphate buffer pH 8.7. (A) Transient state without convection/ $\omega=0$ and several scan rates (r); (1) 20 mV/s, (2) 50 mV/s, (3) 100 mV/s, (4) 200 mV/s; (B) Steady state on a rotating disc r=5 mV/s and several angular velocities (ω); (1) 500 rpm, (2) 1000 rpm, (3) 2000 rpm, (4) 5000 rpm..... 195

Figure A.2.2 Current potential curves obtained on a gold disc anode (S=3.14 mm²) at room temperature. Residual current of 75 mM sodium pyrophosphate buffer pH 8.7 with 20 mM Cbz-ethanolamine. (A) Transient state without convection/ $\omega=0$ and several scan rates (r); (1) 20 mV/s, (2) 50 mV/s, (3) 100 mV/s, (4) 200 mV/s; (B) Steady state on a rotating disc r=5 mV/s and several angular velocities (ω); (1) 500 rpm, (2) 1000 rpm, (3) 2000 rpm, (4) 5000 rpm..... 195

Figure A.2.3 Current potential curves obtained on a gold disc anode (S=3.14 mm²) at room temperature. Residual current of 75 mM sodium pyrophosphate buffer pH 8.7 with 20 mM NADH. (A) Transient state without convection/ $\omega=0$ and several scan rates (r); (1) 20 mV/s, (2) 50 mV/s, (3) 100 mV/s, (4) 200 mV/s; (B) Steady state on a rotating disc r=5 mV/s and several angular velocities (ω); (1) 500 rpm, (2) 1000 rpm, (3) 2000 rpm, (4) 5000 rpm..... 196

Figure A.2.4 Preparative electrolysis (expected to examine the effect of the applied potential dependence of the conversion of NADH at the steady state) achieved using a filter press microreactor on a microstructured gold anode $S=18\text{ cm}^2$. Anolyte: 20 mM NADH in 75 mM sodium pyrophosphate buffer pH 8.7. Catholyte: 75 mM sodium pyrophosphate buffer pH 8.7. $T=40^\circ\text{C}$ and $r=5\text{ mV/s}$; $Q_{\text{anolyte}}=Q_{\text{catholyte}}=50\text{ }\mu\text{L/min}$. (A) Current-potential curve obtained before preparative electrolysis. (B) Temporal evolution of the electrolysis current, under two applied potentials on the anode: (1) E_{peak} , (2) 1 V.196

Figure A.2.5 Preparative electrolysis (expected to examine the effect of the flow rate dependence on the conversion of NADH at the steady state) achieved using a filter press microreactor on a microstructured gold anode $S=18\text{ cm}^2$. Anolyte: 20 mM NADH with 20 mM Cbz-ethanolamine and 20 U/mL HLADH in 75 mM sodium pyrophosphate buffer pH 8.7. Catholyte: 75 mM sodium pyrophosphate buffer pH 8.7. $T=40^\circ\text{C}$; $Q_{\text{anolyte}}=Q_{\text{catholyte}}$. (1) 50 $\mu\text{L/min}$, (2) 500 $\mu\text{L/min}$, (3) 1000 $\mu\text{L/min}$, (4) 2600 $\mu\text{L/min}$. (A) Current-potential curve obtained before preparative electrolysis; $r=5\text{ mV/s}$. (B) Flow rate dependence of the maximum current evolution. (C) Temporal evolution of the electrolysis current, at $E_{\text{applied on the anode}}=1\text{ V}$197

Figure A.2.6 Preparative electrolysis (expected to examine the effect of the temperature dependence on the conversion of NADH at the steady state) achieved using a filter press microreactor on a microstructured gold anode $S=18\text{ cm}^2$. Anolyte: 20 mM NADH with 20 mM Cbz-ethanolamine and 20 U/mL HLADH in 75 mM sodium pyrophosphate buffer pH 8.7. Catholyte: 75 mM sodium pyrophosphate buffer pH 8.7. $Q_{\text{anolyte}}=Q_{\text{catholyte}}=50\text{ }\mu\text{L/min}$; (1): $T=10^\circ\text{C}$, (2): $T=25^\circ\text{C}$, (3): $T=50^\circ\text{C}$. (A) Current-potential curve obtained before preparative electrolysis; $r=5\text{ mV/s}$; (B) Temperature dependence of the maximum current evolution; (C) Temperature dependence of the half wave potential; (D) Temporal evolution of the electrolysis current, at $E_{\text{applied on the anode}}=1\text{ V}$198

Figure A.2.7 Current-potential curve for the applied potential dependence of the conversion of NADH at the steady state, obtained during preparative electrolysis achieved using a filter press microreactor on a microstructured gold anode $S=18\text{ cm}^2$. Anolyte: 20 mM NADH with 20 mM Cbz-ethanolamine and 20 U/mL HLADH in 75 mM sodium pyrophosphate buffer pH 8.7. Catholyte: 75 mM sodium pyrophosphate buffer pH 8.7. Electrolysis time: 2 min. $Q_{\text{anolyte}}=Q_{\text{catholyte}}=50\text{ }\mu\text{L/min}$. (1): 0.6 V, (2): 0.8 V, (3): 1 V...199

Figure A.2.8 Preparative electrolysis (expected to examine the effect of the NADH concentration dependence on the conversion of NADH at the steady state) achieved using a filter press microreactor on a microstructured gold anode $S=18\text{ cm}^2$. $T=40^\circ\text{C}$. $Q_{\text{anolyte}}=Q_{\text{catholyte}}=50\text{ }\mu\text{L/min}$ Catholyte: 75 mM sodium pyrophosphate buffer pH 8.7. Anolyte: NADH with 20 mM Cbz-ethanolamine and 20 U/mL HLADH in 75 mM sodium pyrophosphate buffer pH 8.7. $[\text{NADH}]^\circ$: (1) 3 mM, (2) 7 mM, (3) 13 mM. (A) Current-potential curve obtained before preparative electrolysis; $r=5\text{ mV/s}$; (B) Peak current dependence of the $[\text{NADH}]^\circ$; (C) Temporal evolution of the electrolysis current, at $E_{\text{applied on the anode}}=1\text{ V}$200

Figure A.2.9 Current-potential curve for the batch HLADH catalyzed oxidation of Cbz-amino propanol obtained by using a filter press microreactor on a microstructured gold made anode $S=18\text{ cm}^2$ at $r=5\text{ mV/s}$ after 30 min of enzymatic reaction. Anolyte: Reaction medium contained in a side batch reactor used for the HLADH catalyzed oxidation of Cbz-amino propanol, $[\text{NADH}]\approx 1.2\text{ mM}$. Catholyte: 100 mM sodium pyrophosphate buffer pH 8.7. $T=25^\circ\text{C}$; $Q_{\text{anolyte}}=Q_{\text{catholyte}}=1\text{ mL/min}$201

Figure A.2.10 Potential-time curve for the batch coupled HLADH catalyzed oxidation of Cbz-amino propanol and electrochemical regeneration of NAD^+ obtained by electrolysis using a filter press microreactor on a microstructured gold made anode $S= 18 \text{ cm}^2$. Anolyte: Reaction mixture (18.7 mM Cbz- β -amino propanol in 100 mM sodium pyrophosphate buffer pH 8.7, 37.4 mM NAD^+ and 100 U/mL HLADH in a volume of 10 mL). Catholyte: 100 mM sodium pyrophosphate buffer pH 8.7. Electrolysis time: 22 h at 0.5 mA. $T=25^\circ\text{C}$; $Q_{\text{anolyte}}= Q_{\text{catholyte}}=1 \text{ mL/min}$201

Figure A.2.11 Potential-time curve for the fed-batch coupled HLADH catalyzed oxidation of Cbz-amino propanol and electrochemical regeneration of NAD^+ obtained by electrolysis using a filter press microreactor on a microstructured gold made anode $S= 18 \text{ cm}^2$. Anolyte: Reaction mixture (18.7 mM Cbz- β -amino propanol in 100 mM sodium pyrophosphate buffer pH 8.7, 37.4 mM NAD^+ and 100 U/mL HLADH in a volume of 10 mL with 5 mM Cbz- β -amino propanol pulses added at 4 and 26 h). Catholyte: 100 mM sodium pyrophosphate buffer pH 8.7. Electrolysis time: 48 h at 0.5 mA. $T=25^\circ\text{C}$; $Q_{\text{anolyte}}= Q_{\text{catholyte}}=1 \text{ mL/min}$202

CHAPTER 1
INTRODUCTION

1. INTRODUCTION

1.1 Biotransformation

Biotransformation is the chemical reaction catalyzed by microorganisms in terms of growing or resting cells or by isolated enzymes.

Whole cells are often employed for synthetic reactions that require cofactors, since their regeneration is generally easier and less expensive in metabolically active cells. Nevertheless, their use as catalysts has several disadvantages as: low specific activities, possible generation of unwanted by-products due to the presence of other enzymes and more complicated processes as a consequence of the cell growth.

On the other hand, isolated enzymes are remarkable catalysts due to the following characteristics: capability of accepting a wide range of complex molecules as substrates, high specific enzymatic activities, possibility of external regeneration of their cofactors and exquisite stereo-specificity, catalyzing reactions with unparalleled chiral (enantio) and positional (regio) selectivities. Both isolated enzymes and whole cells are used in industry, and are an active area of research (Schmid, Dordick et al. 2001).

A critical consideration in any biotransformation application is the acquisition and development of a suitable biological catalyst. Hence, the ideal biotransformation system should include:

- *An efficient enzyme production system:* With a readily available microbial source, genetically stable and nonpathogenic strain.
- *An efficient biocatalyst:* Such as resting cells or purified enzymes with high stereoselectivity, high activity in the desired reaction, flexible substrate selectivity and minimal side reactions.
- *A stable biocatalyst:* Stable under optimal reaction conditions, acquiescent to immobilization/stabilization and amenable to bioreactor restrictions.

1.2 Enzymes

Enzymes catalyze the basic chemical reactions of the metabolism of all living organisms. Most of them are proteins (a few are ribonucleic acids or ribonucleoproteins) and the catalytic part is located in a relatively small active site, where the substrates bind and are chemically processed into products. They are derived from renewable resources, present high specificity and selectivity in reactant and product stereochemistry, work under mild conditions of temperature, pH and pressure, require nontoxic and noncorrosive conditions and are biodegradable (Cherry and Fidantsef 2003; Gavrilescu and Chisti 2005).

Even though the enzymes are naturally tailored to perform catalysis under physiological conditions, the main challenge in biocatalysis is to transform these physiological catalysts into process catalysts in the industrial field. This goal is not easy to achieve due to their complex molecular structures, intrinsic fragility (instability) and high cost of production (Illanes 2008). The production of enzymes by the development of fermentation processes, based on the use of selected production strains, made possible to manufacture them as purified, well-characterized preparations to be tuned to fit into the industrial scale. In recent years, the introduction of protein engineering and directed evolution has provided tailor-made enzymes (Figure 1.2.1) and it has further improved manufacturing processes and enabled the commercialization of new enzymes.

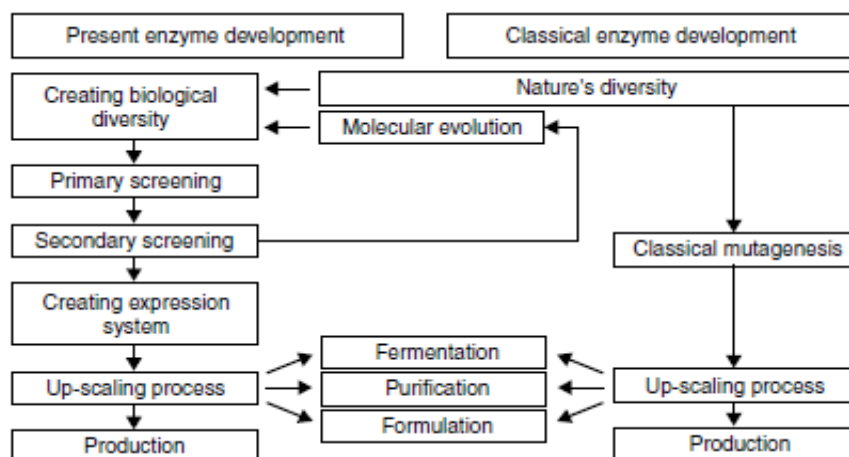


Figure 1.2.1 Classical vs present development of enzymes (Kirk et al., 2002).

Further immobilization of the biological agent confers advantages in biotransformation processes such as facilitating reuse and stabilization improvement. In addition, immobilized biocatalyst reactors and membrane bioreactors are used in continuous systems (Burton 2001).

The specific property that distinguishes one enzyme from another is the chemical reaction (and also the reverse reaction) that the enzymes catalyze, so they are classified based on this fact.

The catalyzed chemical reaction (and also the reverse reaction) is the specific property that distinguishes one enzyme from another, and they are classified based on this fact.

The Nomenclature Committee of the International Union of Biochemistry and Molecular Biology (NC-IUBMB) gives to every enzyme four numbers after the abbreviation EC. The first number indicates one of the six kinds of the reaction types that can be catalyzed by the enzyme, the second number is related to chemical structures changed in the process, the third defines the properties of the enzyme and the characteristics of the catalyzed reaction and the fourth is a running number. The main classification and the properties of the enzymes are summarized in table 1.2.1.

Table 1.2.1 Summary of the enzymes classification based on the International Union of Biochemistry and Molecular Biology (IUBMB) guidelines. Adapted from Buchholz and coworkers (Buchholz, Kasche et al. 2005).

Enzyme class	Function	Remarks
1. Oxidoreductases	Oxidation-reduction reactions	Cosubstrate required Two-substrate reaction
2. Transferases	Group transfer reactions	Two-substrate reactions, one substrate must be activated The donor is a cofactor (coenzyme) charged with the group to be transferred
3. Hydrolases	Strictly transferases that transfer groups to H ₂ O	Two substrate reactions, one of these is H ₂ O
4. Lyases	Non-hydrolytic bond-breaking reactions	One substrate reactions= bond breaking Two-substrate reactions=bond formation
5. Isomerases	Isomeration reactions	One-substrate reactions
6. Ligases	Bond-formation reactions	Require ATP as cobsustrate Two-substrate reactions

Regarding the industrial application of the enzymes, about 75% of their use (considering their value) is accounted for the detergent, food and starch processing industries and some special ones account for around 10% of the enzyme market. Their uses in the development of new drugs, medical diagnostics and other numerous analytical applications are being increased (Gavrilescu and Chisti 2005). It is estimated that no less than 50% of the enzymes marketed today come from manipulated organisms by genetic and protein engineering techniques (Illanes 2008).

New uses are being developed for enzymes in biotransformation of chemicals, food and feed, agricultural and textile sectors. Table 1.2.2 presents a summary of enzyme applications.

Table 1.2.2 Industrial enzymes applications (Gavrilescu and Chisti 2005).

Enzyme	Substrate	Reaction catalyzed	Industry
Proteases	Proteins	Proteolysis	Detergents, food, pharmaceutical, chemical synthesis
Carbohydrases	Carbohydrates	Hydrolysis of carbohydrates to sugars	Food, feed, pulp and paper, sugar, textiles, detergents
Lipases	Fats and oils	Hydrolysis of fats to fatty acids and glycerol	Food, effluent treatment, detergents, fine chemicals
Pectinases	Pectins	Clarification of fruit juices	Food, beverages
Cellulases	Cellulose	Hydrolysis of cellulose	Pulp, textile, feed, detergents
Amylases	Polysaccharides	Hydrolysis of starch into sugars	Food

1.3 Oxidoreductases

Oxidoreductases, as seen in table 1.2.1 catalyze oxidation-reduction reactions with a transfer of electrons from a reductant (donor) to an oxidant (acceptor). They involve biological oxidation and reduction, and thus respiration and fermentation processes (Dixon and Webb 1979). Most of all the oxidoreductases need cofactors, either organic redox coenzymes, transition metal ions or both.

Coenzymes are organic compounds with low molecular weight and they act in dissociation/association equilibrium with the catalysts so they have the functions as a co-substrate, e.g. nicotinamide adenine dinucleotide (NAD^+) that transfers hydride (H^-) or they are bound to the respective enzyme, such as electron transferring cofactors flavin adenine dinucleotide (FAD) y flavin mononucleotide (FMN). The metal ion or other non-protein group is called the prosthetic group and is bound covalently to the active site of the enzyme.

Oxidoreductases represent about 25% of all presently known enzymes, and represent a very large and diverse class of enzymes. They are classified in oxidases, peroxidases, oxygenases and dehydrogenases or reductases.

Oxidases catalyze oxidations by consumption of O_2 as electron acceptor without incorporation of the oxygen into the final product. Most of the oxidases are flavoproteins which are proteins that contain a riboflavin-derived nucleic acid as flavin adenine dinucleotide (FAD) or flavin mononucleotide (FMN).

Peroxidases are enzymes that are specific for the oxidation of a wide range of substrates using peroxide as oxidant, usually hydrogen peroxide. Peroxidases have no requirement for expensive cosubstrates.

Oxygenases catalyze the hydroxylation of a wide variety of organic substrates. They include either one (monooxygenases) or two (dioxygenases) oxygen atoms into the substrate.

Dehydrogenases will be presented in the next section.

1.3.1 Dehydrogenases

Dehydrogenases are the most useful oxidoreductases for preparative applications (Buchholz, Kasche et al. 2005). They catalyze the oxidation of a substrate by transferring hydrogen atoms to a coenzyme that acts as an acceptor. Enzymatic addition or removal of the elements of hydrogen to or from an organic molecule in general requires the action of the coenzyme, so the dehydrogenases are either NAD^+ or FAD-dependent oxidoreductases.

The general mechanism proceeds by: the formal transfer of a hydride and a proton; or the transfer of two electrons and two protons; or the transfer of a hydrogen atom, an electron, and a proton; or any of several other sequences.

The best known oxidoreductases, which comprise the major classes of these enzymes, are *pyridine nucleotide-dependent dehydrogenases*. They catalyze the dehydrogenation of an alcohol group to a ketone or aldehyde coupled with the reduction of NAD^+ to NADH.

Some significant enzymes belonging to this class are alcohol dehydrogenase, lactate dehydrogenase, glyceraldehyde-3-P dehydrogenase and glutamate dehydrogenase.

Alcohol dehydrogenases (ADH; EC 1.1.1.1) are zinc metalloenzymes of broad specificity. They oxidize a wide range of aliphatic and aromatic alcohols to their corresponding aldehydes and ketones, using NAD^+ as a coenzyme. The most studied ones are obtained from yeast and horse liver. Figure 1.3.1 shows the dehydrogenation of ethanol, which represents the natural substrate for ADH.

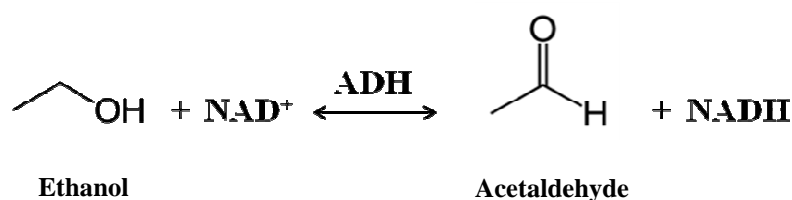


Figure 1.3.1 Reaction of the dehydrogenation of ethanol by alcohol dehydrogenase.

Horse liver alcohol dehydrogenase (HLADH) is a symmetrical dimer, with two identical chains that contain one binding site for NAD^+ and two sites for Zn^{2+} ; one of the zinc ions is directly concerned with catalysis. Yeast alcohol dehydrogenase (YADH) is a tetramer and each chain binds one NAD^+ and one Zn^{2+} (Brändén, Jörnvall et al. 1975). Alcohol dehydrogenase is found as isoenzyme in humans and higher animals, with multiple molecular forms for the same enzyme (Briganti, Ping Fong et al. 1989; Eklund, MÜLLER-Wille et al. 1990). Isoenzymes act by similar catalytic mechanisms, although they have different selectivity for different substrates, except for ethanol. YADH is highly selective for ethanol, but reacts slowly with the higher alcohols.

Instead, HLADH accepts a broad range of substrates from ethanol to octanol and benzyl alcohol.

The *kinetic mechanism* of the oxidation of alcohols (ethanol as an example) proceeds with the reduction of NAD^+ by a formal hydride transfer to NADH; a proton is released and ethanol is oxidized to acetaldehyde. It is known that zinc plays an important role in the mechanism of ADHs. In the dehydrogenation of an alcohol, the C-H and O-H bonds must be broken. The C-H bond is cleaved by transferring the hydride to NAD^+ ; in the case of ADH the problem of breaking the O-H bond is solved by the function of the catalytic Zn^{2+} . The coordination of the OH group with Zn^{2+} substantially increases the acidity of the alcohol and facilitates the dissociation of the proton. The acid strengthening effect of Zn^{2+} is amplified at the active site by the presence of NAD^+ complexed with ADH. The role of the Zn^{2+} is to contribute to cleaving the O-H bond.

The structure and detailed mechanism of the alcohol dehydrogenases, focusing on the HLADH, will be described in the next section.

1.4 Horse liver alcohol dehydrogenase (HLADH)

Horse liver alcohol dehydrogenase (HLADH; EC 1.1.1.1) is a dimer with a molecular weight of 80000 Da (Eklund, Nordström et al. 1974). There are two forms of the subunits, S and E of the dimer, which differ only by six residues in their amino acid composition (Eklund, Brändén et al. 1976). The S form is active on hydroxy-steroids, and both forms are active on ethanol. When isolated from liver, the enzyme consists of about 40-60% of the EE dimer, the remainder being SS and ES.

1.4.1 Structure

The structure of ADH reveals much about the active site, including the structural relationship of Zn^{2+} to the substrates. Structures of the free enzyme and ternary complexes show two domains, a dinucleotide binding domain (Rossmann fold) and a substrate binding domain, with an intervening cleft in the free enzyme. The cleft closes on ternary complex formation, and modeling studies suggest that this results from the substrate binding domain closing on the dinucleotide fold by sliding motion (Colonna-Cesari, Perahia et al. 1986). HLADH is a metalloenzyme with two zinc ions in each

subunit (Sund 1970). One Zn^{2+} is used to maintain its conformation (Sytkowski and Vallee 1976; Sytkowski and Vallee 1979) while the other also participates in the catalytic reaction.

The structure of the ternary complex of HLADH with NAD^+ and difluorobenzyl alcohol bound to the active site is presented in figure 1.4.1 (Rubach and Plapp 2002). The enzyme is in its closed conformation with the alcoholic group of the difluorobenzyl alcohol (pink) directly ligated to Zn^{2+} (red). Like all zinc metalloenzymes in which the metal participates in catalysis, Zn^{2+} in the free enzyme has a molecule of water in its coordination sphere (Vallee and Auld 1990). Zinc coordinated with water is displaced by the alcoholic group of the substrate during formation of the ternary complex. In the NAD^+ (black) binding site, the nicotinamide ring lies in a pocket lined with hydrophobic amino acid side chains to which hydride transfer occurs.

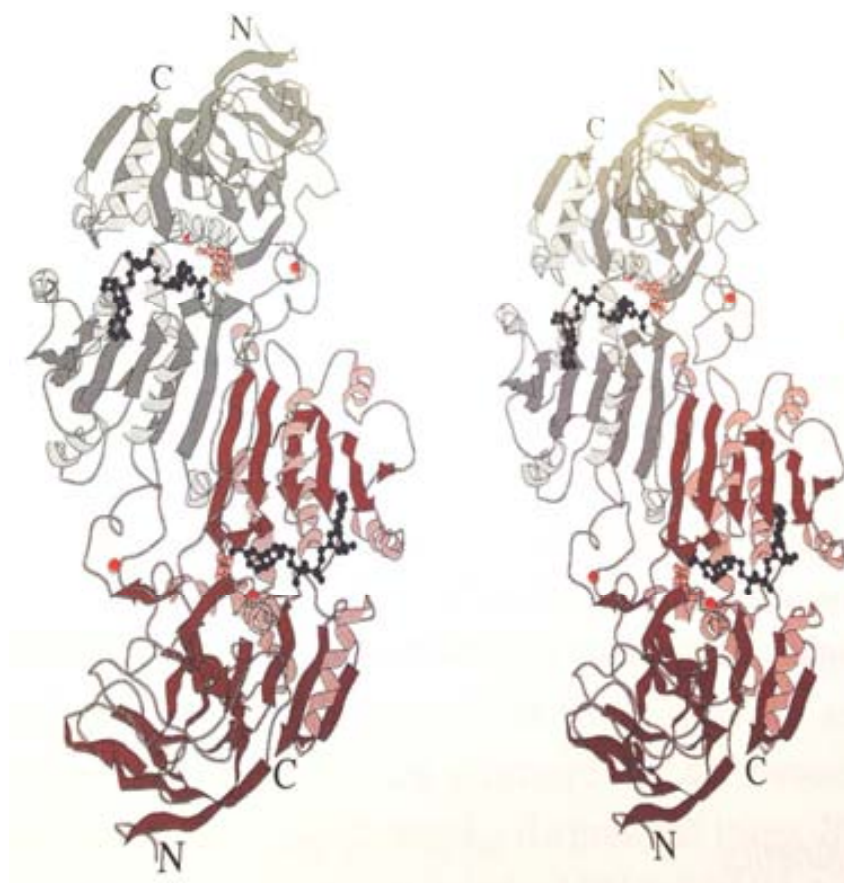


Figure 1.4.1 Structure of horse liver alcohol dehydrogenase-ternary complex of ADH with NAD^+ and difluorobenzyl alcohol. Dimeric structure showing the overall chain fold for the subunits: NAD^+ (black), difluorobenzyl alcohol (pink) and two Zn^{2+} ions (red) per monomer. (Frey A. and Hageman D. 2007).

1.4.2 Mechanism

The reaction catalyzed by HLADH follows an ordered mechanism, with NAD^+ binding to free enzyme when primary alcohols and aldehydes, such as ethanol and acetaldehyde or benzyl alcohol and benzaldehyde, are the substrates (Wratten and Cleland 1963; Shearer, Kim et al. 1993). In higher alcohols, dissociation of NAD^+ from a ternary complex can be detected (Silverstein and Boyer 1964).

The two active sites are in clefts between the coenzyme-binding core and the catalytic domains. Substrates bind in a hydrophobic pocket in the cleft with their oxygen atoms ligated to the zinc atoms of the catalytic domains. When coenzymes bind, the active site clefts close up by a rigid body rotation of the catalytic domains toward the coenzyme-binding domains (Eklund and Brändén 1979; Eklund, Samama et al. 1981).

The three dimensional structure has been used as a model for the active enzyme-substrate complex, but the *pro-R* hydrogen of substrate was oriented away from the nicotinamide ring in the observed mode of binding, so that rotation around single bonds of the substrate appeared to be required for direct hydrogen transfer. The complex is formed with good substrates at kinetically saturating levels. Taking the oxidation of ethanol as example, the composition of the complex should reflect the internal equilibrium on the surface of the enzyme, which favors NAD^+ -alcohol over NADH -benzaldehyde (Eklund, Plapp et al. 1982; Shearer, Kim et al. 1993). However, it has also been suggested that the complex contains NADH , and maybe an abortive complex with the alcohol (Bignetti, Rossi et al. 1979; Schneider, Cedergren-Zeppezauer et al. 1985). This complex could be formed as the enzyme slowly oxidizes benzaldehyde to benzoic acid (Anderson and Dahlquist 1980), which removes the aldehyde that maintains the internal equilibrium of reactants bound to the enzyme (Shearer, Kim et al. 1993).

The reactions involved in the mechanism of horse liver alcohol dehydrogenase are strongly pH-dependent (Pettersson 1987; LeBrun, Park et al. 2004). For example, the bimolecular association of NAD^+ is faster at pH below the pK of about 9.2 for free (apo) enzyme (Kvassman and Pettersson 1979; Sekhar and Plapp 1988), whereas the unimolecular dissociation of the enzyme- NAD^+ complex is faster at pH below a pK of 7.6 for the complex (Kvassman and Pettersson 1979). Binding of NAD^+ is a two-step

reaction, where the bimolecular association is followed by a limiting unimolecular step (Brändén, Jörnvall et al. 1975; Eklund, Samama et al. 1981; Eklund and Brändén 1987; Sekhar and Plapp 1988). The limiting rate constant for NAD^+ association decreases as pH is lowered below 7.6 (Sekhar and Plapp 1988).

1.4.3 Applications

Horse liver alcohol dehydrogenase has a broad substrate specificity, being active for the oxidation of a variety of primary, secondary, branched and cyclic alcohols (Merritt and Tomkins 1959; Sund and Theorell 1963; Dalziel and Dickinson 1966); specifically α -amino alcohols with nonpolar side chains, such as L-leucinol, L-phenylalaninol, and L-valinol (Andersson and Wolfenden 1982), n-alcohols ranging from ethanol to 1-decanol (Schirmer, Liu et al. 2002), short, middle and long-chain aliphatic alcohols (Cea, Wilson et al. 2009); reduction of ketones (Peters 1998; Goldberg, Schroer et al. 2007); asymmetric reduction of arylpropionic aldehydes (Giacomini, Galletti et al. 2007), reduction of substituted cyclohexanones and decalones (Graves, Clark et al. 1965; Dutler and Brändén 1981), synthesis of optically pure or enantiomerically enriched lactones (Haslegrave and Jones 1982; Naemura, Fujii et al. 1986; Shigematsu, Matsumoto et al. 1995; Martins, Viljoen et al. 2001); and stereospecific oxidation of only one of the enantiotopic hydroxy group of meso diols possessing acyclic, monocyclic and bicyclic structures (Jakovac, Goodbrand et al. 1982; Ng, YUAN et al. 1984; Boratyński, Kielbowicz et al. 2010).

1.5 Regeneration of the cofactor NAD^+

Although the costs for the oxidized cofactors NAD^+ and NADP^+ are more than fivefold lower than the cost for their reduced form, NADH and NADPH , their stoichiometric use is not economically feasible.

The regeneration of nicotinamide cofactors is a crucial step for an economic use of the enzymes (Chenault and Whitesides 1987; van der Donk and Zhao 2003; Zhao and van der Donk 2003; Hollmann and Schmid 2004; Wichmann and Vasic-Racki 2005; Hollmann, Hofstetter et al. 2006). In addition, cofactor regeneration simplifies product isolation, prevents problems of product inhibition by the cofactor, and can drive

thermodynamically unfavorable transformations by coupling to favorable regeneration reactions.

Whereas regeneration of the reduced forms of the pyridine nucleotide cofactors has been extensively investigated, recycling of NAD^+ has been less developed. Even so, various *in situ* regeneration methods have been devised to allow the use of catalytic quantities (Hummel and Kula 1989; Iwuoha and Smyth 2003).

The effectiveness of an *in situ* cofactor regeneration process is typically measured in terms of turnover numbers (TN, defined as the number of moles of product formed per mole of cofactor per unit time) and total turnover numbers (TTN, defined as the number of moles of product formed per mole of cofactor during the course of a complete reaction) of the cofactor (Katz, Heleg-Shabtai et al. 1998). TTNs of 10^3 to 10^5 are maybe sufficient to make a process economically viable depending on the value of the reaction product.

1.5.1 Chemical regeneration

Chemical cofactor regeneration systems use oxidants such as quinoid structures (Hilt, Jarbawi et al. 1997; Hilt, Lewall et al. 1997; Pival, Klimacek et al. 2008), and transition metals (Hollmann, Witholt et al. 2002; Hollmann, Kleeb et al. 2005). These methods are attractive since they are robust and allow phosphorylated and non-phosphorylated nicotinamide cofactors regenerate. However, to avoid the generation of hazardous hydrogen peroxide, molecular oxygen has to be substituted by an anode as terminal electron acceptor, resulting in complicated reaction set-ups (Hollmann and Schmid 2004). 2,2'-azino-bis(3-ethylbenzothiazoline-6-sulphonic acid) (ABTS) and electrochemical regeneration is a fast and efficient combination to promote ADH-catalyzed oxidation reactions (Schröder, Steckhan et al. 2003).

On the other side, chemical methods require cumbersome reaction conditions as well as expensive and/or toxic reagents, produce unwanted side products, and therefore have not been preferred for commercial or preparative applications. This could be the reason why very few examples of chemical methods of cofactor regeneration have been reported (Wichmann and Vasic-Racki 2005).

1.5.2 Photochemical regeneration

Photochemical regeneration of NAD^+ has been investigated during the past years due to its potential to use solar energy to promote chemical reactions. Hence, a couple of light-driven regeneration systems for NAD(P)^+ have been evaluated (Willner and Mandler 1989).

Absorption of light can either accelerate the primary electron transfer from NAD(P)H to a mediator (reductive quenching) or facilitate the reoxidation of the reduced mediator by the terminal electron acceptor (oxidative quenching). For reductive quenching, photosensitizers such as tin porphyrins (Handman, Harriman et al. 1984; Saiki and Amao 2003), methylene blue (Julliard and Le Petit 1982) and other dyes (Willner and Mandler 1989) have been reported. For oxidative quenching, $[\text{Ru}^{\text{III}}(\text{bpy})_3]^{3+}$ complexes in combination with viologens have been used among other systems. Usually, molecular oxygen or protons serve as terminal electron acceptors (Handman, Harriman et al. 1984; Willner and Mandler 1989). Using molecular oxygen can be an inconvenient, due to reactive, partially reduced oxygen species which are involved (Steckhan, Herrmann et al. 1991). Molecular oxygen was replaced by the anode as terminal electron acceptor and coupled the resulting photo-electrochemical NAD(P)^+ regeneration system to oxidation reactions catalyzed by various alcohol dehydrogenases (Ruppert and Steckhan 1989).

Next to soluble photosensitizers, semi-conductors (e.g. TiO_2) were reported for NAD^+ regeneration (Kawamoto, Aoki et al. 1989). Nonetheless, low performances (TTN) of the photosensitizers and coenzymes constitute a disadvantage.

Photoexcitation results in the formation of strong oxidizing agents and reactive radicals, which potentially interfere with the desired reaction. Accordingly, photochemical regeneration of NAD(P)^+ is not very well developed yet (Willner and Mandler 1989).

1.5.3 Enzymatic regeneration of NAD^+

There are two different ways to achieve enzymatic regeneration: the use of substrate-coupled reaction systems and the use of a second enzyme to catalyze the cofactor regeneration reaction (figure 1.5.1).

In the substrate-coupled reaction systems, one enzyme that uses both the reduced and oxidized forms of a cofactor is applied to catalyze both the desired synthesis of the product from one substrate and the cofactor regeneration reaction with a second substrate. Since the same enzyme is required to catalyze two separated reactions simultaneously, it is usually difficult to achieve thermodynamically-favorable reaction conditions for both reactions in the same reaction medium.

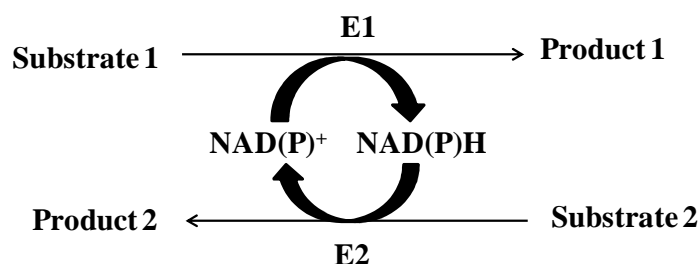


Figure 1.5.1 Enzymatic regeneration of cofactors. For substrate-coupled regeneration, the two enzymes are the same, $E1=E2$; for enzyme coupled regeneration, $E1$ and $E2$ represent two different enzymes (Liu and Wang 2007).

The use of a second enzyme, which has been adapted for the majority of cofactor regeneration processes, usually allow more options of substrates for the cofactor regeneration reaction, and makes it much easier to achieve large thermodynamic driving forces for both reactions. In either way, it is desirable to make value-added products from the second substrates applied for cofactor regeneration; otherwise, the second substrates have to be either very cheap or easily regenerated for reuse.

NAD^+ can be recycled from $NADH$ by using $NADH$ oxidases in an enzyme coupled regeneration method. This method has some drawbacks, as the production of H_2O_2 which damages most proteins, hence catalase must be added (van der Donk and Zhao 2003).

Some studies have provided a potentially attractive alternative (Riebel, Gibbs et al. 2002; Geueke, Riebel et al. 2003). Certain $NADH$ oxidases generate water as reduced product involving an enzyme-bound flavine adenine dinucleotide (FAD) and a redox-active cysteine residue in the enzyme's active site (Claiborne, Conn Mallett et al. 2001).

Unlike methods that use ADH, lactate dehydrogenase or glutamate dehydrogenase for $NAD(P)^+$ regeneration, this method does not generate by-products, but the oxygen sensitivity of the protein is currently still a disadvantage.

Enzymatic cofactor regeneration has some disadvantages, such as high enzyme cost, enzyme instability, and restricted reaction conditions.

1.5.4 Electrochemical regeneration

Electrochemistry is a promising tool for the regeneration of the different cofactors and coenzymes. There are several advantages of the use of electrochemical regeneration: the supply of redox equivalents is basically mass-free since only electron transfer reactions are involved, no cosubstrate is required and no coproduct is formed, the use of a second enzyme can be avoided, electrons are among the cheapest redox equivalents available (Wandrey 2004) and the technique is environmentally friendly.

In electrochemical regeneration systems not only co-substrates are replaced by electrons but also regeneration enzymes or mediators are in some cases not necessary anymore; for example, during direct cofactor regeneration at electrodes. For efficient usage of the reduction equivalents it is possible to influence the selectivity of the electron transfer by adjusting the electrode potential or by changing the chemical nature of the electrode surface. The selectivity of the regeneration reaction could be adapted to a given process by the choice of the mediator that shuttles reduction equivalents from electrode to cofactor using indirect cofactor regeneration strategies (Arns, Heineman et al. 2001).

This kind of regeneration is applicable to a broad range of reaction conditions in terms of reaction medium, temperature, pH, etc., being compatible with the optimal environment conditions for the enzymatic catalysis (Hollmann and Schmid 2004).

The bioelectrochemical conversion can be conveniently monitored by the electric current, the current being related to the amount of product formed by the following equation:

$$\text{moles product} = \frac{I \cdot t}{F \cdot n} \quad (1.1)$$

In which

I = current (A)

t = time (s)

F = Faraday's number (96500 C/mol)

n = number of electrons transferred for the corresponding reaction

This principle allows the selectivity and specificity of the bioelectrochemical reactions to be monitored.

Synthesis where the cofactor NAD(P)^+ has to be regenerated to its oxidized state can be carried out with direct, indirect and enzyme-coupled electrochemical cofactor regeneration (figure 1.5.2).

Direct regeneration means that the species to be regenerated reacts at the electrode. Indirect regeneration means that another substance (mediator) acts as an electron shuttle between the electrode and the cofactor used. If a second enzyme is used as the electron shuttle the process is called enzyme-coupled electrochemical cofactor regeneration.

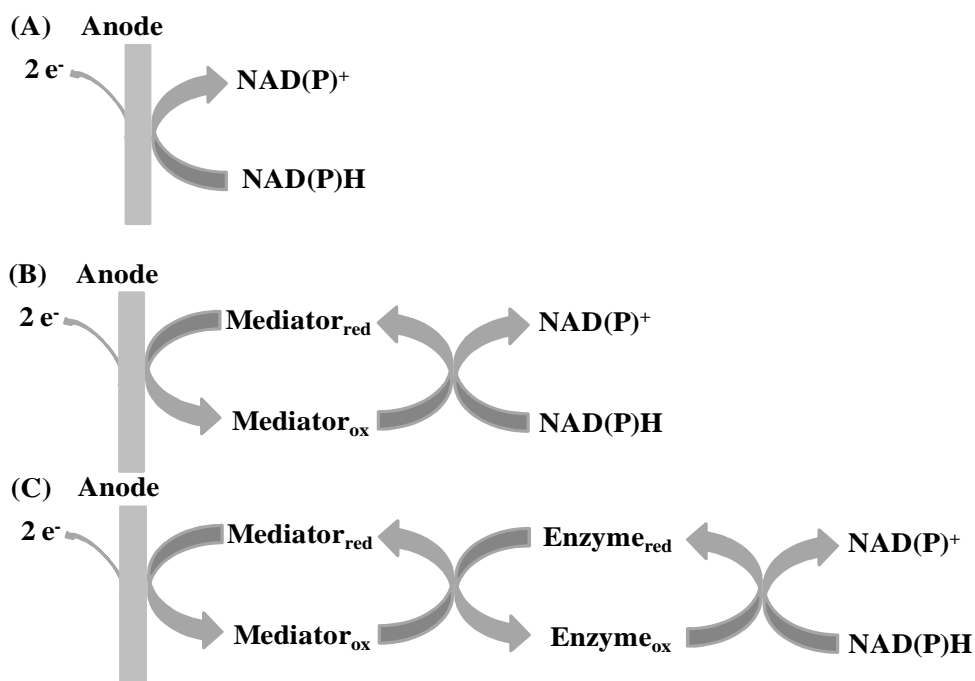


Figure 1.5.2 NAD(P)^+ -dependent oxidation reactions: (A) direct electrochemical regeneration, (B) indirect electrochemical regeneration, (C) enzyme-coupled electrochemical regeneration.

1.5.4.1 Direct anodic regeneration of NAD(P)^+

The electrochemistry of the redox-coupled $\text{NAD(P)}^+/\text{NAD(P)H}$ has been studied extensively (Gorton 2002). Direct anodic oxidation of NAD(P)H generally occurs at high overpotentials, on which the electrode material has a significant influence, e.g. $\text{C} \approx -400$, $\text{Pt} \approx -700$, and $\text{Au} \approx -1000$ mV vs. Saturated Calomel Electrode (SCE),

respectively (Blaedel and Jenkins 1975; Samec and Elving 1983). The exact mechanism of NAD(P)H oxidation is still controversial, but it seems that follows an ECE-mechanism (sequential Electrochemical-Chemical- Electrochemical steps).

Dimerization of the intermediate radical species has been reported (Gorton 2002). However, since the dimer is oxidized yielding enzymatically active NAD(P)⁺, this side-reaction does not limit the applicability of direct anodic NAD(P)⁺ regeneration. The high overpotential observed in the direct electrochemical oxidation of NADH is attributed to the very high potential of the NADH^{•+}/NADH couple, making this step rate limiting in the overall process. The required overpotentials can be lowered significantly via oxidative pretreatment of the anode surface (Fassouane, Laval et al. 1990; Biade, Bourdillon et al. 1992; Obón, Casanova et al. 1997; Anne, Bourdillon et al. 1999).

One consequence of the high overpotentials needed for direct anodic NAD(P)⁺ regeneration is that it can only be used for reactions with substrates that are oxidation-stable to avoid side reactions. Nevertheless, some synthetic applications of this approach have been reported. Direct electrochemical NAD⁺ regeneration was coupled to the glucose dehydrogenase (GDH, EC 1.1.1.47) catalyzed oxidation of glucose to gluconic acid (Fassouane, Laval et al. 1990). In a plugged-flow reactor setup, the authors efficiently regenerated NAD⁺ at oxidatively pretreated carbon electrodes (E= +700 mV vs. SCE). The selectivity of the electrochemical regeneration was estimated to yield over 99.95% enzymatically active NAD⁺ and up to 335 turnovers for the nicotinamide cofactor were achieved. The electrochemical step was found to be overall rate-limiting; thus, the rate of the electrochemical regeneration required an optimization of the ratio of electrode surface to reactor volume, raising the anode potential. However, the stability of GDH activity decreased drastically, which could be partially alleviated with poly(ethyleneimine) (Obón, Casanova et al. 1997).

Furthermore, both the anodic and the cathodic current were studied to drive thermodynamical unfavorable deracemization reactions catalyzed by alcohol- and amino acid-dehydrogenases (Fassouane, Laval et al. 1990; Biade, Bourdillon et al. 1992). For example, L-alanine dehydrogenase (L-Ala DH, EC. 1.4.1.1) was coupled to anodic regeneration of NAD⁺ together with cathodic regeneration of the racemic substrate (Anne, Bourdillon et al. 1999).

In general, direct electrochemical regeneration of NAD(P)^+ is an efficient method that does not require additional reaction components. High yields of enzymatically active oxidized nicotinamide coenzymes are obtained. However, this kind of regeneration is not suitable for easily oxidizable substrates, because direct anodic oxidation will significantly lower the specificity of the overall reaction.

1.5.4.2 Mediated electrochemical regeneration of NAD(P)^+

To avoid the high overpotential necessary for the direct electrochemical oxidation of NAD(P)H , various chemical redox agents can be used as electron carriers. They are called redox mediators. Due to the mainly chemical oxidation of NADH , they are able to lower the working potential to the formal potential of the mediator. Mediators are used as soluble monomers as well as immobilized on the electrode surface (Gorton and Domínguez 2002).

The mechanism of the mediated electrochemical regeneration of the oxidized nicotinamide adenine dinucleotide initiates with the oxidation of the mediator at a suitable potential. The reduced NAD(P)H will be oxidized by the oxidized mediator. The reduced mediator can then be re-oxidized at the electrode. At the cathode, the reduction of oxygen occurs. The oxidized NAD(P)^+ can be used in an enzymatic reaction. NAD(P)H oxidation using electron transfer mediators follows a Michaelis–Menten mechanism (Lobo, Miranda et al. 1997).

Mediated oxidation of NADH can be accomplished with a large number of compounds such as metal complexes (Hilt and Steckhan 1993; Hilt, Lewall et al. 1997), quinones (Pariante, Tobalina et al. 1996; Ciszewski and Milczarek 2000; Prieto-Simón and Fàbregas 2004; Ghanem, Chrétien et al. 2009), fluorenones (Mano and Kuhn 1999; Mano, Thienpont et al. 2001; Munteanu, Mano et al. 2002), phenazines (Curulli, Carelli et al. 1997; Lu, Bai et al. 2010; Arechederra, Addo et al. 2011), phenoxazine and phenothiazines (Lobo, Miranda et al. 1996), and even conducting polymers (Bartlett, Birkin et al. 1997; Toh, Bartlett et al. 2003) and Self Assembled Monolayers (SAM) (Ju, Xiao et al. 2002; Barzegar, Moosavi-Movahedi et al. 2009). Generally, two-electron proton acceptor type mediators exhibit higher reaction rates than single electron mediators for NAD(P)H oxidation and yield enzymatically active NAD(P)^+ as the reaction product (Santos, Gorton et al. 2002). Some chemical substances can be used as

either dyes or redox mediators, e.g., methylene green, methylene blue, or Meldola's Blue. However, besides the potential hazardous effects, some of the substances, as well as their precursors and degradation products, are carcinogenic and/or mutagenic in nature (Manu and Chaudhari 2002).

For preparative implementation, mostly soluble mediators or derivatives have been employed to accomplish NAD(P)^+ regeneration. For example, flavins have been used to regenerate NAD^+ for oxidation reactions catalyzed by horse liver alcohol dehydrogenase (HLADH) (Jones and Taylor 1976). Molecular oxygen serves as terminal electron acceptor making the overall reaction thermodynamically feasible. The unfavorable rate of the hydride transfer from NADH to flavin requires an excess of concentration of flavin to obtain reasonable reaction rates. The rate of the hydride transfer can be increased by several orders of magnitude e.g. by NADH oxidases or flavin oxidoreductases (Schmid, Hollmann et al. 2002). The advantage of using molecular oxygen as terminal electron acceptor is the high thermodynamic driving force as well as the convenient reaction setup. Furthermore, the collateral formation of hydrogen peroxide is a considerable problem for this setup, which can be overcome if an anode serves as electron sink instead of O_2 .

Alternatively, 1,10-phenanthroline-5,6-dione (PDon) derivatives have been used to regenerate NAD(P)^+ electrochemically (Hilt, Jarbawi et al. 1997; Hilt, Lewall et al. 1997). Electrochemical regeneration of the oxidized mediators was performed at moderate overpotentials. Both regeneration approaches were coupled to oxidation reactions catalyzed by HLADH yielding full conversion of the substrate (e.g. meso-3,4-dihydroxymethylcyclohexene) to the optically pure product at a gram scale with turnover numbers for NAD^+ and the mediator of up to 90 and 900, respectively.

In a similar approach, the one-electron acceptor ABTS (2,2'-azinobis (3-ethylbenzothiazoline-6-sulfonate)) (Schröder, Steckhan et al. 2003) has been used. With the same enzyme-substrate couple, nearly full conversion (94%) of meso-3,4-dihydroxymethylcyclohexene (48 mM) to the optically pure product was achieved. Despite the more anodic electrode potential applied (+850 mV vs. Ag/ AgCl), initial rates of oxidation using the ABTS mediator were approximately one order of magnitude slower than for PDon (approximately 1.5 h^{-1} for ABTS).

Mediated electrochemical regeneration of NAD(P)^+ is an efficient method to promote preparative oxidations catalyzed by dehydrogenases, compared to the current state-of-the-art in enzymatic approaches (van der Donk and Zhao 2003).

1.5.4.3 Electroenzymatic regeneration of NAD(P)^+

Various enzymatic approaches have been evaluated to accelerate the electron transfer from NAD(P)H to the oxidized mediator. This concept can be beneficial for synthetic applications, where downstream processing can be greatly facilitated if separation of enzymes and mediators is not necessary. For example, ferrocene was co-immobilized together with diaphorase (NADPH dehydrogenase; EC 1.6.99.1) in poly acrylic acid on a graphite anode, for the regeneration of NAD^+ in oxidation reactions catalyzed by HLADH (Kashiwagi and Osa 1993; Osa, Kashiwagi et al. 1994). Methyl viologen (N,N'-dimethyl-4,4'-bipyridyl, MV^{2+}) is another frequently used mediator for bioelectrocatalytic regeneration of NAD^+ , as the diaphorase/ MV^{2+} system for generation of energy. A series of NAD^+ -dependent dehydrogenases were used to successively oxidize methanol to carbon dioxide. The released reducing equivalents were transferred via NADH to the anode compartment of the biofuel-cell and channeled to the electrode via diaphorase/ MV^{2+} -catalysis (Palmore, Bertschy et al. 1998).

Taken as a whole, bioelectrochemical regeneration of NAD(P)^+ is frequently used within electrochemical biosensors.

1.5.4.4 Microreactors

Microreactors are defined as tridimensional structures with a series of small interconnecting channels with diameter on the order of 10–100 μm (Ehrfeld, Hessel et al. 1999; Ehrfeld, Hessel et al. 2000), created on a flat surface in which small quantities of reagents are manipulated. The main feature of the microreactors is their surface area to volume ratio (between 20 and 1000 cm^{-1}), which is considerable higher than the traditional reactors ($\sim 1 \text{ cm}^{-1}$), (Löwe and Ehrfeld 1999; Jähnisch, Hessel et al. 2004).

Decreased channel dimensions of microreactors present numerous advantages that lead to increased reaction efficiency as high surface area to volume ratio, fast diffusion

transport, enhanced heat transfer and thus reduced energy demands, good process control, high throughput and usage of minimal (microlitres) reagent volumes.

The high specific surface area improves the heat and mass transfer rates in the microreactors. The heat transfer efficiency significantly reduces the heating and cooling time of the reaction mixture, allowing the isothermal behavior of the reaction. Temperature control permits an enhancement of the selectivity, conversion and purity of the products. Low channel dimensions reduce the diffusion time, and the mass transfer rate is minimized compared to the reaction rate. Also, a local turbulence flow can be created in certain microreactors to improve the mixing.

Microreactors were proved to be useful in a wide range of applications from their requirement of an integral component within the framework of process miniaturization to catalytic screening, process intensification (Pohar and Plazl 2009), and on-site and on-demand production of chemicals (Tudorache, Mahalu et al. 2011). Although a great majority of the reaction systems that are studied in microreactors are connected with chemical synthesis, biocatalysis in a microreactor is a promising alternative (Thomsen and Nidetzky 2009).

An interesting application of microreactors is the regeneration of NADH. The feasibility of continuous electroregeneration of NADH in a filter press microreactor (figure 1.5.3), using FAD/FADH₂ as a redox mediator, was experimentally demonstrated (Choban, Waszczuk et al. 2004; Kane 2005; Yoon, Choban et al. 2005; Tzedakis, Kane et al. 2006; Tzedakis, Kane et al. 2006; Cheikhou and Tzedakis 2008; Tzedakis, Cheikhou et al. 2010). In addition, an indirect method for the electrogeneration of NADH was chosen since the direct electroregeneration of NADH seems not to be selective (Jaegfeldt 1981; Cantet, Bergel et al. 1996; Kane 2005).

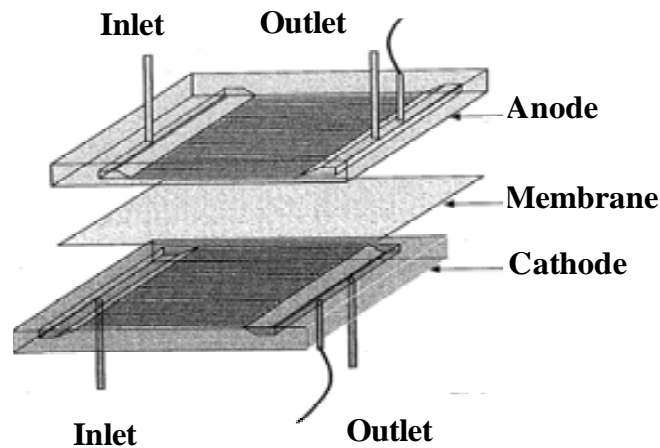


Figure 1.5.3 Internal distribution of a filter press microreactor used for the electrochemical regeneration of NADH.

Concerning the filter-press microreactor, some electrochemical aspects should be taken into account to calculate the concentration of an electrochemically active compound:

$$C_A = C_A^o \cdot e^{-\frac{S \cdot k}{Q}} \quad \text{If } I = I_{\text{lim}} \quad (1.2)$$

$$C_A = C_A^o - \frac{I}{n \cdot F \cdot Q} \quad \text{If } I < I_{\text{lim}} \quad (1.3)$$

Where:

C_A^o : Initial concentration (mol/m³)

C_A : Concentration (mol/m³)

Q : Volumetric flow (m³/s)

S : Surface (m²)

k : Electrochemical reaction rate constant (m/s).

I : Current (A)

n : Number of electrons transferred in the reaction

F : Faraday constant 96500 C/mol

I_{lim} : Limiting current (A)

Moreover, the overall mass balance in the microreactor for a generic compound A involved in (bio) chemical and electrochemical reactions is presented:

$$F_A^o - F_A = dF_A + \frac{I}{n.F} - r_A \cdot dV \quad (1.4)$$

Developing the terms of the equation (1.4):

$$Q.C_A^o - Q.C_A = Q \cdot \frac{\partial C_A}{\partial x} \cdot dx + \frac{i.l}{nF} dx - r_A \cdot \pi \cdot R^2 dx \quad (1.5)$$

Defining the integral from 0 to a length L, the contribution of the electrochemical and (bio) chemical reaction can be clearly observed:

$$\int_{C_A^o}^{C_A} dC_A = -\frac{i.l}{\eta.F.Q} dx + \frac{r_A \cdot \pi \cdot R^2}{Q} dx \quad (1.6)$$

Electrochemical (Bio)chemical
reaction reaction

Where:

- F_A^o : Inlet molar flow (mol/s)
- F_A : Outlet molar flow (mol/s)
- r_A : Chemical reaction rate ($\text{mol} \cdot \text{s}^{-1} \cdot \text{m}^{-3}$)
- V : Volume (m^3)
- x : Distance (m)
- L : Distance at the outlet (m)
- i : Current (A)
- l : length (m)
- R : Radio (m)

Owing to the advantages of the use of the microreactors and the proven applicability to the regeneration of nicotinamide cofactors (NADH), an evaluation of the feasibility of the system for the regeneration of NAD^+ is proposed.

1.6 Engineering of the reaction media and enzymatic reactors

Biocatalysis in organic solvents is an area of interest since their convenient features compared to traditional application of enzymes in aqueous medium. Some of the advantages of the introduction of organic solvents are: increasing the solubility of

nonpolar substrates and products, shifting the thermodynamic equilibrium in favor of synthesis over hydrolysis, changes in the enantioselectivity of the reaction when one organic solvent is changed to another; reduction or elimination of unwanted water-dependent side reactions and elimination of microbial contamination in the reaction mixture (Dordick 1991; Carrea and Riva 2000; Castro and Knubovets 2003). However, not all these advantages are relevant to all the categories of organic-solvent reaction media and reactions, and of course disadvantages of using organic solvent are present. The main one is that most enzymes are denatured or highly inactivated in the presence of organic solvents (Ru, Dordick et al. 1999; Ogino and Ishikawa 2001).

Organic media biocatalysis can be performed in homogeneous or heterogeneous media. The first case includes a) cosolvent systems, water/ solvents mixture with mainly water and a relatively small amount of a water-miscible solvent and b) low water content systems consisting mainly in organic solvent. Heterogeneous media involve two-phase systems of a water-immiscible organic solvent and aqueous buffer.

In homogeneous systems there are not diffusional limitations for substrates and products. When cosolvents are used, substrate and product concentrations at the enzyme surface can be easily controlled in order to manipulate the product conversion rate and to prevent enzyme inhibition. In presence of organic solvents with low water, hydrophobic substrates and products are easily dissolved but enzymes can be inactivated.

In heterogeneous biocatalysis, organic solvents allow increasing the solubility of the substrate and/or products and the enzyme can remain in the aqueous phase without significant deactivation. Nevertheless, the main drawbacks are low and difficult to control reaction rates and the poor reproducibility at large scale.

Numerous attempts have been used to improve enzyme activity and stability in non-aqueous media, following strategies including: covalent attachment of the enzyme with amphipathic compounds (PEG, aldehydes and imidoesters) (DeSantis and Jones 1999; Ogino and Ishikawa 2001; Salleh, Basri et al. 2002); non-covalent interaction with lipids or surfactants (Kamiya, Inoue et al. 2000; Ogino and Ishikawa 2001); entrapment in water-in-oil microemulsions or reverse micelles (Pera, Baigori et al. 2003); immobilization on appropriate insoluble supports (synthetic polyhydroxylic matrices,

porous inorganic carriers, polymers and molecular sieves) (Persson, Wehtje et al. 2002; Yan, Li et al. 2002), etc.

Preparative reactions by HLADH immobilized have been performed on inorganic (Grunwald, Wirz et al. 1986; Van Elsacker, Lemiere et al. 1989; Parida, Datta et al. 1992) or organic systems (Drueckhammer, Sadozai et al. 1987; Lortie, Villaume et al. 1989; Van Elsacker, Lemiere et al. 1989; Bradshaw, Lalonde et al. 1992; Kawakami, Abe et al. 1992).

About the design of *enzymatic reactors*, batch stirred tank reactors (STR) and continuous ultrafiltration-membrane reactors (UFMR) are generally employed with soluble enzymes, while batch stirred tank reactors (STR), continuous stirred tank reactors (CSTR), packed-bed reactors (PBR) and fluidized bed reactors (FBR) are the main configuration of reactors for immobilized enzymes.

Both batch and continuous stirred tank reactors are the most used systems in aqueous reaction medium with soluble enzymes, due to their simplicity. A relevant advantage of the use of stirred tank reactors is that allows an easy control of temperature and pH. However, enzymes usually exhibit poor stability and are difficult to recover in such systems, leading to low productivity. Otherwise, the use of packed bed reactors permits the preservation and reuse of immobilized enzymes and they are frequently used due to their generally high efficiency and ease of operation. However, difficult control of temperature and pH, dead zones, compression of the bed, forming of preferential ways and external diffusion limitations are presented.

Fed-batch reactors constitute a useful modification of the batch reactors. This kind of configuration allows the dosage of the substrate in established periods of time, making possible to improve the selectivity by reducing side reactions, as well as allowing the production when the substrate has a low solubility in the reaction media.

Several examples for the use of batch reactors in reactions catalyzed by several ADHs have been reviewed (Devaux-Basseguy, Bergel et al. 1997). Therefore, batch reactors coupled with cofactor regeneration were studied for the reduction of ketones and aldehydes, aldehyde production, steroid functionalization, synthesis of amino acids and preparation of hydroxyl acids and alcohols. The fed-batch configuration has been

applied successfully as well to obtain propargylic alcohols and (S)-Benzyl- α -d₁ alcohol (Wong, Gordon et al. 1981; Schubert, Hummel et al. 2002).

1.7 Synthesis of aminopolyols

Aminopolyols are amino alcohols with multiple hydroxyl functional groups. They can be obtained by the aldol addition of dihydroxyacetone phosphate (DHAP) to amino aldehydes catalyzed by DHAP-dependent aldolases (Espelt, Parella et al. 2003; Suau, Alvaro et al. 2006) (e.g. Cbz-glycinal catalyzed by RhuA, figure 1.7.1).

Aminopolyols are precursors of iminocyclitols (polyhydroxy-N-heterocycles) which are potent inhibitors of glycosidases and glycosyltransferases (Compain and Martin 2001). They are therapeutic targets for the design of new antibiotics, as well as antimetastatic, antihyperglycemic or immunostimulatory agents (Wong, Halcomb et al. 1995; Stütz and Wiley 1999; Lillelund, Jensen et al. 2002).

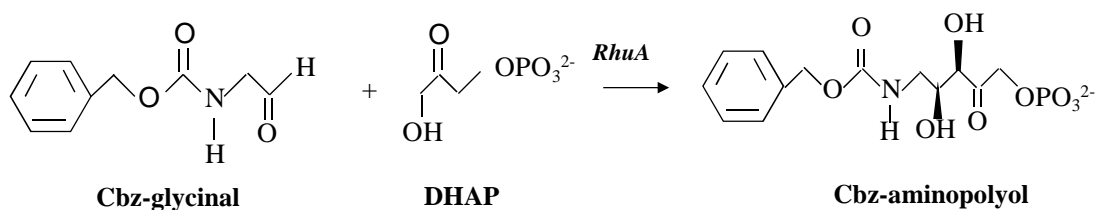


Figure 1.7.1 Aldol addition of DHAP to Cbz-amino aldehyde catalyzed by a DHAP dependent aldolase.

Iminocyclitols can be obtained from Cbz-aminopolyols by the removal of the phosphate group by acid phosphatase and following hydrogenation (Espelt, Parella et al. 2003) (figure 1.7.2).

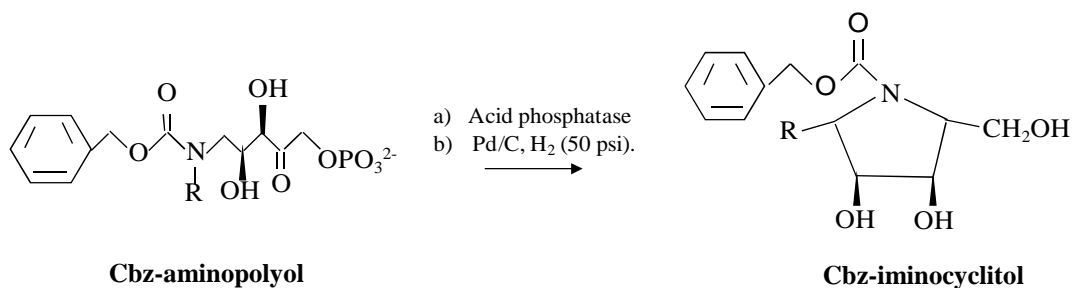


Figure 1.7.2 Obtention of iminocyclitols from aminopolyols.

The use of N-protecting groups as benzyloxycarbonyl (Cbz) or tertbutyloxycarbonyl (Boc) for amino aldehydes represents a complement for orthogonal protection, specifically when using the aldol adducts as chiral building blocks.

1.7.1 Aldolases

Aldolases are a specific group of lyases (aldehyde-lyases; EC 4.1.2) which catalyze stereoselective aldol additions of aldehydes and ketones (Asano, Nash et al. 2000; Compain and Martin 2001).

As indicated before, one interesting application of aldolases is the synthesis of iminocyclitols (Fechter, Stutz et al. 1999; Koeller and Wong 2000; Espelt, Parella et al. 2003).

Aldolases are classified according to their catalytic mechanism:

- *Class I aldolases*: exhibit a conserved lysine residue in the active site which forms a Schiff base intermediate with the donor compound to generate an enamine nucleophile.
- *Class II aldolases*: a divalent metal ion promotes the enolization of the donor substrate via Lewis acid complexation. The nucleophilic enamine or enolate then attacks the carbonyl carbon of the acceptor substrate forming the new C–C bond.

Furthermore, aldolases can be classified based on the donor substrate (Fessner 1998; López-Santín, Alvaro et al. 2008):

- *Dihydroxyacetone phosphate (DHAP)-dependent aldolases* catalyze the reversible asymmetric addition of DHAP to D-glyceraldehyde-3-phosphate (G3P) or L-lactaldehyde, leading to four complementary diastereomers. Four class II aldolases are included in this group: fructose-1,6-biphosphate aldolase (FruA; EC 4.1.2.13), fuculose-1-phosphate aldolase (FucA; EC 4.1.2.17), rhamnulose-1-phosphate aldolase (RhuA; EC 4.1.2.19) and tagatose-1,6-biphosphate aldolase (TagA; EC 4.1.2.40).
- *Pyruvate and phosphoenolpyruvate-dependent aldolases* catalyze the aldol addition between pyruvate or phosphoenolpyruvate (PEP) and different

aldehydes giving products with a new stereogenic center. N-acetylneuraminic acid aldolase (NeuA; EC 4.1.3.3) is the best known enzyme of this group.

- *Acetaldehyde dependent aldolases* catalyze the C-C bond formation between two aldehydes. This group only has one member, which is 2-deoxy-D-ribose 5-phosphate aldolase (DERA; EC 4.1.2.4). The donor is not only restricted to acetaldehyde; propanal, acetone and fluoroacetone are used as well.
- *Glycine dependent aldolases (PEP)* use pyridoxal-5-phosphate (PLP) as cofactor and catalyze the reversible formation of β -hydroxy- α -amino carbonic acid. The best studied enzymes of this group are threonine aldolases (TA; EC 4.1.2.5), which catalyze the reaction of threonine and glycine, and serine hydroxymethyltransferases (SHMT; EC 2.1.2.1).

1.7.1.1 DHAP-dependent aldolases

Dihydroxyacetone phosphate-dependent aldolases are very useful in the asymmetric synthesis of conventional, uncommon carbohydrates, and hydroxylated products. They catalyze the aldol addition of the DHAP donor substrate to a variety of non-natural aldehyde acceptors. Usually, the stereoselectivity is controlled by the enzyme, regardless of the structure and stereochemistry of the substrate acceptor (Wong, Halcomb et al. 1995; Wong, Halcomb et al. 1995). Particularly, DHAP aldolases catalyze the obtention of aminopolyols, precursors of iminocyclitols as mentioned above.

The mechanism of DHAP-dependent aldolases is an ordered two-substrate reaction (Dreyer and Schulz 1996). DHAP binds the zinc ion with its hydroxyl and keto oxygen atoms, conducting to an enediolate intermediate, before the entrance of the acceptor aldehyde. FucA and RhuA are homotetramers with a Zn^{2+} atom in each subunit and the formed enediolate is linked to the carbonyl group of the acceptor aldehyde by either the *si* face (FucA) or the *re* face (RhuA). Thus, aldol addition products with 3R, 4R configuration are obtained in the case of FucA, and 3R, 4S configuration in the case of RhuA. Moreover, enediolate can be decomposed into two final reaction products: inorganic phosphate and a small amount of methylglyoxal (Richard 1993).

Nevertheless, DHAP is usually unstable in reaction conditions (Fessner and Walter 1997). In aqueous medium, DHAP suffers decomposition and isomeration. DHAP decomposition is irreversible; it follows a first order kinetics in a pH range between 7-9 (Phillips and Thornalley 1993), and becomes almost negligible at temperature lower than 4°C. The decomposition involves the same enediolate intermediate as the aldol addition, and the presence of class II aldolases also catalyzes the non-desired DHAP degradation (Suau, Alvaro et al. 2006).

Rhamnulose-1-phosphate aldolase (RhuA; E.C. 4.1.2.19) is a class II Zn^{2+} dependent aldolase and cleaves L-rhamnulose-1-phosphate (R1P) into L-lactaldehyde and dihydroxyacetone phosphate (DHAP) (Figure 1.7.3). The reverse direction consists on C-C bond formation, creating two new chiral centers, which is an attractive feature for the enzymatic synthesis of novel compounds (Bednarski, Simon et al. 1989; Fessner, Sinerius et al. 1991; Wong, Halcomb et al. 1995; Espelt, Parella et al. 2003).

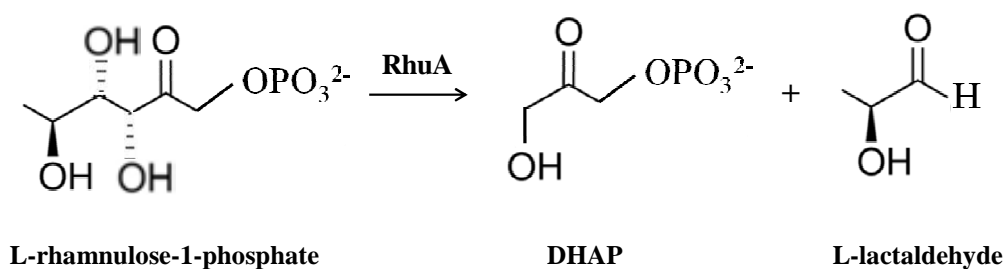


Figure 1.7.3 Reaction of L-rhamnulose-1-phosphate decomposition catalyzed by RhuA.

RhuA is a homotetramer, and each subunit has 274 amino acids with a polypeptide mass of 30145 Da. The N-terminal domain extends like an antenna into the solvent whereas the C-terminal domain forms most of the tetramer interface and thus the core of the enzyme. Moreover, the C-domain provides the three histidines fixing the Zn^{2+} ion at the active center. During catalysis, DHAP backed up by the crucial base Glu117 and bound to the N-domain contacts the Zn^{2+} ion in the C-domain and also the aldehyde (pink), which is most likely bound to the C-domain (blue and transparent green) (Joerger, Mueller-Dieckmann et al. 2000; Kroemer, Merkel et al. 2003) as illustrated in Figure 1.7.4.

One promising synthetic reaction catalyzed by these enzymes is the aldol addition starting from N-protected α -amino aldehydes (Jurczak and Golebiowski 1989) as Cbz-

aminoaldehydes (e.g. (S)-Cbz-alaninal) to form aminopolyols (Ardao, Alvaro et al. 2011) . The protected α -amino aldehydes can be synthesized chemically (Ardao, Benaiges et al. 2006; Calveras, Bujons et al. 2006; Suau, Álvaro et al. 2008; Calveras, Egido-Gabás et al. 2009). However they meet several difficulties such as low selectivity, lack of control and predictability of the obtained product structure and high cost of oxidizing agents that are often environmentally unsuitable. Cbz-alaninal was obtained efficiently by oxidation of Cbz-ethanolamine using oxidoreductases (CPO) (Pešić, López et al. 2012).

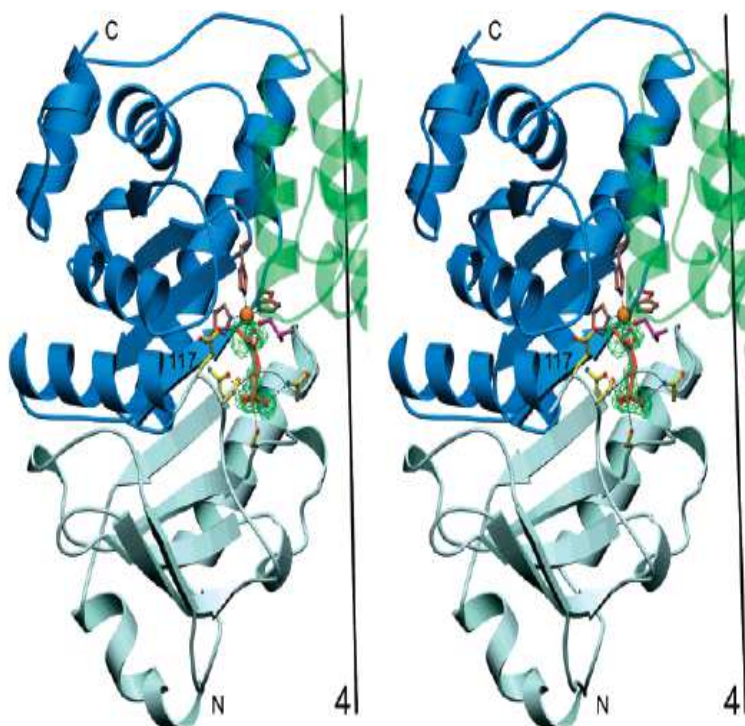


Figure 1.7.4 Structure of the C₄-symmetric RhuA with its molecular fourfold axis (Grueninger and Schulz 2008).

Cbz-amino aldehydes can be also obtained by oxidation of commercial Cbz-amino alcohols using horse liver alcohol dehydrogenase (e.g Cbz-ethanolamine, figure 1.7.5). The reaction had to be carried out in the presence of semicarbazide to trap the produced aldehyde (Andersson and Wolfenden 1982). The resulting α -amino aldehyde semicarbazone was subsequently hydrolyzed at pH 1 in the presence of formaldehyde, regenerating the aldehyde.

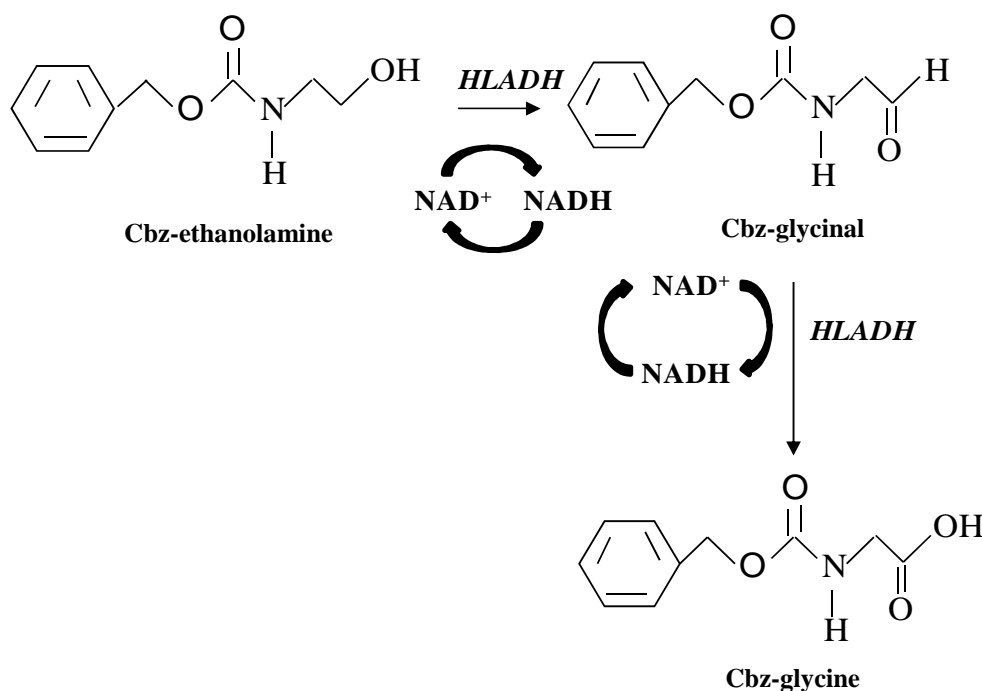


Figure 1.7.5 Oxidation of Cbz-amino alcohols by horse liver alcohol dehydrogenase.

1.8 Oxidation of β -amino alcohols to β -amino acids

β -amino acids are 1,3-difunctionalized compounds that acquire significance due to their biologically important properties, their occurrence in natural products, and the use as valuable intermediates in the design and construction of novel biologically and medicinally important molecules (Cole 1994; Juaristi 1997; Abdel-Magid, Cohen et al. 1999; Juaristi and Lopez-Ruiz 1999).

β -amino acids have been found as components in a variety of natural products and exhibit pharmacological properties: for example, emeriamine has hypoglycemic and anti-etogenic activities in rats (Kanamaru, Shinagawa et al. 1985; Shinagawa, Kanamaru et al. 1987) and cispentacin is an antifungal compound (Juaristi 1997). Functionalized β -amino acids are key components of a variety of bioactive molecules such as taxol, one of the most active antitumor agents which contain a α -hydroxy β -amino acid side chain (Winkler and Subrahmanyam 1992; Nicolaou and Guy 1995). Unsaturated β -amino acid ADDA is present in the antibiotics cyanovinfen RR, nodularin, as well as microcystin LR (Namikoshi, Rinehart et al. 1989). β -Tyrosine, a β -aryl- β -amino acid, is present in jasplakinolide which is a sponge metabolite with potent

insecticidal, antifungal and anthelmintic properties (Crews, Manes et al. 1986). Other representative examples include cryptophycin, a potent tumor-selective depsipeptide (Shih, Gossett et al. 1999), and the aminopeptidase inhibitors bestatin and amastatin (Roers and Verdine 2001).

Furthermore, β -amino acids mimic the secondary structure of natural peptide sequences (peptidomimetics). The most widely studied peptidomimetics are oligomers of β -amino acids, which have been shown to adopt a range of stable secondary structures such as α -helices, β -turns and β -sheets. These characteristics facilitate interactions with receptors and enzymes and prevent peptidase degradation (Cheng, Gellman et al. 2001; Steer, Lew et al. 2002; Seebach, Beck et al. 2004; Seebach, Kimmerlin et al. 2004; English, Chumanov et al. 2006). Also, they have utility as chiral auxiliaries, chiral ligands, chiral building blocks and intermediates in the synthesis of β -lactams that show potent antibiotic activity (Hart and Ha 1989; Palomo, Aizpurua et al. 1991).

β -amino acids can be obtained using different synthetic strategies, such as the chiral pool approach, enzymatic resolutions, diastereoselective reactions with chiral auxiliaries and catalytic asymmetric synthesis (Cole 1994; Juaristi 1997; Abdel-Magid, Cohen et al. 1999; Juaristi and Lopez-Ruiz 1999).

The use of chemoenzymatic methods for the preparation of enantiomerically pure β -amino acids increased in the latest years (Sih 1997; Soloshonok 1997). Based on the lipase-catalyzed kinetic resolution several β -amino acids were synthesized as: alicyclic β -aminocarboxylic acid from 2,2,2-trifluoroethyl esters (Csomós, Kanerva et al. 1996; Kanerva, Csomós et al. 1996), both enantiomers of cispentacin from carbinol (Theil and Ballschuh 1996; Sánchez, Rebolledo et al. 1997), (S)-3-aminobutyric acid and taxol's side chain (Sánchez, Rebolledo et al. 1997; Lee and Kim 1998).

The feasibility of the synthesis of Cbz- β -amino acids from Cbz- β -amino alcohols by horse liver alcohol dehydrogenase (e.g. Cbz- β -amino propanol, figure 1.8) is interesting due to the exceptional oxidative activity of this enzyme. As mentioned above, HLADH catalyzes the reversible interconversion of a wide variety of aldehyde/alcohol substrate pairs and the dimerization and oxidation of aldehydes (Abeles and Lee 1960; Dalziel and Dickinson 1965; Hinson and Neal 1975). In the other hand, it has been proven that HLADH recognizes Cbz- α -amino alcohols (Andersson and Wolfenden 1982).

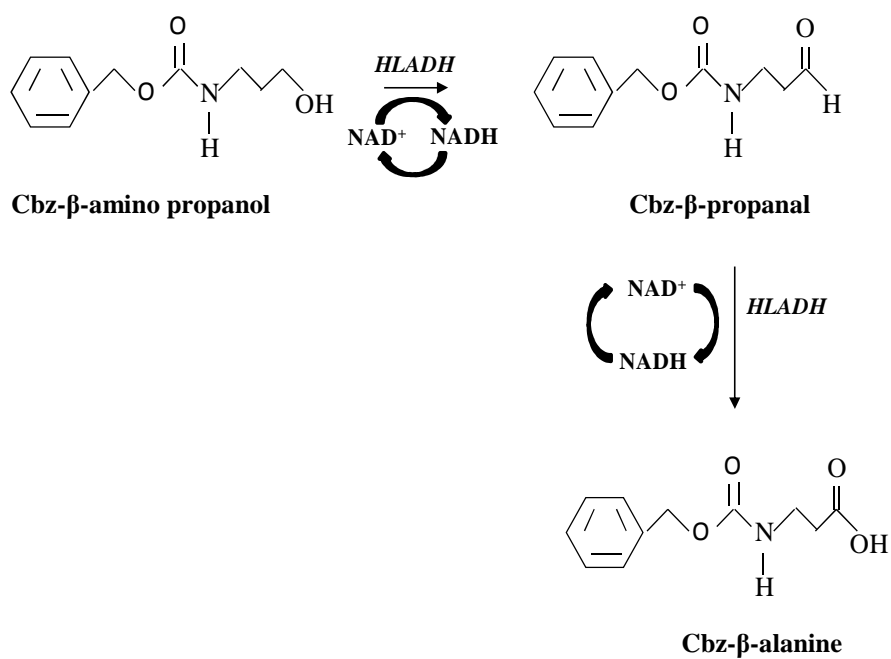


Figure 1.8.1 Oxidation of Cbz-β-amino alcohols by horse liver alcohol dehydrogenase.

CHAPTER 2
OBJECTIVES

2. OBJECTIVES

The general objective of this thesis is the study of the oxidative capacity of the enzyme alcohol dehydrogenase from horse liver (HLADH) using amino alcohols as substrates, for the synthesis of: (i) β -aminoacids and (ii) α -amino aldehydes with further production of α -aminopolyols by their aldol addition with dihydroxyacetone phosphate (DHAP).

This thesis as part of the projects “Integrated biotechnological processes for the obtention of bioactive compounds” (CTQ2008-00578/PPQ) and “Novel alternatives for microbial production of enzymes and multienzymatic stereoselective synthesis” (CTQ2011-28398-C02-01), financed by the Spanish Ministry of Science and Innovation, involved specific objectives, presented as follows:

- Development of the methodology for the synthesis of the α -amino aldehyde Cbz-glycinal by HLADH catalyzed oxidation of the α -amino alcohol Cbz-ethanolamine.
- Coupling the reactions of oxidation of Cbz-ethanolamine by HLADH and aldol addition of the Cbz-glycinal formed with dihydroxyacetone phosphate (DHAP) catalyzed by rhamnulose-1-phosphate aldolase (RhuA) for the production of the corresponding Cbz-aminopolyols.
- Determination of the feasibility of HLADH to recognize β -amino alcohols (Cbz- β -amino propanol) as substrates for the synthesis of β -aminoacids (Cbz- β -alanine) and establishment of the operational conditions to improve their productivity.
- Evaluation of the most appropriate regeneration system for the nicotinamide adenine dinucleotide (NAD^+) cofactor to be coupled with the oxidation of Cbz-ethanolamine and Cbz- β -amino propanol as a strategy for the enhancement of the process productivity and cost reduction.

CHAPTER 3
GENERAL MATERIALS AND
METHODS

3. GENERAL MATERIALS AND METHODS

3.1 Materials

Horse liver alcohol dehydrogenase was obtained from a horse liver, which was purchased from a horse slaughterhouse, and also it was acquired as an expressed enzyme in *E.coli* from Evocatal (Düsseldorf, DE). Rhamnulose-1-phosphate aldolase (RhuA) was expressed in *E. coli* as a fusion protein containing a hexa-histidine tag (Vidal, Durany et al. 2003). Yeast alcohol dehydrogenase (YADH) was expressed in *E.coli* and it was provided by the Faculty of Chemistry, University of Belgrade, Serbia. Bis(cyclohexylamine) rhamnulose-1-phosphate was synthesized using a modification of the method detailed by Fessner (Fessner, Schneider et al. 1993). Cbz-ethanolamine, Cbz-glycine, Cbz- β -aminopropanol, Cbz- β -alanine, Cbz- β -alaninal, NAD^+ , semicarbazide hydrochloride, semicarbazide 6% wt. on silica gel and dihydroxyacetone phosphate hemimagnesium salt hydrate were purchased from Sigma Aldrich (St. Louis, MO, USA). NADH was obtained from either Sigma Aldrich (St. Louis, MO, USA) or Acros Organics (Morris Plains, NJ, USA). Cbz-glycinal was purchased from Sunshine ChemLab, Inc (Downingtown, PA, USA). Fast flow chelating sepharose was purchased from Amersham Biosciences (Uppsala, Sweden). 10% crosslinked agarose beads (10 BCL) were purchased from Iberagar (Coima, Portugal). All other chemicals were obtained as the highest grade commercially available.

3.2 Obtention of enzymes

3.2.1 Purification of Horse liver alcohol dehydrogenase

Horse liver alcohol dehydrogenase (HLADH) was extracted from horse liver according to a modification of the method detailed by Dalziel (Dalziel 1961).

Horse liver (1 kg) was soaked with 2 L of water for 2 h at room temperature to extract proteins. The mixture was centrifuged (Beckman J2-21, 10000 rpm, 1 h, 4°C) and the precipitate was discarded. The supernatant extract was mixed with 300 g/L $\text{NH}_4(\text{SO}_4)_2$ on an ice bath at pH 6.5 for 2 h to precipitate catalase and ferritin, which were removed by centrifugation (Beckman J2-21, 10000 rpm, 1 h, 4°C). The red clear supernatant

obtained was mixed with 110 g/L $\text{NH}_4(\text{SO}_4)_2$ on an ice bath at pH 6.5 for 2 h. The resulting precipitate, containing the enzyme was separated as above.

The precipitate, containing HLADH, was resuspended in a minimum volume of cold 50 mM sodium phosphate buffer, pH 7.0. More buffer was added gradually under cold shaking until a crystalline precipitate was formed (haemoglobin and aldolase). The suspension was centrifuged (Beckman J2-21, 1000 rpm, 1 h, 4°C) and the precipitate was discarded. Further centrifuging was sometimes necessary to obtain a clear red solution.

The solution was heated at 52°C for 15 min, cooled and centrifuged (Beckman J2-21, 10000 rpm, 1 h, 4°C). The precipitate of denatured protein was washed with buffer, and the mixture of supernatant and washings were dialysed against 50 mM sodium phosphate buffer pH 7.0 (3 x 2 L) and then against 50 mM sodium phosphate buffer pH 6.0 (2 x 2 L). The partially purified HLADH was stored at -20°C.

3.2.2 Purification of rhamnulose-1-phosphate aldolase (RhuA) on immobilized metal-chelate affinity chromatography (IMAC)

The affinity between imidazole rings from histidine residues and the ions immobilized on the chromatographic resin followed the procedure developed by Ardao (Ardao 2009) for the purification of *E. coli* recombinant RhuA containing hexa-histidine tag.

First, 0.84 L of the fermentation broth containing a fusion protein expressed in *E. coli* according to Ruiz (Ruiz, Pinsach et al. 2009) was centrifuged (Beckman J2-21, 9700 rpm, 35 min, 4°C), and the obtained supernatant (0.74 L) was discarded. The pellet was resuspended and homogenized in lysis buffer (50 mM sodium phosphate, 300 mM NaCl, 20 mM imidazole, pH 8.0) to reach the cell density OD=80. Resuspended cells were disrupted by one-shot high pressure disruption (Constant Systems LTD One Shot) (21kPa, 4°C) and this process was repeated until the value of cell density was less than 10% of the initial one. The insoluble debris was removed by centrifugation (Beckman J2-21, 9700 rpm, 35 min, 4°C), and supernatant was loaded to a chromatographic column (Amersham Biosciences XK 50/20) containing 400 mL of high density cobalt-chelate affinity resin, Co-IDA (GE Healthcare 17-0575-02). The loading was performed

using a FPLC system (fast protein liquid chromatography) which consisted of peristaltic pumps (Pharmacia LKB Pump P-500), an UV detector adjusted to 280 nm (Pharmacia Monitor UVM) and fractions collector (Amersham Biosciences Frac-200). After the loading, the column was washed repeatedly with the lysis buffer, in order to eliminate other proteins. Then, the elution of RhuA was performed using elution buffer (50 mM sodium phosphate, 300 mM NaCl, 300 mM imidazole, pH 8.0). The fractions containing proteins were tested for RhuA activity, and those showing activity were precipitated with $(\text{NH}_4)_2\text{SO}_4$ at the concentration of 0.4 g/mL, and centrifuged (Beckman J2-21, 9700 rpm, 35 min, and 4°C). After removing the supernatant, the precipitated enzyme was resuspended in 0.4 g/mL $(\text{NH}_4)_2\text{SO}_4$. The enzyme suspension was stored at 4°C.

Previously to use, the metal-chelate support was charged with the Co^{2+} metal ions. For that, the resin was packed into the column, washed with 3 volumes of Milli-Q H_2O and then 3 volumes of 0.2 M CoCl_2 pH 4.7, which passed through the column at a flow rate of 1 mL/min. Finally, the column was washed with 5 volumes of Milli-Q H_2O , equilibrated with 20% (v/v) ethanol and stored at 4°C.

3.3 Synthesis of L-rhamnulose-1-phosphate

L-rhamnulose-1-phosphate was synthesized as a cyclohexylamine salt by aldol addition of dihydroxyacetone phosphate (DHAP) and L-lactaldehyde, enzymatically catalyzed by rhamnulose-1-phosphate aldolase (RhuA) (Figure 3.3.1) and further neutralization with cyclohexylamine, according to the reported procedure (Fessner, Schneider et al. 1993) modified by Ardao (Ardao 2009).

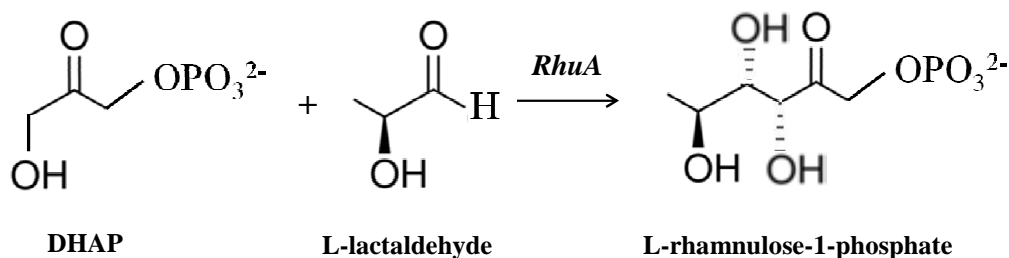


Figure 3.3.1 Enzymatic synthesis scheme of L-rhamnulose-1-phosphate catalyzed by rhamnulose-1-phosphate aldolase (RhuA).

For the obtention of L-rhamnulose-1-phosphate, L-lactaldehyde was synthesized from D-threonine and ninhydrin (Figure 3.3.2) according to the reported method (Zagalak, Frey et al. 1966) and modified by Ardao (Ardao 2009).

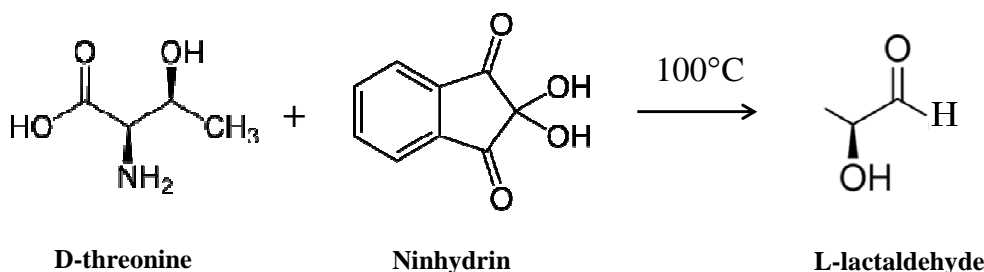


Figure 3.3.2 Reaction of oxidative decarboxylation of D-threonine by ninhydrin for the synthesis of L-lactaldehyde.

First, 25 mmol of D-threonine and 51.1 mmol of ninhydrin were dissolved in 400 mL of 0.05 M sodium citrate buffer at pH 5.4 and incubated in a glycerol bath at 100°C using vigorous magnetic stirring. A condenser coil was applied to retain the NH₃ liberated during the reaction. After 2 h of reaction, the mixture was left to cool down and then vacuum filtered (10-16 μm).

The reaction mixture was purified by ion exchange chromatography, in order to remove the purple side product of the reaction of ninhydrin with NH₃. First, an anionic exchange resin (Dowex 1x8, HCO₃⁻ form) was added until the pH of the reaction mixture was adjusted to 6.5 and was left on vigorous magnetic stirring for approximately 3 h. Then, the resin was separated by filtration and the reaction mixture was further treated with a cationic exchange resin (Dowex 50x8, H⁺ form), that was added in the amount required to obtain pH 4.0. After 1 h of vigorous stirring, the resin was separated by filtration and the liquid mixture was concentrated by vacuum to obtain the volume of 50-100 mL. The treatment with the ion exchange resins had to be repeated until complete elimination of the purple color. Finally, the solution of L-lactaldehyde was concentrated by vacuum to a volume of 25 mL, and was stored at 4°C, pH 4.0 and inert atmosphere.

The concentration of L-lactaldehyde was determined by an indirect method based on the reduction of L-lactaldehyde in the presence of KBH₄ and the formed 1,2-propanediol

was quantified using HPLC according to the methodology described in the section 3.4.5.1.

Then, 10 mmol of DHAP hemimagnesium salt hydrate and synthesized L-lactaldehyde were dissolved in 250 mL of Milli-Q H₂O and the pH was adjusted to 7.5 with KOH and 10 U of RhuA were added to react at 35°C with mild magnetic stirring. Samples were withdrawn periodically and incubated for 1 minute at 100°C in order to stop the enzymatic reaction. DHAP, L-lactaldehyde and L-rhamnulose-1-phosphate were quantified as specified in the sections 3.4.4 and 3.4.5.1 respectively. When no further consumption was detected, the reaction was stopped by incubating the reaction mixture at the temperature of 100°C.

L-rhamnulose-1-phosphate was purified by ion exchange chromatography. The reaction mixture was filtrated through carbon coal to remove the possible organic impurities. The filtrated reaction mixture was loaded to a chromatography column containing 140 mL of anion exchange resin (Dowex 1x8, HCO₃⁻ form), and then washed with 2 volumes of Milli-Q H₂O. Fractions of 50 mL of the eluted liquid were collected and the content of L-lactaldehyde and L-rhamnulose-1-phosphate were measured (section 3.4.5.1). The L-rhamnulose-1-phosphate retained on the resin was eluted with a solution of 0.2 M NaHCO₃. Fractions of 50 mL were collected during the elution and analyzed by HPLC (section 3.4.5.1) to determine the content of L-rhamnulose-1-phosphate based on the L-lactaldehyde concentration.

The column was washed with a solution of 0.7 M NaHCO₃ in order to recover the sugar that could have possibly remained on the column. Finally, the fractions containing L-rhamnulose-1-phosphate were lyophilized, dissolved in 100 mL of Milli-Q H₂O, treated with cationic exchange resin (Dowex 50x8, H⁺ form) and maintained on vigorous magnetic stirring to eliminate remaining bicarbonate. Once no CO₂ release was observed, the solution was vacuum filtered (10-16 µm) to separate the resin, then neutralized with cyclohexylamine and lyophilized. The cyclohexylamine salt was stored at -20°C under inert atmosphere.

3.4 Analytical methods

3.4.1 Horse liver alcohol dehydrogenase enzymatic activity assay

Horse liver alcohol dehydrogenase activity was determined spectrophotometrically in an UV-Visible Spectrophotometer Cary 50 (Varian, Palo Alto, CA, USA) using quartz cuvettes by monitoring the decrease of the NADH concentration at 340 nm ($\epsilon_{340}=6220 \text{ M}^{-1}\text{cm}^{-1}$) when benzaldehyde was reduced to benzyl alcohol, following the protocol established in-house by the manufacturer Evocatal (Düsseldorf, DE) (Figure 3.4.1).

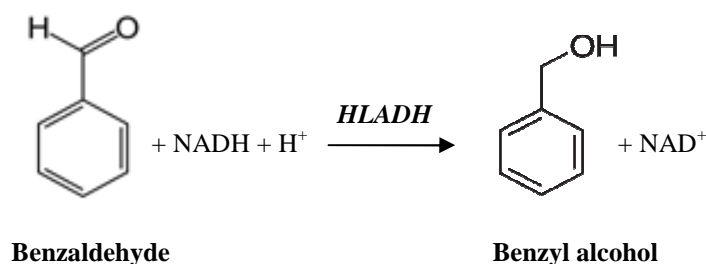


Figure 3.4.1 Reaction scheme for the determination of the enzymatic activity of horse liver alcohol dehydrogenase (HLADH).

0.05 mL of the sample was added to the assay mixture which contained 50 mM trietanolamine buffer pH 7, 3 mM benzaldehyde and 0.25 mM NADH (previous incubation at 30°C) in a final volume of 1 mL. The reaction was carried out at 30°C for one minute. One unit of HLADH activity is defined as the amount of enzyme that converts 1 μmol of NADH per minute.

3.4.2 RhuA enzymatic activity assay

The activity of RhuA was determined spectrophotometrically in an UV-Visible Spectrophotometer Cary 50 (Varian, Palo Alto, CA, USA) using a coupled enzymatic assay according to the procedure of Chiu y Feingold (Chiu and Feingold 1969), adapted by Vidal (Vidal 2006). In the first step, rhamnulose 1-phosphate is cleaved to L-lactaldehyde and DHAP catalyzed by RhuA; in the second step, DHAP is reduced using rabbit muscle glycerol 3-phosphate dehydrogenase (α -GDH) and NADH (Figure 3.4.2).

The activity was measured by following the decrease of the absorbance at 340 nm caused by NADH consumption ($\epsilon_{340 \text{ nm}}=6220 \text{ M}^{-1}\text{cm}^{-1}$)

The second reaction in the sequence was performed with high GDH enzymatic activity in order to not limit the global reaction rate. Therefore, the observed reaction rate corresponds to the rate of DHAP formation catalyzed by RhuA.

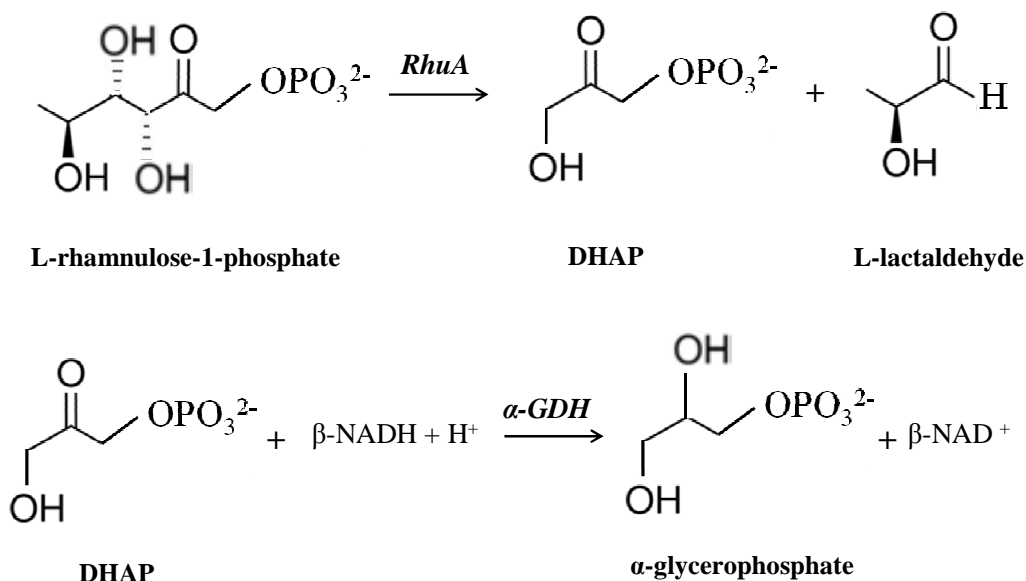


Figure 3.4.2 Reaction scheme for the determination of the enzymatic activity of rhamnulose-1-phosphate aldolase (RhuA).

0.01 mL of the sample was added to the assay mixture that contained 50 mM TrisHCl buffer pH 7.5, 0.15 mM NADH, 2 mM bis (cyclohexylamine) rhamnulose 1-phosphate and 2.5 U/mL GDH on a final volume of 1 mL. The absorbance was measured at 25°C at a wavelength of 340 nm.

One unit of RhuA activity is defined as the amount of enzyme required to convert 1 μmol of rhamnulose 1-phosphate to DHAP per minute at 25°C and pH 7.5.

3.4.3 Determination of protein concentration

The total protein content was determined using the well-known Bradford colorimetric method (Bradford 1976) modified by Pierce Biotechnology, Inc (Rockford, IL, USA).

The reagent Coomassie[®] dye binds the protein in an acidic medium and immediate shift in the absorption maximum occurs from 465 nm to 595 nm with a concomitant color change from brown to blue.

To determine the protein concentration, 30 μ L of the sample was added to 1.5 mL of Coomassie[®] previously stabilized at room temperature and the resulting solution was well mixed. After 10 min incubation the absorbance was measured at 595 nm. Protein concentration was estimated employing a concentration-absorbance calibration curve, using bovine serum albumin (BSA) as standard.

3.4.4 DHAP concentration assay

Dihydroxyacetone phosphate concentration was determined spectrophotometrically in an UV-Visible Spectrophotometer Cary 50 (Varian).

DHAP is reduced using rabbit muscle glycerol 3-phosphate dehydrogenase (GDH) and reduced nicotine adenine dinucleotide (NADH). 0.01 mL of the DHAP sample was added in a 1 mL quartz cuvette that contained the assay mixture composed of 0.2 mM NADH in 100 mM Tris HCl buffer pH 7.5 and maintained at 25°C. The assay was initiated upon addition of α -GDH with final activity of 0.5 U/mL. DHAP concentration in the sample was measured by the decrease of NADH absorbance at 340 nm ($\epsilon_{340\text{nm}}=6220\text{ M}^{-1}\text{cm}^{-1}$) before GDH addition.

3.4.5 Quantification of substrates and products

3.4.5.1 Concentration of L-lactaldehyde and L-rhamnulose-1-phosphate

The qualitative determination of L-lactaldehyde and L-rhamnulose-1-phosphate was performed by using an analytical HPLC Dionex UltiMate 3000 with Waters 2410 IR detector employing a reversed-phase column X Bridge C18, 5 μ m, 4.6x250 mm from Waters (Wexford, Ireland) at 30°C. The mobile phase consisted of 5 mM H₂SO₄ in Milli-Q H₂O, which was pumped at a flow rate of 0.6 mL/min.

For the quantification of L-lactaldehyde, a reduction was carried out by adding the stoichiometric quantity of KBH₄, considering the yield of the reaction of synthesis to be

100% to 2 mL of the reaction sample. The mixture was incubated at room temperature at magnetic stirring for 3 h. 1,2-propanediol was quantified using an analytical HPLC Dionex UltiMate 3000 with Waters 2410 IR detector under the same conditions mentioned above, from peak areas by the external standard method based on a prior calibration with samples of known concentration. The result corresponded to the concentration of L-lactaldehyde initially present in the sample.

3.4.5.2 Concentration of carboxybenzyl (Cbz) compounds

The concentration of the Cbz compounds, substrates: Cbz-ethanolamine and Cbz- β -amino propanol; products: Cbz-glycinal, Cbz-glycine, Cbz-aminopolyol, Cbz- β -amino propanal and Cbz- β -alanine were estimated by an analytical HPLC Dionex Ultimate 3000 coupled with a Variable Wavelength Ultimate 3000 Detector (Sunnyvale, USA), equipped with a reversed-phase column X Bridge C18, 5 μ m, 4.6 x 250 mm Waters (Wexford, Ireland) at 30°C. The solvent system consisted of solvent A, composed of 0.1% (v/v) trifluoroacetic acid (TFA) in H₂O, and solvent B, composed of 0.095% (v/v) trifluoroacetic acid (TFA) in H₂O:acetonitrile (1:4). The samples were eluted at a flow rate of 1 mL/min using a gradient from 20 to 36% B for 25 min. Samples of 30 μ L were injected, and peaks were detected at 200 nm. The compounds were quantified from peak areas by the external standard method based on a prior calibration with samples of known concentration.

CHAPTER 4

OXIDATION OF CBZ-AMINOALCOHOLS

CATALYZED BY HORSE LIVER ALCOHOL

DEHYDROGENASE

POSTER (Chapter 4 and 5):

Milja Pešić, Rossmery A. Rodríguez Hinestroza, Marta Enrich, M. Dolors Benaiges, Carmen López, Gregorio Álvaro, Josep López-Santín. *“One-pot enzymatic oxidation and aldol addition for the synthesis of aminopolyols from aminoalcohols: peroxidase vs. alcohol dehydrogenase approaches”*. BIOTRANS, October (2011). Sicily, Italy.

4. OXIDATION OF CBZ-AMINO ALCOHOLS CATALYZED BY HORSE LIVER ALCOHOL DEHYDROGENASE

4.1 Introduction

Horse liver alcohol dehydrogenase catalyzes the oxidation of α -amino alcohols with non polar side chains as reported by Andersson and Wolfenden (Andersson and Wolfenden 1982). The interest of the present work is their oxidation to α -amino aldehydes for a further aldol addition to dihydroxyacetone phosphate (DHAP) catalyzed by aldolases to obtain aminopolyols. Aminopolyols are precursors of iminocyclitols which exhibit biological activity and therapeutic properties as inhibitors of glycosidases and glycosyltransferases (Compain and Martin 2001), targets for the design of new antibiotic, antimetastatic, antihyperglycemic or immunostimulatory agents as pointed out in section 1.7 (Wong, Halcomb et al. 1995; Stütz and Wiley 1999; Lillelund, Jensen et al. 2002).

The oxidation of Cbz-ethanolamine catalyzed by HLADH to obtain Cbz-glycinal was proposed (figure 4.1.1). The main limitation of this study is that the Cbz-glycinal rendered to the acid Cbz-glycine, because of the dismutation and/or oxidation of aldehydes by HLADH (Abeles and Lee 1960; Dalziel and Dickinson 1965; Hinson and Neal 1975).

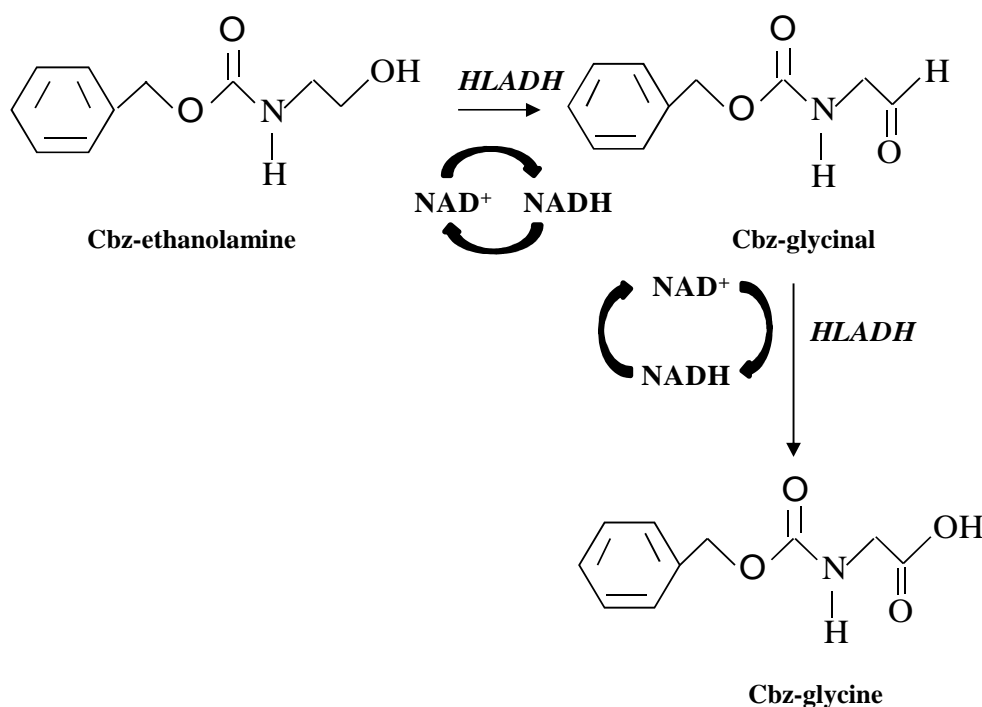


Figure 4.1.1 Oxidation of Cbz-ethanolamine by horse liver alcohol dehydrogenase.

Based on this fact the presence of an aldehyde trapping agent could be necessary to avoid the oxidation to the acid. Semicarbazide hydrochloride has been used (Andersson and Wolfenden 1982) since it forms a Schiff base with the Cbz-aminoaldehyde obtained (Cbz-glycinal) as illustrated in figure 4.1.2. This compound, an α -amino aldehyde semicarbazone (Cbz-glycinal semicarbazone) can be hydrolyzed at pH 1.0 in order to dissociate the Schiff base, the presence of an aldehyde in excess as formaldehyde is necessary to entrap the semicarbazide, regenerating the Cbz-glycinal and avoiding a further formation of the Schiff base of the semicarbazide and the Cbz-glycinal at pH 8.7.

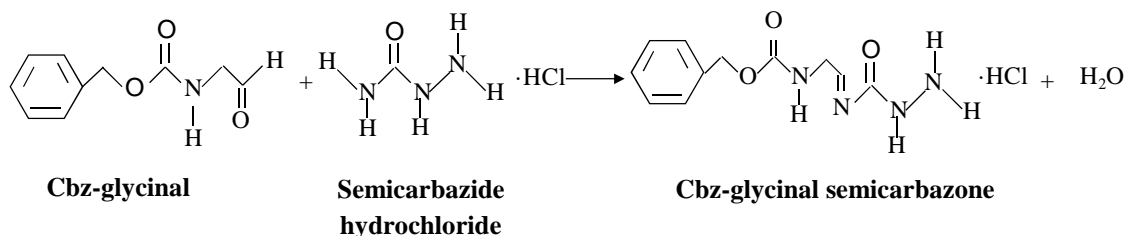


Figure 4.1.2 Schiff base formed by semicarbazide hydrochloride and Cbz-glycinal.

Besides, the study of the feasibility to obtain Cbz-glycinal from the Cbz-ethanolamine oxidation by HLADH without semicarbazide hydrochloride was proposed. This was carried out at several conditions, including an evaluation of reaction medium engineering and the use of amino supports (MANA-agarose) as an alternative to trap the Cbz-glycinal.

4.2 Methods

4.2.1 Comparison of different types of ADH and feasibility of the oxidation of Cbz-ethanolamine

Alcohol dehydrogenases from several origins, as yeast (YADH) and horse liver (HLADH) were studied. In addition, two kinds of HLADH were employed, an in house partially purified enzymatic solution from a horse liver according to section 3.2.1, and a commercial enzyme expressed in *E.coli*.

Enzymatic activity assays were performed as indicated in section 3.4.1, and protein concentration was determined as described in section 3.4.3. Specific enzymatic activity was calculated as the enzymatic activity with respect to the protein concentration per mg of protein.

The kinetic parameters of the Cbz-ethanolamine oxidation catalyzed by ADHs were determined according to Michaelis-Menten kinetics.



$$r = \frac{k_{cat} \cdot [E]_0 \cdot [S]}{K_M + [S]} \quad (4.2)$$

With:

$$r_{max} = k_{cat} \cdot [E]_0 \quad (4.3)$$

The Michaelis-Menten equation (4.2) can be rearranged to give convenient graphical representations as the proposed by Lineweaver and Burk (Lineweaver and Burk 1934) (equation 4.4). Thereby, a plot of $1/r$ against $1/[S]$ gives a straight line of slope K_M/r_{max} and with intercepts on the x and y axes of $-1/K_M$ and $1/r_{max}$ respectively.

$$\frac{1}{r} = \frac{K_M}{[S]} \cdot \frac{1}{r_{max}} + \frac{1}{r_{max}} \quad (4.4)$$

These kinetic parameters were determined performing the oxidation of Cbz-ethanolamine. Therefore, 5 mM Cbz-ethanolamine and 5 mM NAD⁺ were dissolved in 50 mM sodium pyrophosphate buffer pH 8.7 at room temperature. The reaction was initiated when ADH was added to the medium. The final concentrations of ADH were 20 U/mL HLADH in house (UAB), 1.44 U/mL commercial HLADH and 0.042 U/mL YADH. These values were the highest activities obtained limited by the enzyme availability.

The course of the reactions was continuously monitored by measuring the concentration of reactants and products by HPLC, following the method presented in section 3.4.5.2 and reaction rate was calculated as the slope of concentration vs. time at different times.

4.2.2 Oxidation of Cbz-ethanolamine catalyzed by HLADH using semicarbazide hydrochloride

Oxidation of Cbz-ethanolamine by HLADH using semicarbazide hydrochloride as trapping agent was performed by dissolving 5 or 20 mM Cbz-ethanolamine in 50 mM sodium pyrophosphate buffer pH 8.7. Then, 5 or 20 mM NAD⁺ and semicarbazide hydrochloride within the range of 150-600 mM were dissolved, and the pH was readjusted to 8.7. The reaction was initiated when HLADH was added to the reaction medium to reach a final concentration of 16-80 U/mL. The reaction was performed at room temperature under stirring and protected from light. Moreover, the effect of the pH was studied at pH 7.0, 8.0 and 8.7.

The course of the reactions was continuously monitored by measuring the concentration of the reactants and products by HPLC, following the method presented in section 3.4.5.2. The enzymatic activity of HLADH was analyzed according to section 3.4.1. The conversion was calculated as the percentage of Cbz-ethanolamine consumption with respect to the initial concentration. Yield was estimated as the production of Cbz-glycinal semicarbazone with respect to the initial concentration of Cbz-ethanolamine. Productivity was defined as the Cbz-ethanolamine consumed per unit of reaction time.

To obtain Cbz-glycinal from Cbz-glycinal semicarbazone the following scheme (figure 4.2.1) was proposed, adapted from a methodology found in the literature (Andersson and Wolfenden 1982).

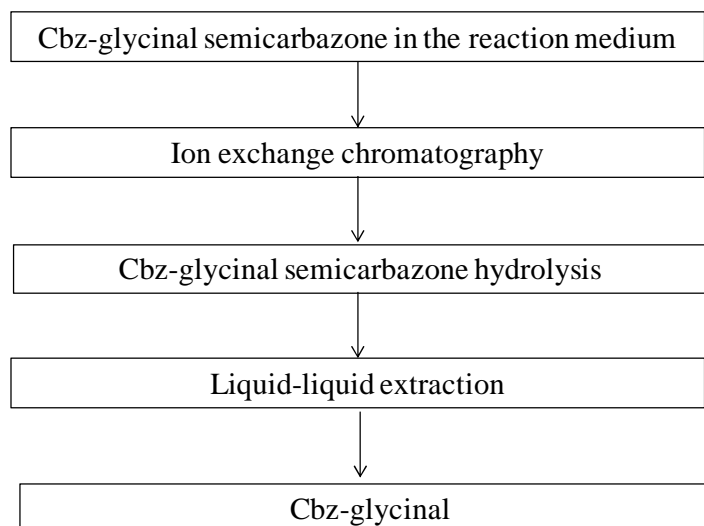


Figure 4.2.1 Scheme of the work up of Cbz-glycinal semicarbazone to obtain Cbz-glycinal. Adapted from Andersson and Wolfenden (Andersson and Wolfenden 1982).

To perform the ion exchange chromatography the reaction mixture was injected to a column (1.6 x 2 cm) packed with 4 mL CM Sephadex at 0.1 mL/min. The packed resin was previously equilibrated with 5 mM triethylammonium bicarbonate pH 7.2. Cbz-glycinal semicarbazone was eluted by applying a linear gradient of 5 to 400 mM triethylammonium bicarbonate pH 7.2 at a flow rate of 0.1 mL/min and room temperature. Fractions were collected every 10 min for 2 h. The aliquots containing Cbz-glycinal semicarbazone were pooled.

Cbz-glycinal semicarbazone was 10-fold diluted with 50% v/v methanol and it was treated by adding 20-50 fold molar excess of formaldehyde and the pH was adjusted at 1.0. The solution was stirred at room temperature using horizontal agitation and after 2 h, the pH was adjusted to 7.0. Finally, one volume of diethyl ether was used to extract Cbz-glycinal.

Also, semicarbazide 6% (w/w) on silica gel was tested as an alternative trapping agent in the HLADH catalyzed oxidation of Cbz-ethanolamine by adding 1500 μ mol of semicarbazide in 5 mL of reaction medium.

The concentration of Cbz-glycinal semicarbazone, Cbz-glycinal, Cbz-glycine and Cbz-ethanolamine were analyzed by HPLC, following the method described in section 3.4.5.2.

4.2.3 Preparation of the support glyoxal-agarose and MANA-agarose

The monoaminoethyl-N-aminoethyl (MANA)-agarose support was prepared from glyoxal-agarose resin according to the method reported by Fernández-Lafuente and coworkers (Fernandez-Lafuente, Rosell et al. 1993). Glyoxal-agarose resin was prepared by etherification of 10% crosslinked agarose gel with glycidol, and further sodium periodate oxidation of the resulting glyceryl-agarose.

15 mL of 10BCL agarose gel were washed thoroughly with distilled water and were suspended in 11.6 mL of a solution that contained 0.32 M NaOH, 0.14 M NaBH₄ and 2.04 M glycidol. The reaction was left on mild agitation in the rotary evaporator for approximately 19 h at room temperature. Then, the agarose was vacuum-filtered and washed with distilled water (10 volumes) to eliminate the remaining reagents.

The resulting glyceryl-agarose was oxidized with 400 μmol NaIO₄/mL agarose, during approximately 60 min. The supernatant was monitored periodically to measure the remaining sodium periodate. The formation of aldehyde groups was calculated from the consumption of NaIO₄, which was analyzed by colorimetric detection of the iodine liberated from the oxidation with 10% (w/v) KI in the presence of a saturated solution of NaHCO₃. The absorbance was measured at 500 nm using a UV-Visible Spectrophotometer Cary 50 (Varian, Palo Alto, CA, USA). When the oxidation was finished, the glyoxal-agarose was vacuum filtered and washed with distilled water.

MANA-agarose support was prepared by the reaction of glyoxal-agarose with ethylenediamine and further reduction with sodium borohydride during a reaction time of 2 h. The standard conditions determined by Fernández-Lafuente and coworkers (Fernandez-Lafuente, Rosell et al. 1993) were employed in order to obtain ≈99% of conversion from aldehyde groups to amino groups in the support.

15 g of glyoxal-agarose were suspended in 135 mL of 0.1 M sodium bicarbonate buffer at pH 10.0 with 2 M ethylenediamine. The suspension was left under mild horizontal

stirring for 2 h. Then, 1.5 g of NaBH₄ was added to the suspension to reach 10 mg/mL, and it was left again on mild horizontal stirring for another 2 h in order to finish the reduction of the Schiff bases. The reduced gel was vacuum filtered and washed with 150 mL of a solution containing 0.1 M sodium acetate + 1 M NaCl at pH 5.0, with 150 mL of a solution of 0.1 M sodium bicarbonate and 1 M NaCl at pH 10.0, and finally with 750 mL of distilled water.

4.2.4 Immobilization of HLADH

Immobilization of HLADH on 10BCL glyoxal-agarose support was performed by adapting the procedure used by Bolivar and coworkers (Bolivar, Wilson et al. 2006). To perform the immobilization, 1 mL (≈1 g) of 10BCL glyoxal-agarose support was resuspended in 9 mL of 100 mM sodium phosphate buffer pH 10.0 and the pH was readjusted. Afterwards, to study the immobilization at low and high charge, 10/1000 U of HLADH were added and left to immobilize on the support under mild horizontal stirring at room temperature. In addition, a blank was prepared following the same method but adding water instead of the support. The enzymatic activity of the supernatant, suspension and the blank were continuously monitored. When no activity was detected in the supernatant, the support was reduced with 1 mg/mL sodium borohydride for 30 min at 4°C under mild stirring. Finally, the immobilized enzyme was washed with an excess of distilled water.

The retained activity and the immobilization yield were defined as follows:

$$\text{Retained activity (\%)} = \frac{\text{Suspension activity}_{f_t} - \text{Supernatant activity}_{f_t}}{\text{Suspension activity}_{i_t}} \cdot 100 \quad (4.5)$$

$$\text{Immobilization yield (\%)} = \frac{\text{Suspension activity}_{i_t} - \text{Supernatant activity}_{f_t}}{\text{Suspension activity}_{i_t}} \cdot 100 \quad (4.6)$$

Where:

i_t: Initial time

f_t: Final time

4.2.5 Oxidation of Cbz-ethanolamine catalyzed by HLADH

The oxidation of Cbz-ethanolamine was carried out by dissolving 20 mM Cbz-ethanolamine and 20 mM NAD⁺ in 50 mM sodium pyrophosphate and sodium phosphate buffer. The reaction was initiated when HLADH was added to the reaction medium to reach a final activity of 20-500 U/mL. The reaction was performed at temperatures ranging from 25-40°C under stirring and protected from light. Several conditions were studied:

- MANA-agarose support as Cbz-glycinal trapping agent. It was evaluated in proportions of MANA-agarose:reaction medium (v/v) (1:1 and 1:10) under mechanic stirring at 25°C.
- The use of cosolvents by adding 4% (v/v) dimethylformamide (DMF) at 25°C.

A preliminary stability evaluation of HLADH was carried out by adding 15 U/mL HLADH in 50 mM phosphate buffer pH 8.7 and 4% DMF at 25°C under horizontal stirring. The enzymatic activity was monitored using the method described in section 3.4.1.

The course of the reactions was monitored according to section 4.2.2.

4.2.6 Oxidation of Cbz-ethanolamine to Cbz-glycinal using immobilized HLADH

Immobilized HLADH was employed for Cbz-ethanolamine oxidation in aqueous medium and ethyl acetate biphasic medium 50% (v/v). The reactions were performed using the general procedure described in section 4.2.5 but adding 2.0 g of immobilized HLADH equivalent to a final theoretical activity of 50 U/mL_{support} in a final volume of 7 mL at pH 8.7 and 37°C under mechanic stirring.

The course of the reactions was monitored according to section 4.2.2.

4.3 Results and discussion

4.3.1 Selection of the biocatalyst and feasibility of the oxidation of Cbz-ethanolamine by ADH

In the interest to obtain Cbz-amino aldehydes, the oxidation of Cbz-amino alcohols catalyzed by alcohol dehydrogenases (ADH) was proposed. Alcohol dehydrogenases from different sources as yeast (YADH) and horse liver (HLADH) were studied to determine the most convenient catalyst for the oxidation of a Cbz-ethanolamine. Table 4.3.1 shows the results obtained from the preliminary analysis of enzymatic activities and protein concentration of ADHs from different sources.

Table 4.3.1 Enzymatic activity of ADH from different sources

Enzyme	Enzymatic activity (U/mL)	Protein concentration (mg/mL)	Specific enzymatic activity (U/mg)
Commercial HLADH	8.6	20.01	0.430
In house HLADH	690.0	141.7	4.869
YADH	0.25	1.1	0.226

Results show that HLADH extracted from horse liver presents the highest enzymatic activity respect to the assay substrate, benzaldehyde. This value is 80 and 2760-fold higher than commercial HLADH and YADH, respectively. Since in house HLADH was partially purified, higher enzymatic activity could correspond to higher protein concentration. In terms of specific activity, in house HLADH is 11.3 and 21.5-fold more active than commercial HLADH and YADH, respectively. Nevertheless, in house HLADH specific enzymatic activity has the highest value of the tested enzymes. These findings indicate that in house HLADH is the most appropriate enzyme in terms of enzymatic activity.

On the other hand, the enzymes were evaluated as biocatalysts in the oxidation of 5 mM Cbz-ethanolamine with 5 mM NAD⁺ at pH 8.7 and room temperature. The enzymatic activity employed was different for every enzyme, being 20 U/mL in house HLADH,

1.44 U/mL commercial HLADH and 0.042 U/mL YADH. Figure 4.3.1 represents only the evolution of the in house HLADH reaction since the YADH reaction showed values of Cbz-glycinal and Cbz-glycine lower than 1 mM, and commercial HLADH only reacted at 24 h.

The kinetic parameters were calculated using Lineweaver and Burk plot (Lineweaver and Burk 1934) presented in equation 4.4. The plot of $1/r$ against $1/[S]$ for the three enzymes provides the value of r_{\max} , K_M and k_{cat} . Table 4.3.2 compares the kinetic values calculated for ADH from different sources.

Table 4.3.2 Kinetic parameters of Cbz-ethanolamine oxidation catalyzed by ADH from different sources. The reactions were performed with 5 mM Cbz-ethanolamine in 50 mM sodium pyrophosphate buffer pH 8.7, 5 mM NAD^+ and a final enzymatic activity of 20 U/mL in house HLADH, 1.44 U/mL commercial HLADH and 0.042 U/mL YADH in a final volume of 5 mL.

Enzyme	r_{\max} ($\text{mol}\cdot\text{L}^{-1}\cdot\text{h}^{-1}$)	K_M (mol/L)	k_{cat} ($\text{mol}\cdot\text{U}^{-1}\cdot\text{h}^{-1}$)	k_{cat}/K_M ($\text{L}\cdot\text{U}^{-1}\cdot\text{h}^{-1}$)
Comercial HLADH	*	*	*	*
In house HLADH	$2.57\cdot 10^{-5}$	0.0046	$1.29\cdot 10^{-9}$	$2.79\cdot 10^{-7}$
Yeast alcohol dehydrogenase (YADH)	$1.25\cdot 10^{-8}$	0.0041	$3.00\cdot 10^{-10}$	$7.31\cdot 10^{-8}$

* There was no reaction until 24 h.

Cbz-ethanolamine in presence of commercial HLADH only reacted after 24 h with a 1.2% yield Cbz-glycinal. Hence, there was no data to perform the kinetic calculations. Concerning the maximum rate (r_{\max}), the value obtained by in house HLADH was 2056-fold higher than the YADH. This was expected since YADH enzymatic activity is 480-fold lower than in house HLADH and r_{\max} is reached when all the enzyme sites are saturated with the substrate. However, the Michaelis constant (K_M) is practically the same for both enzymes indicating that both have the same affinity for the substrate. The catalytic constant k_{cat} for in house HLADH is 4.3-fold higher than that for YADH. This fact points out that in house HLADH provided the highest value of the product converted per active site. Finally, these results pointed that in house HLADH is more efficient in the oxidation of Cbz-ethanolamine. In that sense, Figure 4.3.1 presents the

concentration and the enzymatic activity profile of the Cbz-ethanolamine oxidation catalyzed by HLADH extracted from horse liver.

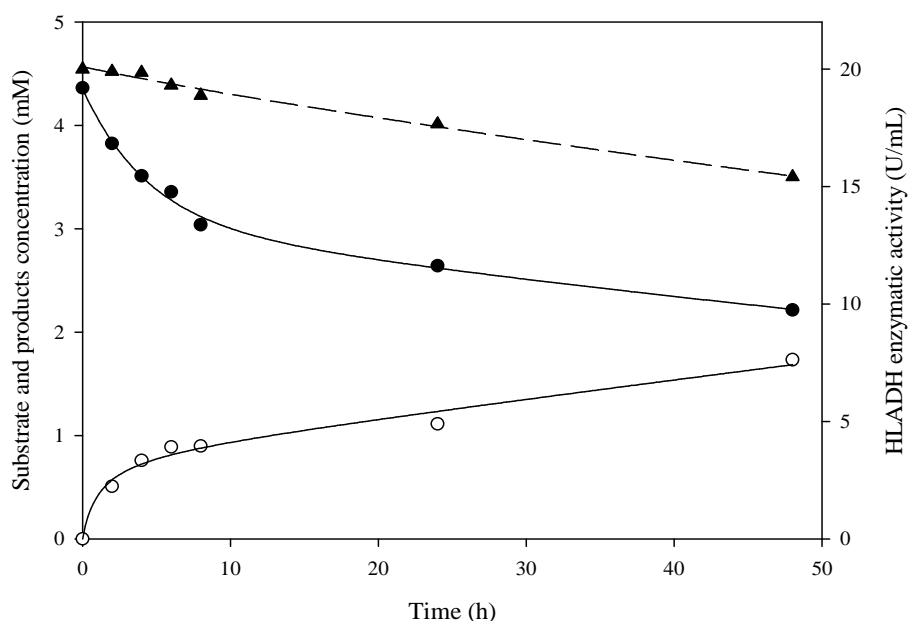


Figure 4.3.1 Time course of the preliminary batch oxidation of Cbz-ethanolamine. Cbz-ethanolamine (●), Cbz-glycine (○), HLADH (▲). The reaction was performed with 5 mM Cbz-ethanolamine in 50 mM sodium pyrophosphate buffer pH 8.7, 5 mM NAD^+ , 20 U/mL HLADH enzymatic activity at room temperature (20-22°C) in a final volume of 5 mL for 48 h.

Cbz-ethanolamine was directly oxidized to the acid Cbz-glycine with no aldehyde detected. This result is consistent with the phenomenon of dismutation and/or oxidation of aldehydes by HLADH (Abeles and Lee 1960; Dalziel and Dickinson 1965; Hinson and Neal 1975). Therefore, Cbz-ethanolamine conversion was 44.7% and Cbz-glycine yield 39.7% at 48 h reaction time. In addition, there was no peak of the aldehyde, Cbz-glycinal, or a new product in the chromatogram. Thus, the difference between conversion and yield ($\approx 11\%$) can be attributed to an experimental uncertainty. Concerning the enzymatic activity, the enzyme was stable at the reaction conditions, reaching 77.0% of remaining activity at 48 h.

4.3.2 HLADH catalyzed oxidation of Cbz-ethanolamine

In order to obtain Cbz-glycinal as oxidative product from Cbz-ethanolamine instead of Cbz-glycine, several studies were carried out to try to stop the oxidation to the intermediate stage which is the aldehyde compound. The results are presented in the next sections.

4.3.2.1 Oxidation of Cbz-ethanolamine catalyzed by HLADH in aqueous medium using semicarbazide hydrochloride for aldehyde entrapment

Due to the high oxidative capacity of HLADH, the use of an aldehyde trapping agent, such as nitrogenous bases, can be a good method to avoid further oxidation of the aldehyde to the acid. Semicarbazide as a hydrochloride salt has been widely used as an aldehyde trapping agent. It belongs to a family of chemicals called hydrazines. Accordingly, it was employed to produce α -amino aldehydes from α -amino alcohols catalyzed by HLADH (Andersson and Wolfenden 1982) by formation of semicarbazone and further purification of the α -aminoaldehyde.

Owing to the requirement of semicarbazide hydrochloride, a modification of the methodology reported by Andersson and Wolfenden (Andersson and Wolfenden 1982) was employed for the oxidation of 5 mM Cbz-ethanolamine with 5 mM NAD^+ , 16 U/mL HLADH at pH 8.7 and room temperature. The concentration of semicarbazide hydrochloride used was the same as the one proposed by the authors (300 mM) and one half (150 mM). Figure 4.3.2 shows the effect of the semicarbazide concentration in the oxidation of Cbz-ethanolamine.

The highest yield at 24 h reaction of Cbz-glycinal semicarbazone (27.0%) was obtained with 300 mM of semicarbazide hydrochloride. The yield was 1.5-fold enhanced if compared to the one obtained with 150 mM semicarbazide hydrochloride (17.9%). Consequently, Cbz-glycine yield was 15.3%, which is 1.3-fold lower compared with 150 mM semicarbazide hydrochloride (19.3%). In that sense the conversion of Cbz-ethanolamine was similar, resulting in 39.2% and 43.0% using 150 and 300 mM semicarbazide hydrochloride. In addition, the remaining enzymatic activity obtained was similar in both cases and around 95%. These results were expected since increasing

semicarbazide hydrochloride concentration provides more available amino groups to trap the aldehyde formed, hence the amount of aldehyde oxidized to acid decreased.

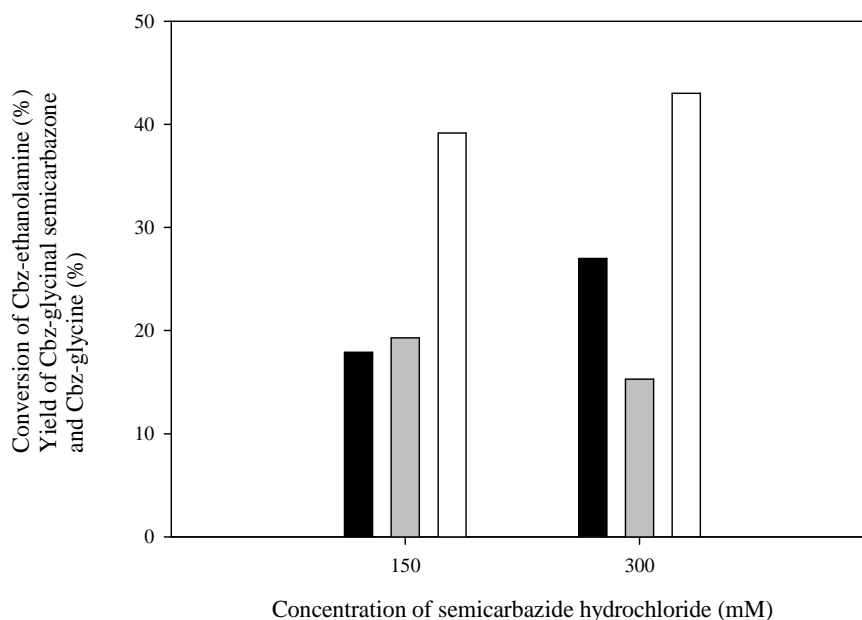


Figure 4.3.2 Influence of the concentration of semicarbazide hydrochloride in the yield of Cbz-glycinal semicarbazone (black bars) and Cbz-glycine (gray bars) and conversion of Cbz-ethanolamine (white bars). The reactions were performed with 5 mM Cbz-ethanolamine in 50 mM sodium pyrophosphate buffer pH 8.7, 5 mM NAD⁺ and HLADH activity of 16 U/mL at room temperature (20-22°C) in a final volume of 5 mL for 24 h.

In the interest to improve the productivity of the reaction the highest concentration of Cbz-ethanolamine in aqueous media was employed. This value was around 20 mM according to Pešić (Pešić 2012).

Moreover, the effect of using a higher semicarbazide hydrochloride concentration (600 mM) was studied since the concentration of Cbz-ethanolamine was higher. The reaction was monitored for 48 h. Figure 4.3.3 compares the oxidation of 20 mM Cbz-ethanolamine with 20 mM NAD⁺, 16 U/mL HLADH at pH 8.7 and room temperature for both semicarbazide hydrochloride concentrations, 300 and 600 mM.

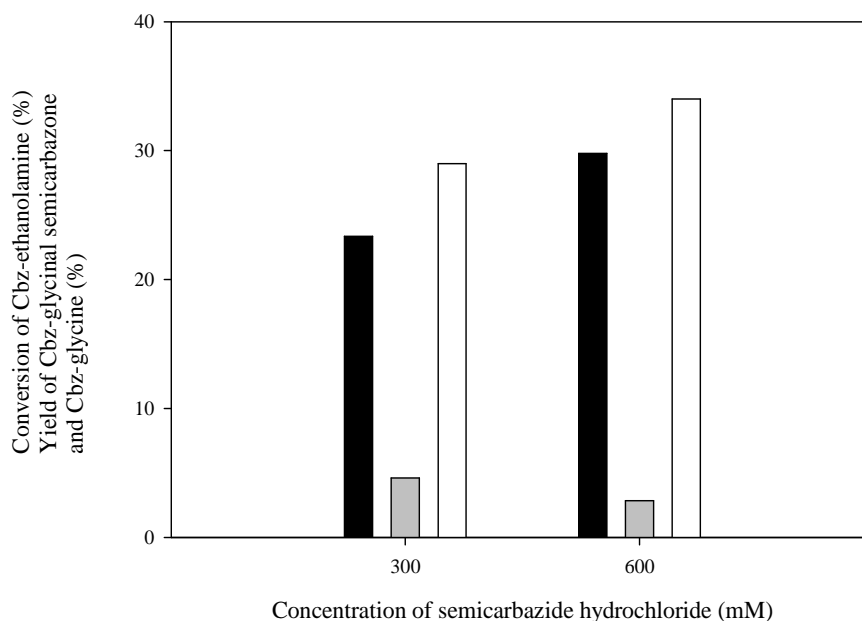


Figure 4.3.3 Influence of the concentration of semicarbazide hydrochloride in the yield of Cbz-glycinal semicarbazone (black bars) and Cbz-glycine (gray bars) and Cbz-ethanolamine conversion (white bars). The reactions were performed with 20 mM Cbz-ethanolamine in 50 mM sodium pyrophosphate buffer pH 8.7, 20 mM NAD⁺ and HLADH activity of 16 U/mL at room temperature (20-22°C) in a final volume of 5 mL for 48 h.

Yield of Cbz-glycinal semicarbazone was 1.3-fold enhanced with the increase of the concentration of semicarbazide hydrochloride. This value was 29.8% with 600 mM compared to 23.4% with 300 mM. Therefore, Cbz-glycine formed was 1.7 fold-decreased, obtaining 2.8% and 4.6% for 600 and 300 mM, respectively. This behavior was expected, based on the explanation presented above and taking in account that the Cbz-ethanolamine converted was 29.0 and 34.1% for 300 and 600 mM, respectively. On the other hand, the variation in the yield of Cbz-glycinal semicarbazone was lower between 300 and 600 mM compared to 150 mM and 300 mM. This could be an indication of the approximation to the saturation point of the semicarbazide hydrochloride. Besides, yield of Cbz-glycinal semicarbazone was 2.3-fold improved in the case of 300 mM semicarbazide hydrochloride concentration in contrast with the same concentration but using 5 mM Cbz-ethanolamine (figure 4.3.2). This result was a consequence of the increment in the initial Cbz-ethanolamine concentration that promoted the rate of the Cbz-glycinal formation. Regarding the remaining enzymatic activity, even it was similar for both cases, with the value of 75%. This is lower than the

presented in figure 4.3.2, because the reaction time was increased since the initial concentration of Cbz-ethanolamine was higher.

i. Effect of the pH

HLADH-catalyzed oxidation of alcohols takes place at pH values in a range of 7.0 to 9.0 (Kvassman and Pettersson 1979; Sekhar and Plapp 1988) ; the use of basic pH is common since this helps to ameliorate the unfavorable equilibrium. Based on this fact, the influence of the pH in the yield of Cbz-glycinal semicarbazone and Cbz-glycine was studied in the range mentioned for the oxidation of 20 mM Cbz-ethanolamine with 20 mM NAD⁺ and 16 U/mL HLADH at room temperature using the highest concentration of semicarbazide hydrochloride evaluated (600 mM). The results obtained from the analysis of the variation of the pH can be seen in figure 4.3.4.

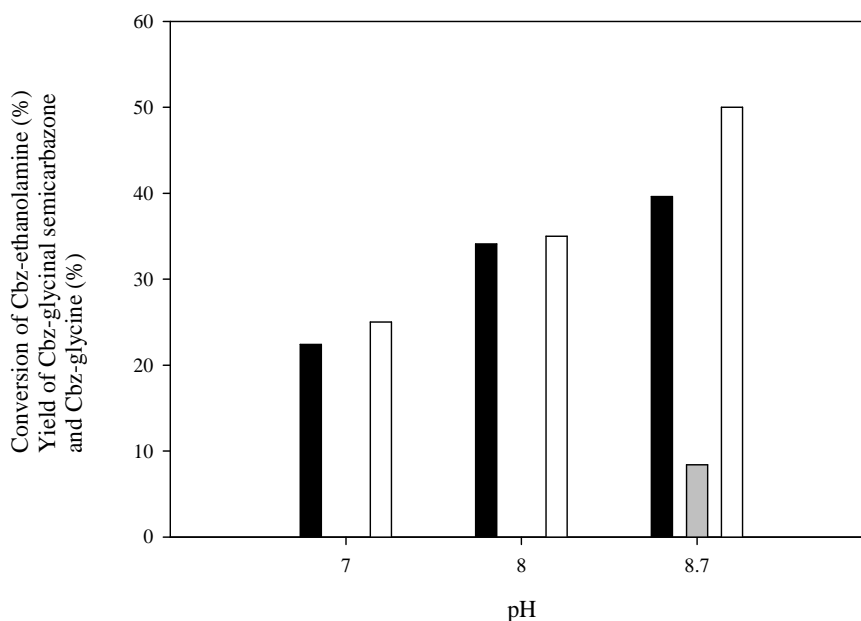


Figure 4.3.4 Effect of the pH in the yield of Cbz-glycinal semicarbazone (black bars) and Cbz-glycine (gray bars) and Cbz-ethanolamine conversion (white bars). The reactions were performed with 20 mM Cbz-ethanolamine, 600 mM semicarbazide hydrochloride, 20 mM NAD⁺ and HLADH activity of 16 U/mL at room temperature (20-22°C) in a final volume of 5 mL for 72 h.

The increase of pH promotes the oxidation of Cbz-ethanolamine with conversion values of 25.3, 32.5 and 50.0% for pH 7.0, 8.0 and 8.7 respectively. As well, the highest production of Cbz-glycinal semicarbazone was at pH 8.7 (39.6%). Nevertheless under this condition there is a measurable formation of Cbz-glycine (8.4% yield). Concerning the HLADH activity, the enzyme was stable at pH 8.0 and 8.7 and a remaining activity of 84.7% was observed at pH 7.0. Having in mind the objective of obtaining Cbz-glycinal, it was necessary to increase the yield of Cbz-glycinal semicarbazone. In that sense, pH 8.7 is the one that better fulfills the requirement, although there is a little formation of Cbz-glycine (8.4%) at 72 h.

ii. Cbz-glycinal semicarbazone formation at higher enzymatic activity

Positive results were found during the studies of the Cbz-ethanolamine oxidation in presence of semicarbazide hydrochloride catalyzed by HLADH. Notwithstanding, it was necessary to rise the enzymatic activity to improve the reaction kinetics. Hence, this value was 5-fold increased to 80 U/mL.

It was previously demonstrated that 600 mM semicarbazide hydrochloride provided the highest yield of Cbz-glycinal semicarbazone and the lowest yield of Cbz-glycine. However, for purification purposes it is more convenient to work with a lower concentration of entrapping agent. For this reason the oxidation was performed with 20 mM Cbz-ethanolamine and 20 mM NAD⁺, 80 U/mL HLADH at pH 8.7, room temperature, using semicarbazide hydrochloride concentration of 300 and 600 mM (see figure 4.3.5 A and B). Table 4.3.3 presents a detailed comparison of both reactions at 151 h. Figure 4.3.5 indicates that in general no significant differences were found between concentrations of 300 and 600 mM of semicarbazide hydrochloride. This also accords with our earlier observations presented in this section. Therefore, table 4.3.3 shows that the yield of Cbz-glycinal semicarbazone was 1.2-fold improved at 600 mM semicarbazide hydrochloride, with a value of 84.4% compared to 71.9% with 300 mM. Meanwhile, the yield of Cbz-glycine (6.0%) was 2-fold lower than at 300 mM (11.9%). These findings support the idea that at 600 mM the effect of the production of Cbz-glycine can be reduced, although the yield of Cbz-semicarbazone is not significantly improved.

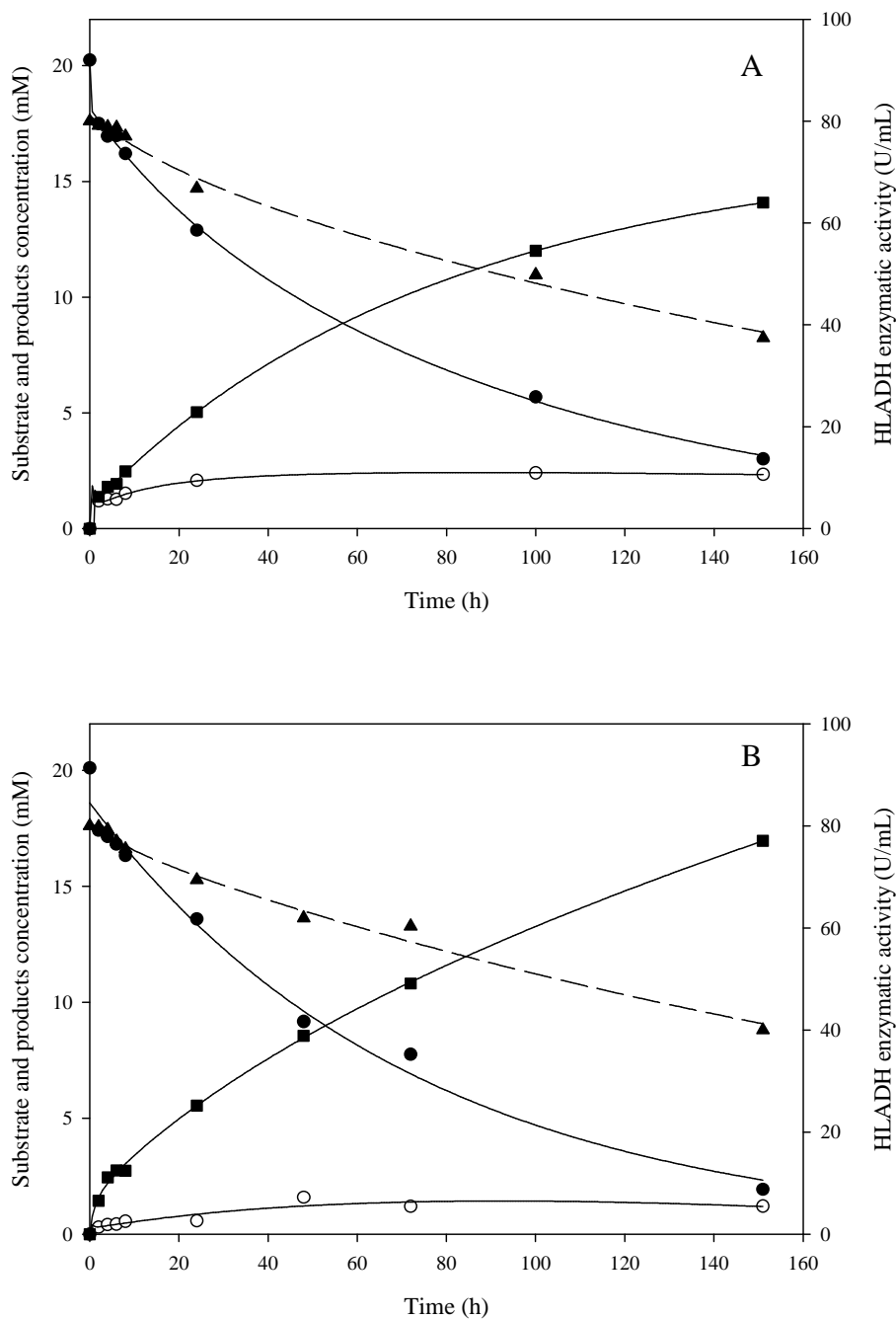


Figure 4.3.5 Concentration profile of Cbz-ethanolamine oxidation using semicarbazide hydrochloride 300 mM (A) and 600 mM (B). The reactions were performed with 20 mM Cbz-ethanolamine in 50 mM sodium pyrophosphate buffer pH 8.7, 20 mM NAD⁺ and HLADH activity of 80 U/mL at room temperature (20-22°C) for 151 h. Cbz-ethanolamine (●), Cbz-glycine (○), Cbz-glycinal semicarbazone (■), HLADH (▲).

The initial rate of reaction (table 4.3.3), calculated as the Cbz-glycine semicarbazone formed, was 0.72 and 0.69 mM/h at 300 and 600 mM, respectively, corresponding only to 1.1-fold enhanced value. The productivity calculated with reference to Cbz-glycinal semicarbazone formed was 1.1-fold improved, being 0.106 and 0.112 mM/h for 300 and 600 mM, respectively.

Again, a minor benefit was observed increasing twice the semicarbazide hydrochloride concentration. Concerning the HLADH activity, it can be observed in figure 4.3.5 A and B that it was stable only during the first 8 h reaction time. Hence, there was a decrease after 24 h until 151 h, when an almost similar value of $\approx 50\%$ remaining activity was found for both concentrations.

These experiments were successful as they were able to demonstrate that from 71.9 up to 84.4% yield of Cbz-glycinal semicarbazone can be obtained. This compound must be further treated to recover the target product Cbz-glycinal. Besides, such high concentration of semicarbazide hydrochloride is not required, as 300 mM is enough to obtain 71.9% of Cbz-glycinal with just 11.9% of Cbz-glycine yield after 151 h.

Table 4.3.3 Summary of HLADH catalyzed oxidation of Cbz-ethanolamine using semicarbazide hydrochloride to obtain Cbz-glycinal semicarbazone. The reactions were performed with 20 mM Cbz-ethanolamine in 50 mM sodium pyrophosphate buffer pH 8.7, 20 mM NAD⁺, 300 mM and 600 mM semicarbazide concentration, and HLADH activity of 80 U/mL at room temperature (20-22°C) in a final volume of 5 mL for 151 h.

Semicarbazide hydrochloride concentration (mM)	Cbz-ethanolamine conversion (%)	Cbz-glycinal semicarbazone yield (%)	Cbz-glycine yield (%)	Initial reaction rate (mM Cbz-glycinal semicarbazone/h)	Productivity (mM Cbz-glycinal semicarbazone produced/h)	HLADH remaining activity (%)
300	84.7	71.9	11.9	0.69	0.106	53.1
600	90.4	84.4	6.0	0.72	0.112	50.0

iii. Cbz-glycinal recovery from Cbz-glycinal semicarbazone

A methodology was proposed for the recovery of the Cbz-glycinal according to the procedure reported by Andersson and Wolfenden (Andersson and Wolfenden 1982), as the main objective of the HLADH catalyzed Cbz-ethanolamine oxidation was to obtain Cbz-glycinal.

The proposed first stage of the purification was the CM Sephadex ion exchange chromatography of the reaction mixture equilibrated with 5 mM triethylammonium bicarbonate pH 7.2. The intention was to separate the Cbz-glycinal semicarbazone from the other components by its elution following the procedure presented in section 4.2.2. Figure 4.3.6 provides the distribution of the Cbz-glycinal semicarbazone, Cbz-ethanolamine and Cbz-glycine for different elution fractions.

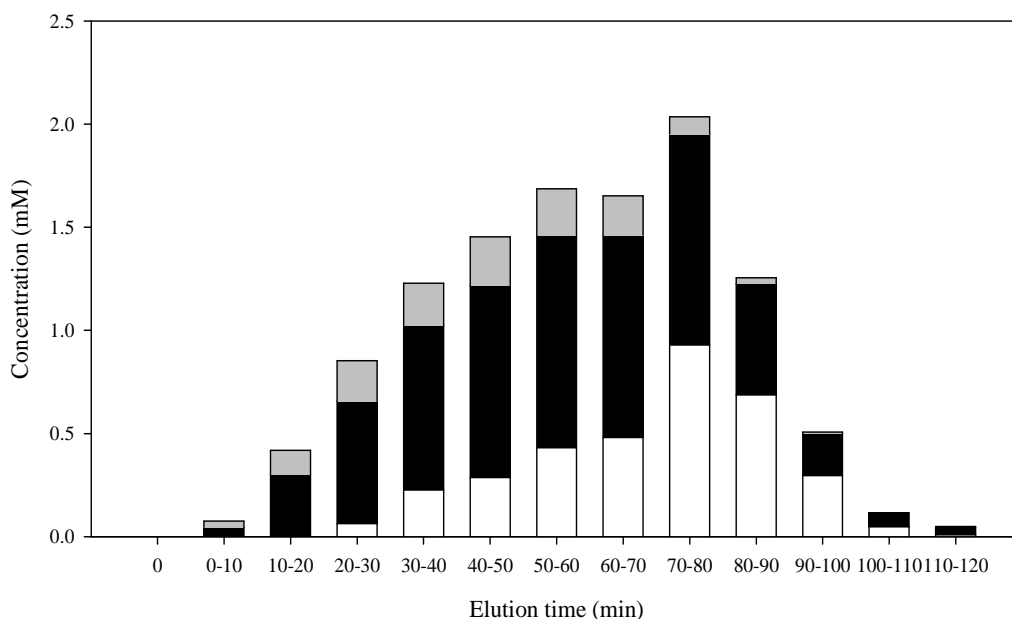


Figure 4.3.6 Elution of Cbz-glycinal semicarbazone in the CM Sephadex ion exchange chromatography. The resin was previously equilibrated with 5 mM triethylammonium bicarbonate pH 7.2 and the elution was performed by applying a linear gradient of 5 to 400 mM triethylammonium bicarbonate pH 7.2 at room temperature (20-22°C) and a flow rate of 0.1 mL/min. Cbz-ethanolamine (white), Cbz-glycinal semicarbazone (black) and Cbz-glycine (gray).

This graphic shows that Cbz-glycinal semicarbazone was present in high concentrations in most of the aliquots. Specifically, it was observed in the aliquots from 10 to 100 min. On the other hand, Cbz-ethanolamine and Cbz-glycine were eluted at 30-100 min and at 10-90 min, respectively. This distribution leads to discard this chromatography step since Cbz-glycinal semicarbazone can not be separated efficiently of the other two compounds.

Then, separation was directly attempted by an acid hydrolysis of the reaction mixture at pH 1.0 in order to reverse the Schiff base between the Cbz-glycinal and semicarbazide hydrochloride (Andersson and Wolfenden 1982). An excess of formaldehyde was necessary to capture the free semicarbazide hydrochloride and render Cbz-glycinal at pH 7.0. The amount of Cbz-glycinal recovered by this procedure was 38.3% and 48.5% by using 20 and 50-fold excess of formaldehyde respectively. This excess was calculated in reference to the initial semicarbazide hydrochloride concentration (300 mM). In the interest to enhance the recovery of Cbz-glycinal, the hydrolysis was also performed at higher temperature, but there was not any significant difference.

As the obtained Cbz-glycinal was pretended to be used as substrate for the aldolic condensation of DHAP catalyzed by RhuA in order to produce Cbz-aminopolyol, additional purification steps were necessary to remove the formaldehyde in excess, which could react with DHAP in presence of aldolases.

Several organic solvents as diethyl ether, chloroform, ethyl acetate and hexane were used to extract the Cbz-glycinal; however, no good recovery of the Cbz-glycinal was obtained. The best solvent was found to be diethyl ether. Nevertheless, a poor partition coefficient (1.3) was determined comparing the organic phase with a Cbz-glycinal partition of 57% and the aqueous phase with 43%. As formaldehyde and formaldehyde semicarbazone were mainly dissolved in the aqueous phase, the organic phase was evaporated to remove the solvent and the traces of the formaldehyde adding an extra step and reducing the Cbz-glycinal recovery to $\approx 1\%$.

These findings demonstrate that Cbz-glycinal recovered from Cbz-glycinal semicarbazone using this methodology is not adequate to perform the aldolic addition of

DHAP catalyzed by aldolases, since the recovery percentage in the organic phase was very low.

On the other hand, semicarbazide 6% (w/w) on silica gel was also employed with no positive results since it did not provide an adsorption of the Cbz-glycinal formed, the reaction renders directly to Cbz-glycine.

4.3.2.2 Evaluation of the support MANA-agarose for aldehyde entrapment

MANA-agarose support was proposed as a Cbz-glycinal trapping agent since it has amino groups and it was expected to follow the same mechanism of semicarbazide hydrochloride, reacting with aldehyde groups of the target compound. The use of this kind of support can provide several advantages, such as an easier separation and desorption because of their solid state, no requirement of other aldehydes, and reusability.

MANA-agarose was prepared from glyoxal-agarose according to the procedure described in section 4.2.4. The preparation of glyoxal-agarose was made by etherification of agarose gels with glycidol and further oxidation of the resulting glyceryl-agarose by sodium periodate. The amount of sodium periodate added was 400 μmol per mL agarose providing 389 μmol of aldehyde groups per mL agarose.

Figure 4.3.7 presents the results of the oxidation of 20 mM Cbz-ethanolamine, 20 mM NAD^+ and 20 U/mL HLADH in presence of MANA-agarose gel in different proportions with respect to the reaction medium at pH 8.7 and 25°C.

Similar values of the Cbz-ethanolamine conversion of around 24% were obtained in both proportions of MANA-agarose: reaction medium (1:10 and 1:1) (v/v). Moreover, the yield of Cbz-glycine was very low with values of 5.2 and 1.0% for proportions of 1:10 and 1:1 respectively. One unanticipated finding was the decrease of enzymatic activity, with a remaining value of $\approx 23\%$ for both conditions.

Hence, it could be conceivably hypothesized that there was a formation of Cbz-glycinal and it was trapped in the MANA-agarose gel. Another implication of this is the possibility of the adsorption of Cbz-ethanolamine in the support. A further study was

carried out to verify this assumption by adding the reaction medium using the same conditions mentioned above without enzyme, using MANA-agarose:reaction medium (1:1) but a low adsorption of 14.4% Cbz-ethanolamine was obtained after 168 h.

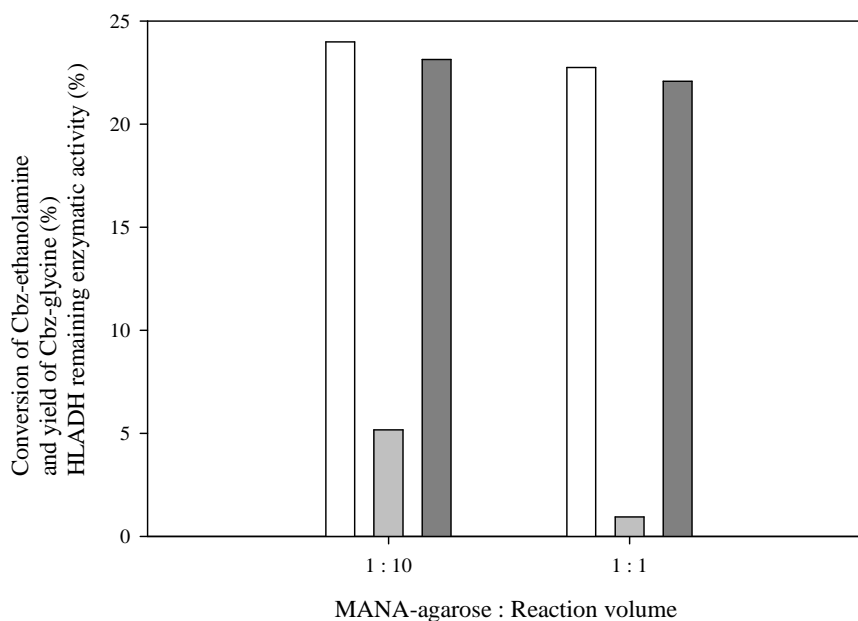


Figure 4.3.7 Study of the use of MANA-agarose gel in the oxidation of Cbz-ethanolamine. The reactions were performed with 20 mM Cbz-ethanolamine in 50 mM sodium pyrophosphate buffer pH 8.7, 20 mM NAD⁺ and HLADH activity of 20 U/mL at 25°C for 72 h using MANA-agarose:reaction medium (v/v) (1:10 and 1:1). Cbz-ethanolamine conversion (white bars), Cbz-glycine yield (gray bars) and HLADH remaining activity (dark gray bars).

Consequently, with the purpose of determining if Cbz-glycinal was formed and it was adsorbed in MANA-agarose, the reaction medium was adjusted to pH 1.0 to reverse the Schiff base. There was no recovery of Cbz-glycinal which could imply some of the following assumptions: there was no formation, the concentration was very low or the Schiff base is not so easily reverted in these conditions. Taken together, these findings could suggest that there was a little adsorption of Cbz-ethanolamine and its oxidation with HLADH only provides Cbz-glycine.

Regarding the HLADH enzymatic activity, the decrease can not be related to the reaction medium because of its previously demonstrated high stability. The evidence of this reaction could indicate that there was adsorption in the support. In fact, MANA-agarose was widely used as support for enzyme immobilization by covalent attachment

at acidic, neutral and alkaline pH. Thereby, HLADH was immobilized in MANA-agarose at neutral pH as reported by Bolivar and coworkers (Bolivar, Wilson et al. 2006). Although the monoaminoethyl-*N*-aminoethyl groups have a double positive charge at neutral or acid pH value and just one charge at moderate alkaline pH, these results pointed out that the adsorption is still suitable at pH 8.7.

4.3.2.3 Oxidation of Cbz-ethanolamine in aqueous medium with cosolvents

The use of cosolvents enables the improvement of the solubility of the hydrophobic compounds with respect to the aqueous medium. The main objective of their employment is to solubilize the Cbz-glycinal formed in the reaction. Nevertheless, the cosolvent concentration in the reaction medium should be low to avoid the enzyme deactivation.

Dimethylformamide (DMF) was employed by Ardao (Ardao 2009) to perform the aldolic addition of DHAP by RhuA and (*S*)-Cbz-alaninal. According to her results, DMF was selected as cosolvent for the HLADH catalyzed oxidation of Cbz-ethanolamine to promote the formation of Cbz-glycinal. Figure 4.3.8 provides the preliminary evaluation of HLADH enzymatic activity in 4% v/v DMF at pH 8.7.

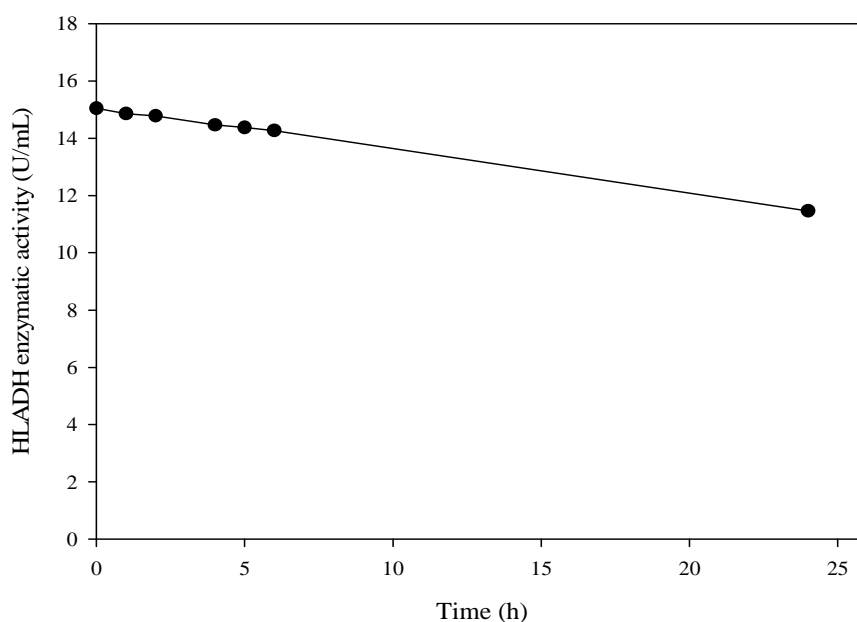


Figure 4.3.8 Stability of HLADH in presence of 75 mM sodium pyrophosphate buffer pH 8.7 and 4% v/v DMF during 24 h.

Overall, HLADH was shown to be rather stable in the medium containing 4% v/v DMF at pH 8.7; the loss of enzymatic activity was only 3.1% during the first 6 h. However, after the 6 h there was a gradual decrease to obtain a remaining activity of 76.2% at 24 h.

The oxidation of 20 mM Cbz-ethanolamine was performed with 20 mM NAD⁺, 20 U/mL of HLADH at pH 8.7 and 25°C using 4% (v/v) DMF. Figure 4.3.9 represents the concentration profile and enzymatic activity of that reaction.

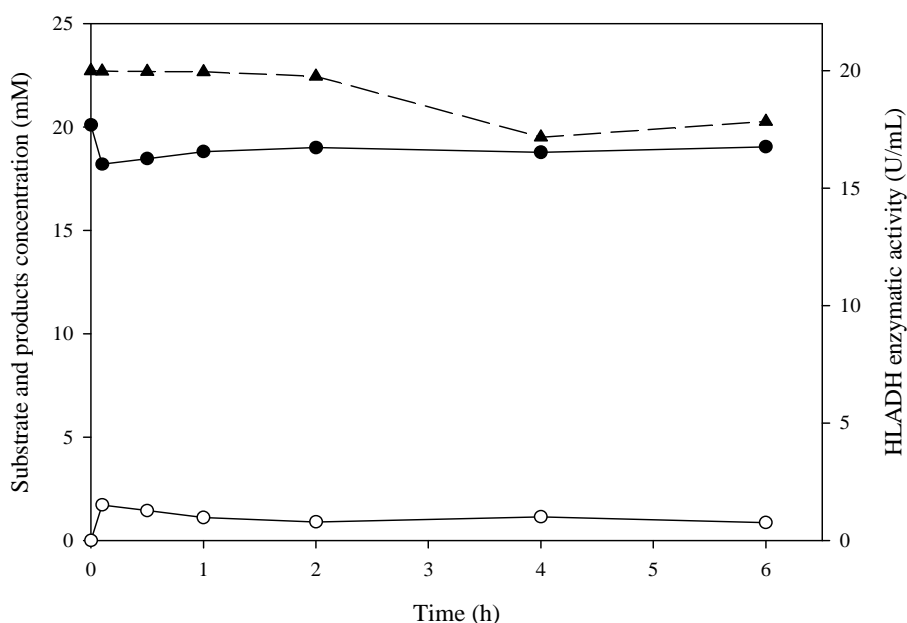


Figure 4.3.9 Time course of the Cbz-ethanolamine oxidation catalyzed by HLADH in presence of 4% (v/v) DMF. The reaction was performed with 20 mM Cbz-ethanolamine in 75 mM sodium pyrophosphate buffer pH 8.7, 4% v/v DMF, 20 mM NAD⁺ and 20 U/mL HLADH at 25°C. Cbz-ethanolamine (●), Cbz-glycine (○), HLADH (▲).

This graphic is quite revealing. First, unlike the other Cbz-ethanolamine oxidations previously performed, practically there is no conversion of the substrate. Only in the first 30 min the reaction yielded 8.5% Cbz-glycine which disappeared with time and there was no formation of the Cbz-glycinal. The enzyme was stable with a slight decrease from 4 h until 89.2% at 6 h. The behavior of the concentration profile of the substrate and products and the enzymatic activity could suggest an inhibition of the enzyme. Therefore, it has been reported that DMF is strongly HLADH inhibitory (Jones and Schwartz 1982).

4.3.2.4 Use of immobilized HLADH for the oxidation of Cbz-ethanolamine

The deactivation of the soluble enzymes in presence of organic solvents is a drawback, so it was necessary to define a proper immobilization methodology that provides enzyme stability in the oxidation of Cbz-ethanolamine.

i. Immobilization of HLADH in glyoxal-agarose

Glyoxal-agarose support has been used successfully in the stabilization of several enzymes by multipoint covalent attachment with high activity recoveries (Blanco and Guisán 1989; Alvaro, Fernandez-Lafuente et al. 1990; Guisán, Bastida et al. 1991). Therefore, HLADH was effectively immobilized on this support providing operational and organic solvent stability and applicability to NAD⁺ cofactor recycling system (Bolivar, Wilson et al. 2006).

Glyoxal-agarose was prepared according to the procedure described in section 4.2.4. As presented in section 4.3.2.2 glyoxal-agarose provided 389 μmol of aldehyde groups per mL agarose.

Afterwards, HLADH was immobilized at low (10 U in 10 mL support) and high load (1000 U in 10 mL support) at pH 10.0, following the procedure described in section 4.2.6. Figure 4.3.10 presents the results obtained at low (A) and high load (B).

There was a complete immobilization of HLADH on glyoxal-agarose after 1 h of incubation of the support with low enzymatic load (A). In addition, 78.1% retained activity with respect to the initial suspension was obtained. Such positive results were expected as they had been reported by Bolivar and coworkers (Bolivar, Wilson et al. 2006). By contrast, high load immobilization (B) presented a different behavior. A period of 3 h was required to obtain 85.0% immobilization yield, corresponding to a 1.2-fold decrease compared to low load at 1 h. On the other hand, only 15.0% retained activity was obtained using high load of enzyme. A possible explanation for this might be the saturation of the support and the diffusion limitations of the HLADH immobilized on glyoxal-agarose. Accordingly, it can be established that 21.2% loss of enzymatic activity was because of the immobilization process itself, whereas the rest of the apparent activity loss can be mainly attributed to the diffusion limitations.

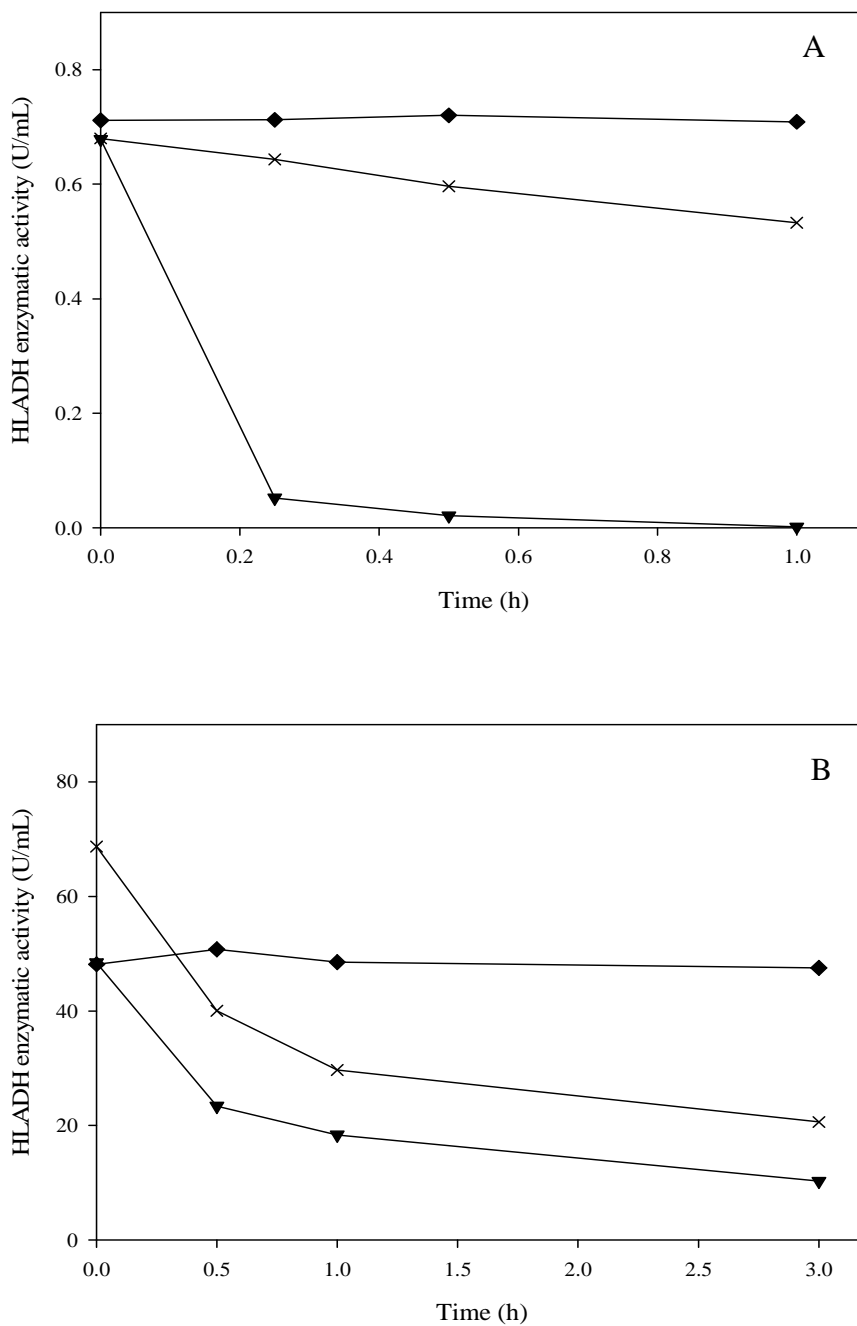


Figure 4.3.10 Time course of HLADH immobilization on glyoxal-agarose. The immobilization was performed with 1 g agarose in 10 mL of 100 mM sodium bicarbonate buffer pH 10.0 at room temperature (20-22°C). The immobilization was carried out using low (A) and high (B) load of enzyme. Measured activities in supernatant (▼), suspension (x) and blank (◆).

ii. Immobilized-HLADH catalyzed oxidation of Cbz-ethanolamine in aqueous medium

Reactions catalyzed by immobilized enzymes have different kinetic properties compared to the soluble enzymes. Thus, the reaction rate depends not only on the reaction itself, but also on the transport of the substrates and the products to and from the interior of the particle. Consequently, Cbz-ethanolamine oxidation in aqueous media (20 mM) was proposed using a stoichiometric amount of NAD^+ , 2 g of 50 U/mL_{support} immobilized HLADH at pH 8.7 and 37°C in a final volume of 7 mL. Figure 4.3.11 shows the concentration profile.

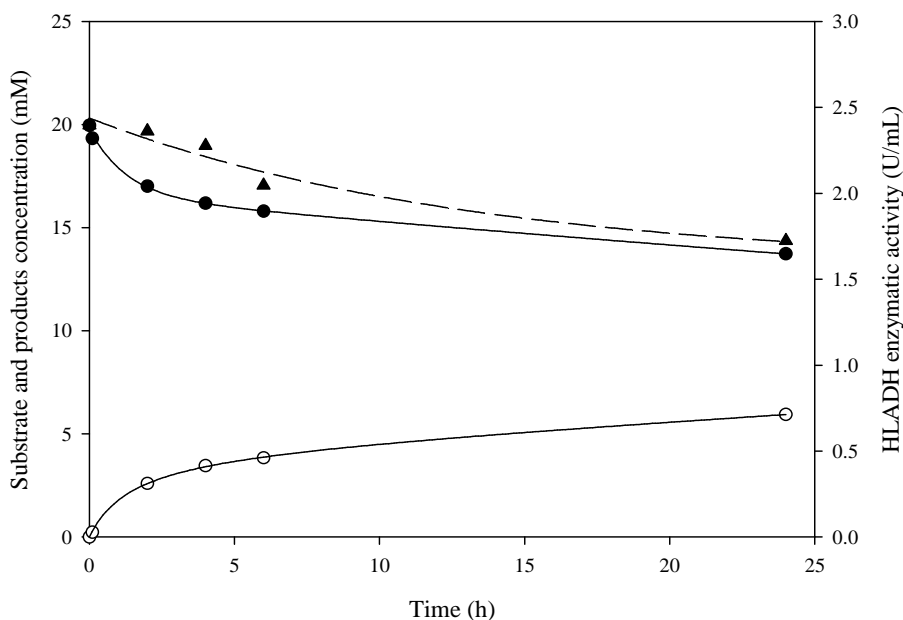


Figure 4.3.11 Time course of the Cbz-ethanolamine oxidation catalyzed by immobilized HLADH on glyoxal-agarose in aqueous medium. The reaction was performed with 20 mM Cbz-ethanolamine in 75 mM sodium pyrophosphate buffer pH 8.7, 20 mM NAD^+ , 2 g of 50 U/mL_{support} immobilized HLADH at 37°C in a final volume of 7 mL. Cbz-ethanolamine (●), Cbz-glycine (○), HLADH (▲).

There was no production of Cbz-glycinal in aqueous medium, but 29.8% yield of Cbz-glycine was obtained at 24 h. The enzymatic activity obtained was apparent because of the diffusion limitations at high load immobilizations. Also, the remaining enzymatic activity was 71.9% at 24 h, because of a deactivation of the enzyme by the organic solvent.

iii. Immobilized-HLADH catalyzed oxidation of Cbz-ethanolamine in biphasic medium

Finally, in an attempt to obtain Cbz-glycinal from the oxidation of Cbz-ethanolamine, a biphasic system was proposed. The intention was to promote the diffusion of the Cbz-glycinal into the organic phase while the enzyme remained in the aqueous phase, which probably stopped the further oxidation into Cbz-glycine. Figure 4.3.12 shows the oxidation of 20 mM Cbz-ethanolamine, 20 mM NAD⁺, 2 g of 50 U/mL_{support} immobilized HLADH in reaction medium:ethyl acetate (1:1) at pH 8.7 and 37°C.

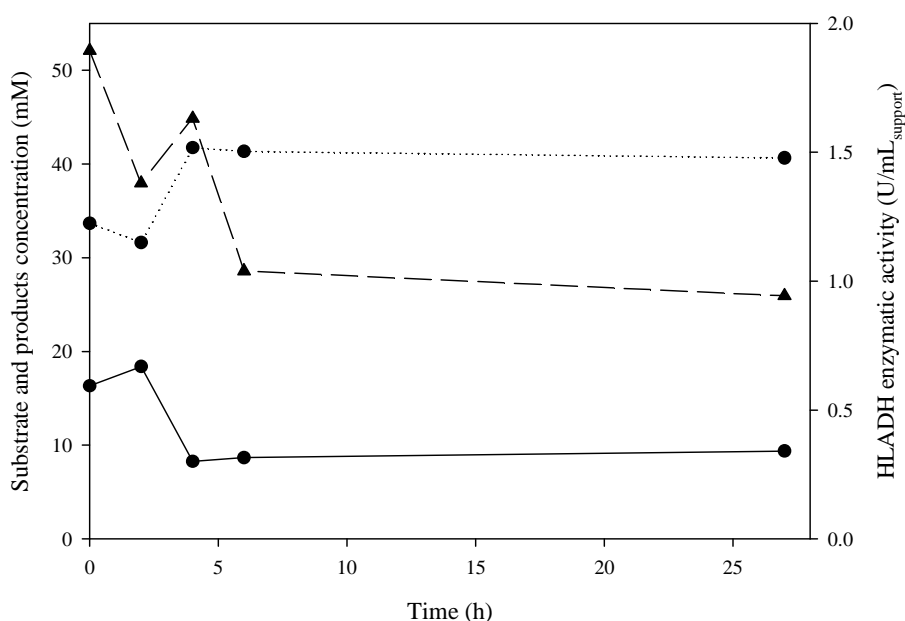


Figure 4.3.12 Time course of the Cbz-ethanolamine oxidation catalyzed by immobilized HLADH on glyoxal-agarose in biphasic medium. The reaction was performed with 20 mM Cbz-ethanolamine in 75 mM sodium pyrophosphate buffer pH 8.7, 20 mM NAD⁺, 2 g of 50 U/mL_{support} immobilized HLADH at 37°C in reaction medium:ethyl acetate (1:1) for a final volume of 7 mL. Cbz-ethanolamine (●), aqueous phase (solid line), organic phase (dotted line), HLADH (▲).

Contrary to expectations, there was no reaction of Cbz-ethanolamine. Only a partition of Cbz-ethanolamine in the organic and aqueous phase was observed during the time. Remaining enzymatic activity was 47.2% at 24 h of reaction.

4.4 Conclusions

HLADH catalyzed oxidation of Cbz-ethanolamine was successfully performed using semicarbazide hydrochloride as Cbz-glycinal trapping agent. The most appropriate concentration of semicarbazide hydrochloride employed was 300 mM yielding 71.9% Cbz-glycinal semicarbazone. However, the recovery of Cbz-glycinal was not very effective since it implied several purification steps. It was necessary to add up to 50-fold excess of formaldehyde in the acid hydrolysis and only 48.5% Cbz-glycinal was recovered. Cbz-glycinal was obtained with a high concentration of formaldehyde which is a major inconvenience when the aldehyde Cbz-glycinal is tried to react with DHAP in the further RhuA catalyzed aldolic condensation to obtain aminopolyols.

Meanwhile, in order to obtain Cbz-glycinal from Cbz-ethanolamine oxidation by HLADH several alternatives were studied with no positive results. Supports with amino groups as MANA-agarose and semicarbazide on silica gel and an evaluation of the engineering media were not able to promote the formation of Cbz-glycinal. Even when it was obtained in a low yield ($\approx 4\%$ maximum) it always turned out rendering to Cbz-glycine.

The results of this chapter demonstrated the high oxidative capacity of HLADH. The aim of obtaining Cbz-glycinal could not be accomplished without a trapping agent. Nevertheless, HLADH recognizes Cbz-amino alcohols, which represents an interesting finding. Further applications can be proposed based on this fact.

CHAPTER 5

**COUPLING OF THE HLADH CATALYZED
OXIDATION OF CBZ-AMINO ALCOHOLS
AND ALDOL ADDITION FOR THE
PRODUCTION OF CBZ-AMINOPOLYOLS**

5. COUPLING OF THE HLADH CATALYZED OXIDATION OF CBZ-AMINO ALCOHOLS AND ALDOL ADDITION FOR THE PRODUCTION OF CBZ-AMINOPOLYOLS

5.1 Introduction

Dihydroxyacetone phosphate-dependent aldolases employ dihydroxyacetone phosphate (DHAP) as donor substrate to catalyze reactions with a relatively broad range of different acceptor aldehydes. They have been widely used to synthesize C-labeled sugars, deoxy sugars and fluoro sugars. Therefore, DHAP aldolases catalyze the formation of aminopolyols, precursors of iminocyclitols which are potent inhibitors of glycosidases and glycosyltransferases (Compain and Martin 2001), therapeutic targets for the design of new antibiotics and antimetastatic, antihyperglycemic or immunostimulatory agents (Wong, Halcomb et al. 1995; Stütz and Wiley 1999; Lillelund, Jensen et al. 2002).

An interesting application of these aldol addition reactions is to obtain Cbz-aminopolyols from Cbz-aminoaldehydes using rhamnulose-1-phosphate aldolase (RhuA) (Ardao, Alvaro et al. 2011; Pešić 2012). One pot oxidation of Cbz-ethanolamine using chloroperoxidase with aldol addition catalyzed by RhuA was successfully performed by Pešić (Pešić, López et al. 2013).

The aim of this chapter is to obtain Cbz-aminopolyols by coupling the oxidation of Cbz-ethanolamine by HLADH and the aldol addition with DHAP catalyzed by RhuA. The first reaction, consisting of Cbz-ethanolamine oxidation by HLADH, should produce the intermediary Cbz-glycinal. In presence of RhuA and DHAP, the aldol addition is expected to take place, avoiding the further oxidation of Cbz-glycinal to Cbz-glycine and producing the corresponding Cbz-aminopolyol ((3R)-5-[(Benzyloxy) carbonyl] amino)-5-deoxy-1-O-phosphonopent-2-ulose). Figure 5.1.1 illustrates the coupled system.

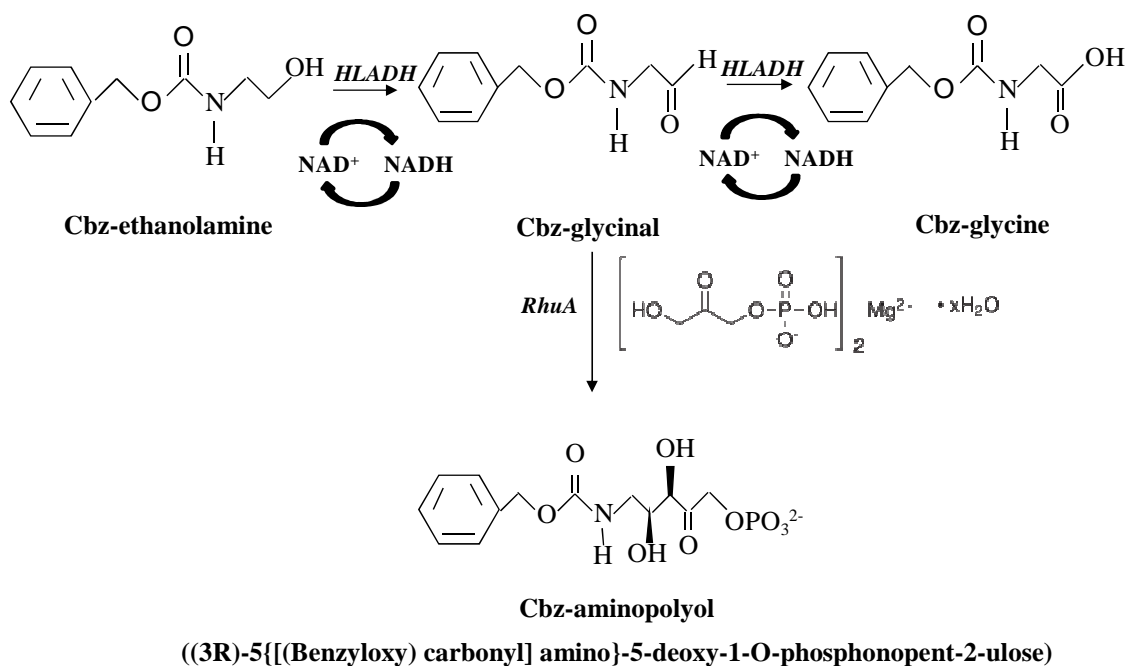


Figure 5.1.1 Coupled oxidation of Cbz-ethanolamine by HLADH and aldol addition catalyzed by RhuA

5.2 Methods

5.2.1 Coupled oxidation of Cbz-ethanolamine by HLADH and aldol addition catalyzed by RhuA

Coupled oxidation of Cbz-ethanolamine by HLADH and aldol addition catalyzed by RhuA were carried out by dissolving 20 mM Cbz-ethanolamine in 50 mM sodium phosphate buffer at pH ranging from 7.0 to 8.0. 20 mM NAD⁺ and 40 mM DHAP were solubilized and the pH was readjusted. An amount of RhuA was added to the reaction medium to reach 60 to 80 U/mL in a final volume of 5 mL. The reaction was initiated when HLADH was added to a final concentration between 20-450 U/mL. The reaction was performed at room temperature (20-22°C), under stirring and protected from light.

The course of the reactions was continuously monitored by measuring the concentration of the reactants and products formed by HPLC, following the method presented in section 3.4.5.2. The enzymatic activity of HLADH was analyzed according to section 3.4.1. DHAP concentration was determined as described in section 3.4.4.

The conversion was calculated as the percentage of Cbz-ethanolamine consumption with respect to their initial concentration. Yield was estimated as the production of Cbz-glycine/Cbz-glycinal/coupled reaction product with respect to the initial concentration of Cbz-ethanolamine.

5.2.2 Study of DHAP degradation

The study of DHAP degradation was performed in the reaction medium with Cbz-ethanolamine as described in section 5.2.1, using 20 U/mL HLADH and 30 U/mL RhuA, but without adding NAD⁺, at 4°C. The concentration of DHAP was monitored continuously following the procedure presented in section 3.4.4.

5.2.3 Coupled Cbz-ethanolamine oxidation and aldol addition with DHAP pulses

DHAP pulses addition in the coupled oxidation and aldol addition was carried out following the methodology described in section 5.2.1., with addition of 40 mM DHAP every 2 h during the first 6 h and then every 24 h. The reactions were monitored according to section 5.2.1.

5.2.4 Analysis of coupled reaction product by LC-MS

Unknown product from coupled reaction was tried to identify as putative Cbz-aminopolyol by Bruker micrOTOF-Q Mass Spectrometer (Bruker Daltonik, Bremen, Germany), equipped with an electrospray ionization source from Bruker and coupled with 1200 RR HPLC from Agilent (Agilent Technologies, Santa Clara, CA, USA). The analytic column employed was a reversed-phase column X Bridge C18, 5 μ m, 4.6 x 250 mm from Waters (Wexford, Ireland). The mobile phase consisted of a solvent A, with 2.5% v/v formic acid (HCOOH) in H₂O, and solvent B, with 8% v/v 1:4 HCOOH in H₂O/CH₃CN. The elution was carried out at 0.7 mL/min flow rate using a gradient from 20% B to 36% B over 20 min with peaks detection at 270 nm. The mass spectrometer was operated both in the positive and negative ion mode.

5.3 Results and discussion

5.3.1 Preliminary studies of the coupled oxidation of Cbz-ethanolamine by HLADH and DHAP aldol addition catalyzed by RhuA

5.3.1.1 Selection of the coupled reaction conditions

Determining the best reaction conditions for coupled enzymatic reactions involved the study of compatibility of both enzymes. HLADH catalyzed oxidation of alcohols occurs in a pH ranging from 7.0 up to 9.0 (Kvassman and Pettersson 1979; Sekhar and Plapp 1988), while RhuA is active in pH ranging from 6.0-9.0 and shows its optimum activity at 7.5 (Chiu and Feingold 1969). Regarding temperature, it was recommended to work at 4°C because of the chemical degradation of DHAP at higher values, as reported by Suau and coworkers (Suau, Alvaro et al. 2006).

In order to determine the best coupled reaction conditions, oxidation of 20 mM Cbz-ethanolamine was carried out with 20 mM NAD⁺ and 40 mM DHAP, adding HLADH and RhuA to reach 20 and 60 U/mL respectively, in a final volume of 5 mL. The effect of the pH was evaluated at 7.0 and 8.0 according to the explanation presented above. On the other hand, although recommended temperature is 4°C in order to avoid the chemical degradation of DHAP, at so low temperatures the rate of oxidation of Cbz-ethanolamine was very low as demonstrated in chapter 4, so room temperature (20-22°C) was selected as first approach. Nevertheless, in the following section (5.3.2) the reactions at 4 and 25°C will be compared. Figure 5.3.1 presents the results of the pH effect in the coupled reactions.

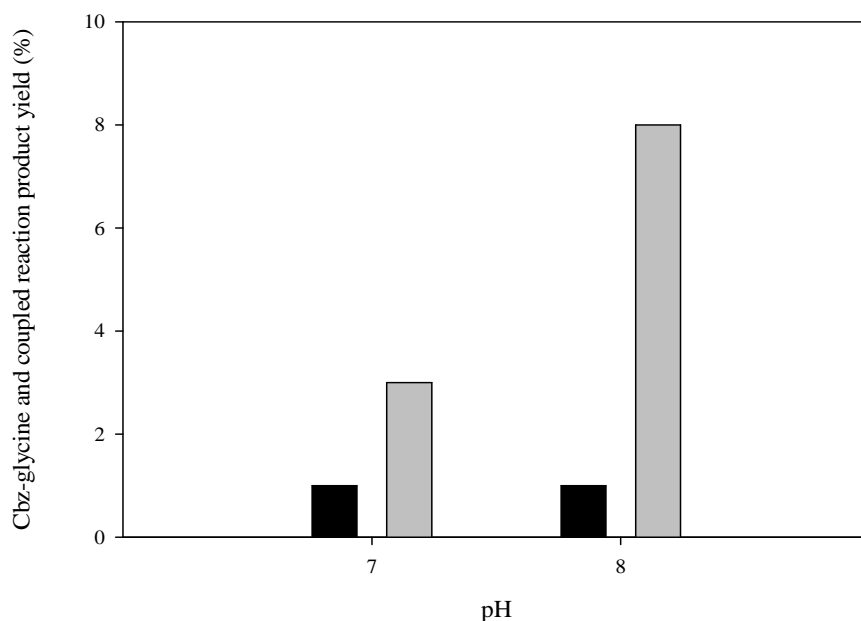


Figure 5.3.1 Effect of the pH in the coupled oxidation of Cbz-ethanolamine by HLADH and the aldol addition catalyzed by RhuA. The reactions were performed using 20 mM Cbz-ethanolamine with 20 mM NAD⁺ and 40 mM DHAP, adding HLADH and RhuA to reach 20 and 60 U/mL, respectively, in a final volume of 5 mL at pH 7 and 8 at room temperature (20-22°C) in 48 h reaction time. Coupled reaction product (black bars) and Cbz-glycine (gray bars).

Comparisons of the coupled reactions were made at pH 7.0 and 8.0 at 48 h of reaction. A new peak appeared in the chromatogram that could be an evidence of the formation of Cbz-aminopolyol, because it was observed at the same retention time obtained by Pešić (Pešić 2012) following the same analytical procedure. Hence, the yield obtained at both pH was $\approx 1\%$, a very low value corresponding to the small peak. Concerning the intermediate and undesired product, Cbz-glycinal was not detected and Cbz-glycine was present with a yield of 3.1 and 8.2% for pH 7.0 and 8.0, respectively. The highest concentration of acid was formed at higher pH as demonstrated in chapter 4. Regarding the enzymatic activity of the enzymes, although HLADH is more stable at higher pH (chapter 4) low remaining activities of 29.3 and 40.2% were obtained at pH 7.0 and pH 8.0, respectively. However, RhuA showed stability under these conditions, with 84.0% remaining activity at pH 7.0 and 96.4% at pH 8.0. Thus, the most adequate pH in terms of enzymatic preservation for the coupled reaction is 8.0 since it provided more stability to both enzymes HLADH and RhuA.

On the other hand, interferences were found in the determination of DHAP concentration. The quantification method is based on the reduction of DHAP by rabbit muscle glycerol 3-phosphate dehydrogenase (GDH) and NADH (section 3.4.4); the NADH formed in the oxidation of Cbz-ethanolamine interferes in the determination giving a false value of the absorbance and a consequently incorrect value of concentration.

5.3.1.2 DHAP degradation

It is well known that DHAP can be degraded by chemical and enzymatic mechanisms (Suau, Alvaro et al. 2006). The chemical degradation pathway was studied at pH 7 (Suau, Alvaro et al. 2006) and it was reduced using low temperatures. The enzymatic degradation of DHAP was evaluated by means of 40 mM DHAP with RhuA to a final concentration of 30 U/mL in presence of 20 mM Cbz-ethanolamine in 50 mM sodium phosphate buffer pH 8 and 20U/mL of HLADH, which can not react in absence of NAD^+ . The study was performed at 4°C in a final volume of 5 mL. The results are presented in figure 5.3.2.

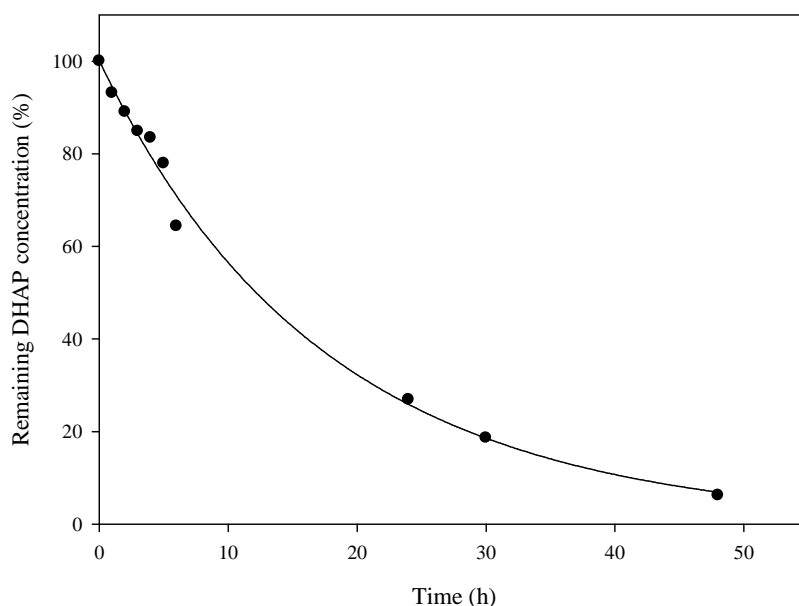


Figure 5.3.2 Enzymatic DHAP degradation at pH 8 and 4°C. The medium consisted of 20 mM Cbz-ethanolamine, 40 mM DHAP, HLADH and RhuA in final enzymatic activities of 20 and 30 U/mL, respectively in a volume of 5 mL.

Figure 5.3.2 evidences the enzymatic degradation of DHAP. Particularly, after the first 6 h of reaction the remaining concentration was 64.1% and then a marked decrease occurred, reaching 6.3% at 48 h. A reasonable approach to tackle the effect of the degradation could be the addition of DHAP in several pulses in the coupled reaction combined to a low temperature (4°C).

5.3.2 Coupled enzymatic reaction for the synthesis of Cbz-aminopolyol with DHAP pulses addition

DHAP pulses addition was proposed for the coupled oxidation based on the findings presented above. In order to enhance the kinetics of the Cbz-ethanolamine oxidation, the enzymatic activity of HLADH was 23-fold increased. As well, in order to promote the formation of Cbz-aminopolyol, RhuA enzymatic activity was 1.3-fold increased. As the DHAP concentration can not be monitored, the addition of several pulses of DHAP was proposed: 40 mM every 2 h during the first 6 h of reaction and then 40 mM every 24 h to guarantee a high concentration of DHAP available for the aldol addition. Concerning the temperature, 4 and 25°C were evaluated to establish comparisons. Figure 5.3.3 shows the substrate and products concentration profile, as well as the enzymatic activity during the combined reaction with DHAP pulses at 4 (A) and 25°C (B).

Coupled reaction yielded 11.2% of the unknown product at 52 h and 25°C, although there was no formation of this product at 4°C. Concerning the intermediary Cbz-glycinal, it was only present at 4°C with 1.0% yield. On the other hand, it was further oxidized to Cbz-glycine and presumably converted to Cbz-aminopolyol at 25°C. The undesired product, Cbz-glycine was the mostly formed yielding 16.3 and 64.2% at 4 and 25°C, respectively, corresponding to 4-fold increased yield at 25°C.

The stability of the enzymes was higher at low temperatures, as expected. Therefore, HLADH remaining activity was 1.3-fold increased, corresponding to 60.1 and 45.0% for 4 and 25°C, respectively. Besides, RhuA showed a similar behavior with 1.3 fold-increased at 4°C, yielding 61.2% remaining activity compared to 47.2% at 25°C.

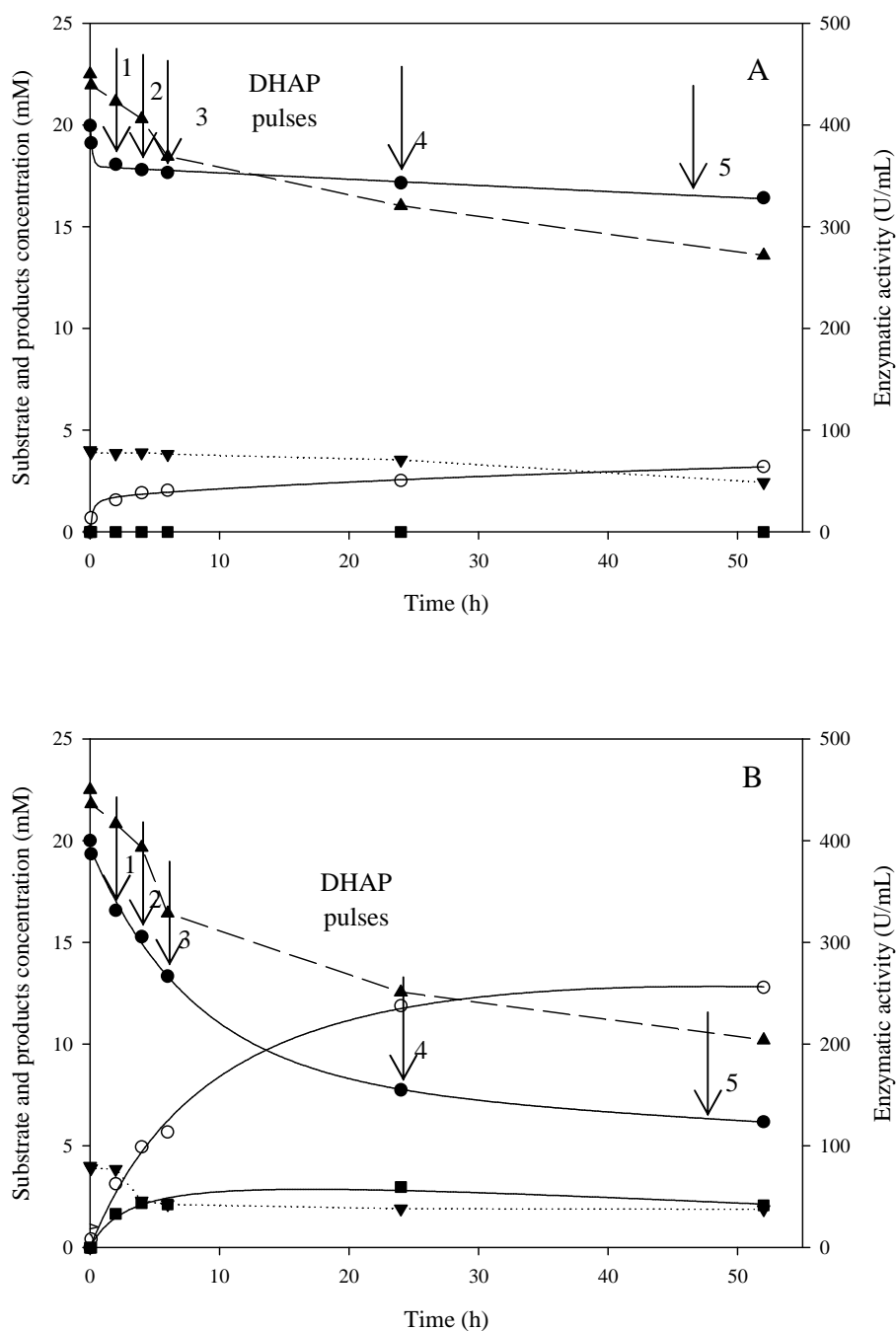


Figure 5.3.3 Time course of coupled Cbz-ethanolamine oxidation by HLADH and DHAP aldol addition catalyzed by RhuA at 4°C (A) and 25°C (B). The reactions were performed using 20 mM Cbz-ethanolamine with 20 mM NAD^+ and 40 mM DHAP, adding HLADH and RhuA to reach 450 and 80 U/mL, respectively, in a final volume of 5 mL at pH 8 with 40 mM DHAP pulses every 2 h during the first 6 h and then every 24 h during 52 h of reaction. Cbz-ethanolamine (●), Cbz-glycine (○), coupled reaction product (■), HLADH (▲), RhuA (▼).

Besides the known compounds, all the chromatograms showed a new peak from HLADH. This was studied since it overlaid the possible Cbz-aminopolyol peak. Hence,

the adsorption of HLADH in activated carbon was proposed with the intention of removing this peak. Therefore, 400 U/mL HLADH were vacuum-filtered with activated carbon and then the filtrated sample was injected in the HPLC in order to compare the area of the peak with respect to the initial sample. A reduction of 28.0% in the peak area was obtained with similar enzymatic activity for both initial and filtrated sample. Nevertheless, this reduction was not enough since it was still necessary to subtract the initial value (assuming that it was constant in time).

Then, the analysis of the unknown product was carried out by LC-MS using micrOTOF-Q in order to identify it as a possible Cbz-aminopolyol. According to Pešić (Pešić 2012) the molecular mass of the corresponding Cbz-aminopolyol is 363. The experimental results of the isotropic distribution both in negative and positive ion mode indicated a molecular mass of 204 which evidenced that the peak does not correspond to Cbz-aminopolyol. Furthermore, the existence of more than one compound in this peak was found, and it can be due to the presence of other clusters.

5.4 Conclusions

The purpose of this chapter was to obtain Cbz-aminopolyol by the coupled oxidation of Cbz-ethanolamine using HLADH and DHAP aldol addition catalyzed by RhuA. No formation of the corresponding Cbz-aminopolyol was obtained by evaluating several conditions as pH, temperature and DHAP pulses addition to minimize the chemical and enzymatic degradation of DHAP and promote Cbz-aminopolyol formation. The most important limitation lies in the fact that Cbz-glycinal can not be obtained by HLADH catalyzed oxidation of Cbz-ethanolamine. Even in presence of high available concentration of DHAP and RhuA activity, the reaction rate of the further oxidation into Cbz-glycine was considerably higher than the rate of formation of Cbz-aminopolyol. Although it seemed that some Cbz-aminopolyol was formed, its absence was confirmed by LC-MS. The present study confirms previous findings and contributes additional evidence that corroborates the high capacity of HLADH to directly oxidize amino alcohols into amino acids, which will serve as a base of future studies about this subject.

CHAPTER 6
HORSE LIVER ALCOHOL
DEHYDROGENASE CATALYZED
OXIDATION OF CBZ-AMINO ALCOHOLS
TO CBZ-AMINO ACIDS

POSTER (Chapter 6 and 7):

Rossmery A. Rodríguez-Hinestroza, Carmen López, Theodore Tzedakis, Josep López-Santín, M. Dolors Benaiges. "*Enzymatic synthesis of β -amino acids using Horse liver alcohol dehydrogenase and electrochemical cofactor regeneration*". Biotrans, July (2013), Manchester, UK.

6. HORSE LIVER ALCOHOL DEHYDROGENASE CATALYZED OXIDATION OF CBZ- β -AMINO ALCOHOLS TO CBZ- β -AMINO ACIDS

6.1 Introduction

Due to β -amino acids have a similar structure to α -amino acids, they are involved in the synthesis of biologically active compounds. Specifically, they exhibit significant biological and pharmacological properties (Cole 1994; Juaristi 1997; Abdel-Magid, Cohen et al. 1999; Juaristi and Lopez-Ruiz 1999). As described in section 1.8, β -amino acids have shown hypoglycemic and anti-etogenic activities in rats (Kanamaru, Shinagawa et al. 1985; Shinagawa, Kanamaru et al. 1987), insecticidal, antifungal and antihelminthic properties (Crews, Manes et al. 1986; Juaristi 1997) and they are antibiotics and antitumor agents, (Namikoshi, Rinehart et al. 1989; Winkler and Subrahmanyam 1992; Nicolaou and Guy 1995; Shih, Gossett et al. 1999). Besides, they facilitate interactions with receptors and enzymes and prevent peptidase degradation (Cheng, Gellman et al. 2001; Steer, Lew et al. 2002; Seebach, Beck et al. 2004; Seebach, Kimmerlin et al. 2004; English, Chumanov et al. 2006), they act as aminopeptidase inhibitors (Roers and Verdine 2001) and chiral auxiliaries, chiral ligands, chiral building blocks and intermediates in the synthesis of β -lactams (Hart and Ha 1989; Palomo, Aizpurua et al. 1991).

The high oxidative capacity of HLADH demonstrated in previous chapters was a significant finding since that this enzyme can oxidize alcohols rendering to the corresponding acids. Therefore, HLADH catalyzed oxidation of Cbz- β -amino alcohols to obtain Cbz- β -amino acids was proposed. Specifically, Cbz- β -amino propanol was selected as a model in order to produce its corresponding acid, Cbz- β -alanine. Figure 6.1.1 presents the scheme of the reaction.

On the other hand, the study of regeneration of nicotinamide cofactor was proposed because of its economic importance, in order to increase the productivity of the reaction and other advantages summarized in section 1.5 from the literature (Chenault and Whitesides 1987; van der Donk and Zhao 2003; Zhao and van der Donk 2003;

Hollmann and Schmid 2004; Wichmann and Vasic-Racki 2005; Hollmann, Hofstetter et al. 2006).

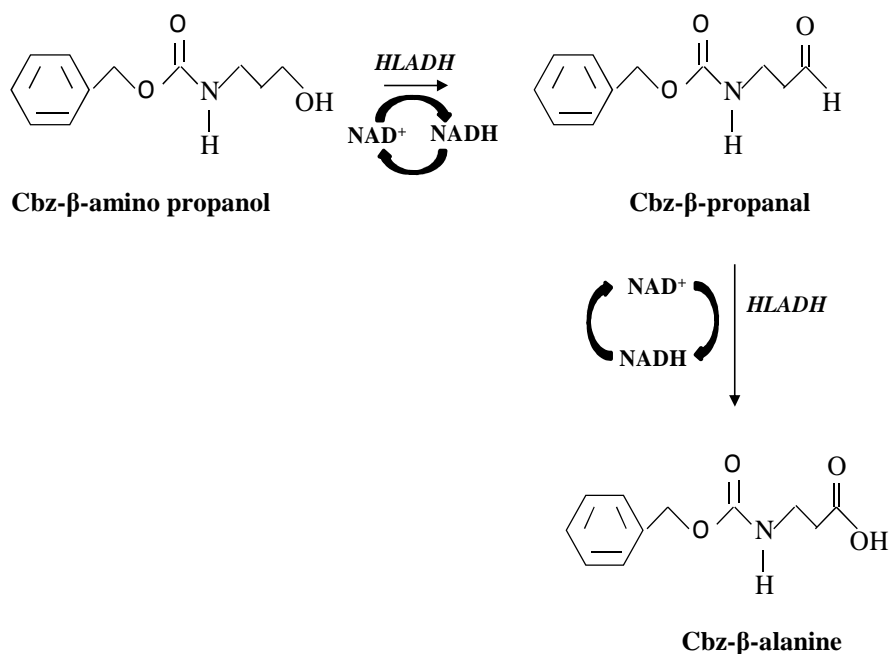


Figure 6.1.1 Oxidation of Cbz-β-amino propanol by horse liver alcohol dehydrogenase.

Enzymatic substrate-coupled regeneration of NAD⁺ was studied as a simple method to regenerate the cofactor NAD⁺. Also, only a cosubstrate is required, since HLADH catalyzes the reversible oxidation of alcohols. Acetaldehyde was selected to oxidize the formed NADH based on the results obtained in previous reports (Lemiere, Lepoivre et al. 1985; Orbegozo, Lavandera et al. 2009). Figure 6.1.2 shows the HLADH catalyzed oxidation of Cbz-β-amino propanol coupled with the NAD⁺ regeneration using acetaldehyde as cosubstrate.

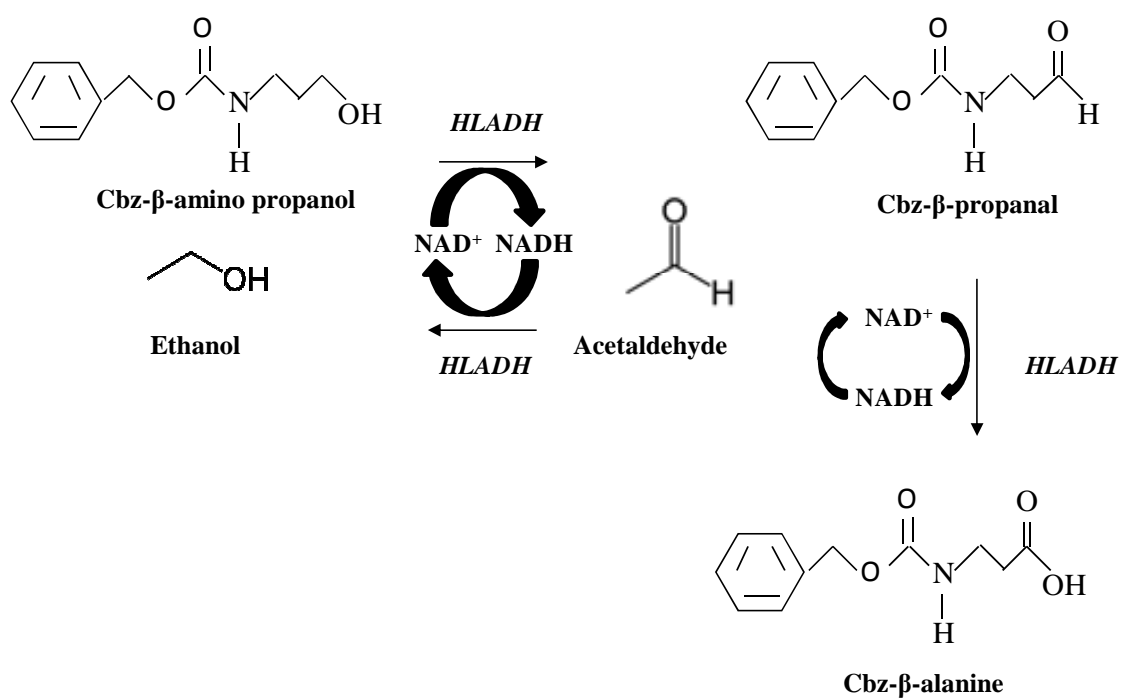


Figure 6.1.2 Oxidation of Cbz- β -amino propanol catalyzed by HLADH coupled with the enzymatic regeneration of NAD⁺ using acetaldehyde as cosubstrate.

6.2 Methods

6.2.1 Batch oxidation of Cbz- β -amino propanol catalyzed by HLADH

Batch oxidation of Cbz- β -amino propanol was performed by dissolving (10mM or maximal solubility) Cbz- β -amino propanol and (one half or the stoichiometric value) NAD⁺ in 100 mM sodium pyrophosphate buffer pH 8.7. The reaction was initiated when HLADH was added to the reaction medium to reach 100 U/mL in a final volume of 5 mL. It was performed under stirring, protected from light at the corresponding temperature.

The study of the influence of the temperature was carried out following the methodology presented above at several temperatures: 25, 30 and 40°C.

Temperature increment caused the precipitation of some impurities of the enzymatic solution, which were quantified by measuring the volume variation in time of several aliquots of reaction medium at 40°C.

The study of maximal solubility of Cbz- β -amino propanol and Cbz- β -alanine was carried out in two separated vials adding Cbz- β -amino propanol (1), and Cbz- β -alanine (2) in 100 mM sodium pyrophosphate buffer pH 8.7 in enough quantity to assure sobresaturation. The vials were magnetically stirred overnight at 25°C. The solubility of the Cbz- β -amino propanol and Cbz- β alanine was determined by the HPLC method presented in section 3.4.5.2.

To increase the solubility of Cbz- β -amino propanol several cosolvents were studied: dimethylformamide (DMF), 1,4-dioxane, acetonitrile (ACN), and dimethylsulfoxide (DMSO). The solid was solubilized in the cosolvent and then 100 mM sodium pyrophosphate buffer pH 8.7 was added to reach the concentration of 4% (v/v) in order to preserve enzymatic activity. The samples were analyzed qualitatively by observing the turbidity at 25°C.

The course of the reactions was continuously monitored by measuring the concentration of Cbz- β -amino propanol and the formed Cbz- β -alanine by HPLC as presented in

section 3.4.5.2, and the enzymatic activity of HLADH was analyzed using the method described in section 3.4.1.

The conversion was calculated as the percentage of the consumption of Cbz- β -amino propanol with respect to the initial concentration of Cbz- β -amino propanol. The yield was estimated as the production of Cbz- β -alanine with respect to the initial concentration of Cbz- β -amino propanol. The productivity was calculated as the Cbz- β -amino propanol consumed per unit of time during the reaction. The initial reaction rate was represented as the rate of Cbz- β -amino propanol consumption during the period of linear change in concentration.

6.2.2 Fed-batch oxidation of Cbz- β -amino propanol

Fed-batch reaction of Cbz- β -amino propanol was initiated following the same procedure of the batch configuration (section 6.2.1), but employing 112.2 mM as initial concentration of NAD⁺. Pulses of solid Cbz- β -amino propanol were added when the concentration decreased around 5 mM in order to restore the initial concentration of substrate. The reaction was performed using mechanic stirring in a final volume of 5 mL.

The course of the reaction and the calculations were made according to section 6.2.1.

6.2.3 Oxidation coupled to enzymatic cofactor regeneration

To perform the batch oxidation coupled to the enzymatic cofactor regeneration, the same methodology described in section 6.2.1 was followed. The maximal solubility of Cbz- β -aminopropanol was used with a stoichiometric amount of cofactor NAD⁺, and adding 200 mM acetaldehyde at 25°C in a final volume of 5 mL.

Fed-batch operation was carried out following the same procedure, but pulses of solid Cbz- β -amino propanol were added when the concentration decreased 5 mM.

The monitoring of the reaction and the calculations were made according to section 6.2.1. Total turnover number (TTN) was calculated as the number of moles of Cbz- β -alanine formed per initial mol of NAD⁺ during the course of the complete reaction.

6.3 Results and discussion

6.3.1 Preliminary studies of batch oxidation of Cbz- β -amino propanol catalyzed by HLADH

It has been demonstrated in chapter 4 that the enzyme HLADH recognizes amino alcohols as substrates rendering to amino acids. Taking advantage of this fact, it is envisaged to study the feasibility of the HLADH catalyzed oxidation of β -amino alcohols to β -amino acids which are interesting compounds due to their biological activity (Cole 1994; Juaristi 1997; Abdel-Magid, Cohen et al. 1999; Juaristi and Lopez-Ruiz 1999).

In order to perform a preliminary test to determine the HLADH oxidative capacity to recognize β -amino alcohols, Cbz- β -amino propanol (Cbz-3-amino propanol) was chosen to obtain Cbz- β -alanine. Similar reaction conditions as the oxidation of Cbz-ethanolamine that allowed the production of Cbz-glycine (e.g. half of the stoichiometric amount of NAD^+ and pH 8.7) were employed since those can promote the oxidation of Cbz- β -amino propanol to the corresponding acid.

Figure 6.3.1 presents the evolution of batch oxidation of 10 mM Cbz- β -amino propanol with 10 mM NAD^+ , catalyzed by 100 U/mL HLADH at pH 8.7 and 25°C in a final volume of 5 mL.

Figure 6.3.1 shows that, as a matter of fact, HLADH oxidizes Cbz- β -amino propanol to the corresponding acid, Cbz- β -alanine. This also accords with our earlier observations in chapter 4, which showed that Cbz-ethanolamine oxidation by HLADH renders to the acid, Cbz-glycine. As well, this finding is in agreement with previous studies reported in the literature that were mentioned in chapter 4, which indicate that HLADH catalyzes the dismutation and further oxidation of aldehydes (Abeles and Lee 1960; Dalziel and Dickinson 1965; Hinson and Neal 1975). Near 50% conversion was attained after 72 h as corresponding to the NAD^+ concentration employed. It has to be noticed that 2 mole of NAD^+ are stoichiometrically necessary per mole of substrate. Besides, 0.075 mM/h productivity was obtained in that period of time. Overall, the evolution of the enzymatic activity reveals stability of the HLADH. After 24 h, around 90% of remaining activity

can be observed, reaching 78.6 % at 72 h. Such stability was expected, based on the obtained results in the previous chapter. This characteristic represents a very positive reason for the use of HLADH as biocatalyst in this kind of reactions.

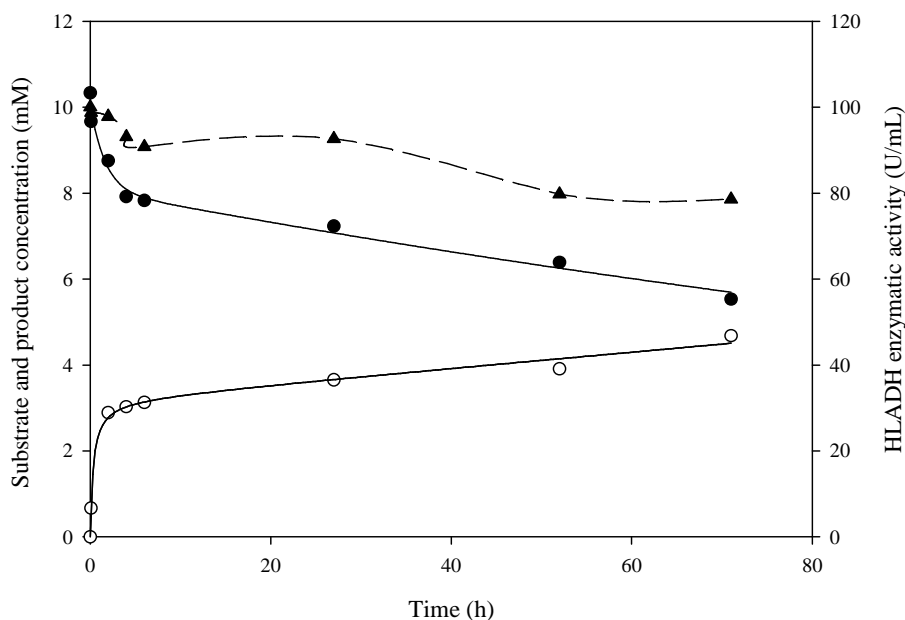


Figure 6.3.1 Time course of the preliminary batch oxidation of Cbz- β -amino propanol. The reaction was performed with 10 mM Cbz- β -amino propanol in 100 mM sodium pyrophosphate buffer pH 8.7, 10 mM NAD⁺ and 100 U/mL HLADH in a final volume of 5 mL at 25°C for 72 h. Cbz- β -amino propanol (●), Cbz- β -alanine (○), HLADH enzymatic activity (▲).

Owing to the good results presented above, the evaluation of the influence of the temperature in the Cbz- β -amino propanol oxidation was proposed, as part of the preliminary studies of the HLADH capacity to oxidize β -amino alcohols.

HLADH was partially purified from a horse liver, then some impurities tend to precipitate, being significant at 40°C. In addition, based on experimental observations, it was assumed that the precipitates formed at both 25°C and 30°C are similar and negligible.

Taking this fact into account, the effect of the temperature in the oxidation of Cbz- β -amino propanol to Cbz- β -alanine catalyzed by HLADH was studied at 25, 30 and 40°C and results are compared in table 6.3.1.

Table 6.3.1 Effect of the temperature in the preliminary batch oxidation of Cbz- β -amino propanol to Cbz- β -alanine catalyzed by HLADH after 50 h of reaction. The reactions were performed with 10 mM Cbz- β -amino propanol in 100 mM sodium pyrophosphate buffer pH 8.7, 10 mM NAD⁺ and 100 U/mL HLADH at 25°C.

Temperature (°C)	Cbz- β -amino propanol conversion (%)	Cbz- β -alanine yield (%)	Productivity (mM Cbz- β -amino propanol/h)	Initial reaction rate (mM Cbz- β -amino propanol/h)	HLADH remaining enzymatic activity (%)
25	38.3	37.1	0.074	0.79	82.7
30	42.5	39.5	0.084	0.85	84.1
40	49.4	30.5	0.087	0.94	80.8

On average, the remaining enzymatic activity was similar in all the cases with high values ($> 80\%$). Moreover, Cbz- β -amino propanol conversion increased with temperature, as expected. Nevertheless, it can be observed that Cbz- β -alanine yield decreased at 40°C . Consequently, the difference between conversion and yield is around 20%. However, these differences observed at 25 and 30°C were only around 3%. Hence, the existence of a secondary reaction involving the substrate or a reaction of Cbz- β -alanine degradation at 40°C could be conceivably hypothesized, although additional chromatographic peaks were not observed. Despite this, a clear benefit in the productivity was obtained by increasing the temperature.

In order to elucidate the significant gap between conversions and yields at 40°C , the study of the possible reaction or degradation of Cbz- β -alanine was proposed. Figure 6.3.2 shows the reactions of 10 mM Cbz- β -alanine 5 mM, $\text{NAD}^+:\text{NADH}$ (1:1) in 100 mM sodium pyrophosphate buffer pH 8.7, using 100 U/mL HLADH in a volume of 5 mL at 25 and 40°C .

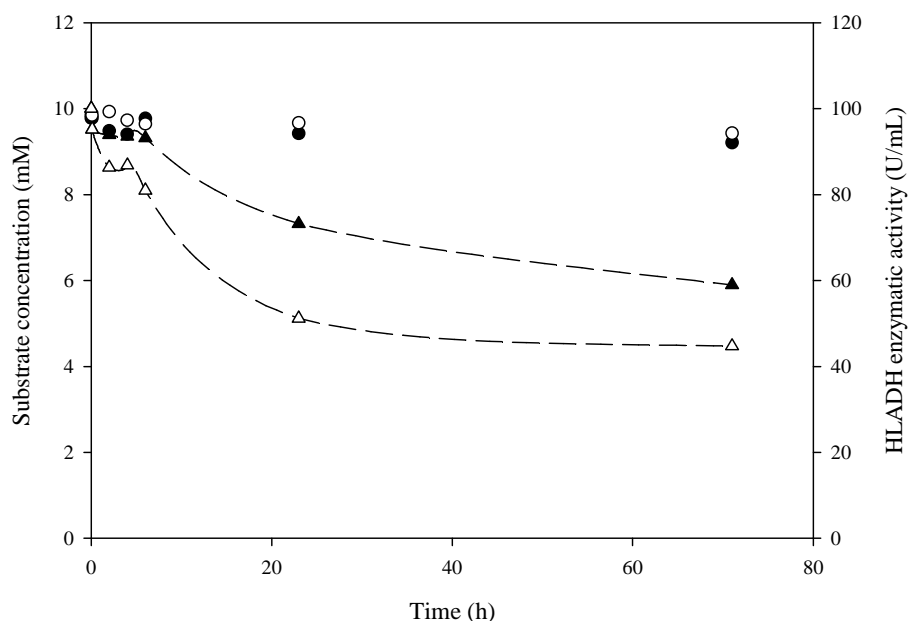


Figure 6.3.2 Reaction of Cbz- β -alanine using $\text{NAD}^+:\text{NADH}$ (1:1) at several temperatures. The reactions were performed with 10 mM Cbz- β -alanine in 100 mM sodium pyrophosphate buffer pH 8.7, 5 mM $\text{NAD}^+:\text{NADH}$ (1:1) and 100 U/mL HLADH in a final volume of 5 mL at 25°C for 72 h. Cbz- β -alanine: 25°C (●), 40°C (○); HLADH enzymatic activity: 25°C (▲), 40°C (△).

From the graph above we can see that there is no reaction of Cbz- β -alanine at both 25 and 40°C. Then, the small variation of the concentration found along time was attributed to experimental uncertainty, because there was not Cbz- β -amino propanol formed or the presence of another peak in the chromatogram. In addition, HLADH showed less stability in Cbz- β -alanine and maybe due to the presence of NADH; in fact, at the end of the reaction the remaining activity was 59.0% and 44.7% for 25 and 40°C respectively. Interestingly, this experiment allowed demonstrating that the equilibrium in the Cbz- β -amino propanol oxidation to Cbz- β -alanine is completely shifted to the acid production.

Turning now to the experimental evidence presented in table 6.3.1, conversion and productivity increased with the temperature as expected. Despite that, the precipitation of the impurities and the gap between conversion and yield at 40°C represents an inconvenience and a source of experimental errors. Besides, the enhancement of the conversion and productivity is not so significant between 25 and 30°C. Therefore, the temperature selected was 25°C.

6.3.2 Batch oxidation of Cbz- β -amino propanol for the synthesis of Cbz- β -alanine catalyzed by HLADH

Solubility studies of Cbz- β -amino propanol and Cbz- β -alanine in aqueous phase were performed in 100 mM sodium pyrophosphate buffer pH 8.7 at 25°C. The values obtained were 18.7 mM and 19.4 mM for Cbz- β -amino propanol and Cbz- β -alanine, respectively.

Trying to optimize the synthesis of Cbz- β -alanine from Cbz- β -amino propanol, the value of solubility of Cbz- β -amino propanol in 100 mM sodium pyrophosphate buffer pH 8.7 was chosen. This solution was diluted when the enzyme was added and provided an initial concentration between 13 and 17 mM. As well, a stoichiometric amount of NAD⁺ (1 mole of substrate requires 2 moles of NAD⁺ for complete oxidation) was proposed, and 25°C was selected as working temperature as indicated in the previous section. In addition, 100 U/mL of HLADH was employed based on the analysis presented in chapter 4.

Figure 6.3.3 provides the results obtained from the batch oxidation of 18.7 mM Cbz- β -amino propanol with 37.4 mM NAD^+ , 100 U/mL HLADH at pH 8.7 and 25°C in a final volume of 5 mL.

Strong evidence of the enhancement in conversion and yield was found when the Cbz- β -amino propanol oxidation was performed employing stoichiometric NAD^+ amount. Indeed, Cbz- β -amino propanol was completely converted to Cbz- β -alanine at 72 h of reaction. Accordingly, high concentration of substrate and cofactor shifted the equilibrium to the production of the acid and the initial reaction rate was 2.51 mM/h, 3.2-fold higher than the obtained in section 6.3.1. Likewise, there was a significant difference of Cbz- β -amino propanol conversion compared to the preliminary studies, as it was 2.1-fold improved at 50 h of reaction. Correspondingly, the productivity obtained was 0.24 mM/h.

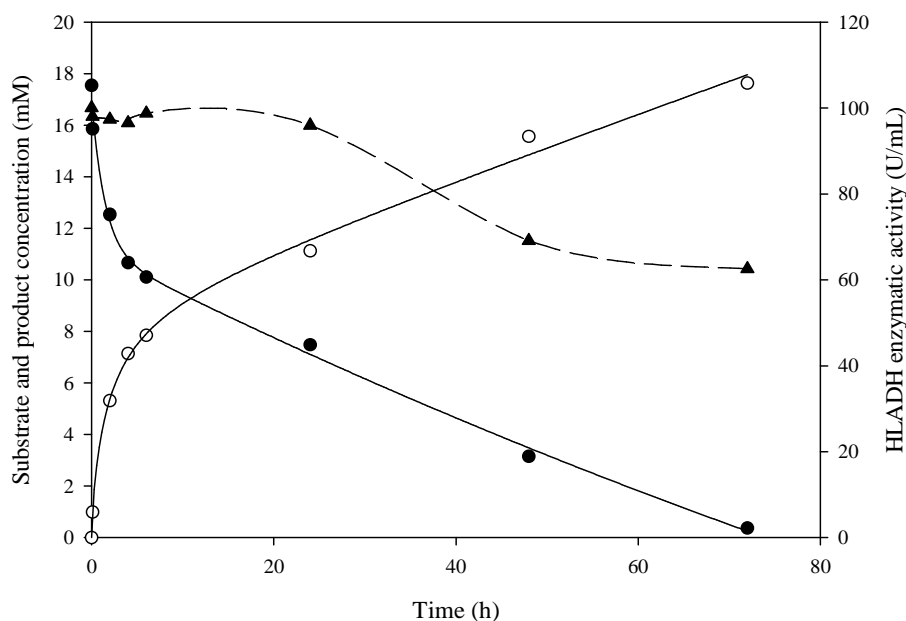


Figure 6.3.3 Time course of the batch oxidation of Cbz- β -amino propanol to Cbz- β -alanine. The reaction was performed with 18.7 mM Cbz- β -amino propanol in 100 mM sodium pyrophosphate buffer pH 8.7, 37.4 mM NAD^+ and 100 U/mL HLADH in a final volume of 5 mL at 25°C for 72 h. Cbz- β -amino propanol (\bullet), Cbz- β -alanine (\circ), HLADH enzymatic activity (\blacktriangle).

Concerning the HLADH enzymatic activity, the general evolution in the first 24 h showed stability, but a decrease was observed at 48 h of reaction, reaching 62.5% remaining activity at 72 h. The reason for this could be the reduction of the pH due to acid production, which causes enzyme instability.

In an attempt to increase the productivity of the synthesis of Cbz- β -alanine the use of water miscible organic solvents (cosolvents) was proposed. Cosolvents enabled the use of high concentrations of poorly water-soluble substrates as Cbz- β -amino propanol. However, as mentioned in chapter 4, the major drawback is that some of them can strongly inhibit the enzyme HLADH at low concentrations (Jones and Schwartz 1982).

No significant improvement in Cbz- β -amino propanol solubility was found with the use of cosolvents, achieving solubility values below 30 mM. These findings point out that the use of these cosolvents does not provide a significant benefit for the productivity. Furthermore, according to section 4.3.2.3, DMF and DMSO are strong HLADH inhibitors at low concentrations as well as 1,4-dioxane, and acetonitrile interacts with the cofactor (Jones and Schwartz 1982). Besides, potential HLADH substrates as alcohols and ketones have to be excluded. Other cosolvents proposed by Jones and Schwartz (Jones and Schwartz 1982) as N-methyl-2-pyrrolidone (NMP), hexamethylphosphoramide (HMPA), and diglyme are toxic and carcinogenic.

6.3.3 Fed-batch oxidation of Cbz- β -amino propanol to Cbz- β -alanine catalyzed by HLADH

Following the objective of productivity enhancement in the synthesis of Cbz- β -alanine, a fed-bath reactor was proposed. Poor solubility of Cbz- β -amino propanol (section 6.3.2) in water represents a disadvantage for the obtention of Cbz- β -alanine. Nevertheless, the addition of solid substrate pulses can represent a clear benefit. Therefore, the pulse addition was optimized using an initial excess of cofactor NAD^+ as 3-fold higher than the stoichiometric requirement for the initial substrate concentration, to maintain relatively high reaction rates. Figure 6.3.4 presents the evolution of the oxidation of 18.7 mM Cbz- β -amino propanol with 112.2 mM NAD^+ and 100 U/mL HLADH in a final volume of 5 mL at pH 8.7 and 25°C.

Fed-batch Cbz- β -alanine production resulted in 88.4% yield at 96 h after the addition of three Cbz- β -amino propanol pulses. Consequently, the productivity was 0.56 mM/h which corresponds to 2.3-fold improved value compared with batch reaction. Besides, the initial reaction rate was 4.16 mM/h, corresponding to 1.7-fold higher than the one obtained in batch mode, as expected due to the higher initial NAD^+ concentration. As a

consequence of the high initial reaction rate, the first substrate pulse was required after only 3 h of reaction. Other two substrate pulses were needed at 25.5 and 49 h, but after the last pulse there was a significant decrease of the reaction rate. This result seems to be due to the loss of the HLADH enzymatic activity (46% remaining at 49 h), the decrease of the NAD^+ concentration because of its consumption in the reaction and/or by the fact that HLADH oxidations often suffer inhibition by products and NADH (Kochius, Magnusson et al. 2012).

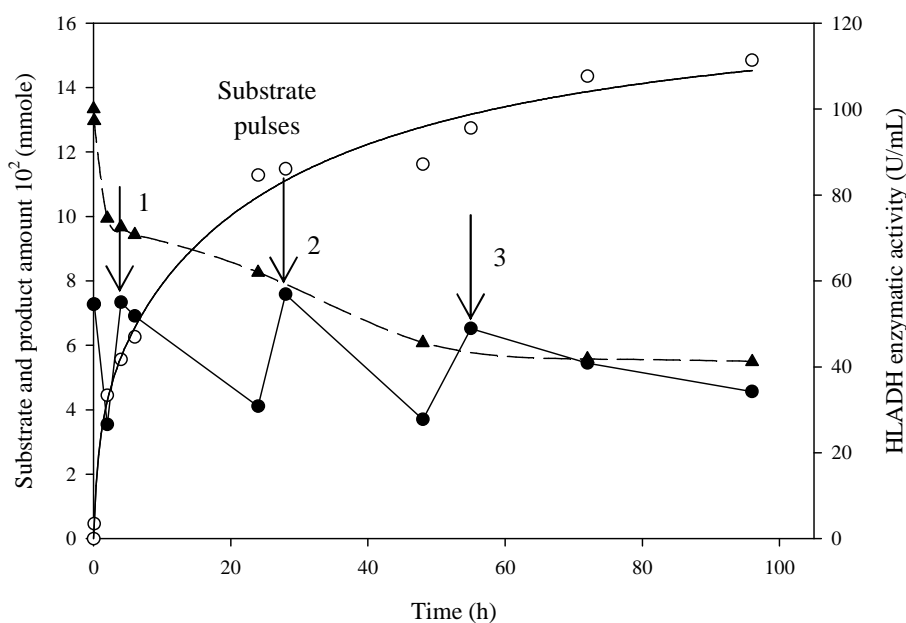


Figure 6.3.4 Time course of the fed-batch oxidation of Cbz- β -amino propanol to Cbz- β -alanine. The reaction was performed with 18.7 mM Cbz- β -amino propanol in 100 mM sodium pyrophosphate buffer pH 8.7, 112.2 mM NAD^+ and 100 U/mL HLADH in a final volume of 5 mL at 25°C for 96 h. 5 mM Cbz- β -amino propanol pulses were added at 3, 25.5 and 45.5 h. Cbz- β -amino propanol (●), Cbz- β -alanine (○), HLADH enzymatic activity (▲).

Interestingly, the solubility of Cbz- β -alanine seemed to be enhanced with the decrease of pH because of the Cbz- β -alanine formation, which allowed the obtention of more than 30 mM. However, it could destabilize the enzyme as mentioned above. Therefore, a significant instability of HLADH was appreciated. Specifically, 25% of activity loss was observed during the first 2 h of reaction, more than the measured at around 48 h in the batch experiment (figure 6.3.3). This trend continues until 96 h reaching 41.2% remaining activity. The main reason for this could be a fast pH decrease due to the attained acid yields ($\approx 50\%$ conversion at 2 h). At this point, it must be considered that

although the concentration of sodium pyrophosphate buffer pH 8.7 is high, it can not effectively buffer such an abrupt reduction of the pH.

6.3.4 Enzymatic substrate-coupled regeneration of NAD⁺

Enzymatic substrate-coupled regeneration of NAD⁺ represents a simple way to regenerate the cofactor NAD⁺. A few enzymes are suitable for the regeneration of oxidized nicotinamide cofactors. Owing that HLADH catalyzes the reversible oxidation of alcohols, only a cosubstrate is required to regenerate NAD⁺.

The system acetaldehyde/HLADH is inexpensive, and represents a common method employed to reoxidize the NADH formed (Weckbecker, Gröger et al. 2010). Lemièrre and coworkers (Lemièrre, Lepoivre et al. 1985) studied several alcoholic substrates as cyclohexanol and 2-cyclohexenol in presence of acetaldehyde, and they were oxidized nearly quantitatively within 1 h and 6 h respectively. Orbegozo and coworkers (Orbegozo, Lavandera et al. 2009) applied this system to oxidize benzyl alcohol with 100% conversion at 23 h.

Given that the use of a stoichiometric amount of cofactor is expensive (Chenault, Simon et al. 1988), a small quantity of cofactor is usually employed in regeneration systems as it was exemplified by Orbegozo and co-workers (Orbegozo, Lavandera et al. 2009). But it has to be noticed that some regeneration methods have been developed using catalytic quantities (Hummel and Kula 1989; Iwuoha and Smyth 2003).

6.3.4.1 Batch oxidation of Cbz-β-amino propanol and enzymatic regeneration of NAD⁺

In order to study the enzymatic substrate-coupled regeneration of NAD⁺ a batch reactor configuration using the system acetaldehyde/HLADH was proposed. Nevertheless, the oxidation of Cbz-β-amino propanol to Cbz-β-alanine catalyzed by HLADH is a slow reaction (section 6.3.2), and, as a consequence, it was necessary to employ a stoichiometric amount of NAD⁺ (1 mole of substrate requires 2 moles of NAD⁺) or at least one half (1 mole of substrate per 1 mole of NAD⁺) for kinetic reasons. Figure 6.3.5 shows the concentration profile of the coupled reaction of 18.7 mM Cbz-β-amino

propanol, 37.4 mM NAD^+ with 200 mM acetaldehyde and 100 U/mL HLADH in a final volume of 5 mL at pH 8.7 and 25 °C.

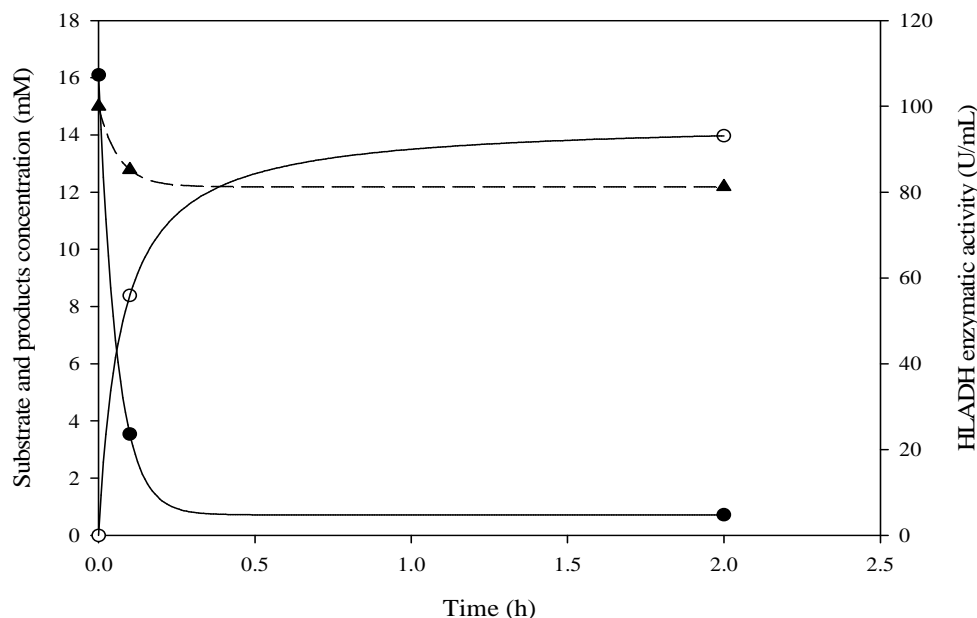


Figure 6.3.5 Time course of the batch synthesis of Cbz- β -alanine using the enzyme substrate-coupled regeneration system acetaldehyde/HLADH. The reaction was performed with 18.7 mM Cbz- β -amino propanol in 100 mM sodium pyrophosphate buffer pH 8.7, 37.4 mM NAD^+ , 200 mM acetaldehyde and 100 U/mL HLADH at 25°C for 2 h. Cbz- β -amino propanol (\bullet), Cbz- β -alanine (\circ), HLADH enzymatic activity (\blacktriangle).

The initial reaction rate was 84.78 mM/h, corresponding to 20.3-fold improved compared to the fed-batch reaction without regeneration using 6-fold higher initial concentration of cofactor. 54.3% Cbz- β -amino propanol conversion was reached in the first 0.1 h of reaction. Taking advantage of this fact, the first 5 mM pulse of substrate was added at 0.5 h resulting in a conversion of 65.2% at 2 h. However, additional 5 mM pulses at 2.5, 4 and 6 h did not have the same effect. The conversion decreased and the reaction stopped at 2 h, as can be confirmed with the evolution profile of Cbz- β -alanine which reached a plateau at 2 h. Despite this, the productivity of Cbz- β -alanine at 2 h (6.84 mM/h) was 12.2-fold improved compared to the fed-batch reaction without regeneration at 96 h. On the other hand, the TTN was calculated to be 0.92, which is consistent with the value of 1 obtained by Weibel (Weibel, Weetall et al. 1971).

Concerning the HLADH enzymatic activity, 8% of activity loss was observed at 0.1 h of reaction. This can be explained by the marked drop of the pH due to the Cbz- β -

alanine formed as mentioned in section 6.3.3, and by the presence of acetaldehyde and the corresponding ethanol, that could deactivate the enzyme (Chenault, Simon et al. 1988). Even so, the enzyme was stable until 24 h with 79.3% remaining activity, supporting the fact that the mayor instability was because of the initial Cbz- β -alanine formed and when the reaction stopped the enzymatic activity only showed a slightly decrease in time.

These results are very positive and quite revealing in several ways. First, Cbz-amino propanol is practically converted (95%) to Cbz- β -alanine in 2 h. This finding is in agreement with Lemière and coworkers (Lemiere, Lepoivre et al. 1985), who showed that the system acetaldehyde/HLADH provides a rapid conversion of alcohols, attributed to the high concentration of regenerated NAD^+ available. Thus, the initial reaction rate (125.5 mM/h) and the productivity (7.69 mM/h) observed were 50 and 32-fold improved, respectively, demonstrating a significant benefit compared to the batch reaction without cofactor regeneration. A total turnover number of 0.48 was obtained, which is consistent with the fact that a high concentration of initial cofactor NAD^+ (stoichiometric) was used.

6.3.4.2 Fed-batch oxidation of Cbz- β -amino propanol and enzymatic regeneration of NAD^+

Finally, based on the positive results obtained with the batch reaction in the previous section, fed-batch configuration was proposed in order to improve the productivity as demonstrated in section 6.3.3. Fed-batch configuration expected to be favorable for a HLADH substrate-coupled regeneration as an excess of a second substrate is required to promote the oxidation of NADH, but some competitiveness for the enzyme by its product formed (ethanol in this case) can be present. Because of the high improvement in the initial reaction rate observed previously, one half of the stoichiometric value of NAD^+ was used for economical reasons. Figure 6.3.6 presents the evolution of the mole profile of the enzymatic substrate-coupled regeneration system acetaldehyde/HLADH applied to the synthesis of Cbz- β -alanine.

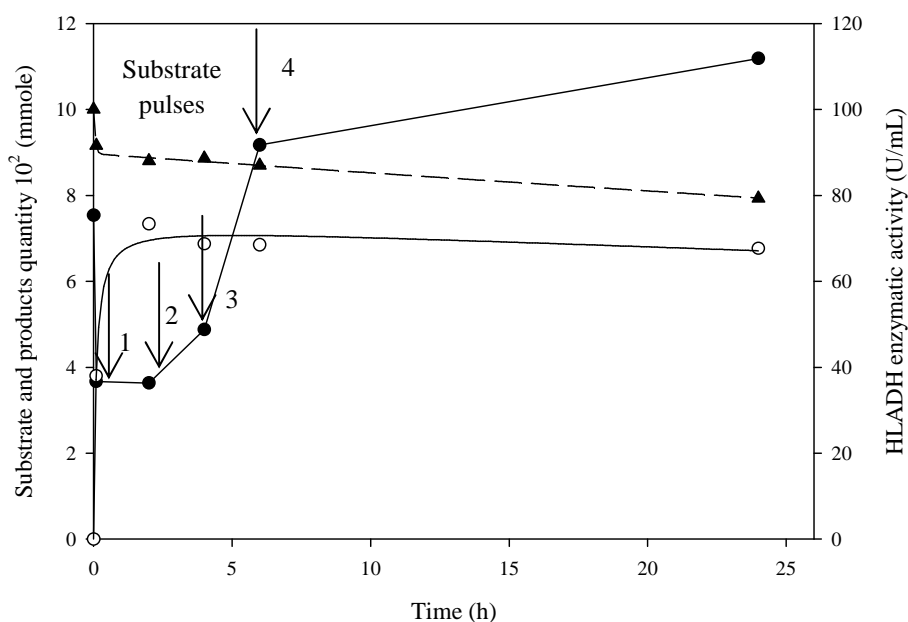


Figure 6.3.6 Time course of the fed-batch synthesis of Cbz- β -alanine using the substrate-coupled regeneration system acetaldehyde/HLADH. The reaction was performed with 18.7 mM Cbz- β -amino propanol in 100 mM sodium pyrophosphate buffer pH 8.7, 18.7 mM NAD⁺, 200 mM acetaldehyde and 100 U/mL HLADH in a final volume of 5 mL at 25°C for 96 h. 5 mM Cbz- β -amino propanol pulses were added at 0.5, 2.5, 4 and 6 h. Cbz- β -amino propanol (●), Cbz- β -alanine (○), HL-ADH enzymatic activity (▲).

There are several possible explanations to the results obtained in this experiment. Considering that the same enzyme catalyzes two separated reactions simultaneously, it is difficult to achieve thermodynamically favorable conditions for both reactions in the same reaction medium (Liu and Wang 2007). Therefore, since acetaldehyde is reduced by HLADH into ethanol using NADH, the ethanol could compete with the Cbz- β -amino propanol for the enzyme, taking into account that ethanol is the natural substrate of HLADH. For this reason, the oxidation of Cbz- β -amino propanol is very fast during the first 2 h, and at this moment enough concentration of ethanol was formed and the competition started. Otherwise, a possible inhibition of HLADH by acetaldehyde has to be noticed (Sund and Theorell 1963). Also, it was observed by Orbegozo and coworkers (Orbegozo, Lavandera et al. 2009) that despite the use of high concentrations of acetaldehyde that should shift the equilibrium, the conversion decreased.

Finally, table 6.3.2 provides a summary of the results obtained in this chapter for the oxidation of Cbz- β -amino propanol to Cbz- β -alanine catalyzed by HLADH.

Table 6.3.2 Summary of the results for the oxidation of Cbz- β -amino propanol to Cbz- β -alanine catalyzed by HLADH. 18.7 mM Cbz- β -amino propanol, 100 U/mL HLADH , pH 8.7 and 25°C were used for all the cases.

Configuration	NAD⁺ regeneration	NAD⁺ initial concentration (mM)	Reaction time (h)	Conversion Cbz-β-amino propanol (%)	Productivity (mM Cbz-β-alanine/h)
Batch	-	Stoichiometric	72	100.0	0.24
Fed-batch	-	3-fold high the stoichiometric value	96	88.4	0.56
Batch	√	Stoichiometric	2	95.5	7.69
Fed-batch	√	One half of the stoichiometric value	2	65.3	6.84

6.4 Conclusions

In this chapter it has been demonstrated that HL-ADH recognizes β -amino alcohols as substrates. Furthermore, their enzymatic oxidation to β -amino acids has been studied, employing Cbz- β -amino propanol as model substrate. The study of the reaction using a stirred tank reactor conducted to set up the best reaction conditions for the production of Cbz- β -alanine. Fed-batch operation, with addition of several pulses of substrate, led to a significant improvement in the productivity.

The high cost of the cofactor pointed out the requirement of NAD^+ regeneration step. Enzymatic coupled-substrate regeneration of NAD^+ was evaluated using the system acetaldehyde/HLADH. The batch configuration provided satisfactory result since an almost complete conversion of Cbz- β -amino propanol to Cbz- β -alanine was obtained in the first two hours of reaction.

Although enzymatic regeneration of NAD^+ could be completed with success in discontinuous oxidation of Cbz- β -amino propanol, the results did not show a significant benefit combining enzymatic regeneration with fed-batch addition of substrate. Based on this fact, other cofactor regeneration systems should be studied in order to optimize the production of Cbz- β -alanine and other amino acid products by horse liver alcohol dehydrogenase.

CHAPTER 7

**HLADH-CATALYZED OXIDATION OF CBZ-
AMINO ALCOHOLS USING
ELECTROREGENERATED NAD⁺ IN A
FILTER-PRESS MICROREACTOR**

The work presented in this chapter was carried out in the research group of Prof. Theodore Tzedakis at the Laboratoire de Génie Chimique, Université Paul Sabatier, Toulouse, France

7. HLADH-CATALYZED OXIDATION OF CBZ-AMINO ALCOHOLS USING ELECTROREGENERATED NAD^+ IN A FILTER-PRESS MICROREACTOR

7.1 Introduction

The regeneration of the cofactor NAD^+ represents an important stage in the establishment of the best conditions for the oxidation of Cbz- α -amino alcohols and Cbz- β -amino alcohols catalyzed by HLADH.

Particularly, the electrochemical regeneration provides several advantages compared to other regeneration methods as summarized by Hollmann (Hollmann and Schmid 2004). As it was explained in section 1.5.4, the electrochemical regeneration of the cofactor NAD^+ can be performed by a direct, indirect and enzyme-coupled operation. Therefore, in the direct regeneration the cofactor reacts by itself at the electrode; the indirect regeneration includes the use of mediators that transfer electrons between the electrode and the cofactor; and finally in the enzyme-coupled electrochemical cofactor regeneration, an enzyme is required for the electron transfer between the cofactor and the electrogenerated mediator. In this work a direct electrochemical regeneration method of the cofactor NAD^+ was proposed due to its simplicity; in addition, it has been proven as an effective method employing alcohol dehydrogenases (Fassouane, Laval et al. 1990; Biade, Bourdillon et al. 1992; Anne, Bourdillon et al. 1999).

The chemical equation of the coupled regeneration system for both oxidations of Cbz-ethanolamine and Cbz- β -amino propanol is presented as follows:

Oxidation of Cbz-ethanolamine:

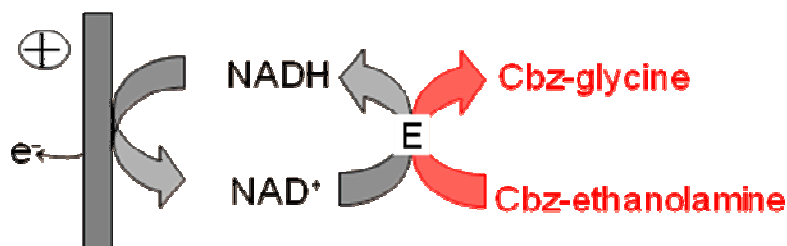
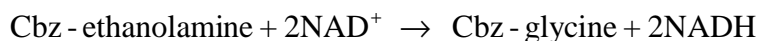


Figure 7.1.1 Scheme of the chemical oxidation of Cbz-ethanolamine and direct electrochemical regeneration of NAD^+ .

Oxidation of Cbz- β -amino propanol:

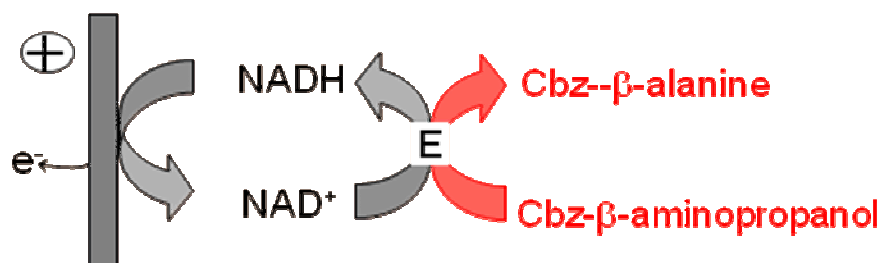


Figure 7.1.2 Scheme of the chemical oxidation of Cbz- β -amino propanol and direct electrochemical regeneration of NAD^+ .

7.2 Materials and methods

7.2.1 Electrokinetic studies

The electrochemical study of the compounds involved in the NADH oxidation was carried out into a three-electrode classical electrochemical cell. An Autolab Potentiostat/Galvanostat PGSTAT30 was used for the oxidation of Cbz-ethanolamine, while the oxidation of Cbz- β -amino propanol was achieved using an EGG instrument, Princeton Applied Research Potentiostat Galvanostat model 283. The working electrode WE (anode) was a rotating disk (platinum and gold) polished before each experiment. Platinum was used as a counter electrode CE (cathode), burned in advance.

The electrode potentials were measured with respect to a saturated calomel electrode SCE (reference electrode: RE) immersed in Luggin capillary. The overall apparatus is illustrated in figure 7.2.1.

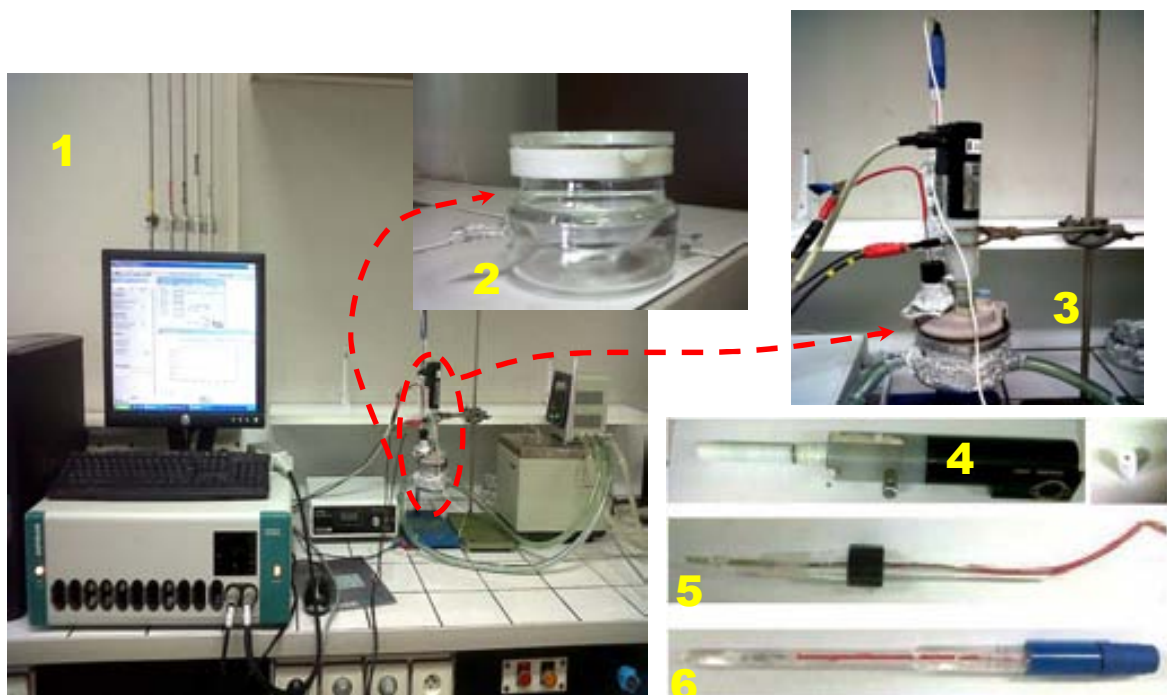


Figure 7.2.1 Apparatus used to carry out electrokinetic studies (1). Insets: (2) Reduced volume (20 mL) Metrohm cell; (3) Cell with electrodes; (4) Working electrode=rotating disc of platinum or gold; (5) Platinum counter electrode; (6) Saturated calomel used as reference electrode.

The current-potential (I vs E) curves were plotted for the compounds involved in the different oxidations of substrates (Cbz-ethanolamine and Cbz- β -amino propanol) catalyzed by HLADH at room temperature (20-22°C). NADH solutions were protected from light and sodium pyrophosphate buffer was used to adjust the pH of all solutions at 8.7.

The estimation of the kinetic parameters of the electrochemical oxidation of NADH was performed using the current-potential curves obtained in transient state by cyclic voltammetry on the disk electrode.

For mass transfer limited phenomenon, cyclic voltammetry provides peak shaped current–potential (I=f (E)) curves. The following equation lies the peak current (I/A) versus the potential scan rate (r /V/s) (Bard and Faulkner 2001; Tzedakis, Cheikhou et al. 2010) at 289K:

$$I_{\text{peak}} \text{ (A)} = 2.99 \cdot 10^5 \cdot n_{\text{overall}} \sqrt{\alpha n_{\text{limstep}} \cdot D_{\text{NADH}} \cdot S \cdot C^{\circ}} \cdot \sqrt{r} \quad (7.1)$$

The peak potential (E_{peak} /V), constant for reversible redox systems, varies linearly versus the natural logarithm of the potential scan rate for irreversible redox systems:

$$E_{\text{Peak}} \text{ (V)} = E^{\circ} - \frac{R \cdot T}{\alpha n_{\text{limstep}} \cdot F} \left(0.78 + \ln \sqrt{\frac{\alpha n_{\text{limstep}} \cdot F \cdot D_{\text{NADH}}}{R \cdot T \cdot (k^{\circ})^2}} \right) + 0.5 \cdot \frac{R \cdot T}{\alpha n_{\text{limstep}} \cdot F} \cdot \ln(r) \quad (7.2)$$

Where:

n_{overall} : electron number (dimensionless)

α : Anodic charge transfer coefficient (dimensionless)

D_{NADH} : Diffusion coefficient (cm²/s)

C° : Initial concentration (mol/cm³)

S : Surface area of the electrode (3.14·10⁻⁴ cm²).

R : Universal constant of gases (8.314 J·mol⁻¹·K⁻¹)

T : Temperature (K)

F : Faraday constant (96500 C/mol)

E° : Standard Potential (for NADH/NAD⁺: 0.32V)

k° = Intrinsic heterogeneous electronic transfer constant (m/s)

r = potential scan rate (V/s)

The examined range for potential scan rates is $20 < r /_{\text{mV/s}} < 200$ in the kind of *cyclic voltammetry without stirring* ($\omega_{\text{rotating disk}} = 0$ rpm). For steady state current potential curves plotted on a *rotating disk anode*, the examined range for angular velocities is in the range: $500 < \omega /_{\text{rpm}} < 5000$ with a fixed scan rate: $r = 5$ mV/s.

For all curves plotted for the regeneration system with Cbz- β -amino propanol the angular velocity ω and the potential scan rate were fixed respectively at 1000 rpm and $r = 5$ mV/s.

7.2.2 Preparative electrolysis

The multichannel filter press microreactor patented by Tzedakis and coworkers (Tzedakis, Kane et al. 2006) to perform the regeneration of NADH (reduction of NAD⁺) was used in the present study to carry out the electrochemical oxidation of NADH (Figure 7.2.2). The microreactor is constituted of two micro-grooved rectangular plates (5 cm x 5 cm x 0.2 cm) made of platinum and gold; both of them were evaluated as working electrode materials and the best material was chosen for preparative electrolysis. Each electrode has about 150 hemicylindrical microchannels ($l = 3$ cm, $r \sim 75$ μm) which permitted to electrolyze from 0.1 to 5 cm³/min. Both anodes WE and cathode CE are separated by a nafion cationic membrane (N1135). A platinum wire was used as pseudoreference electrode. Two large channels (3 mm x 0.7 mm x 40 mm), located at the bottom and at the top of the metal plate, provide uniform distribution of electrolyte to all microchannels as well as uniform output of the electrolyzed solutions (Tzedakis, Kane et al. 2006; Tzedakis, Kane et al. 2006; Cheikhou and Tzedakis 2008). In addition each electrode includes a heat exchanger which allows operating under desired temperature. The microreactor was connected to a potentiostat Autolab PGSTAT30, and a Watson Marlow 2055 peristaltic pump. The feed catholyte tank contained 100 mM sodium pyrophosphate buffer pH 8.7, and was also recirculated through the cathode. The system is illustrated in figure 7.2.2.

Owing to the inconvenience of polishing the electrodes, before every experiment the working solution was recirculated in the WE and the buffer in the CE by several minutes to ensure reproducible results.

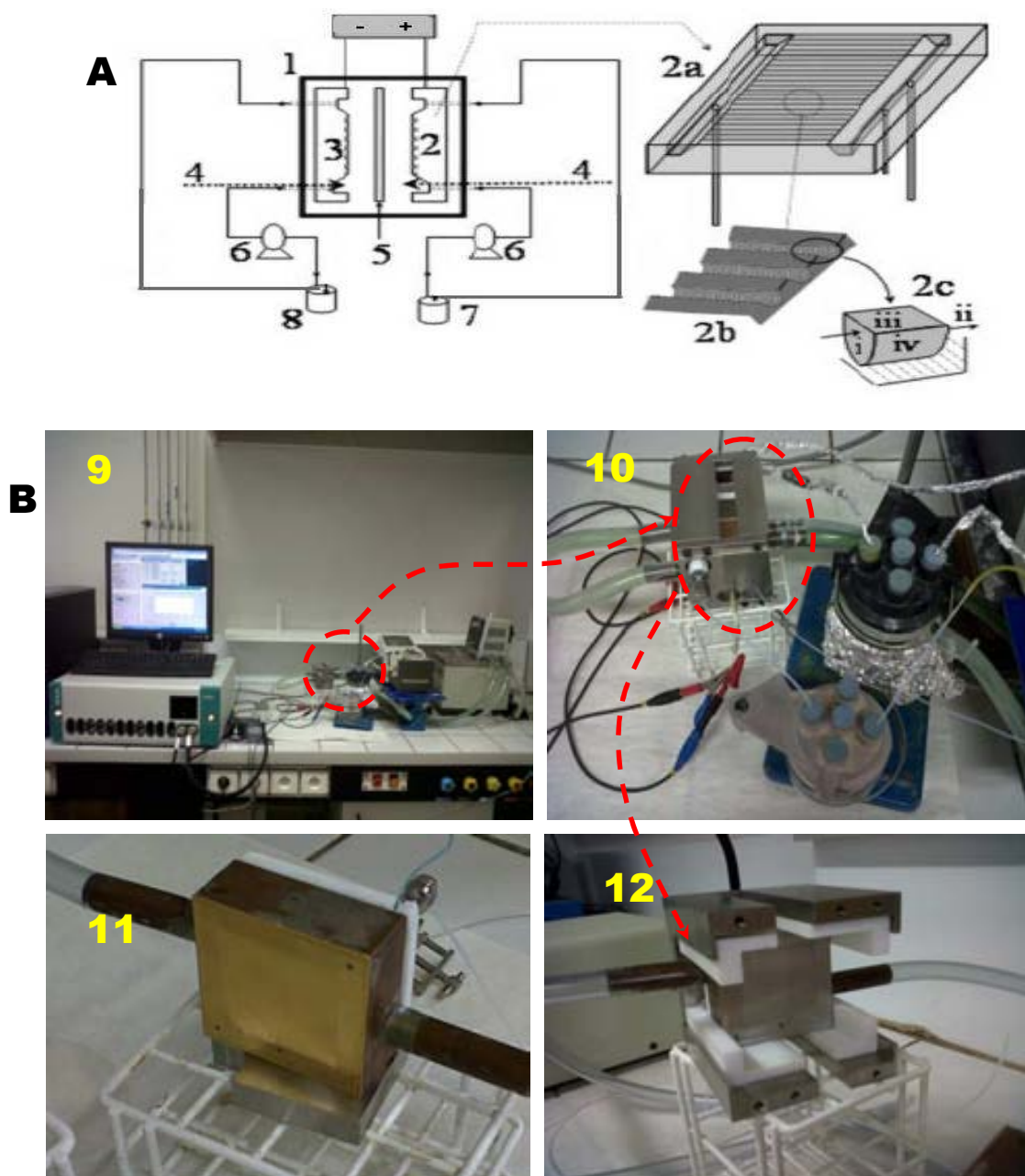


Figure 7.2.2 Schematic representation (A) and pictures (B) of the experimental set-up used to carry out preparative electrolysis. (A) Scheme: (1) Filter-press microreactor; (2, 2a/2b/2c zoom of the microchannels: (i) inlet face, (ii) outlet face, (iii) membrane face, (iv) electrode face) Microstructured anode; (3) Microstructured cathode; (4) ‘pseudo-reference’ electrodes (Pt wire); (5) Nafion cationic membrane; (6) Peristaltic pumps; (7) Anolyte feed storage tank; (8) Catholyte feed storage tank. (B) Pictures: (9) Overall apparatus used; (10) Filter-press microreactor system and feed tanks for anolyte (covered by aluminum foil) and for catholyte; (11 and 12) dismantled microreactor shown micro-grooved anode (gold) and cathode (platinum).

The conversion for electrolysis in continuous mode, for a specie j was calculated according to the following equation:

$$X = \frac{\text{moles number of } j \text{ transformed by electrolysis}}{\text{total moles number of } j} \quad (7.3)$$

For the cofactor NADH:

If the conversion is instantaneous, at the outlet of the microreactor:

$$X = \frac{[\text{NADH}]^{\circ} - [\text{NADH}]_{\text{outlet of } E_{\mu}R}}{[\text{NADH}]^{\circ}} \quad (7.4)$$

$$X = \frac{Q \cdot t \cdot ([\text{NADH}]^{\circ} - [\text{NADH}]_{\text{outlet of } E_{\mu}R})}{Q \cdot t \cdot [\text{NADH}]^{\circ}} \quad (7.5)$$

If the conversion is measured as the accumulated value in the reaction/storage tank, in a specific time, and assuming that the dead volumes (electrochemical microreactor (E_μR) +pipes) are negligible in comparison with the volume of the reaction/storage tank:

$$X = \frac{[\text{NADH}]^{\circ} - [\text{NADH}]_{\text{reaction tank}}}{[\text{NADH}]^{\circ}} \quad (7.6)$$

$$X = \frac{Q \cdot t \cdot ([\text{NADH}]^{\circ} - [\text{NADH}]_{\text{reaction tank}})}{Q \cdot t \cdot [\text{NADH}]^{\circ}} \quad (7.7)$$

The NAD⁺ yield (y) or selectivity was estimated by:

$$y = \frac{\text{produced mole number of NAD}^+}{\text{mole number of NADH consumed}} \quad (7.8)$$

The instantaneous yield at the outlet of the μER is given by:

$$y = \frac{\text{UV measured concentration of NAD}^+}{[\text{NADH}]^{\circ} - [\text{NADH}]_{\text{outlet of the } E_{\mu}R}} \quad (7.9)$$

To calculate the cumulative selectivity inside the reaction/storage tank:

$$y = \frac{\text{UV measured concentration of NAD}^+}{[\text{NADH}]^{\circ} - [\text{NADH}]_{\text{reaction/storage tank}}} \quad (7.10)$$

Faradic yield y_f at a time t was estimated by the equation:

$$y_f = \frac{\text{amount of charge corresponding to the produced mole number of NAD}^+}{\text{overall amount of charge supplied}} \quad (7.11)$$

$$y_f = \frac{2 \cdot F \cdot \text{UV detected concentration of NAD}^+ \text{ into the reaction/storage tank}}{\int_0^t I_{(\text{galvano/potential})} \cdot dt} \quad (7.12)$$

The residence time (τ) within the filter-press microreactor was calculated by equation:

$$\tau = \frac{V}{Q} \quad (7.13)$$

Where:

V=Volume of the microreactor (10^{-9}m^3)

Q= Volumetric flow (m^3/min)

For a flow value of $50 \mu\text{L}/\text{min}$, the residence time is $\approx 0.02 \text{ min}$

7.2.3 Quantification of NADH and NAD⁺

Both the concentrations of NADH and NAD⁺ were determined by UV-Vis spectrophotometry, according to the Beer-Lambert Law, and using a Hewlett Packard 8452A Diode array spectrophotometer.

$$A = \epsilon \cdot l \cdot C \quad (7.14)$$

Where:

A= Absorbance (dimensionless)

ϵ = Molar extinction coefficient ($\text{M}^{-1} \cdot \text{cm}^{-1}$)

l= thickness of the solution analyzed or of the UV cell (cm)

C= Concentration (M)

Calibration curves were plotted for several concentrations of the cofactors in 100 mM sodium pyrophosphate buffer pH 8.7, in order to correlate concentration and absorbance at the wavelength corresponding to the highest absorption value: 340 nm for NADH and 260 nm for NAD⁺.

7.2.4 Quantification of substrate and products by HPLC

The concentration of the reactants, Cbz-ethanolamine and Cbz- β -amino propanol, and the products Cbz-glycine and Cbz- β -alanine, was measured by HPLC, following the method presented in section 3.4.5.2, but using a HPLC Hewlett Packard series 1100.

7.2.5 Electrochemical behavior of the compounds involved in the NADH oxidation

The procedure described in section 7.2.1 was used to plot the current-potential (I vs E) for the compounds involved in the different oxidations of substrates (Cbz-ethanolamine and Cbz- β -amino propanol) catalyzed by HLADH. Same conditions as section 7.2.1 were employed.

The compounds involved and their proper mixtures are presented as follows:

Oxidation of Cbz-ethanolamine

- 75 mM sodium pyrophosphate buffer pH 8.7
- 20 mM Cbz-ethanolamine
- 20 mM NADH
- 300 mM semicarbazide hydrochloride.

Oxidation of Cbz- β -amino propanol

- 100 mM sodium pyrophosphate buffer pH 8.7
- 15 mM Cbz- β -alanine
- 5 mM NADH
- 5 mM NADH +15 mM Cbz- β -amino propanol
- 5 mM NADH + 15 mM Cbz- β -alanine.

7.2.6 Electrochemical oxidation of NADH and systematic study of several physicochemical parameters

The current-potential curves were plotted for the oxidation of 20 mM NADH in the electrochemical microreactor (E μ R) before electrolysis; then during 20 min the preparative electrolysis (explained in section 7.2.3) was carried out in a continuous mode (the steady state was reached after few minutes, as a function of the volumetric flow; in practice after

3 or 4 residence times). As described in section 7.2.1 NADH solutions were protected from light and sodium pyrophosphate buffer was used to adjust the pH of all solutions at 8.7.

Further, a systematic study of several physicochemical parameters was performed for the oxidation of Cbz-ethanolamine: for each parameter a short-time electrolysis (2 min) was carried out in a continuous mode, in order to verify the effect of the corresponding parameter to the NADH conversion.

7.2.7 Enzymatic oxidation catalyzed by HLADH coupled with electrochemical regeneration of NAD⁺

Coupled oxidation of Cbz-ethanolamine or Cbz- β -amino propanol with electrochemical regeneration of NAD⁺ was performed in the system presented in figure 7.2.2. The microreactor was connected to a potentiostat Autolab PGSTAT30 for the Cbz-ethanolamine oxidation, or to a potentiostat EGG instrument, Princeton Applied Research model 283, for the Cbz- β -amino propanol oxidation. The enzymatic reaction was operated on a batch reactor, while the electrochemical operation was performed according to a discontinuous mode. The reaction medium constituted by the buffer, the cofactor NAD⁺, Cbz-ethanolamine, and the enzyme HLADH was introduced into the feed anolyte tank and it was continuously recirculated through the anode to regenerate the NAD⁺.

For the oxidation of Cbz-ethanolamine, 20 mM Cbz-ethanolamine was dissolved in 75 mM sodium pyrophosphate buffer pH 8.7 at 25°C in a final volume of 10 mL. Then, 20 mM NAD⁺ was dissolved, and the pH was readjusted to 8.7. The reaction was initiated when a volume of HLADH was added to the reaction medium to reach 500 U/mL in a final volume of 10 mL at 40°C under magnetic stirring and protected from light. This mixture was pumped into the microreactor at 1 mL/min. The applied anodic potential was 1V/Pt wire.

To perform the batch oxidation of Cbz- β -amino propanol, 18.7 mM Cbz- β -amino propanol was dissolved in 100 mM sodium pyrophosphate buffer pH 8.7 at 25°C. The same procedure as the oxidation of Cbz-ethanolamine was followed but using 37.4 mM NAD⁺, and HLADH to reach 100 U/mL in a final volume of 10 mL and 25°C. However, in that case, the reaction proceeded during 2 h without connection to the microreactor, allowing

enough production of NADH for the electrochemical oxidation. Further, the reaction medium was pumped into the microreactor at 1 mL/min. The applied current was 0.8·limiting current (I_{lim}) which is defined as the maximum value of the current in the horizontal plateau provided by the current-potential curves in steady state. This value can be shown when there is mass transfer limitation.

The fed-batch oxidation of Cbz- β -amino propanol was carried out following the same procedure of the batch configuration but under mechanical stirring, with pulses of 5 mM Cbz- β -amino propanol added in solid state when Cbz- β -amino propanol concentration inside the reactor was lower than 10 mM.

The course of the reactions was continuously monitored by determination of the concentration of the reactants and products as described in section 7.2.4, and the enzymatic activity of HLADH was analyzed according to section 3.4.1 but with a Hewlett Packard 8452A Diode array spectrophotometer. NADH and NAD^+ concentrations were measured according to section 7.2.3.

The conversion was calculated as the percentage of Cbz-ethanolamine/Cbz- β -amino propanol consumption with respect to their initial concentration. Yield was estimated as the production of Cbz-glycine/Cbz- β -alanine with respect to the initial concentration of Cbz-ethanolamine/Cbz- β -amino propanol. Productivity was defined as the Cbz-ethanolamine/Cbz- β -amino propanol consumed per unit of time during the reaction. Total turnover number (TTN) was calculated as the number of moles of Cbz-glycine/Cbz- β -alanine formed per mole of NAD^+ during the course of the complete reaction.

7.3 Results and discussion

7.3.1 Direct electrochemical regeneration of NAD^+ in a three-electrode classical electrochemical cell

As mentioned above, a direct electroregeneration of NAD^+ was chosen to be coupled with the HLADH catalyzed oxidation of Cbz-ethanolamine and the oxidation of Cbz- β -amino propanol, since several advantages and its applications in alcohol dehydrogenases were reported in the literature.

7.3.1.1 Current potential curves for NADH oxidation

Since high overpotentials are required to oxidize NADH, various electrokinetic studies were achieved to determine both the feasibility of the electroregeneration of NAD^+ and the stability of the involved substrates under these conditions (Hollmann and Schmid 2004). Consequently, the electroactivity of the compounds and their mixtures, involved in the HLADH catalyzed-oxidations of Cbz-ethanolamine and Cbz- β -amino propanol, was determined, by plotting their current-potential curves using two electrode materials: platinum and gold.

i. On platinum anode

The study was performed for all the conditions described in section 7.2.5, and current-potential curves are presented in annex 1; figures A.1.1-A.1.3. In order to propose a clear analysis of the results, only the curves obtained for the various reagents (under one value of the potential scan rate for transient state without convection/ $\omega=0$, and one ω of a rotating disc at the steady state $r=5$ mV/s) were presented here as an example (figure 7.3.1).

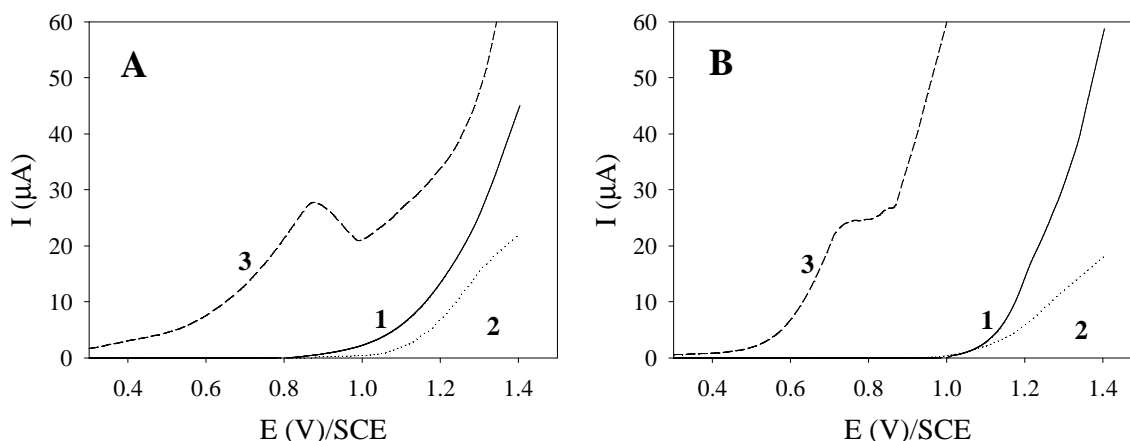


Figure 7.3.1 Current potential curves obtained on a platinum disc anode ($S=3.14 \text{ mm}^2$) at room temperature. (A): transient state without convection/ $\omega=0$; $r=100$ mV/s; (B): steady state on a rotating disc $\omega=1000$ rpm, $r=5$ mV/s. 1: residual current (75 mM sodium pyrophosphate buffer pH 8.7); 2: (1) + 20 mM Cbz-ethanolamine; 3: (1) + 20 mM NADH.

The general voltammetric response was similar in transient (A) and steady state (B). Curve 1 concerns the residual current obtained in sodium pyrophosphate buffer, pH 8.7; in both

cases, it indicates the oxidation of platinum to PtO (shoulder for $E > 0.9$ V / transient state/1.1 V at the steady state), followed by the exponential part attributed to the water oxidation to oxygen ($E > \sim 1.1$ V / transient state/ ~ 1.3 V at the steady state).

Introduction of the Cbz-ethanolamine into the medium (curves 2 Figure 7.3.1) causes the overall current to decrease and the curve is shifted to the anodic potentials ($\Delta E > \sim 0.1$ V). There is no signal attributed to the oxidation of the Cbz-ethanolamine. This means that Cbz-ethanolamine was adsorbed on the platinum electrode and it limited both the platinum and water oxidation. Concerning the behavior of NADH in sodium pyrophosphate buffer at pH 8.7, the curve obtained (3) at the transient state (A) presents three signals: a peak shaped signal ($E_{\text{beginning}} \sim 0.5$ V; $E_{\text{peak}} \sim 0.85$ V) which corresponds to NADH oxidation, followed by a shoulder attributed to the platinum oxidation and the exponential part of the water oxidation. Therefore, the curve obtained at the steady state (B) conditions presents a diffusion plateau ($E_{\text{beginning}} \sim 0.55$ V; $E_{\text{half-wave}} \sim 0.68$ V).

The peak potential is slightly higher to the reported (~ 0.7 V) by Blaedel and Samec (Blaedel and Jenkins 1975; Samec and Elving 1983), translating a certain irreversibility of the system in the present conditions.

ii. On gold anode

Another material (gold-made disk) was used as anode in order to examine the effect of the Cbz-ethanolamine on the oxidation of NADH. The current-potential curves obtained on the gold electrode for all the involved compounds are presented in annex 2; figures A.2.1-A.2.3. As the study performed with platinum, only the effect of one parameter in both transient and steady states is illustrated in figure 7.3.2 as an example.

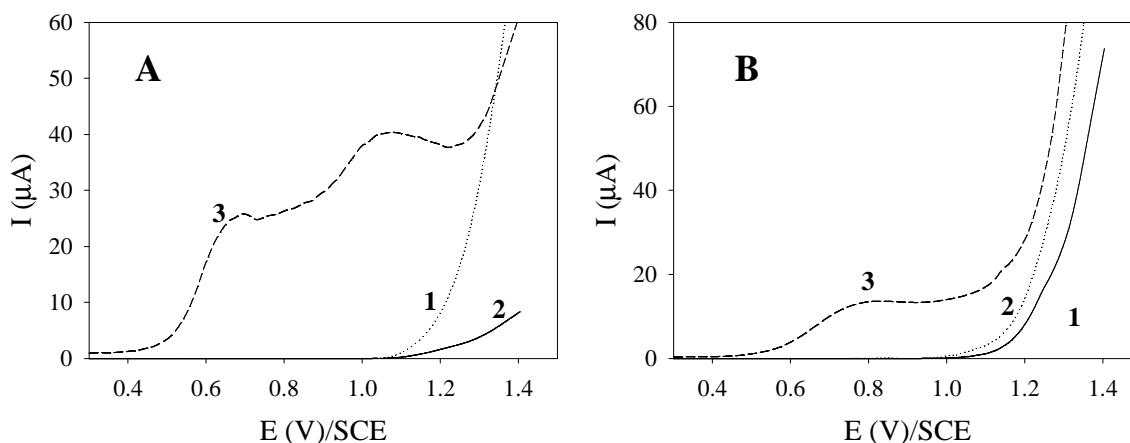


Figure 7.3.2 Current potential curves obtained on a gold disc anode ($S=3.14 \text{ mm}^2$) at room temperature. (A): transient state without convection/ $\omega=0$; $r=100 \text{ mV/s}$; (B): steady state on a rotating disc $\omega= 1000 \text{ rpm}$, $r=5 \text{ mV/s}$. 1: residual current (75 mM sodium pyrophosphate buffer pH 8.7); 2: (1) + 20 mM Cbz-ethanolamine; 3: (1) + 20 mM NADH.

Obtained curves on gold electrode exhibit a similar shape to the curves obtained on platinum in transient (A) and steady state (B).

Curve 1 concerns the residual current obtained in pyrophosphate buffer, pH 8.7; for transient state conditions, curve 1, A, shows several low resolution peaks/shoulder shaped, for potentials higher than 0.85V. Because of their 'low magnitude' these signals were not observed in the chosen scale and they are attributed to the gold anode oxidation ($\text{Au}^0 \rightarrow \text{Au}^{\text{I}} \rightarrow \text{Au}^{\text{III}}$) to lead to various conductive gold oxides. Water oxidation arises after 1.3 V. The same behavior is observed in steady state conditions. Introduction of the Cbz-ethanolamine into the medium (curve 2 Figure 7.3.2, B) does not cause significant changes in the shape of the curve obtained in steady state conditions, except a slight decrease of the potential of water oxidation, probably because the Cbz-ethanolamine slightly limits the oxidation of gold, so water oxidation becomes easier. There is no a signal attributed to the oxidation of the Cbz-ethanolamine. Comparison with platinum allows to conclude that adsorption of the Cbz-ethanolamine on the platinum electrode is stronger than the adsorption on gold.

Concerning the NADH behavior in sodium pyrophosphate buffer at pH 8.7, the curve 3 obtained at the transient state (Figure 7.3.2 A), presents several signals: a peak shaped signal (NADH oxidation; $E_{\text{beginning}} \sim 0.55 \text{ V}$; $E_{\text{peak}} \sim 0.73 \text{ V}$; it corresponds to the value predicted by (Samec and Elving 1983), followed by a shoulder (at least two peaks)

attributed to the gold oxidation as well as the exponential part of the water oxidation. At the steady state (curve 3 Figure 7.3.2, B), the curve presents also three signals: a diffusion plateau (NADH oxidation; $E_{\text{beginning}} \sim 0.55$ V; $E_{\text{half-wave}} \sim 0.79$ V), followed by two shoulders attributed to the gold oxidation as well as the exponential part of the water oxidation ($E > 1.2$ V).

7.3.1.2 Effect of the substrate Cbz- β -amino propanol and the product Cbz- β -alanine on the shape of the current potential curves obtained for NADH oxidation

The current-potential curves, plotted on both platinum and gold disk anodes, for NADH oxidation in presence of the substrate Cbz- β -amino propanol and the product Cbz- β -alanine are indicated in figure 7.3.3. The expected goal was to check the influence of the substrate, as well as the product of the oxidation of Cbz- β -amino propanol catalyzed by HLADH, on the magnitude of the oxidation current of NADH as function of the electrode material.

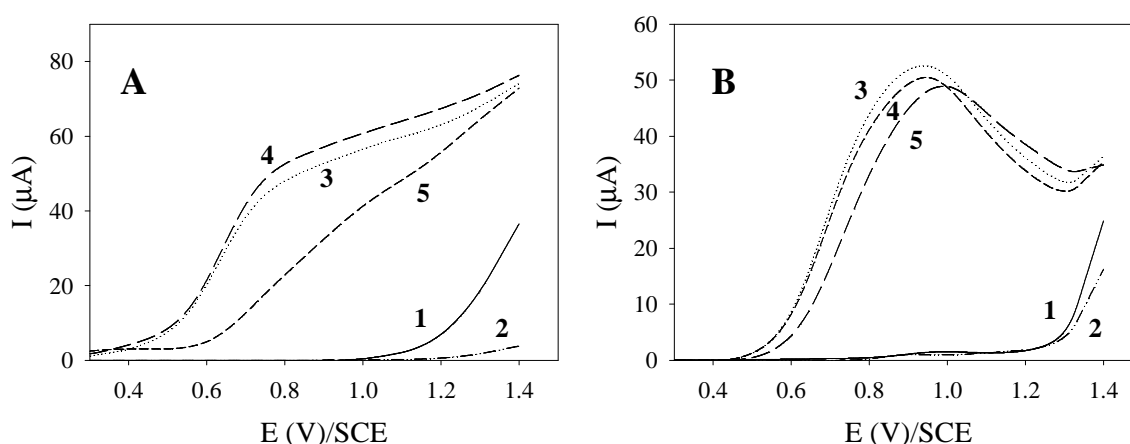


Figure 7.3.3 Current potential curves obtained at the steady state on a rotating disc $\omega = 1000$ rpm, $r = 5$ mV/s; room temperature. (A): platinum disc anode ($S = 3.14$ mm²); (B): gold disc anode ($S = 3.14$ mm²) 1: residual current (100 mM sodium pyrophosphate buffer pH 8.7); 2: (1) + 15 mM Cbz- β -alanine; 3: (1) + 5 mM NADH; 4: (3) + 15 mM Cbz- β -amino propanol; 5: (3) + 15 mM Cbz- β -alanine

For both Pt or Au anodes, the substrate Cbz-amino propanol and the product Cbz- β -alanine does not exhibit electrochemical activity. Indeed, comparison of curves 1 (residual current) and 2 (substrate), does not show additional signal, except a slight decrease in the magnitude of the current, translating a stronger adsorption on platinum.

Regarding the platinum disk, curve 3, A, figure 7.3.3, obtained with NADH, it exhibits a 'normal behavior' with plateau translating a diffusion limited current. Addition of 15 mM Cbz- β -amino propanol (curve 4, A) does not significantly change the shape of the curve, ($\Delta I_{lim} < 5\%$), meaning that oxidation of NADH is not affected by the Cbz- β -amino propanol. Also, the addition of 15 mM Cbz- β -alanine (curve 5, A) appears to have a stronger effect on the NADH oxidation current, hence the oxidation becomes more difficult, higher overvoltage is required and the system appears to become 'more irreversible'. Adsorption of Cbz- β -alanine could be responsible of the decrease of the current magnitude on platinum anode.

On the other hand, concerning the gold disk, the curve 3, B, figure 7.3.3, obtained with NADH, exhibits a 'unusual behavior': a peak shaped signal (instead of a plateau), translating a diffusion limited current, as observed previously in curve Figure 7.3.2, B, 3. Moreover, the addition of 15 mM Cbz- β -amino propanol (curve 4, B) does not significantly change the shape of the curve ($\Delta I_{lim} < 5\%$), meaning that oxidation of NADH is not affected by the Cbz- β -amino propanol. Finally, the addition of 15 mM Cbz- β -alanine (curve 5, B) showed the same behavior of the Cbz- β -amino propanol leading to the same conclusions. The Cbz- β -alanine does not affect the NADH oxidation current.

Comparison of the initial oxidation potential of NADH for gold and platinum shows similar values, so that is not a criterion to choice the electrode material. The main reason appears to be the effect of substrates on the oxidation of NADH. Platinum seems to be partially passivated by the substrate and oxidation of NADH becomes more difficult, because this effect is lower on gold; the gold was retained as anodic material for NADH oxidation for the preparative electrolysis on the microreactor.

Once the working electrode was selected, the electroactivity of semicarbazide hydrochloride was examined, since it was applied as Cbz-glycinal trapping agent in 15-fold excess for the oxidation of Cbz-ethanolamine (section 4.3.2.1). The current-potential curve at the transient state of 0.3 M semicarbazide hydrochloride dissolved in 75 mM sodium pyrophosphate pH 8.7 is presented in figure 7.3.4. (2).

The curve shows several signals: the first one, starting at 0.3 V, is attributed to the oxidation of semicarbazide hydrochloride. Comparison of the potential of this signal with

the potential of the NADH oxidation signal (~ 0.55 V, curve 3, reported from figure 7.3.2 (A)), clearly indicates that the semicarbazide hydrochloride was oxidized before NADH, so it cannot be used in the NAD⁺ regeneration system. Moreover, the semicarbazide hydrochloride oxidation signal appears as a shoulder (instead of a peak), because a second signal is present for potentials higher than 0.7 V; probably a second step of oxidation of this compound arises in the same potential area that the gold oxidation. It has to be noted that the steady state curves were not plotted because electroactivity was proven in transient state.

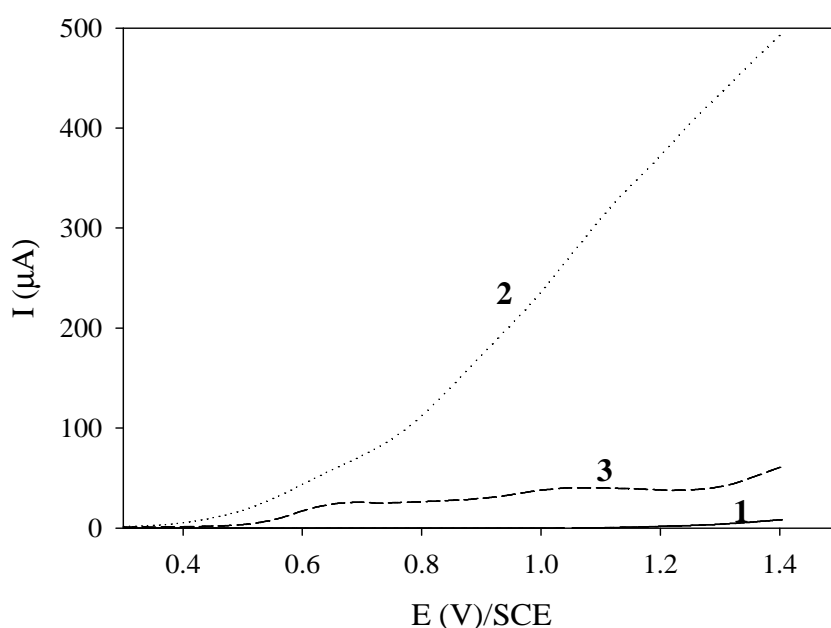


Figure 7.3.4 Current potential curves obtained on a gold disc anode ($S=3.14$ mm²) at transient state and at room temperature. $\omega=0$ rpm, $r=100$ mV/s. 1: residual current (75 mM sodium pyrophosphate buffer pH 8.7); 2: 1+300 mM semicarbazide hydrochloride; 3: 1+ 20 mM NADH.

7.3.1.3 Effect of the potential scan rate on the NADH electrochemical oxidation

Figure 7.3.5 indicates the curves $I=f(E)$ obtained for various potential scan rates. Curves clearly indicate the oxidation of NADH already discussed.

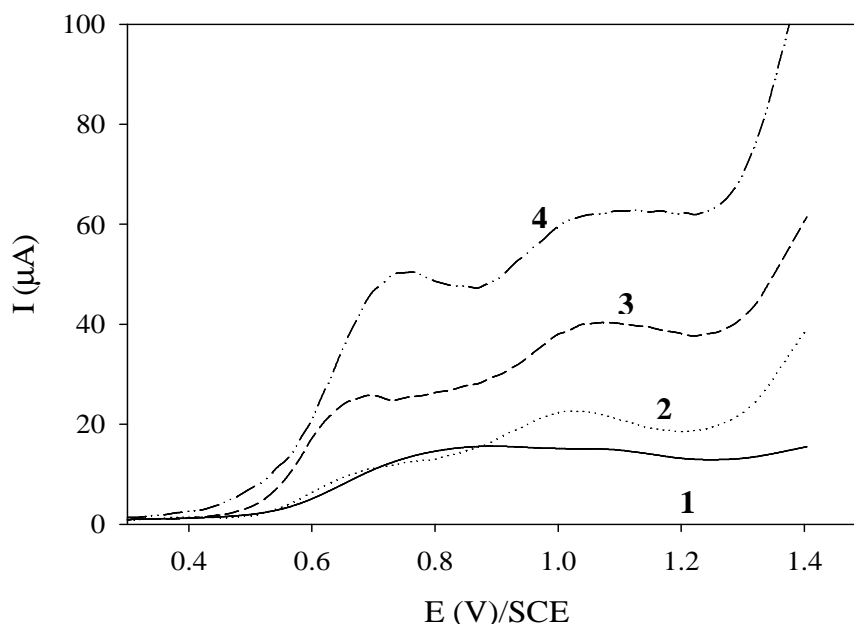


Figure 7.3.5 Current potential curves obtained on a gold disc anode ($S=3.14 \text{ mm}^2$) at room temperature and transient state without convection ($\omega=0$). Electrolyte: 100 mM sodium pyrophosphate buffer pH 8.7. (1) Residual current (100 mV/s); (2), (3) and (4): 15 mM NADH, at 50, 100 and 200 mV/s respectively.

Analysis of the dependence of the magnitude of the current peak with the square root of the potential scan rate seems to be linear (with important uncertainties), and indicates a mass transfer limiting phenomenon (Tzedakis, Cheikhou et al. 2010).

$$I_{\text{Peak(A)}} = 1 \cdot 10^{-4} \cdot r_{(\text{r in V/s})}^{0.5} \quad R^2 = 0.98 \quad (7.15)$$

Further, a lineal correlation between the peak potential and the logarithm of the potential scan rate was found:

$$E_{\text{Peak(V)}} = 0.83 + 0.046 \ln r_{(\text{r in V/s})} \quad R^2 = 0.99 \quad (7.16)$$

The slope of the equation 7.16 allowed determination of the anodic transfer coefficient ($\alpha_{n_{\text{lim.step}}}$)=0.27. This coefficient (defined as: $\alpha = \frac{\partial(\Delta G^{*\circ})}{\partial(\Delta G)} = \frac{\partial(\Delta G^{*\circ})}{+nF \partial(E)}$) indicates how

the free activation enthalpy barrier changes versus the applied potential. For a simple system which exchanges $1 e^-$, $\alpha_{n_{\text{lim.step}}}$ is 0.5. The calculated value (0.27) is a little lower than the one obtained for the electrochemical oxidation of NADH using glassy carbon (0.35) and platinum (0.45) electrodes at pH 7 (Moiroux and Elving 1980).

Combining equation 7.1 with equation 7.15 allowed the determination of the diffusion coefficient of NADH ($D_{\text{NADH}} = 1.1 \cdot 10^{-10} \text{ m}^2/\text{s}$), resulting in a value similar to $2 \cdot 10^{-10} \text{ m}^2/\text{s}$, reported by Moiroux and Elving (Moiroux and Elving 1980) in the conditions mentioned above. It has to be noticed that the reported NADH diffusion coefficients are lower than the diffusivities of classical simple molecules, probably because the higher size of the molecule of NADH.

Taking into account the determined value of ' $\alpha_{\text{n}_{\text{lim,step}}}$ ' and the diffusion coefficient, the combination of equation 7.2 with equation 7.16 allowed to access to the intrinsic heterogeneous electronic transfer constant $k^0 = 2.2 \text{ m/s}$ which is practically the same for the values obtained by Moiroux and Elving (Moiroux and Elving 1980) for a bare electrode. This value indicates that the electrochemical oxidation of NADH appears to be a relatively slow electrochemical system (Tzedakis, Cheikhou et al. 2010).

7.3.2 Oxidation of NADH in a filter-press microreactor at the steady state

The concentration of both NAD⁺ and NADH were determined by UV-Vis spectroscopy at wavelength corresponding to the highest absorption value: 340 nm for NADH and 260 nm for NAD⁺ (Horecker and Kornberg 1948; Silverstein 1965). The slope of the graphics $A=f(C)$ allowed the molar extinction coefficients to be determined (table 7.3.1).

Table 7.3.1 Molar extinction coefficients of NADH and NAD⁺ in 100 mM sodium pyrophosphate buffer pH 8.7 at room temperature.

Compound	Wavelength (nm)	Molar extinction coefficient ($\text{M}^{-1} \cdot \text{cm}^{-1}$)	
		Experimental	Theoretical Reported by (Hald, Lehmann et al. 1975)
NADH	340	5577	6220
	260	14408	14100
NAD ⁺	260	16492	17400

The comparison between the obtained and theoretical molar extinction coefficients of NAD^+ and NADH indicates similar values with a low average error percentage ($\Delta\varepsilon=5\%$), and the differences can be attributed to experimental error or the variability of the analytical equipments employed (dead volumes).

In fact due to the high specific area of the microreactor, it can be assumed that, during one residence time, the NADH is quasi-completely transformed to NAD^+ into the microreactor. Moreover, given that the intermediate radical species formed are oxidized to enzymatically active NAD^+ (Gorton 2002), measurement of the absorbance at 260 nm was not necessary. Most of the compounds absorb at this wavelength, so it could represent a major source of error. Nevertheless, the enzyme HLADH absorbs at 340 nm (as explained in chapter 5) and this value must be subtracted in each measure.

To reach the steady state, the time of electrolysis should be at least $5\tau=0.1$ min. Because of the low flow, the electrolysis should take at least 20 min in order to obtain enough volume to perform all the assays required (1 mL).

The current-potential curve obtained with the microreactor for the oxidation of 20 mM NADH at the steady state is presented in annex 2; figure A.2.4 (A). The signal attributed to the oxidation of NADH appears as a peak located at $E_{\text{peak}}\approx 0.59$ V/Pt wire pseudoreference. Two reasons could explain the peak shape (instead of a diffusion plateau) of the anodic signal: high conversion in the microreactor, or a current decrease caused by the depletion in the concentration, the microreactor acting as a thin layer. The effect that NADH at high concentration causes adsorption and fouling of the surface electrode has been reported in the literature (Aizawa, Coughlin et al. 1975; Blaedel and Jenkins 1975; Samec and Elving 1983)

The electrolysis was performed at both signals E_{peak} (see I vs E curve, annex 2; figure A.2.4 (B)) and 1 V/Pt wire pseudoreference as the value reported by Samec and Elving (Samec and Elving 1983). The 20 min electrolysis and the current-time (I vs t) curves were plotted (Annex 2; figure A.2.4 (B)). The conversion of NADH was determined by the concentration measured by UV, and is presented in figure 7.3.6.

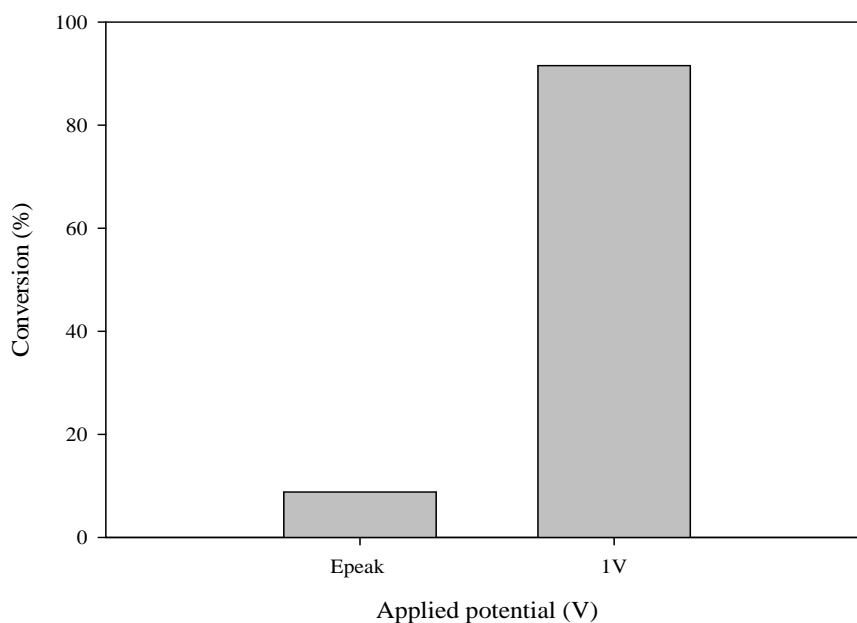


Figure 7.3.6 Applied potential dependence of the conversion of NADH, obtained during preparative electrolysis achieved using a filter press microreactor on a microstructured gold made anode $S = 18 \text{ cm}^2$. Anolyte: 20 mM of NADH in 75 mM sodium pyrophosphate buffer pH 8.7. Catholyte: 75 mM sodium pyrophosphate buffer pH 8.7. $T = 40^\circ\text{C}$; $Q_{\text{anolyte}} = Q_{\text{catholyte}} = 50 \mu\text{L}/\text{min}$.

Figure 7.3.6 shows that the highest conversion of NADH was reached at 1 V with 92% comparing to 9% at 0.59 V. An explanation might be that due to the adsorption of NADH on gold, a high overvoltage was required to reach significant conversions.

7.3.3 Coupled oxidation of Cbz-ethanolamine and electrochemical regeneration of NAD^+

Coupled enzymatic reaction of Cbz-ethanolamine with the electrochemical reaction of NAD^+ can not be performed for the production of Cbz-glycinal, because the semicarbazide hydrochloride (aldehyde trapping agent) is electroactive (section 7.3.1.1). Nevertheless, in order to verify the feasibility of the NAD^+ regeneration without the use of semicarbazide hydrochloride, the coupling reaction of Cbz-ethanolamine and the NAD^+ electrochemical regeneration was performed, to obtain Cbz-glycine as represented in figure 7.1.1. Some difficulties were presented in coupling of both reactions in a filter-press microreactor.

To overcome the low rate of the chemical oxidation of Cbz-ethanolamine without semicarbazide hydrochloride (section 4.3.1), high values of enzymatic activity of HLADH

(500 U/mL) and temperature (40°C) were chosen. However, some proteins and/or cellular debris precipitated in the pipes and inside the microreactor blocked the pipes, the inlet and/or the outlet of the microreactor. Despite the reaction medium was left reacting in the feed tank at room temperature until the next day. At 22 h of reaction the precipitated proteins were removed by microcentrifugation (3 min at 10000 rpm). Then, the reaction medium was pumped into the microreactor, and the electrolysis was performed by 2.2 h on a discontinuous way applying 1 V at 40°C.

The evolution of the enzymatic activity as well as the concentration of Cbz-ethanolamine in the oxidation, at 40°C, of 20 mM Cbz-ethanolamine with 20 mM NAD⁺ at pH 8.7 (in presence of 500 U/mL of HLADH in a final volume of 10 mL), coupled with 2.2 h of NAD⁺ electro regeneration, are shown in figure 7.3.7.

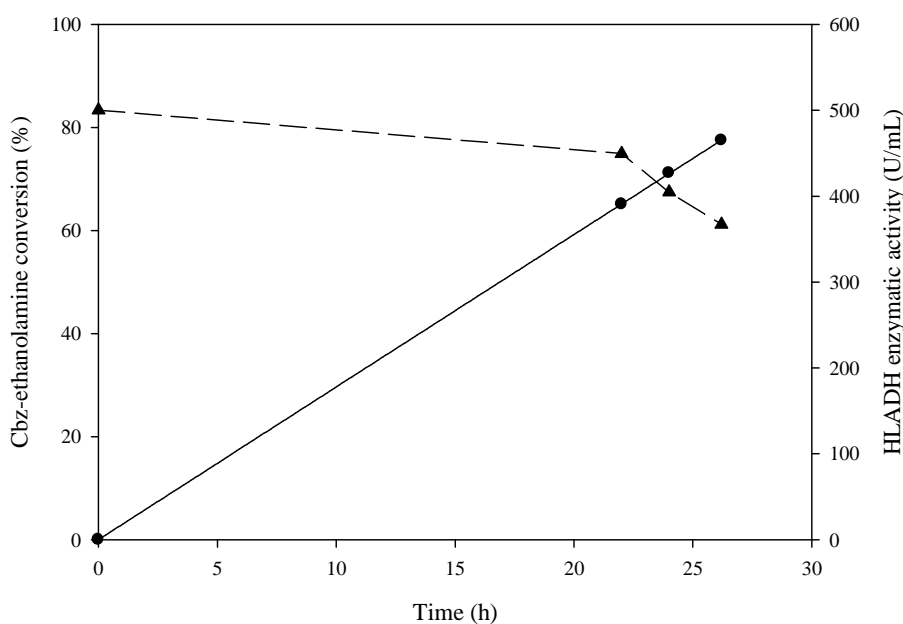


Figure 7.3.7 Oxidation of 20 mM Cbz-ethanolamine with 20 mM NAD⁺ at pH 8.7. HLADH was added to reach 500 U/mL in a final volume of 10 mL at 40°C coupled with 2.2 h of NAD⁺ electroregeneration. Cbz-ethanolamine (●) and HLADH (▲)

As it can be seen, the enzyme HLADH is stable during the reaction at 40°C and the electrolysis. After 2.2 h of electrolysis (performed at 24 h reaction time) the conversion of Cbz-ethanolamine was very low. Given that the rate of the oxidation of Cbz-ethanolamine is very low, the term of biochemical reaction in the mass balance into the microreactor

(equation 1.6, section 1.5.4.4) is negligible for NADH and NAD⁺. The NADH formed in the reaction was oxidized to NAD⁺ with 90% NADH conversion in 2.2 h.

$$\int_{C_{\text{NADH}}^{\circ}}^{C_{\text{NADH}}^{\circ}(1-X_{\text{NADH}})} dC_{\text{NADH}} = -\int_0^x \frac{i.l}{\eta.n.F.Q} dx + \int_0^x \frac{r_A \cdot \pi.R^2}{Q} dx \rightarrow \int_{C_{\text{NADH}}^{\circ}}^{C_{\text{NADH}}^{\circ}(1-X_{\text{NADH}})} dC_{\text{NADH}} = -\int_0^x \frac{i.l}{\eta.n.F.Q} dx \quad (7.17)$$

Electrochemical (Bio)chemical
reaction reaction

7.3.4 Effect of physicochemical parameters on the electrochemical oxidation of NADH

The effect of several physicochemical parameters in the electrochemical oxidation of NADH was evaluated using a filter-press microreactor. This systematic study allowed to examine the effect in the conversion of NADH, and also to establish the best reaction conditions.

As a consequence of the electroactivity of the semicarbazide hydrochloride (section 7.3.1.1) the oxidation of Cbz-ethanolamine to Cbz-glycinal semicarbazone coupled with the electrochemical regeneration of NADH cannot be performed. Owing that the oxidation of Cbz-ethanolamine to Cbz-glycine is very slow, as it was observed in chapter 4, the systematic study of the NADH oxidation was carried out with the reaction medium constituted by the buffer, Cbz-ethanolamine, and enzyme, but adding 20 mM NADH instead of NAD⁺.

Annex 2; figures A.2.5, A.2.6, and A.2.7 present the effect of the flow rate, temperature and concentration of NADH on the NADH oxidation current ($I=f(E)$) and its temporal evolution versus these parameters, respectively.

These curves were plotted before preparative electrolysis using a filter press microreactor. During the electrolysis, the NADH oxidation current was recorded. The conversion of NADH obtained during the electrolysis is presented in figure 7.3.8 (A), (B) and (C).

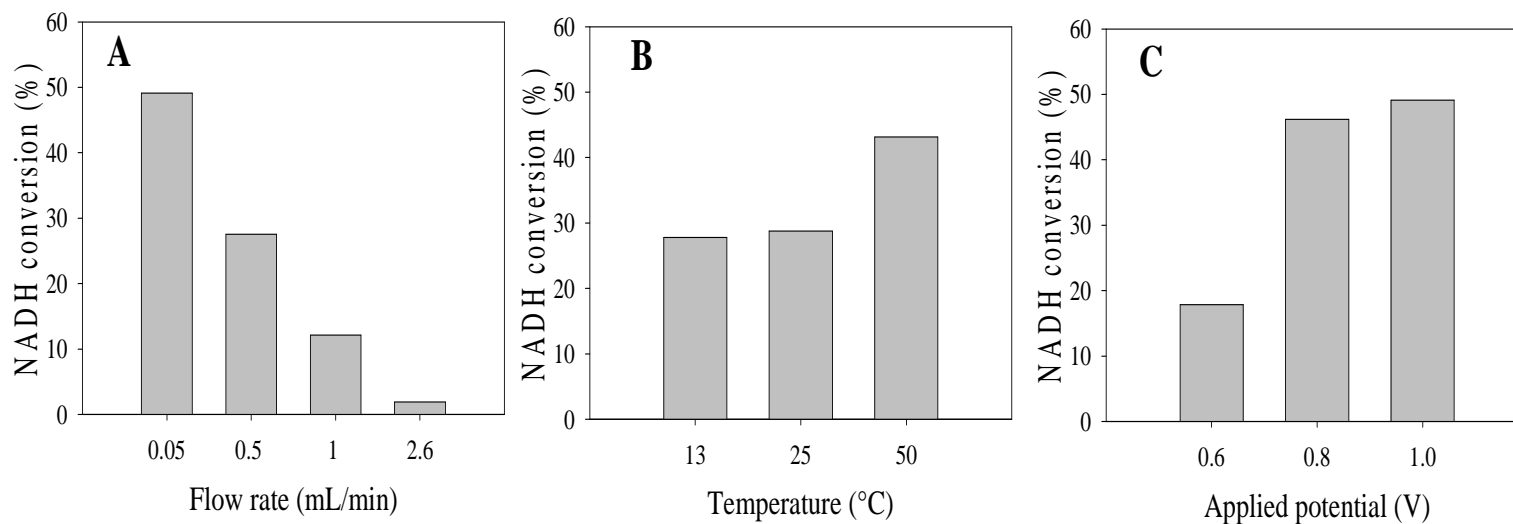


Figure 7.3.8 Flow rate (A), temperature (B) and applied potential (C) dependences of the conversion of NADH, obtained during preparative electrolysis achieved using a filter press microreactor on a microstructured gold made anode $S = 18 \text{ cm}^2$. Analyte: 20 mM NADH, 20 mM Cbz-ethanolamine and 20 U/mL HLADH in 75 mM sodium pyrophosphate buffer pH 8.7. Catholyte: 75 mM sodium pyrophosphate buffer pH 8.7. Electrolysis duration: 2 min. (A): $T = 40^\circ\text{C}$; $E_{\text{applied}} = 1 \text{ V/Pt wire}$; (B): Flow rate $50 \mu\text{L}/\text{min}$; $E_{\text{applied}} = 1 \text{ V/Pt wire}$; (C) $T = 40^\circ\text{C}$; Flow rate $50 \mu\text{L}/\text{min}$.

Overall, the analysis of the current-potential curves presented in annex 2, figure A.2.5 (A), shows that the current rises with the flow rate, as a result of the enhancement of the mass transfer coefficient (Tzedakis, Cheikhou et al. 2010). Assuming for the mass transfer coefficient a power function law with the flow ($k = a \cdot Q^b$) (annex 2; figure A.2.5 (B)), the results lead to propose the following relation:

$$I_{\max}(A) = 3.464 \cdot Q_{L.s^{-1}}^{0.48} \quad \text{and} \quad k = 286 \cdot Q_{L.s^{-1}}^{0.48} \quad (7.18)$$

The figure 7.3.8 (A) shows that the NADH conversion decreases with the flow rate (from 50% to 5%) since the lower residence time (τ) inside the filter-press microreactor (even if the maximum current increased because of the enhancement of the mass transfer). For this microreactor and in these operating conditions the optimal flow rate is in the range of 50 $\mu\text{L}/\text{min}$.

The influences of the temperature on the current-potential and current-time curves are presented in annex 2, figure A.2.6 (A) and (D), respectively. The conversion of NADH is illustrated in figure 7.3.8 (B).

Temperature strongly affects the $I=f(E)$ curves. Hence, increasing temperature has a double effect: the NADH oxidation becomes more rapid/reversible and the starting oxidation potential decreases from ~ 0.6 V to ~ 0.3 V. The curve C (annex A2.6) provides the evolution of the half wave potential ($E_{1/2}$) versus temperature and indicates a linear evolution probably caused by the NADH desorption:

$$E_{(V)} = 0.89 - 0.0084 \cdot T_{(K)} \quad R^2 = 0.99 \quad (7.19)$$

Moreover, the curves are peak shaped, indicating an important depletion of the concentration during the pass in the microreactor. Both, the maximum current (peak) and the limiting current (after concentration depletion) for NADH oxidation increased with the temperature. The curve B (annex A.2.6.) provides the evolution of the limiting current versus temperature.

NADH conversion increased from 30% to 50% in the examined temperature range. This augmentation is relatively low, probably due to the relatively low applied potential, which does not allow achieving important currents. To sum up, the reaction rate of the anodic oxidation of NADH is faster at higher temperature, then the conversion increases

(Liu, Xu et al. 2011). Nevertheless, this effect is more significant at temperatures higher than 25°C.

The influence of the applied potential was monitored, and the current-time curve is presented in the annex 2; figure A.2.7. The conversion of NADH is illustrated in figure 7.3.8 (C). The NADH conversion increases with the potential in the range from 0.6 to 0.8 V/Pt wire, meaning that at 0.6 V the maximum (limiting) current was not achieved. Low difference between 0.8 and 1 V was observed in the NADH conversion to NAD⁺ (around 3%), meaning that the limiting current is achieved at an applied potential slightly higher than 0.8V/Pt wire.

On the other hand, the NADH concentration effect observed in the current-potential and current-time curves is presented in annex 2; figure A.2.8 and the conversion of NADH is presented in figure 7.3.9.

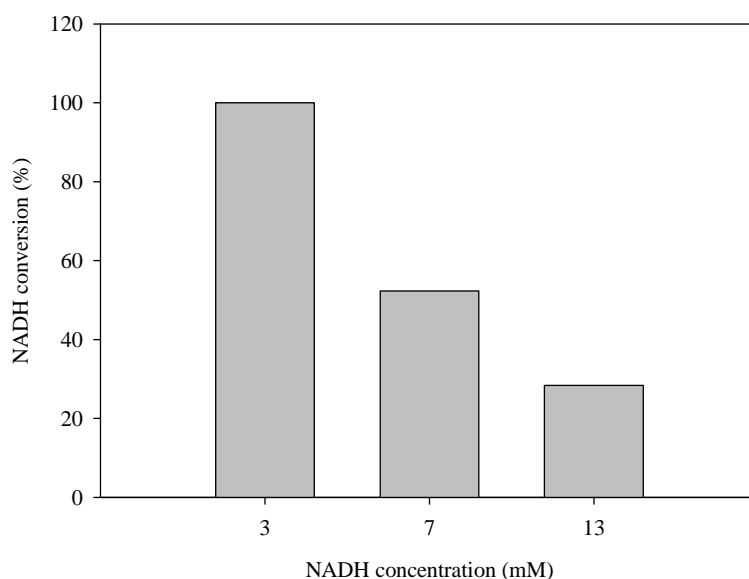


Figure 7.3.9 Effect of the NADH concentration dependence in the conversion of NADH at the steady state, obtained during preparative electrolysis achieved using a filter press microreactor on a microstructured gold made anode $S = 18 \text{ cm}^2$. Anolyte: 20 mM NADH, 20 mM Cbz-ethanolamine and 20 U/mL HLADH in 75 mM sodium pyrophosphate buffer pH 8.7. Catholyte: 75 mM sodium pyrophosphate buffer pH 8.7. Electrolysis time: 2 min at 1 V. $T = 40^\circ\text{C}$; $Q_{\text{anolyte}} = Q_{\text{catholyte}} = 50 \text{ }\mu\text{L}/\text{min}$.

The current-potential curves (annex 2; figure A.2.8 (A)) show an unusual behavior; at low concentration of NADH (3 mM) curves show two waves for oxidation of NADH (0.2/0.6 V, and 0.7/1.2 V). Two effects can be proposed: i) a pre-wave corresponding to

an adsorption of NADH followed to the main wave for NADH oxidation, and ii) two successive mono-electronic oxidations for NADH. This last proposition appears less probable because of the dissymmetric limiting currents. Increasing the concentration of NADH (7 mM, curve 2) caused the increase of the magnitude of the first signal (which appeared at lower potential, and as a peak instead as a wave, probably due to the depletion of concentration, or an adsorption that produces passivation) and a decrease of the second one.

For higher concentrations (13 mM) of NADH, the curve shows an increase of the potential peak and a decrease of its magnitude; this behavior could arise from a stronger passivation of the anode at higher concentrations of NADH. The current peak evolution versus concentration is presented in inset in annex 2; figure A.2.8 (B). This evolution seems to be exponential:

$$I_{\text{peak(A)}} = 1.92 + 6.85 \cdot (1 - e^{-0.035 \cdot T(\text{K})}) \quad (7.20)$$

Figure 7.3.9 shows that conversion decreases with the initial NADH concentration, from ~100% at 3 mM to ~13% at 13 mM; that is the usual behavior of the plug-flow reactor if the flow rate remains constant.

Finally, the electrolysis applying current and potential was examined and the results of the conversion of NADH are presented in figure 7.3.10.

A clear difference of the conversion is observed when $0.8 \cdot I_{\text{max}}$ and the potential of oxidation of NADH (1V) were applied. This finding also supports the hypothesis about the adsorption of NADH, and it can therefore be assumed that in this particular case, the equation $0.8 \cdot I_{\text{max}}$ does not provide a real value of the current required to completely oxidize NADH. The potential obtained, 1 V, was the applied value for the effective oxidation of NADH, in agreement with Samec (Samec and Elving 1983). Nevertheless the values of the potential must be carefully considered because a platinum wire is being used as reference electrode, and this can introduce important errors in the real value of the applied potential.

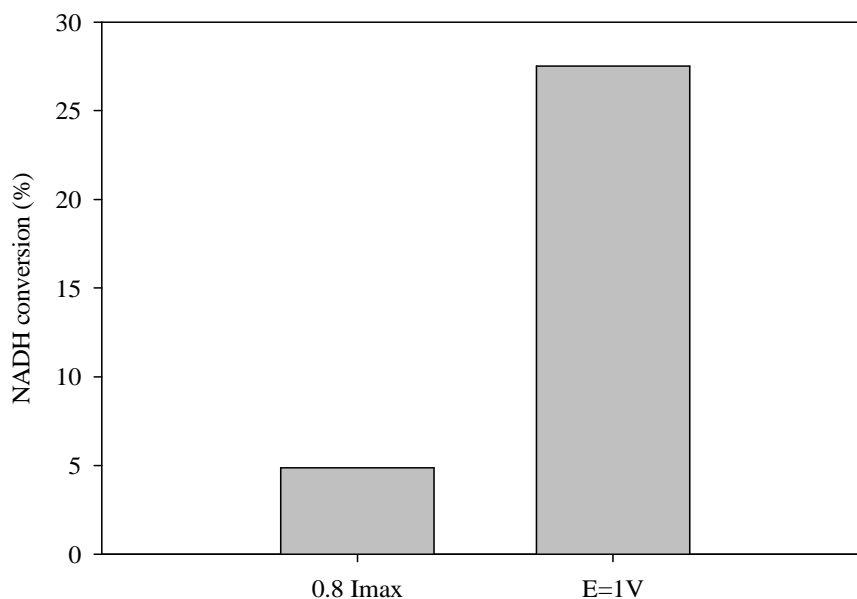


Figure 7.3.10 Comparison of the conversion of 20 mM NADH in reaction medium applying current (0.8·I_{max}) and potential (1 V) at the steady state during preparative electrolysis achieved using a filter press microreactor on a microstructured gold made anode S= 18 cm². Anolyte: 20 mM of NADH, 20 mM Cbz-ethanolamine and 20 U/mL HLADH in 75 mM sodium pyrophosphate buffer pH 8.7. Catholyte: 75 mM sodium pyrophosphate buffer pH 8.7. Electrolysis time: 2 min at 1 V. T=40°C; Q_{anolyte}= Q_{catholyte} =50 μL/min.

7.3.5 Coupled oxidation of Cbz-β-amino propanol and electrochemical regeneration of NAD⁺

The oxidation of Cbz-β-amino propanol (to Cbz-β-alanine) by electrogenerated NAD⁺ was proposed. Thus, it was necessary to determine the optimal reaction conditions. The temperature was chosen as 25°C, based on the positive results previously presented in section 6.3.1. Also, at this temperature the precipitation of the enzymatic solution is reduced compared with that at higher temperatures (section 6.3.1). Indeed, precipitation could block the pipes and the microchannels of the microreactor as described in section 7.3.3. Regarding the flow, 1 mL/min was selected. Although this value does not provide the best conversion of NADH (figure 7.3.8), it was proven experimentally that it did not cause pipe blocking since only small amounts of the enzyme solution precipitated. The other operating conditions employed were the best obtained in section 6.3.2.

Because of the observed high adsorption of the medium (NADH + enzyme) at the electrode, current was applied instead of potential to ensure the complete oxidation of

the NADH formed (soluble and absorbed one). Thus, a current equal to $0.8 \cdot I_{\text{lim}}$ (the I_{lim} obtained from the current-potential curves plotted after 30 min of enzymatic reaction with no electrolysis) was applied (annex 2; figure A.2.9, this curves exhibits a similar shape as the curve 1 of the annex 2; figure A.2.8). The concentration profile of the batch coupled reaction is presented in figure 7.3.11.

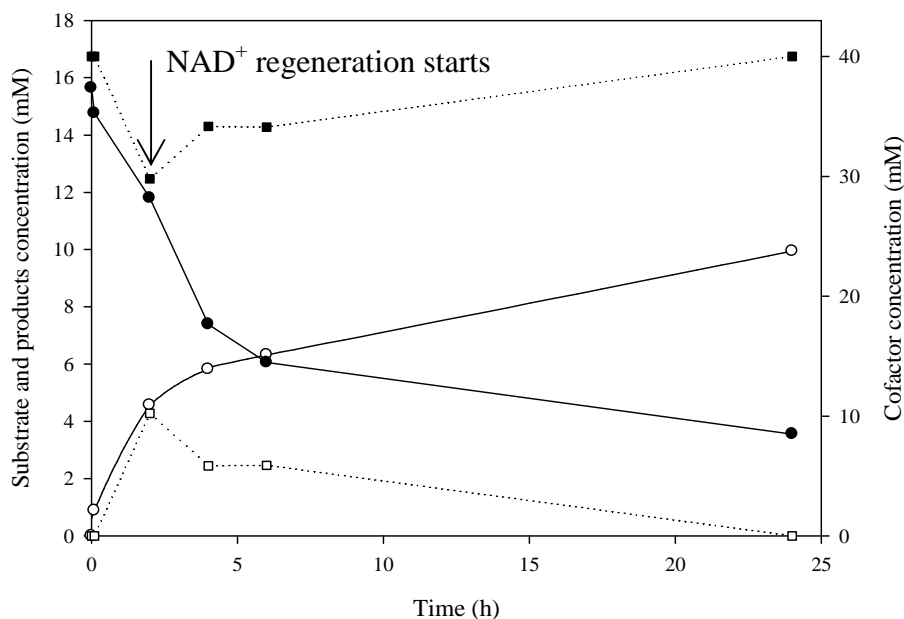


Figure 7.3.11 Time course of the batch coupled oxidation of Cbz-β-amino propanol to Cbz-β-alanine and electrochemical regeneration of NAD⁺ in a filter-press microreactor. The reaction was performed with 18.7 mM Cbz-β-amino propanol in 100 mM sodium pyrophosphate buffer pH 8.7, 37.4 mM NAD⁺ and 100 U/mL HLADH in a final volume of 10 mL at 25°C for 24 h (Anolyte). Catholyte: 100 mM sodium pyrophosphate buffer pH 8.7. Electrolysis time: 2 min at 0.5 mA. $T=40^{\circ}\text{C}$; $Q_{\text{anolyte}} = Q_{\text{catholyte}} = 1 \text{ mL/min}$. Cbz-β-amino propanol (●), Cbz-β-alanine (○), NAD⁺ (■) and NADH (□).

The concentration of NAD⁺ decreased from the initial time until 2 h as it was being consumed in the enzymatic reaction (with no electro-regeneration). The regeneration started after 2 h, when NADH appeared (electrogenerated after applying $0.8 \cdot I_{\text{lim}} \approx 0.5 \text{ mA}$); then the chemical oxidation of NADH was apparent, and it was completely converted into NAD⁺. After 24 h of reaction, substrate conversion was 77.1% and complete NAD⁺ regeneration was achieved.

The temporal evolution of the anode potential, measured versus a platinum wire used as pseudoreference, is presented in annex 2; figure A.2.10. The curve shows that the potential reached around 1.3 V after 15 min of reaction and remained almost constant for higher electrolysis duration. This value of potential could correspond to the

oxidation of water since some bubbles were observed at the outlet of the microreactor. The current was decreased (for 30 min), from 0.5 to 0.2 mA after a reaction duration of 4 h. Meanwhile, there was no change (decrease) in the potential value, so the current was increased again to 0.5 mA, to assure the oxidation of the NADH formed. This could indicate that the efficiency of the regeneration decreased because part of the charge was used to oxidize water.

The profile of the enzymatic activity and a comparison between the coupled reaction and the oxidation of Cbz- β -amino propanol with no regeneration are presented in figure 7.3.12.

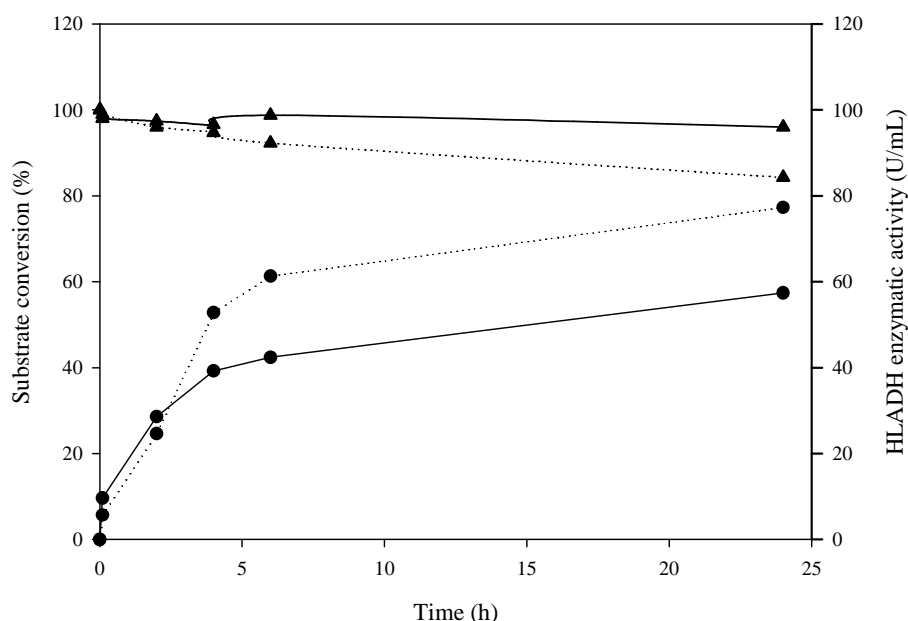


Figure 7.3.12 Comparison of the substrate conversion and HLADH enzymatic activity for the oxidation of Cbz- β -amino propanol. The conversion of Cbz- β -amino propanol (●) and the HLADH enzymatic activity (▲) for the reaction with no regeneration is represented with a solid line and the coupled oxidation with electrochemical regeneration of NAD⁺ with a dotted line.

The conversion of Cbz- β -amino propanol in the coupled regeneration increased when the regeneration of NAD⁺ started at 2 h of reaction; the equilibrium was shifted to the production of Cbz- β -alanine as demonstrated in section 6.3.1. The productivity in the reaction was enhanced and 0.50 mmol/h were obtained, which is 1.3-fold higher than value obtained in the reaction with no regeneration. A TTN of 30 was found.

Concerning the enzymatic activity of HLADH, no significant differences were found between the coupled reaction and the reaction without electroregeneration. When there was no electroregeneration, the enzymatic activity remained practically constant during 24 h. In the coupled reaction there was only a little decrease with time. Such stability with the electroregeneration process was expected, as reported in section 7.3.3.

7.3.6 Coupled fed-batch oxidation of Cbz- β -amino propanol and electrochemical regeneration of NAD⁺

Productivity of the reaction can be improved by employing a fed-batch configuration as presented in section 6.3.3. A good strategy seemed to combine the coupled oxidation of Cbz- β -amino propanol with the electrochemical regeneration of NAD⁺ and the dosage of the solid substrate along time. To guarantee an adequate level of substrate concentration, the pulses were added when a decrease of 5 mM of Cbz- β -amino propanol was observed.

The potential-time curve is presented in annex 2, figure A.2.11, and the concentration profiles are shown in figure 7.3.13.

The concentration of NAD⁺ is affected by two rates: the electroregeneration and the consumption by the enzymatic reaction. Because of the addition of substrate pulses the regeneration is slower than the one corresponding to the batch configuration (figure 7.3.11), and it was necessary to extend the reaction for a long time (until 51 h). The profile of Cbz- β -amino propanol clearly showed the influence of regeneration and the dosage of the substrate. Substrate conversion, calculated as mol of substrate converted per total mol of substrate added, increased very fast. Almost 40% conversion was obtained in 6 h, and 80.4% in 51 h (with 53.2% conversion of NADH). This final conversion is similar to the fed-batch configuration with no regeneration (88.4% at 50 h), but adding 3-fold lower concentration of NAD⁺ (section 6.3.3).

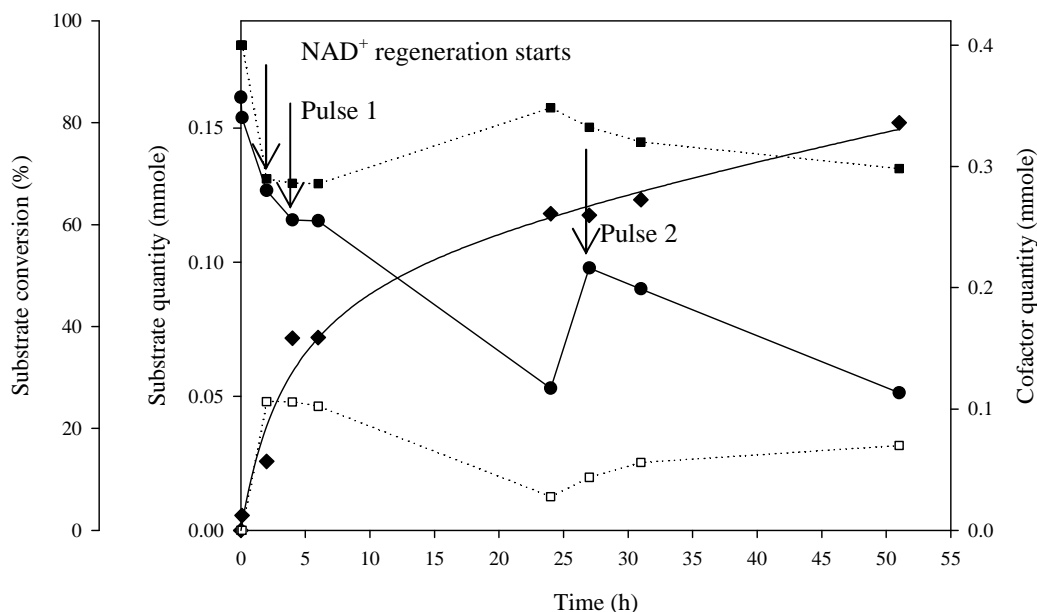


Figure 7.3.13 Time course of the fed-batch coupled oxidation of Cbz- β -amino propanol to Cbz- β -alanine and electrochemical regeneration of NAD^+ in a filter-press microreactor. The reaction was performed with 18.7 mM Cbz- β -amino propanol in 100 mM sodium pyrophosphate buffer pH 8.7, 37.4 mM NAD^+ and 100 U/mL HLADH in a final volume of 10 mL at 25°C for 50 h. 5 mM Cbz- β -amino propanol pulses were added at 4 and 26 h (Anolyte). Catholyte: 100 mM sodium pyrophosphate buffer pH 8.7. Electrolysis time: 48 h at 0.5 mA. $T=40^\circ\text{C}$; $Q_{\text{anolyte}}=Q_{\text{catholyte}}=1$ mL/min. Cbz- β -amino propanol quantity (●), Cbz- β -amino propanol conversion (◆), NAD^+ (■) and NADH (□).

The productivity obtained at 51 h was 0.44 mmol/h; this value is only a little lower than the fed-batch without regeneration (0.56 mmol/h). This difference can be explained by the extra substrate pulse added without regeneration, which was required due to the fast initial rate of the reaction obtained as result of the high initial concentration of NAD^+ available. On the other hand, the evolution of HLADH enzymatic activity is illustrated in figure 7.3.14.

As shown in figure 7.2.14 the HLADH was relatively stable during the first 6 h of reaction, and 70% of remained activity was obtained at 51 h. This can be explained by the results presented in chapter 5 which revealed that during a rapid conversion of Cbz- β -amino propanol to Cbz- β -alanine, pH decreased and caused loss of HLADH activity. The TTN obtained was 56, which is higher than the one obtained in the batch configuration, taking into account that the reaction time was longer.

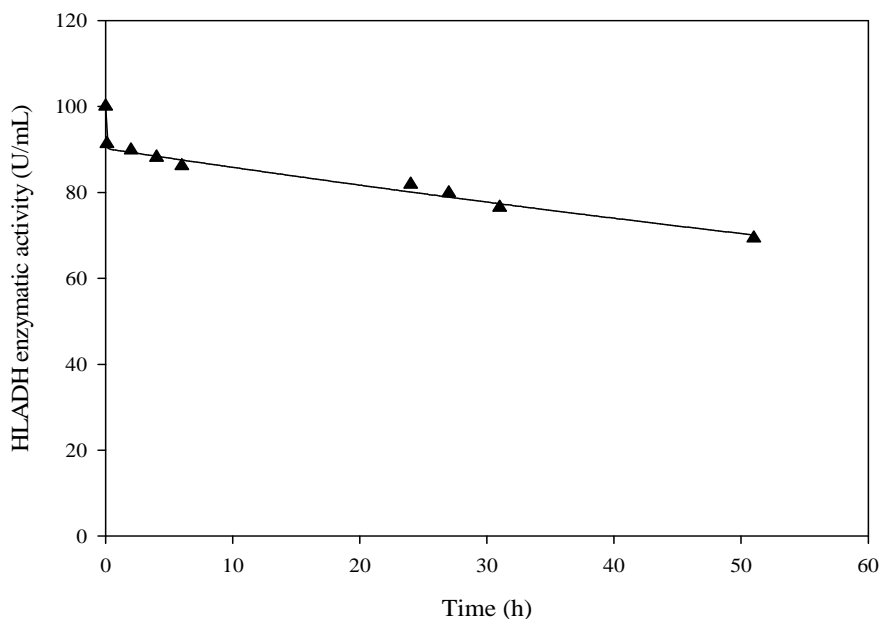


Figure 7.3.14 HLADH enzymatic activity profile for the fed-batch coupled oxidation of Cbz- β -amino propanol and electrochemical regeneration of NAD^+ in a filter-press microreactor.

Concerning the potential-time curve presented in annex 2, figure A.2.11, the same behavior as the batch configuration was found. However, in this case the current applied was not modified.

We compared the enzymatic (section 6.3.4) and electrochemical regeneration of NAD^+ applied to obtain β -alanine. While enzymatic regeneration (section 6.3.4.1) allowed almost complete conversion in 2 h, the reaction stopped at that moment. Hence, fed-batch operation (section 6.3.4.2) could not be performed in an effective way. Several hypotheses were made as a competition for the ethanol formed, or inhibition of the enzyme HLADH. Also, the enzymatic regeneration provided impurities (acetaldehyde and ethanol) in the reaction medium that implies the need for adding an extra separation process for these compounds. On the other hand, the direct electrochemical regeneration does not affect the stability of the enzyme HLADH, fed-batch reaction can be operated efficiently for several days, and only one separation stage is required to recover the cofactor NAD^+ .

7.4 Conclusions

This chapter presents a complete study of the direct electrochemical cofactor NAD^+ regeneration in order to enhance the productivity of the HLADH-catalyzed oxidation of Cbz-ethanolamine and Cbz- β -amino propanol. The direct electrochemical regeneration of NAD^+ was demonstrated by the fact that the NADH was directly oxidized to NAD^+ in both platinum and gold electrodes. NADH oxidation in a filter-press microreactor using a gold cathode allowed obtaining 92% conversion during 20 min of electrolysis in a continuous mode in steady state.

Hence, coupling regeneration of NAD^+ using filter-press microreactor and enzymatic reaction for both substrates was evaluated and optimized to establish the best reaction conditions that allowed an improvement of productivity. However, the HLADH catalyzed oxidation of Cbz-ethanolamine only provides Cbz-glycinal only in presence of the aldehyde trapping agent semicarbazide hydrochloride which is electroactive, so it can not be used in the coupled reaction.

On the other hand, the direct electrochemical regeneration of NAD^+ was successfully coupled with the HLADH catalyzed oxidation of Cbz- β -amino propanol for the production of Cbz- β -alanine. 77.1% Cbz- β -amino propanol conversion and a complete regeneration were obtained at 24 h of reaction using batch operation. The productivity was 0.50 mmol/h, which is 1.3-fold higher than the reaction with no regeneration, and TTN of 30 was obtained.

An improvement in the batch coupled reaction was made by implementing a fed-batch configuration, maintaining the conversion ($\approx 80\%$) with half of complete cofactor regeneration (53.2%) at 51 h, obtaining a TTN of 56. Also, this final conversion was similar to the fed-batch configuration with no regeneration adding 3-fold initial concentration of NAD^+ .

The direct electrochemical regeneration of NAD^+ by coupling with both oxidation of Cbz-ethanolamine and Cbz- β -amino propanol is effective since it is not an invasive method and it was proven that efficiently oxidizes the NADH to NAD^+ . Furthermore,

the use of the electrochemical microreactor presented a clear benefit, as its high in consequence the conversion of NADH.

GENERAL CONCLUSIONS

GENERAL CONCLUSIONS

In house alcohol dehydrogenase from a horse liver (HLADH) showed very good characteristics as biocatalyst for the oxidation of α -amino alcohols, particularly Cbz-ethanolamine with a 4-fold higher specificity constant (k_{cat}/K_M) than that of yeast alcohol dehydrogenase (YADH).

HLADH catalyzed oxidation of Cbz-ethanolamine was successfully accomplished using semicarbazide hydrochloride as aldehyde trapping agent yielding 84%. Cbz-glycinal semicarbazone. Otherwise, yield of the further oxidized product (Cbz-glycine) was only from 6.0-11.9%. Cbz-glycinal semicarbazone was then hydrolyzed at very acidic pH in presence of formaldehyde as semicarbazide trapping agent, obtaining 48.5% of recovery. The separation of the formaldehyde from the mixture was not effective using liquid-liquid extraction with organic solvents due to the poor partition coefficient of the Cbz-glycinal in every system tested. According with these results, the Cbz-glycinal obtained contained a large amount of impurities, particularly formaldehyde, so it was not a good substrate for a further DHAP aldol addition.

Thus, several conditions were studied as the use of supports with amino groups such as MANA-agarose and semicarbazide on silica gel, or the modification of the reaction medium; none of them promoted the production of Cbz-glycinal. Cbz-glycinal was further oxidized rendering Cbz-glycine.

The coupled oxidation of Cbz-ethanolamine by HLADH and aldol addition of DHAP catalyzed with RhuA with DHAP pulses addition did not produce Cbz-aminopolyols. The undesired product Cbz-glycine was formed with 64.1% yield.

Taking advantage of the high oxidative capacity of HLADH, which catalyzes the oxidation of amino alcohols to aminoacids, the enzyme was studied as biocatalyst for the oxidation of β -amino alcohols aiming to produce the highly valued β -aminoacids.

HLADH was able to recognize β -amino alcohols as substrates. Cbz- β -amino propanol was oxidized into Cbz- β -alanine in a batch operation with a complete conversion at 72 h. Fed-batch operation for the synthesis of Cbz- β -alanine provided 2.3-fold improved

productivity (0.56 mM/h) compared with the batch mode. Cbz- β -alanine yield obtained was 88.4% at 96 h employing Cbz-aminopropanol pulse addition.

Enzymatic and electrochemical methods were evaluated for NAD^+ cofactor regeneration. Enzymatic coupled-substrate regeneration of NAD^+ using acetaldehyde improved the initial rate of the batch Cbz- β -amino propanol oxidation with an almost complete conversion to Cbz- β -alanine in the first 2 h of reaction. However, fed-batch operation was not so efficient resulting in a conversion of 65% at 2 h with only one pulse addition of substrate, as the reaction was stopped at 2 h because of the competition for the HLADH with the ethanol formed.

Concerning direct electrochemical regeneration of NAD^+ , it was demonstrated that NADH can be directly oxidized to NAD^+ using platinum and gold electrodes. Therefore, a high conversion of 20 mM NADH (92.0%) was obtained using a filter-press microreactor employing a gold cathode during 20 min of electrolysis in a continuous mode in steady state.

Finally, the direct electrochemical regeneration of NAD^+ using a filter-press microreactor was successfully coupled with the HLADH catalyzed oxidation of Cbz- β -amino propanol for the production of Cbz- β -alanine. A complete regeneration was achieved at 24 h of reaction, with a Cbz- β -amino propanol conversion of 77.1% using a batch operation. Fed-batch operation increased the target compound production maintaining 80.0% conversion and half of the cofactor regeneration at 51 h. Interestingly, this final conversion was similar to the fed-batch configuration with no regeneration adding 3-fold initial concentration of NAD^+ . This fact caused a very positive improvement in cofactor savings.

In general it can be concluded that HLADH is an effective catalyst for the oxidation of Cbz-aminoalcohols. In fact, due to its high oxidative ability the reaction renders directly to Cbz-aminoacids. In order to obtain the intermediate product, Cbz-aminoaldehyde, it is necessary to add an aldehyde trapping agent to produce the corresponding Cbz-aminoaldehyde semicarbazone and a further treatment is required to recover the Cbz-aminoaldehyde.

REFERENCES

REFERENCES

- Abdel-Magid, A. F., J. H. Cohen, et al. (1999). "Chemical Process Synthesis of α -Amino Acids and Esters." Current medicinal chemistry **6**: 955-970.
- Abeles, R. H. and H. A. Lee (1960). "The dismutation of formaldehyde by liver alcohol dehydrogenase." Journal of Biological Chemistry **235**(5): 1499-1503.
- Aizawa, M., R. W. Coughlin, et al. (1975). "Electrochemical regeneration of nicotinamide adenine dinucleotide." Biochimica et Biophysica Acta (BBA)-General Subjects **385**(2): 362-370.
- Alvaro, G., R. Fernandez-Lafuente, et al. (1990). "Immobilization-stabilization of Penicillin G acylase from *Escherichia coli*." Applied Biochemistry and Biotechnology **26**(2): 181-195.
- Anderson, D. and F. Dahlquist (1980). "Determination of the equilibrium distribution between alcohol and aldehyde substrates when bound to horse liver alcohol dehydrogenase using magnetic resonance." Biochemistry **19**(24): 5486-5493.
- Andersson, L. and R. Wolfenden (1982). "A general method of α -aminoaldehyde synthesis using alcohol dehydrogenase." Analytical biochemistry **124**(1): 150-157.
- Anne, A., C. Bourdillon, et al. (1999). "Can the combination of electrochemical regeneration of NAD^+ , selectivity of L- α -amino-acid dehydrogenase, and reductive amination of α -keto-acid be applied to the inversion of configuration of a L- α -amino-acid?" Biotechnology and bioengineering **64**(1): 101-107.
- Ardao, I. (2009). Avances en el desarrollo de bioprocesos: adición aldólica catalizada por rammulosa-1-fosfato aldolasa recombinante. Tesis doctoral, Universitat Autònoma de Barcelona.

- Ardao, I., G. Alvaro, et al. (2011). "Reversible immobilization of rhamnulose-1-phosphate aldolase for biocatalysis: Enzyme loading optimization and aldol addition kinetic modeling." Biochemical Engineering Journal **56**(3): 190-197.
- Ardao, I., M. D. Benaiges, et al. (2006). "One step purification-immobilization of fuculose-1-phosphate aldolase, a class II DHAP dependent aldolase, by using metal-chelate supports." Enzyme and Microbial Technology **39**(1): 22-27.
- Arechederra, M. N., P. K. Addo, et al. (2011). "Poly (neutral red) as a NAD⁺ reduction catalyst and a NADH oxidation catalyst: Towards the development of a rechargeable biobattery." Electrochimica Acta **56**(3): 1585-1590.
- Arns, T., W. R. Heineman, et al. (2001). "Environmental protection and economization of resources by electroorganic and electroenzymatic syntheses." Chemosphere **43**(1): 63-73.
- Asano, N., R. J. Nash, et al. (2000). "Sugar-mimic glycosidase inhibitors: natural occurrence, biological activity and prospects for therapeutic application." Tetrahedron: Asymmetry **11**(8): 1645-1680.
- Bard, A. J. and L. R. Faulkner (2001). Electrochemical Methods, Fundamentals and applications. New York, USA, John Wiley & Sons Inc.
- Bartlett, P. N., P. Birkin, et al. (1997). "Oxidation of β -nicotinamide adenine dinucleotide (NADH) at poly (aniline)-coated electrodes." J. Chem. Soc., Faraday Trans. **93**(10): 1951-1960.
- Barzegar, A., A. A. Moosavi-Movahedi, et al. (2009). "Amplification of electrocatalytic oxidation of NADH based on cysteine nanolayers." Journal of applied electrochemistry **39**(7): 1111-1116.
- Bednarski, M. D., E. S. Simon, et al. (1989). "Rabbit muscle aldolase as a catalyst in organic synthesis." Journal of the American Chemical Society **111**(2): 627-635.
- Biade, A. E., C. Bourdillon, et al. (1992). "Complete conversion of L-lactate into D-lactate. A generic approach involving enzymic catalysis, electrochemical

- oxidation of NADH and electrochemical reduction of pyruvate." Journal of the American Chemical Society **114**(3): 893-897.
- Bignetti, E., G. L. Rossi, et al. (1979). "Microspectrophotometric measurements on single crystals of coenzyme containing complexes of horse liver alcohol dehydrogenase." FEBS Letters **100**(1): 17-22.
- Blaedel, W. and R. A. Jenkins (1975). "Electrochemical oxidation of reduced nicotinamide adenine dinucleotide." Analytical chemistry **47**(8): 1337-1343.
- Blanco, R. M. and J. Guisán (1989). "Stabilization of enzymes by multipoint covalent attachment to agarose-aldehyde gels. Borohydride reduction of trypsin-agarose derivatives." Enzyme and Microbial Technology **11**(6): 360-366.
- Bolivar, J. M., L. Wilson, et al. (2006). "Improvement of the stability of alcohol dehydrogenase by covalent immobilization on glyoxyl-agarose." Journal of Biotechnology **125**(1): 85-94.
- Boratyński, F., G. Kielbowicz, et al. (2010). "Lactones 34 [1]. Application of alcohol dehydrogenase from horse liver (HLADH) in enantioselective synthesis of δ - and ϵ -lactones." Journal of Molecular Catalysis B: Enzymatic **65**(1): 30-36.
- Bradford, M. M. (1976). "A rapid and sensitive method for the quantitation of microgram quantities of protein utilizing the principle of protein-dye binding." Analytical biochemistry **72**(1): 248-254.
- Bradshaw, C. W., J. J. Lalonde, et al. (1992). "Enzymatic synthesis of (R) and (S) 1-deuterohexanol." Applied Biochemistry and Biotechnology **33**(1): 15-24.
- Brändén, C., H. Jörnvall, et al. (1975). *The Enzymes*, Vol, 11 Academic Press, New York.
- Briganti, F., W. Ping Fong, et al. (1989). "In vitro dissociation and reassociation of human alcohol dehydrogenase class I isozymes." Biochemistry(28): 5374-5379.

- Buchholz, K., V. Kasche, et al. (2005). Biocatalysis and Enzyme Technology. Germany, Wiley-VCH.
- Burton, S. G. (2001). "Development of bioreactors for application of biocatalysts in biotransformations and bioremediation." Pure and Applied Chemistry **73**(1): 77-83.
- Calveras, J., J. Bujons, et al. (2006). "Influence of N-amino protecting group on aldolase-catalyzed aldol additions of dihydroxyacetone phosphate to amino aldehydes." Tetrahedron **62**(11): 2648-2656.
- Calveras, J., M. Egado-Gabás, et al. (2009). "Dihydroxyacetone phosphate aldolase catalyzed synthesis of structurally diverse polyhydroxylated pyrrolidine derivatives and evaluation of their glycosidase inhibitory properties." Chemistry-A European Journal **15**(30): 7310-7328.
- Cantet, J., A. Bergel, et al. (1996). "Coupling of the electroenzymatic reduction of NAD⁺ with a synthesis reaction." Enzyme and Microbial Technology **18**(1): 72-79.
- Carrea, G. and S. Riva (2000). "Properties and synthetic applications of enzymes in organic solvents." Angewandte Chemie International Edition **39**(13): 2226-2254.
- Castro, G. R. and T. Knubovets (2003). "Homogeneous biocatalysis in organic solvents and water-organic mixtures." Critical Reviews in Biotechnology **23**(3): 195-231.
- Cea, G., L. Wilson, et al. (2009). "Effect of chain length on the activity of free and immobilized alcohol dehydrogenase towards aliphatic alcohols." Enzyme and Microbial Technology **44**(3): 135-138.
- Ciszewski, A. and G. Milczarek (2000). "Electrocatalysis of NADH oxidation with an electropolymerized film of 1, 4-bis (3, 4-dihydroxyphenyl)-2, 3-dimethylbutane." Analytical chemistry **72**(14): 3203-3209.

- Claiborne, A., T. Conn Mallett, et al. (2001). "Structural, redox, and mechanistic parameters for cysteine-sulfenic acid function in catalysis and regulation." Advances in protein chemistry **58**: 215-276.
- Cole, D. C. (1994). "Recent stereoselective synthetic approaches to β -amino acids." Tetrahedron **50**(32): 9517-9582.
- Colonna-Cesari, F., D. Perahia, et al. (1986). "Interdomain motion in liver alcohol dehydrogenase. Structural and energetic analysis of the hinge bending mode." Journal of Biological Chemistry **261**(32): 15273-15280.
- Compain, P. and O. R. Martin (2001). "Carbohydrate mimetics-based glycosyltransferase inhibitors." Bioorganic & medicinal chemistry **9**(12): 3077-3092.
- Crews, P., L. V. Manes, et al. (1986). "Jasplakinolide, a cyclodepsipeptide from the marine sponge, *Jaspis* sp." Tetrahedron Letters **27**(25): 2797-2800.
- Csomós, P., L. T. Kanerva, et al. (1996). "Biocatalysis for the preparation of optically active β -lactam precursors of amino acids." Tetrahedron: Asymmetry **7**(6): 1789-1796.
- Curulli, A., I. Carelli, et al. (1997). "Enzyme electrode probes obtained by electropolymerization of monomers with PMS and selected dehydrogenase enzymes." Talanta **44**(9): 1659-1669.
- Cheikhou, K. and T. Tzedakis (2008). "Electrochemical microreactor for chiral syntheses using the cofactor NADH." AIChE Journal **54**(5): 1365-1376.
- Chenault, H. K., E. S. Simon, et al. (1988). "Cofactor regeneration for enzyme-catalysed synthesis." Biotechnology and Genetic Engineering Reviews **6**(1): 221-270.
- Chenault, H. K. and G. M. Whitesides (1987). "Regeneration of nicotinamide cofactors for use in organic synthesis." Applied Biochemistry and Biotechnology **14**(2): 147-197.

- Cheng, R. P., S. H. Gellman, et al. (2001). " β -Peptides: from structure to function." Chemical reviews **101**(10): 3219-3232.
- Cherry, J. R. and A. L. Fidantsef (2003). "Directed evolution of industrial enzymes: an update." Current Opinion in Biotechnology **14**(4): 438-443.
- Chiu, T.-H. and D. S. Feingold (1969). "L-rhamnulose-1-phosphate aldolase from *Escherichia coli*. Crystallization and properties." Biochemistry **8**(1): 98-108.
- Choban, E., P. Waszczuk, et al. (2004). "Microfluidic Device and Synthetic Methods." US patent **10**(844,058).
- Dalziel, K. (1961). "Preparation and properties of crystalline alcohol dehydrogenase from liver." Biochemical Journal **80**(2): 440-445.
- Dalziel, K. and F. Dickinson (1965). "Aldehyde mutase." Nature **206**: 255-257.
- Dalziel, K. and F. Dickinson (1966). "The kinetics and mechanism of liver alcohol dehydrogenase with primary and secondary alcohols as substrates." Biochem. J **100**: 34-46.
- DeSantis, G. and J. B. Jones (1999). "Chemical modification of enzymes for enhanced functionality." Current Opinion in Biotechnology **10**(4): 324-330.
- Devaux-Basseguy, R., A. Bergel, et al. (1997). "Potential applications of NAD(P)⁺-dependent oxidoreductases in synthesis: a survey." Enzyme and Microbial Technology **20**(4): 248-258.
- Dixon, M. and E. C. Webb (1979). Enzymes. New York, USA.
- Dordick, J. S. (1991). Principles and Applications of Non-Aqueous Enzymology. Applied Biocatalysis. J. S. Dordick. New York, USA, Marcel Dekker Inc: 1-53.
- Dreyer, M. and G. Schulz (1996). "Refined high-resolution structure of the metal-ion dependent L-fuculose-1-phosphate aldolase (class II) from *Escherichia coli*." Acta Crystallographica Section D: Biological Crystallography **52**(6): 1082-1091.

- Drueckhammer, D. G., S. Sadozai, et al. (1987). "Biphasic one-pot synthesis of two useful and separable compounds using nicotinamide cofactor-requiring enzymes: syntheses of (S)-4-hydroxyhexanoate and its lactone." Enzyme and Microbial Technology **9**(9): 564-570.
- Dutler, H. and C.-I. Brändén (1981). "Correlation studies based on enzyme structure and kinetic results: Deduction of productive substrate orientation in the active-site pocket of horse liver alcohol dehydrogenase." Bioorganic Chemistry **10**(1): 1-13.
- Ehrfeld, W., V. Hessel, et al. (1999). Microreactors, Ullmann's encyclopedia of industrial chemistry, VCH, Weinheim.
- Ehrfeld, W., V. Hessel, et al. (2000). Microreactors, Wiley Online Library.
- Eklund, H., C.-I. Brändén, et al. (1976). "Structural comparisons of mammalian, yeast and bacillar alcohol dehydrogenases." Journal of Molecular Biology **102**(1): 61-73.
- Eklund, H. and C. Brändén (1979). "Structural differences between apo-and holoenzyme of horse liver alcohol dehydrogenase." Journal of Biological Chemistry **254**(9): 3458-3461.
- Eklund, H. and C. Brändén (1987). Alcohol dehydrogenase. Biological Macromolecules and Assemblies: Active Sites of Enzymes. F. A. Jornak, and McPherson, A., Eds. New York, USA, Wiley. **3**: 73-141.
- Eklund, H., P. MÜLLer-Wille, et al. (1990). "Comparison of three classes of human liver alcohol dehydrogenase." European Journal of Biochemistry **193**(2): 303-307.
- Eklund, H., B. Nordström, et al. (1974). "The structure of horse liver alcohol dehydrogenase." FEBS Letters **44**(2): 200-204.
- Eklund, H., B. Plapp, et al. (1982). "Binding of substrate in a ternary complex of horse liver alcohol dehydrogenase." Journal of Biological Chemistry **257**(23): 14349-14358.

- Eklund, H., J.-P. Samama, et al. (1981). "Structure of a triclinic ternary complex of horse liver alcohol dehydrogenase at 2.9 Å resolution." Journal of Molecular Biology **146**(4): 561-587.
- English, E. P., R. S. Chumanov, et al. (2006). "Rational development of β -peptide inhibitors of human cytomegalovirus entry." Journal of Biological Chemistry **281**(5): 2661-2667.
- Espelt, L., T. Parella, et al. (2003). "Stereoselective Aldol Additions Catalyzed by Dihydroxyacetone Phosphate-Dependent Aldolases in Emulsion Systems: Preparation and Structural Characterization of Linear and Cyclic Iminopolyols from Aminoaldehydes." Chemistry – A European Journal **9**(20): 4887-4899.
- Fassouane, A., J. M. Laval, et al. (1990). "Electrochemical regeneration of NAD^+ in a plug-flow reactor." Biotechnology and bioengineering **35**(9): 935-939.
- Fechter, M., A. Stutz, et al. (1999). "Chemical and chemo-enzymatic approaches to unnatural ketoses and glycosidase inhibitors with basic nitrogen in the sugar ring." Curr. Org. Chem **3**: 269-285.
- Fernandez-Lafuente, R., C. Rosell, et al. (1993). "Preparation of activated supports containing low pK amino groups. A new tool for protein immobilization via the carboxyl coupling method." Enzyme and Microbial Technology **15**(7): 546-550.
- Fessner, W.-D. (1998). "Enzyme mediated C • C bond formation." Current Opinion in Chemical Biology **2**(1): 85-97.
- Fessner, W.-D. and C. Walter (1997). Enzymatic CC bond formation in asymmetric synthesis. Bioorganic Chemistry, Springer: 97-194.
- Fessner, W. D., A. Schneider, et al. (1993). "Enzymes in organic-synthesis .6. 6-deoxyl-L-lyxo-hexulose and 6-deoxyl-L-arabino-hexulose 1-phosphates - Enzymatic synthesis by antagonistic metabolic pathways." Tetrahedron-Asymmetry **4**(6): 1183-1192.

- Fessner, W. D., G. Sinerius, et al. (1991). "Diastereoselective Enzymatic Aldol Additions: L-Rhamnulose and L-Fuculose 1-Phosphate Aldolases from *E. coli*." Angewandte Chemie International Edition in English **30**(5): 555-558.
- Frey A., P. and A. Hageman D. (2007). Enzymatic Reaction Mechanisms. New York, USA, Oxford University Press.
- Gavrilescu, M. and Y. Chisti (2005). "Biotechnology—a sustainable alternative for chemical industry." Biotechnology Advances **23**(7–8): 471-499.
- Geueke, B., B. Riebel, et al. (2003). "NADH oxidase from *Lactobacillus brevis*: a new catalyst for the regeneration of NAD." Enzyme and Microbial Technology **32**(2): 205-211.
- Ghanem, M. A., J.-M. Chrétien, et al. (2009). "Electrochemical and solid-phase synthetic modification of glassy carbon electrodes with dihydroxybenzene compounds and the electrocatalytic oxidation of NADH." Bioelectrochemistry **76**(1): 115-125.
- Giacomini, D., P. Galletti, et al. (2007). "Highly efficient asymmetric reduction of arylpropionic aldehydes by horse liver alcohol dehydrogenase through dynamic kinetic resolution." Chemical Communications(39): 4038-4040.
- Goldberg, K., K. Schroer, et al. (2007). "Biocatalytic ketone reduction—a powerful tool for the production of chiral alcohols—part I: processes with isolated enzymes." Applied microbiology and biotechnology **76**(2): 237-248.
- Gorton, L. (2002). "Electrochemistry of NAD(P)⁺/NAD(P)H." Encyclopedia of electrochemistry.
- Gorton, L. and E. Domínguez (2002). "Electrocatalytic oxidation of NAD(P)H at mediator-modified electrodes." Reviews in Molecular Biotechnology **82**(4): 371-392.

- Graves, J. M., A. Clark, et al. (1965). "Stereochemical Aspects of the Substrate Specificity of Horse Liver Alcohol Dehydrogenase." Biochemistry **4**(12): 2655-2671.
- Grueninger, D. and G. E. Schulz (2008). "Antenna domain mobility and enzymatic reaction of L-rhamnulose-1-phosphate aldolase." Biochemistry **47**(2): 607-614.
- Grunwald, J., B. Wirz, et al. (1986). "Asymmetric oxidoreductions catalyzed by alcohol dehydrogenase in organic solvents." Journal of the American Chemical Society **108**(21): 6732-6734.
- Guisán, J. M., A. Bastida, et al. (1991). "Immobilization-stabilization of α -chymotrypsin by covalent attachment to aldehyde-agarose gels." Biotechnology and bioengineering **38**(10): 1144-1152.
- Hald, E., P. Lehmann, et al. (1975). "Molar Absorptivities of β -NADH and β -NAD at 260 nm." Clinical chemistry **21**(7): 884-887.
- Handman, J., A. Harriman, et al. (1984). "Photochemical dehydrogenation of ethanol in dilute aqueous solution." Nature **307**(5951): 534-535.
- Hart, D. J. and D. C. Ha (1989). "The ester enolate-imine condensation route to. beta.-lactams." Chemical reviews **89**(7): 1447-1465.
- Haslegrave, J. A. and J. B. Jones (1982). "Enzymes in organic synthesis. 25. Heterocyclic ketones as substrates of horse liver alcohol dehydrogenase. Highly stereoselective reductions of 2-substituted tetrahydropyran-4-ones." Journal of the American Chemical Society **104**(17): 4666-4671.
- Hilt, G., T. Jarbawi, et al. (1997). "An Analytical Study of the Redox Behavior of 1, 10-Phenanthroline-5, 6-dione, its Transition-Metal Complexes, and its N-Monomethylated Derivative with regard to their Efficiency as Mediators of NAD (P)⁺ Regeneration." Chemistry-A European Journal **3**(1): 79-88.
- Hilt, G., B. Lewall, et al. (1997). "Efficient In-Situ Redox Catalytic NAD(P)⁺ Regeneration in Enzymatic Synthesis Using Transition-Metal Complexes of 1,

- 10-Phenanthroline-5, 6-dione and Its N-Monomethylated Derivative as Catalysts." Liebigs Annalen **1997**(11): 2289-2296.
- Hilt, G. and E. Steckhan (1993). "Transition metal complexes of 1, 10-phenanthroline-5, 6-dione as efficient mediators for the regeneration of NAD⁺ in enzymatic synthesis." J. Chem. Soc., Chem. Commun.(22): 1706-1707.
- Hinson, J. A. and R. A. Neal (1975). "An examination of octanol and octanal metabolism to octanoic acid by horse liver alcohol dehydrogenase." Biochimica et Biophysica Acta (BBA)-Enzymology **384**(1): 1-11.
- Hollmann, F., K. Hofstetter, et al. (2006). "Non-enzymatic regeneration of nicotinamide and flavin cofactors for monooxygenase catalysis." Trends in Biotechnology **24**(4): 163-171.
- Hollmann, F., A. Kleeb, et al. (2005). "Coupled chemoenzymatic transfer hydrogenation catalysis for enantioselective reduction and oxidation reactions." Tetrahedron: Asymmetry **16**(21): 3512-3519.
- Hollmann, F. and A. Schmid (2004). "Electrochemical regeneration of oxidoreductases for cell-free biocatalytic redox reactions." Biocatalysis and Biotransformation **22**(2): 63-88.
- Hollmann, F., B. Witholt, et al. (2002). "[Cp*Rh(bpy)(H₂O)]²⁺: a versatile tool for efficient and non-enzymatic regeneration of nicotinamide and flavin coenzymes." Journal of Molecular Catalysis B: Enzymatic **19**: 167-176.
- Horecker, B. L. and A. Kornberg (1948). "The extinction coefficients of the reduced band of pyridine nucleotides." Journal of Biological Chemistry **175**(1): 385-390.
- Hummel, W. and M. R. Kula (1989). "Dehydrogenases for the synthesis of chiral compounds." European Journal of Biochemistry **184**(1): 1-13.
- Illanes, A. (2008). Enzyme Biocatalysis. Principles and Applications. United Kingdom, Springer.

- Iwuoha, E. I. and M. R. Smyth (2003). "Reactivities of organic phase biosensors: 6. Square-wave and differential pulse studies of genetically engineered cytochrome P450_{cam} (CYP101) bioelectrodes in selected solvents." Biosensors and Bioelectronics **18**(2): 237-244.
- Jaegfeldt, H. (1981). "A study of the products formed in the electrochemical reduction of nicotinamide-adenine-dinucleotide." Journal of Electroanalytical Chemistry and Interfacial Electrochemistry **128**: 355-370.
- Jähnisch, K., V. Hessel, et al. (2004). "Chemistry in microstructured reactors." Angewandte Chemie International Edition **43**(4): 406-446.
- Jakovac, I. J., H. B. Goodbrand, et al. (1982). "Enzymes in organic synthesis. 24. Preparations of enantiomerically pure chiral lactones via stereospecific horse liver alcohol dehydrogenase catalyzed oxidations of monocyclic meso diols." Journal of the American Chemical Society **104**(17): 4659-4665.
- Joerger, A. C., C. Mueller-Dieckmann, et al. (2000). "Structures of l-fuculose-1-phosphate aldolase mutants outlining motions during catalysis." Journal of Molecular Biology **303**(4): 531-543.
- Jones, J. B. and H. M. Schwartz (1982). "Enzymes in organic synthesis. 23. Effects of organic solvents on horse liver alcohol dehydrogenase-catalyzed oxidation." Canadian Journal of Chemistry **60**(8): 1030-1033.
- Jones, J. B. and K. E. Taylor (1976). "Nicotinamide coenzyme regeneration. Flavin mononucleotide (riboflavin phosphate) as an efficient, economical, and enzyme-compatible recycling agent." Canadian Journal of Chemistry **54**(19): 2969-2973.
- Ju, H., Y. Xiao, et al. (2002). "Electrooxidative coupling of a toluidine blue O terminated self-assembled monolayer studied by electrochemistry and surface enhanced Raman spectroscopy." Journal of Electroanalytical Chemistry **518**(2): 123-130.

- Juaristi, E. (1997). *Enantioselective Synthesis of β -Amino Acids*, Wiley-VCH: New York.
- Juaristi, E. and H. Lopez-Ruiz (1999). "Recent Advances in the Enantioselective Synthesis of β -Amino Acids." *Current medicinal chemistry* **6**: 983-1004.
- Julliard, M. and J. Le Petit (1982). "Regeneration of NAD^+ and NADP^+ cofactors by photosensitized electron transfer." *Photochemistry and Photobiology* **36**(3): 283-290.
- Jurczak, J. and A. Golebiowski (1989). "Optically active N-protected α -amino aldehydes in organic synthesis." *Chemical reviews* **89**(1): 149-164.
- Kamiya, N., M. Inoue, et al. (2000). "Catalytic and Structural Properties of Surfactant-Horseradish Peroxidase Complex in Organic Media." *Biotechnology progress* **16**(1): 52-58.
- Kanamaru, T., S. Shinagawa, et al. (1985). "Emeriamine, an antidiabetic β -aminobetaine derived from a novel fungal metabolite." *Life sciences* **37**(3): 217-223.
- Kane, C. (2005). Conception et réalisation de microréacteurs électrochimiques – Application à la régénération électroenzymatique de NADH et potentialités en synthèse. Thèse de doctorat, Université Paul Sabatier – Toulouse III.
- Kanerva, L. T., P. Csomós, et al. (1996). "Approach to highly enantiopure β -amino acid esters by using lipase catalysis in organic media." *Tetrahedron: Asymmetry* **7**(6): 1705-1716.
- Kashiwagi, Y. and T. Osa (1993). "Electrocatalytic oxidation of NADH on thin poly (acrylic acid) film coated graphite felt electrode coimmobilizing ferrocene and diaphorase." *Chemistry Letters* **22**(4): 677-680.
- Katz, E., V. Heleg-Shabtai, et al. (1998). "Surface reconstitution of a de novo synthesized hemoprotein for bioelectronic applications." *Angewandte Chemie International Edition* **37**(23): 3253-3256.

- Kawakami, K., T. Abe, et al. (1992). "Silicone-immobilized biocatalysts effective for bioconversions in nonaqueous media." Enzyme and Microbial Technology **14**(5): 371-375.
- Kawamoto, T., A. Aoki, et al. (1989). "Novel photocatalytic NAD⁺ recycling system with a semiconductor in organic solvent." Journal of fermentation and bioengineering **67**(5): 361-362.
- Kochius, S., A. O. Magnusson, et al. (2012). "Immobilized redox mediators for electrochemical NAD (P)⁺ regeneration." Applied microbiology and biotechnology **93**(6): 2251-2264.
- Koeller, K. M. and C.-H. Wong (2000). "Complex carbohydrate synthesis tools for glycobiologists: enzyme-based approach and programmable one-pot strategies." Glycobiology **10**(11): 1157-1169.
- Kroemer, M., I. Merkel, et al. (2003). "Structure and catalytic mechanism of L-rhamnulose-1-phosphate aldolase." Biochemistry **42**(36): 10560-10568.
- Kvassman, J. and G. Pettersson (1979). "Effect of pH on coenzyme binding to liver alcohol dehydrogenase." European Journal of Biochemistry **100**(1): 115-123.
- LeBrun, L. A., D.-H. Park, et al. (2004). "Participation of histidine-51 in catalysis by horse liver alcohol dehydrogenase." Biochemistry **43**(11): 3014-3026.
- Lee, D. and M.-J. Kim (1998). "Lipase-catalyzed transesterification as a practical route to homochiral *syn*-1, 2-diols. The synthesis of the taxol side chain." Tetrahedron Letters **39**(15): 2163-2166.
- Lemiere, G., J. Lepoivre, et al. (1985). "Hlad-catalyzed oxidations of alcohols with acetaldehyde as a coenzyme recycling substrate." Tetrahedron Letters **26**(37): 4527-4528.
- Lillelund, V. H., H. H. Jensen, et al. (2002). "Recent developments of transition-state analogue glycosidase inhibitors of non-natural product origin." Chemical reviews **102**(2): 515-554.

- Lineweaver, H. and D. Burk (1934). "The determination of enzyme dissociation constants." Journal of the American Chemical Society **56**(3): 658-666.
- Liu, H., Q. Xu, et al. (2011). "The Effect of Temperature on the Electrochemical Behavior of the V (IV)/V (V) Couple on a Graphite Electrode."
- Liu, W. and P. Wang (2007). "Cofactor regeneration for sustainable enzymatic biosynthesis." Biotechnology Advances **25**(4): 369-384.
- Lobo, M., A. Miranda, et al. (1996). "Electrocatalytic detection of nicotinamide coenzymes by poly (o-aminophenol)-and poly (o-phenylenediamine)-modified carbon paste electrodes." Analytica chimica acta **325**(1): 33-42.
- Lobo, M. J., A. J. Miranda, et al. (1997). "Amperometric biosensors based on NAD(P)⁺ dependent dehydrogenase enzymes." Electroanalysis **9**(3): 191-202.
- López-Santín, J., G. Alvaro, et al. (2008). "6.5 Use of Aldolases for Asymmetric Synthesis." Enzyme Biocatalysis: 333.
- Lortie, R., I. Villaume, et al. (1989). "Enzymatic production of long-chain aldehydes in a fixed bed reactor using organic solvents and cofactor regeneration." Biotechnology and bioengineering **33**(2): 229-232.
- Löwe, H. and W. Ehrfeld (1999). "State-of-the-art in microreaction technology: concepts, manufacturing and applications." Electrochimica Acta **44**(21): 3679-3689.
- Lu, B., J. Bai, et al. (2010). "Electrosynthesis and efficient electrocatalytic performance of poly (neutral red)/ordered mesoporous carbon composite." Electrochimica Acta **55**(15): 4647-4652.
- Mano, N. and A. Kuhn (1999). "Immobilized nitro-fluorenone derivatives as electrocatalysts for NADH oxidation." Journal of Electroanalytical Chemistry **477**(1): 79-88.

- Mano, N., A. Thienpont, et al. (2001). "Adsorption and catalytic activity of trinitrofluorenone derivatives towards NADH oxidation on different electrode materials." Electrochemistry communications **3**(10): 585-589.
- Manu, B. and S. Chaudhari (2002). "Anaerobic decolorisation of simulated textile wastewater containing azo dyes." Bioresource technology **82**(3): 225-231.
- Martins, F. J., A. M. Viljoen, et al. (2001). "Enantioselective synthesis of amino acids from pentacyclo [5.4. 0.0². 6.0³. 10.0⁵. 9] undecane-8, 11-dione." Tetrahedron **57**(8): 1601-1607.
- Merritt, A. D. and G. M. Tomkins (1959). "Reversible oxidation of cyclic secondary alcohols by liver alcohol dehydrogenase." Journal of Biological Chemistry **234**(10): 2778-2782.
- Moiroux, J. and P. J. Elving (1980). "Mechanistic aspects of the electrochemical oxidation of dihydronicotinamide adenine dinucleotide (NADH)." Journal of the American Chemical Society **102**(21): 6533-6538.
- Munteanu, F.-D., N. Mano, et al. (2002). "Mediator-modified electrodes for catalytic NADH oxidation: high rate constants at interesting overpotentials." Bioelectrochemistry **56**(1): 67-72.
- Naemura, K., T. Fujii, et al. (1986). "Selective and stereospecific horse liver alcohol dehydrogenase-catalyzed reduction of cage-shaped meso-diketone. An efficient access to optically active D3-trishomocubane derivative." Chemistry Letters(6): 923-926.
- Namikoshi, M., K. L. Rinehart, et al. (1989). "Total synthesis of Adda, the unique C₂₀ amino acid of cyanobacterial hepatotoxins." Tetrahedron Letters **30**(33): 4349-4352.
- Ng, G., L.-C. YUAN, et al. (1984). "Enzymes in organic synthesis. XXIX: Preparations of enantiomerically pure cis-2, 3-and 2, 4-dimethyl lactones via horse liver alcohol dehydrogenase-catalyzed oxidations." Tetrahedron **40**(8): 1235-1243.

- Nicolaou, K. C. and R. K. Guy (1995). "The conquest of Taxol." Angewandte Chemie International Edition in English **34**(19): 2079-2090.
- Obón, J. M., P. Casanova, et al. (1997). "Stabilization of glucose dehydrogenase with polyethyleneimine in an electrochemical reactor with NAD(P)⁺ regeneration." Biotechnology progress **13**(5): 557-561.
- Ogino, H. and H. Ishikawa (2001). "Enzymes which are stable in the presence of organic solvents." Journal of bioscience and bioengineering **91**(2): 109-116.
- Orbegozo, T., I. Lavandera, et al. (2009). "Biocatalytic oxidation of benzyl alcohol to benzaldehyde via hydrogen transfer." Tetrahedron **65**(34): 6805-6809.
- Osa, T., Y. Kashiwagi, et al. (1994). "Electroenzymatic oxidation of alcohols on a poly (acrylic acid)-coated graphite felt electrode terimmobilizing ferrocene, diaphorase and alcohol dehydrogenase." Chemistry Letters **23**(2): 367-370.
- Palmore, G. T. R., H. Bertschy, et al. (1998). "A methanol/dioxygen biofuel cell that uses NAD⁺-dependent dehydrogenases as catalysts: application of an electroenzymatic method to regenerate nicotinamide adenine dinucleotide at low overpotentials." Journal of Electroanalytical Chemistry **443**(1): 155-161.
- Palomo, C., J. M. Aizpurua, et al. (1991). "A convenient method for β -lactam formation from β -amino acids using phenyl phosphorodichloridate reagent." The Journal of organic chemistry **56**(6): 2244-2247.
- Parida, S., R. Datta, et al. (1992). "Supported aqueous-phase enzymatic catalysis in organic media." Applied Biochemistry and Biotechnology **33**(1): 1-14.
- Pariante, F., F. Tobalina, et al. (1996). "Electrodeposition of redox-active films of dihydroxybenzaldehydes and related analogs and their electrocatalytic activity toward NADH oxidation." Analytical chemistry **68**(18): 3135-3142.
- Pera, L. M., M. D. Baigori, et al. (2003). "Enzyme Behaviour in Non-conventional Systems." Indian Journal of Biotechnology **2**(3): 356-361.

- Persson, M., E. Wehtje, et al. (2002). "Factors governing the activity of lyophilised and immobilised lipase preparations in organic solvents." ChemBioChem **3**(6): 566-571.
- Pešić, M. (2012). Biocatalyst and bioprocess engineering for the synthesis of aminopolyols by enzymatic oxidation an aldol addition. Tesis doctoral, Universitat Autònoma de Barcelona.
- Pešić, M., C. López, et al. (2012). "Chloroperoxidase catalyzed oxidation of Cbz-ethanolamine to Cbz-glycinal." Biochemical Engineering Journal.
- Pešić, M., C. López, et al. (2013). "From amino alcohol to aminopolyol: one-pot multienzyme oxidation and aldol addition." Applied microbiology and biotechnology: 1-11.
- Peters, J. (1998). "Dehydrogenases-Characteristics, Design of Reaction Conditions, and Applications." Biotechnology Set, Second Edition: 391-473.
- Pettersson, G. (1987). "Liver alcohol dehydrogenase." CRC Critical Reviews in Biochemistry **21**: 349-389.
- Phillips, S. A. and P. J. Thornalley (1993). "The formation of methylglyoxal from triose phosphates." European Journal of Biochemistry **212**(1): 101-105.
- Pival, S. L., M. Klimacek, et al. (2008). "Novel Chemo-Enzymatic Mimic of Hydrogen Peroxide-Forming NAD(P)H Oxidase for Efficient Regeneration of NAD⁺ and NADP⁺." Advanced Synthesis & Catalysis **350**(14-15): 2305-2312.
- Pohar, A. and I. Plazl (2009). "Process intensification through microreactor application." Chemical and Biochemical Engineering Quarterly **23**(4): 537-544.
- Prieto-Simón, B. and E. Fàbregas (2004). "Comparative study of electron mediators used in the electrochemical oxidation of NADH." Biosensors and Bioelectronics **19**(10): 1131-1138.

- Richard, J. (1993). "Mechanism for the formation of methylglyoxal from triosephosphates." Biochemical society transactions **21**(2): 549-553.
- Riebel, B. R., P. R. Gibbs, et al. (2002). "Cofactor regeneration of NAD⁺ from NADH: novel water-forming NADH oxidases." Advanced Synthesis and Catalysis **344**(10): 1156-1168.
- Roers, R. and G. L. Verdine (2001). "Concise enantio- and diastereoselective synthesis of α -hydroxy- α -methyl- β -amino acids." Tetrahedron Letters **42**(21): 3563-3565.
- Ru, M. T., J. S. Dordick, et al. (1999). "Optimizing the salt-induced activation of enzymes in organic solvents: Effects of lyophilization time and water content." Biotechnology and bioengineering **63**(2): 233-241.
- Rubach, J. K. and B. V. Plapp (2002). "Mobility of fluorobenzyl alcohols bound to liver alcohol dehydrogenases as determined by NMR and X-ray crystallographic studies." Biochemistry **41**(52): 15770-15779.
- Ruiz, J., J. Pinsach, et al. (2009). "Alternative production process strategies in E. coli improving protein quality and downstream yields." Process Biochemistry **44**(9): 1039-1045.
- Ruppert, R. and E. Steckhan (1989). "Efficient photoelectrochemical in-situ regeneration of NAD(P)⁺ coupled to enzymatic oxidation of alcohols." Journal of the Chemical Society, Perkin Transactions **2**(7): 811-814.
- Saiki, Y. and Y. Amao (2003). "Bio-mimetic hydrogen production from polysaccharide using the visible light sensitization of zinc porphyrin." Biotechnology and bioengineering **82**(6): 710-714.
- Salleh, A. B., M. Basri, et al. (2002). "Modified enzymes for reactions in organic solvents." Applied Biochemistry and Biotechnology **102**(1-6): 349-357.
- Samec, Z. and P. J. Elving (1983). "Anodic oxidation of dihydronicotinamide adenine dinucleotide at solid electrodes; mediation by surface species." Journal of Electroanalytical Chemistry and Interfacial Electrochemistry **144**(1): 217-234.

- Sánchez, V. M., F. Rebolledo, et al. (1997). "*Candida antarctica* lipase catalyzed resolution of ethyl (\pm)-3-aminobutyrate." Tetrahedron: Asymmetry **8**(1): 37-40.
- Santos, A. d. S., L. Gorton, et al. (2002). "Nile blue adsorbed onto silica gel modified with niobium oxide for electrocatalytic oxidation of NADH." Electrochimica Acta **47**(20): 3351-3360.
- Schirmer, C., Y. Liu, et al. (2002). "Horse liver alcohol dehydrogenase as a probe for nanostructuring effects of alcohols in water/nonionic surfactant systems." The Journal of Physical Chemistry B **106**(30): 7414-7421.
- Schmid, A., J. Dordick, et al. (2001). "Industrial biocatalysis today and tomorrow." Nature **409**(6817): 258-268.
- Schmid, A., F. Hollmann, et al. (2002). "Oxidation of alcohols." Enzyme Catalysis in Organic Synthesis: A Comprehensive Handbook, Second Edition: 1108-1170.
- Schneider, G., E. Cedergren-Zeppezauer, et al. (1985). "Active site specific cadmium (II)-substituted horse liver alcohol dehydrogenase: crystal structures of the free enzyme, its binary complex with NADH, and the ternary complex with NADH and bound p-bromobenzyl alcohol." Biochemistry **24**(25): 7503-7510.
- Schröder, I., E. Steckhan, et al. (2003). "*In situ* NAD⁺ regeneration using 2, 2'-azinobis (3-ethylbenzothiazoline-6-sulfonate) as an electron transfer mediator." Journal of Electroanalytical Chemistry **541**: 109-115.
- Schubert, T., W. Hummel, et al. (2002). "Highly enantioselective preparation of multifunctionalized propargylic building blocks." Angewandte Chemie International Edition **41**(4): 634-637.
- Seebach, D., A. K. Beck, et al. (2004). "The World of β - and γ -Peptides Comprised of Homologated Proteinogenic Amino Acids and Other Components." Chemistry & biodiversity **1**(8): 1111-1239.
- Seebach, D., T. Kimmerlin, et al. (2004). "How we drifted into peptide chemistry and where we have arrived at." Tetrahedron **60**(35): 7455-7506.

- Sekhar, V. C. and B. V. Plapp (1988). "Mechanism of binding of horse liver alcohol dehydrogenase and nicotinamide adenine dinucleotide." Biochemistry **27**(14): 5082-5088.
- Shearer, G. L., K. Kim, et al. (1993). "Alternative pathways and reactions of benzyl alcohol and benzaldehyde with horse liver alcohol dehydrogenase." Biochemistry **32**(41): 11186-11194.
- Shigematsu, H., T. Matsumoto, et al. (1995). "Horse liver alcohol dehydrogenase-catalyzed enantioselective reduction of cyclic ketones: The effect of the hydrophobic side chain of the substrate on the stereoselectivity of the reaction." Tetrahedron: Asymmetry **6**(12): 3001-3008.
- Shih, C., L. S. Gossett, et al. (1999). "Synthesis and biological evaluation of novel cryptophycin analogs with modification in the β -alanine region." Bioorganic & medicinal chemistry letters **9**(1): 69-74.
- Shinagawa, S., T. Kanamaru, et al. (1987). "Chemistry of emeriamine and its analogs and their inhibitory activity in long-chain fatty acid oxidation." Journal of medicinal chemistry **30**(8): 1458-1463.
- Sih, C. J. (1997). Enantioselective Synthesis of β -Amino Acids E. Juaristi. New York, USA, Wiley-VCH 433-441.
- Silverstein, E. (1965). "Separation and purification of oxidized and reduced nicotinamide adenine dinucleotides." Analytical biochemistry **12**(2): 199-212.
- Silverstein, E. and P. Boyer (1964). "Equilibrium reaction rates and the mechanisms of liver and yeast alcohol dehydrogenase." Journal of Biological Chemistry **239**(11): 3908-3914.
- Soloshonok, V. A. (1997). Enantioselective Synthesis of β -Amino Acids E. Juaristi. New York, USA Wiley-VCH: 443-464.
- Steckhan, E., S. Herrmann, et al. (1991). "Analytical study of a series of substituted (2, 2'-bipyridyl)(pentamethylcyclopentadienyl) rhodium and-iridium complexes

- with regard to their effectiveness as redox catalysts for the indirect electrochemical and chemical reduction of NAD(P)⁺." Organometallics **10**(5): 1568-1577.
- Steer, D. L., R. A. Lew, et al. (2002). "β-amino acids: versatile peptidomimetics." Current medicinal chemistry **9**(8): 811-822.
- Stütz, A. E. and J. Wiley (1999). Iminosugars as glycosidase inhibitors: nojirimycin and beyond, Wiley-VCH Weinheim.
- Suau, T., G. Álvaro, et al. (2008). "Performance of an immobilized fuculose-1-phosphate aldolase for stereoselective synthesis." Biocatalysis and Biotransformation **27**(2): 136-142.
- Suau, T., G. Alvaro, et al. (2006). "Influence of secondary reactions on the synthetic efficiency of DHAP-aldolases." Biotechnology and bioengineering **93**(1): 48-55.
- Sund, H. (1970). Pyridine nucleotide-dependent dehydrogenases. Symposium on Pyridine Nucleotide-Dependent Dehydrogenases (1969: University of Konstanz), Springer-Verlag.
- Sund, H. and H. Theorell (1963). "Alcohol dehydrogenases." The enzymes **7**: 25-83.
- Sytkowski, A. J. and B. L. Vallee (1976). "Chemical reactivities of catalytic and noncatalytic zinc or cobalt atoms of horse liver alcohol dehydrogenase: differentiation by their thermodynamic and kinetic properties." Proceedings of the National Academy of Sciences **73**(2): 344-348.
- Sytkowski, A. J. and B. L. Vallee (1979). "Cadmium-109 as a probe of the metal binding sites in horse liver alcohol dehydrogenase." Biochemistry **18**(19): 4095-4099.
- Theil, F. and S. Ballschuh (1996). "Chemoenzymatic synthesis of both enantiomers of cispentacin." Tetrahedron: Asymmetry **7**(12): 3565-3572.

- Thomsen, M. and B. Nidetzky (2009). "Stereoselective and environmentally friendly reactions." Modern biocatalysis, Wiley-VCH Verlag GmbH, Weinheim: 43-54.
- Toh, C.-S., P. N. Bartlett, et al. (2003). "The effect of calcium ions on the electrocatalytic oxidation of NADH by poly (aniline)-poly (vinylsulfonate) and poly (aniline)-poly (styrenesulfonate) modified electrodes." Physical Chemistry Chemical Physics **5**(3): 588-593.
- Tudorache, M., D. Mahalu, et al. (2011). "Biocatalytic microreactor incorporating HRP anchored on micro-/nano-lithographic patterns for flow oxidation of phenols." Journal of Molecular Catalysis B: Enzymatic **69**(3): 133-139.
- Tzedakis, T., K. Cheikhou, et al. (2010). "Electrochemical study in both classical cell and microreactors of flavin adenine dinucleotide as a redox mediator for NADH regeneration." Electrochimica Acta **55**(7): 2286-2294.
- Tzedakis, T., C. Kane, et al. (2006). "French Patent, n (04.12305, 2004)." US patent.
- Tzedakis, T., C. Kane, et al. (2006). Method for electrochemical reaction and electrochemical reactor with microchannels and method for making same, WO Patent 2,006,053,962.
- Vallee, B. L. and D. S. Auld (1990). "Active-site zinc ligands and activated H₂O of zinc enzymes." Proceedings of the National Academy of Sciences **87**(1): 220-224.
- van der Donk, W. A. and H. Zhao (2003). "Recent developments in pyridine nucleotide regeneration." Current Opinion in Biotechnology **14**(4): 421-426.
- Van Elsacker, P., G. Lemiere, et al. (1989). "The HLADH-catalyzed oxidoreduction in a two-phase system "organic solvent-moistened glass beads"." Bioorganic Chemistry **17**(1): 28-35.
- Vidal, L. (2006). Producción de aldolasas recombinantes: de la biología molecular al desarrollo de procesos. Tesis doctoral, Universitat Autònoma de Barcelona.

- Vidal, L., O. Durany, et al. (2003). "High-level production of recombinant His-tagged rhamnulose 1-phosphate aldolase in Escherichia coli." Journal of Chemical Technology and Biotechnology **78**(11): 1171-1179.
- Wandrey, C. (2004). "Biochemical reaction engineering for redox reactions." The Chemical Record **4**(4): 254-265.
- Weckbecker, A., H. Gröger, et al. (2010). Regeneration of nicotinamide coenzymes: principles and applications for the synthesis of chiral compounds. Biosystems Engineering I, Springer: 195-242.
- Weibel, M. K., H. H. Weetall, et al. (1971). "Insolubilized coenzymes: the covalent coupling of enzymatically active NAD⁺ to glass surfaces." Biochemical and biophysical research communications **44**(2): 347-352.
- Wichmann, R. and D. Vasic-Racki (2005). Cofactor regeneration at the lab scale. Technology transfer in biotechnology, Springer: 225-260.
- Willner, I. and D. Mandler (1989). "Enzyme-catalysed biotransformations through photochemical regeneration of nicotinamide cofactors." Enzyme and Microbial Technology **11**(8): 467-483.
- Winkler, J. D. and D. Subrahmanyam (1992). "Studies directed towards the synthesis of taxol: preparation of C-13 oxygenated taxane congeners." Tetrahedron **48**(34): 7049-7056.
- Wong, C. H., J. Gordon, et al. (1981). "Regeneration of NAD(P)H using glucose-6-sulfate and glucose-6-phosphate dehydrogenase." The Journal of organic chemistry **46**(23): 4676-4679.
- Wong, C. H., R. L. Halcomb, et al. (1995). "Enzymes in organic synthesis: application to the problems of carbohydrate recognition (part 1)." Angewandte Chemie International Edition in English **34**(4): 412-432.

- Wong, C. H., R. L. Halcomb, et al. (1995). "Enzymes in organic synthesis: application to the problems of carbohydrate recognition (part 2)." Angewandte Chemie International Edition in English **34**(5): 521-546.
- Wratten, C. C. and W. Cleland (1963). "Product Inhibition Studies on Yeast and Liver Alcohol Dehydrogenases." Biochemistry **2**(5): 935-941.
- Yan, A.-X., X.-W. Li, et al. (2002). "Recent progress on immobilization of enzymes on molecular sieves for reactions in organic solvents." Applied Biochemistry and Biotechnology **101**(2): 113-129.
- Yoon, S. K., E. R. Choban, et al. (2005). "Laminar flow-based electrochemical microreactor for efficient regeneration of nicotinamide cofactors for biocatalysis." Journal of the American Chemical Society **127**(30): 10466-10467.
- Zagalak, B., P. A. Frey, et al. (1966). "Stereochemistry of conversion of D and L 1,2-propanediols to propionaldehyde." Journal of Biological Chemistry **241**(13): 3028-3035.
- Zhao, H. and W. A. van der Donk (2003). "Regeneration of cofactors for use in biocatalysis." Current Opinion in Biotechnology **14**(6): 583-589.

ANNEXES

ANNEXES

Annex 1. Platinum electrode studies

i. Buffer

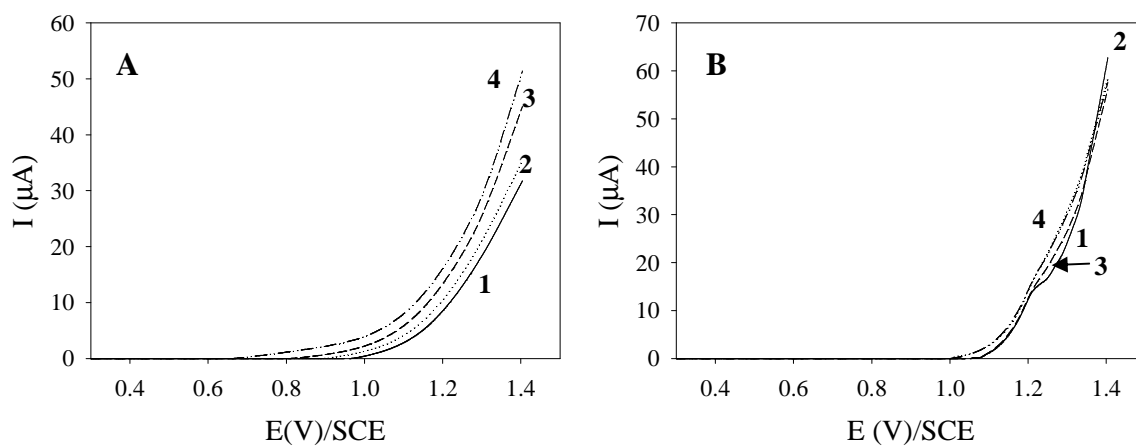


Figure A.1.1 Current potential curves obtained on a platinum disc anode ($S=3.14 \text{ mm}^2$) at room temperature. Residual current of 75 mM sodium pyrophosphate buffer pH 8.7. (A) Transient state without convection/ $\omega=0$ and several scan rates (ν); (1) 20 mV/s, (2) 50 mV/s, (3) 100 mV/s, (4) 200 mV/s; (B) Steady state on a rotating disc $\nu=5 \text{ mV/s}$ and several angular velocities (ω); (1) 500 rpm, (2) 1000 rpm, (3) 2000 rpm, (4) 5000 rpm.

ii. Buffer with 20 mM Cbz-ethanolamine

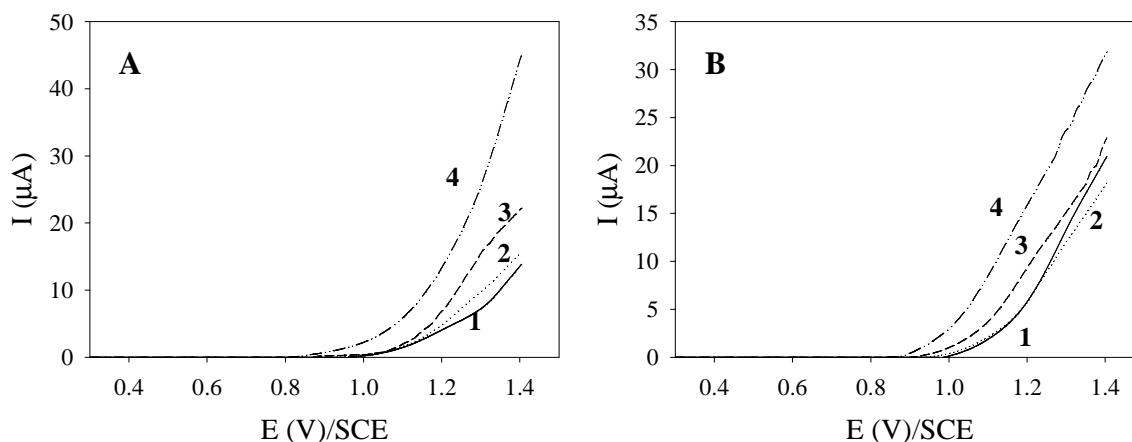


Figure A.1.2 Current potential curves obtained on a platinum disc anode ($S=3.14 \text{ mm}^2$) at room temperature. Residual current of 75 mM sodium pyrophosphate buffer pH 8.7 with 20 mM Cbz-ethanolamine (A) Transient state without convection/ $\omega=0$ and several scan rates (r); (1) 20 mV/s, (2) 50 mV/s, (3) 100 mV/s, (4) 200 mV/s; (B) Steady state on a rotating disc $r=5 \text{ mV/s}$ and several angular velocities (ω); (1) 500 rpm, (2) 1000 rpm, (3) 2000 rpm, (4) 5000 rpm.

iii. Buffer with 20 mM NADH

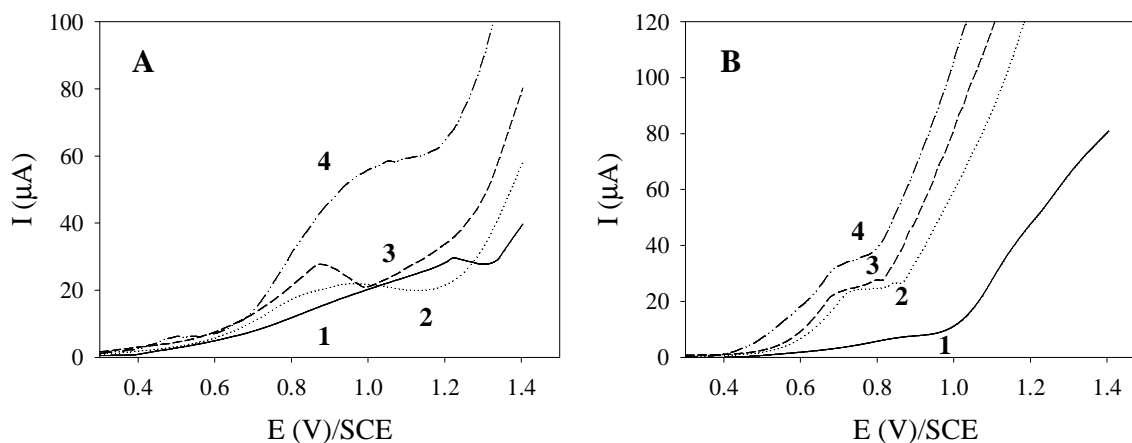


Figure A.1.3 Current potential curves obtained on a platinum disc anode ($S=3.14 \text{ mm}^2$) at room temperature. Residual current of 75 mM sodium pyrophosphate buffer pH 8.7 with 20 mM NADH. (A) Transient state without convection/ $\omega=0$ and several scan rates (r); (1) 20 mV/s, (2) 50 mV/s, (3) 100 mV/s, (4) 200 mV/s; (B) Steady state on a rotating disc $r=5 \text{ mV/s}$ and several angular velocities (ω); (1) 500 rpm, (2) 1000 rpm, (3) 2000 rpm, (4) 5000 rpm.

Annex 2. Gold electrode studies

i. Buffer

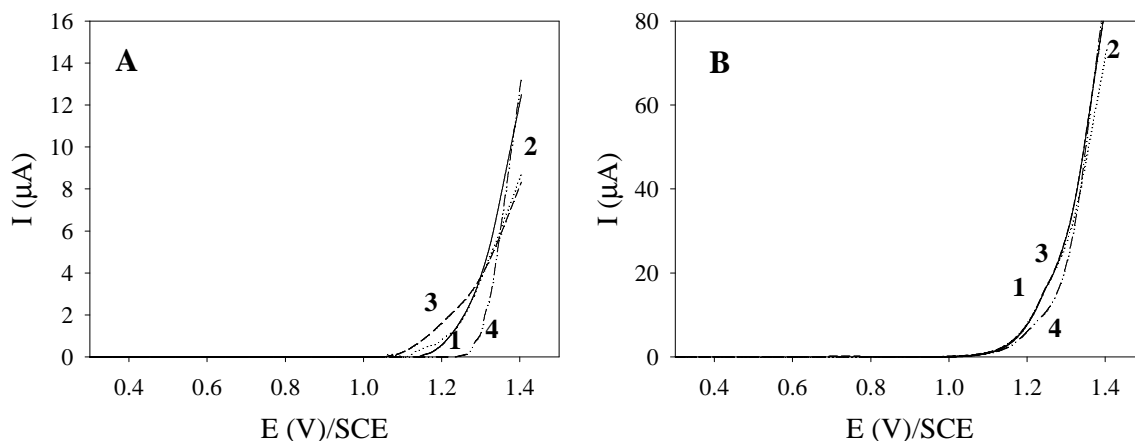


Figure A.2.1 Current potential curves obtained on a gold disc anode ($S=3.14$ mm²) at room temperature. Residual current of 75 mM sodium pyrophosphate buffer pH 8.7. (A) Transient state without convection/ $\omega=0$ and several scan rates (r); (1) 20 mV/s, (2) 50 mV/s, (3) 100 mV/s, (4) 200 mV/s; (B) Steady state on a rotating disc $r=5$ mV/s and several angular velocities (ω); (1) 500 rpm, (2) 1000 rpm, (3) 2000 rpm, (4) 5000 rpm.

ii. Buffer with 20 mM Cbz-ethanolamine

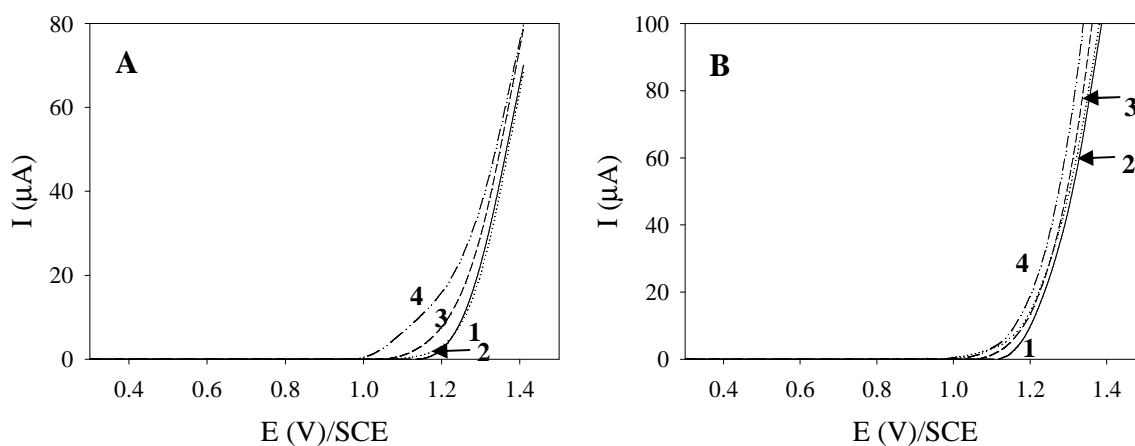


Figure A.2.2 Current potential curves obtained on a gold disc anode ($S=3.14$ mm²) at room temperature. Residual current of 75 mM sodium pyrophosphate buffer pH 8.7 with 20 mM Cbz-ethanolamine. (A) Transient state without convection/ $\omega=0$ and several scan rates (r); (1) 20 mV/s, (2) 50 mV/s, (3) 100 mV/s, (4) 200 mV/s; (B) Steady state on a rotating disc $r=5$ mV/s and several angular velocities (ω); (1) 500 rpm, (2) 1000 rpm, (3) 2000 rpm, (4) 5000 rpm.

iii. Buffer with 20 mM NADH

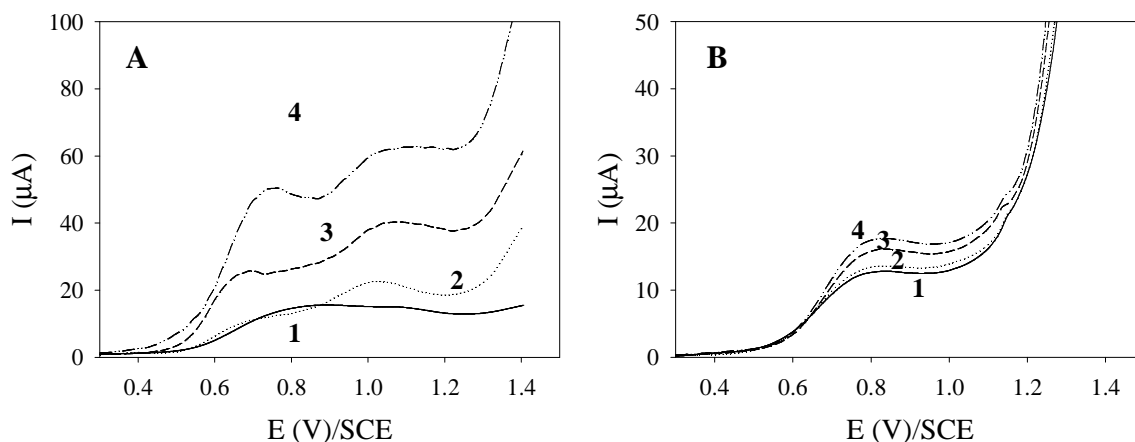


Figure A.2.3 Current potential curves obtained on a gold disc anode ($S=3.14$ mm²) at room temperature. Residual current of 75 mM sodium pyrophosphate buffer pH 8.7 with 20 mM NADH. (A) Transient state without convection/ $\omega=0$ and several scan rates (r); (1) 20 mV/s, (2) 50 mV/s, (3) 100 mV/s, (4) 200 mV/s; Steady state on a rotating disc $r=5$ mV/s and several angular velocities (ω); (1) 500 rpm, (2) 1000 rpm, (3) 2000 rpm, (4) 5000 rpm.

iv. Preparative electrolysis

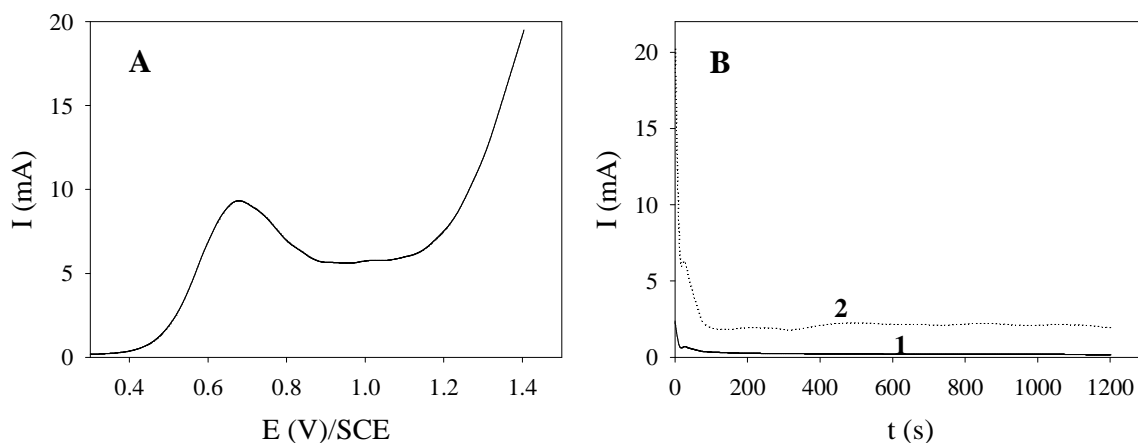


Figure A.2.4 Preparative electrolysis (expected to examine the effect of the applied potential dependence of the conversion of NADH at the steady state) achieved using a filter press microreactor on a microstructured gold anode $S=18$ cm². Anolyte: 20 mM NADH in 75 mM sodium pyrophosphate buffer pH 8.7. Catholyte: 75 mM sodium pyrophosphate buffer pH 8.7. $T=40^\circ\text{C}$ and $r=5$ mV/s; $Q_{\text{anolyte}}=Q_{\text{catholyte}}=50$ $\mu\text{L}/\text{min}$. (A) Current-potential curve obtained before preparative electrolysis. (B) Temporal evolution of the electrolysis current, under two applied potentials on the anode: (1) E_{peak} , (2) 1 V.

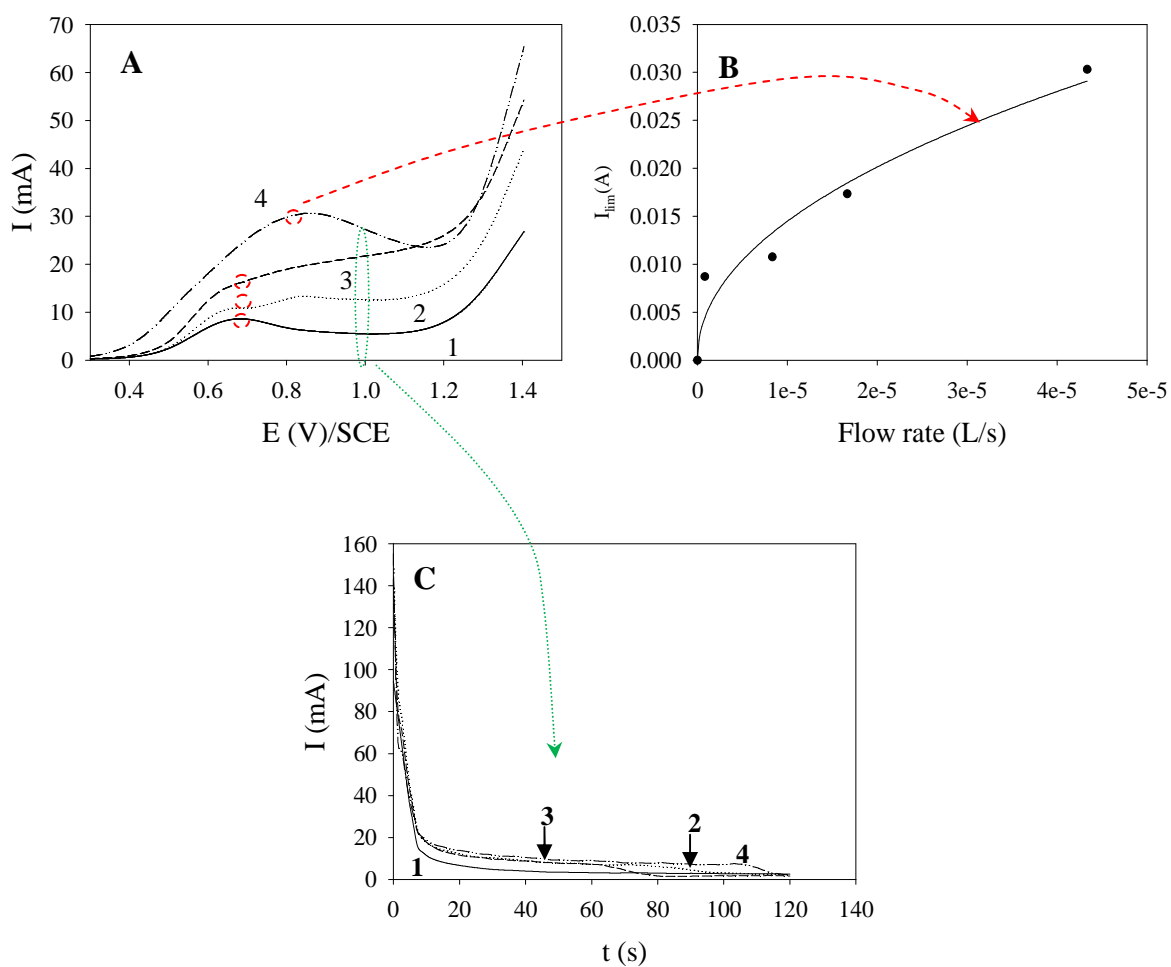


Figure A.2.5 Preparative electrolysis (expected to examine the effect of the flow rate dependence on the conversion of NADH at the steady state) achieved using a filter press microreactor on a microstructured gold anode $S = 18 \text{ cm}^2$. Anolyte: 20 mM NADH with 20 mM Cbz-ethanolamine and 20 U/mL HLADH in 75 mM sodium pyrophosphate buffer pH 8.7. Catholyte: 75 mM sodium pyrophosphate buffer pH 8.7. $T = 40^\circ\text{C}$; $Q_{\text{anolyte}} = Q_{\text{catholyte}}$. (1) 50 $\mu\text{L}/\text{min}$, (2) 500 $\mu\text{L}/\text{min}$, (3) 1000 $\mu\text{L}/\text{min}$, (4) 2600 $\mu\text{L}/\text{min}$. (A) Current-potential curve obtained before preparative electrolysis; $r = 5 \text{ mV}/\text{s}$. (B) Flow rate dependence of the maximum current evolution. (C) Temporal evolution of the electrolysis current, at $E_{\text{applied on the anode}} = 1 \text{ V}$.

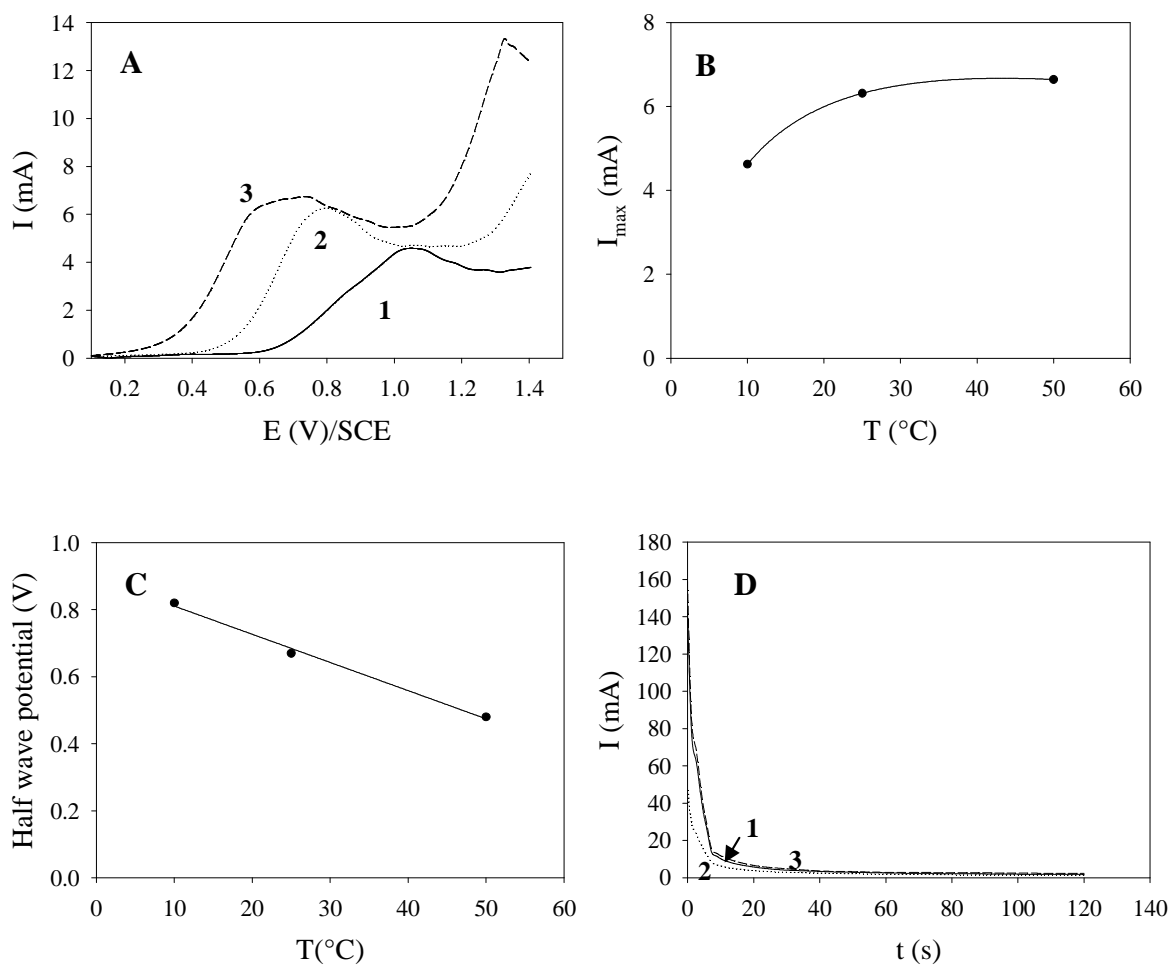


Figure A.2.6 Preparative electrolysis (expected to examine the effect of the temperature dependence on the conversion of NADH at the steady state) achieved using a filter press microreactor on a microstructured gold anode $S = 18 \text{ cm}^2$. Anolyte: 20 mM NADH with 20 mM Cbz-ethanolamine and 20 U/mL HLADH in 75 mM sodium pyrophosphate buffer pH 8.7. Catholyte: 75 mM sodium pyrophosphate buffer pH 8.7. $Q_{\text{anolyte}} = Q_{\text{catholyte}} = 50 \text{ } \mu\text{L}/\text{min}$; (1): $T = 10^\circ\text{C}$, (2): $T = 25^\circ\text{C}$, (3): $T = 50^\circ\text{C}$. (A) Current-potential curve obtained before preparative electrolysis; $r = 5 \text{ mV}/\text{s}$; (B) Temperature dependence of the maximum current evolution; (C) Temperature dependence of the half wave potential; (D) Temporal evolution of the electrolysis current, at $E_{\text{applied on the anode}} = 1 \text{ V}$.

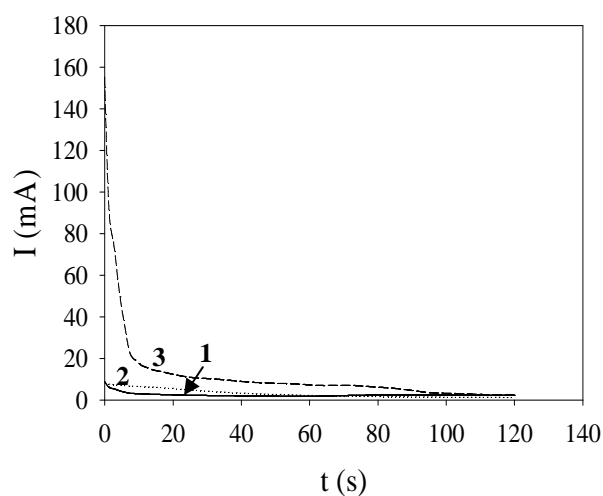


Figure A.2.7 Current-potential curve for the applied potential dependence of the conversion of NADH at the steady state, obtained during preparative electrolysis achieved using a filter press microreactor on a microstructured gold anode $S = 18 \text{ cm}^2$. Analyte: 20 mM NADH with 20 mM Cbz-ethanolamine and 20 U/mL HLADH in 75 mM sodium pyrophosphate buffer pH 8.7. Catholyte: 75 mM sodium pyrophosphate buffer pH 8.7. Electrolysis time: 2 min. $Q_{\text{analyte}} = Q_{\text{catholyte}} = 50 \text{ }\mu\text{L}/\text{min}$. (1): 0.6 V, (2): 0.8 V, (3): 1 V.

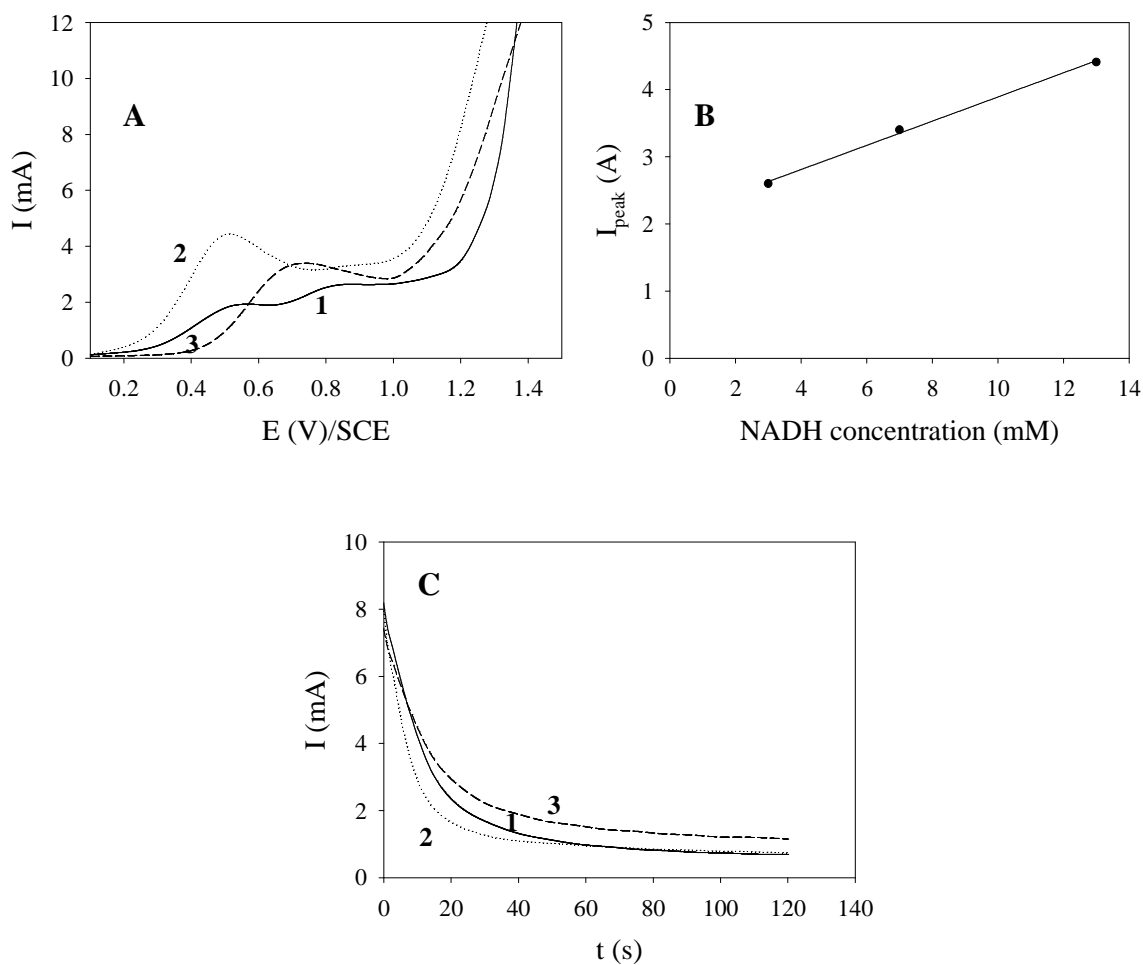


Figure A.2.8 Preparative electrolysis (expected to examine the effect of the NADH concentration dependence on the conversion of NADH at the steady state) achieved using a filter press microreactor on a microstructured gold anode $S = 18 \text{ cm}^2$. $T = 40^\circ\text{C}$. $Q_{\text{analyte}} = Q_{\text{catholyte}} = 50 \text{ }\mu\text{L}/\text{min}$ Catholyte: 75 mM sodium pyrophosphate buffer pH 8.7. Anolyte: NADH with 20 mM Cbz-ethanolamine and 20 U/mL HLADH in 75 mM sodium pyrophosphate buffer pH 8.7. $[\text{NADH}]^\circ$: (1) 3 mM, (2) 7 mM, (3) 13 mM. (A) Current-potential curve obtained before preparative electrolysis; $r = 5 \text{ mV}/\text{s}$; (B) Peak current dependence of the $[\text{NADH}]^\circ$; (C) Temporal evolution of the electrolysis current, at $E_{\text{applied on the anode}} = 1 \text{ V}$.

v. Coupled HLADH catalyzed Cbz-amino propanol oxidation and electroregeneration of NAD^+

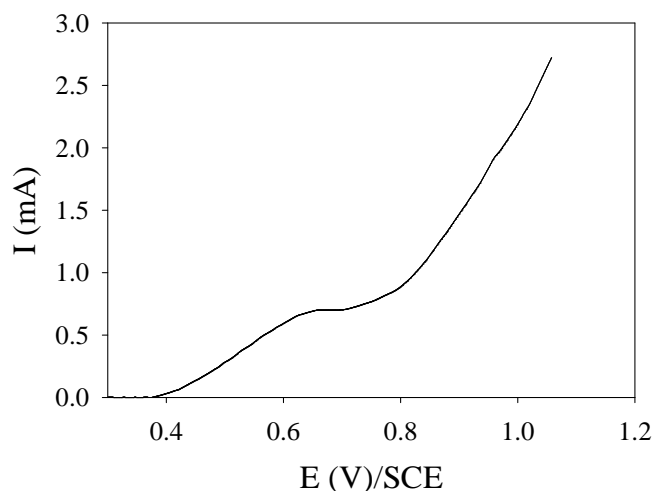


Figure A.2.9 Current-potential curve for the batch HLADH catalyzed oxidation of Cbz-amino propanol obtained by using a filter press microreactor on a microstructured gold made anode $S= 18 \text{ cm}^2$ at $r=5 \text{ mV/s}$ after 30 min of enzymatic reaction. Anolyte: Reaction medium contained in a side batch reactor used for the HLADH catalyzed oxidation of Cbz-amino propanol, $[\text{NADH}] \approx 1.2 \text{ mM}$. Catholyte: 100 mM sodium pyrophosphate buffer pH 8.7. $T=25^\circ\text{C}$; $Q_{\text{anolyte}}=Q_{\text{catholyte}}=1 \text{ mL/min}$.

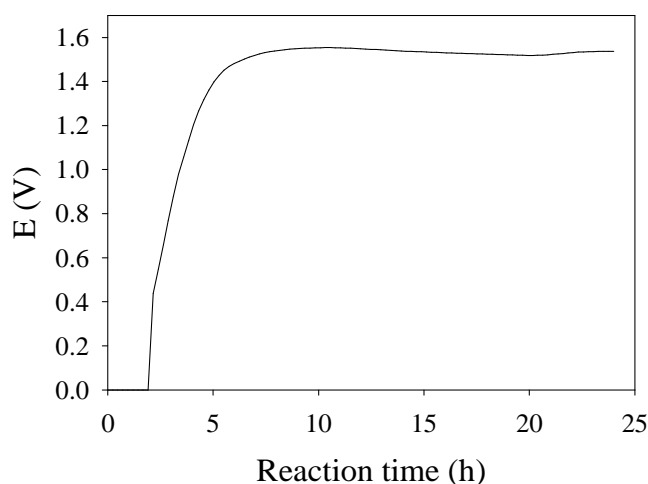


Figure A.2.10 Potential-time curve for the batch coupled HLADH catalyzed oxidation of Cbz-amino propanol and electrochemical regeneration of NAD^+ obtained by electrolysis using a filter press microreactor on a microstructured gold made anode $S= 18 \text{ cm}^2$. Anolyte: Reaction mixture (18.7 mM Cbz- β -amino propanol in 100 mM sodium pyrophosphate buffer pH 8.7, 37.4 mM NAD^+ and 100 U/mL HLADH in a volume of 10 mL). Catholyte: 100 mM sodium pyrophosphate buffer pH 8.7. Electrolysis time: 22 h at 0.5 mA. $T=25^\circ\text{C}$; $Q_{\text{anolyte}}=Q_{\text{catholyte}}=1 \text{ mL/min}$.

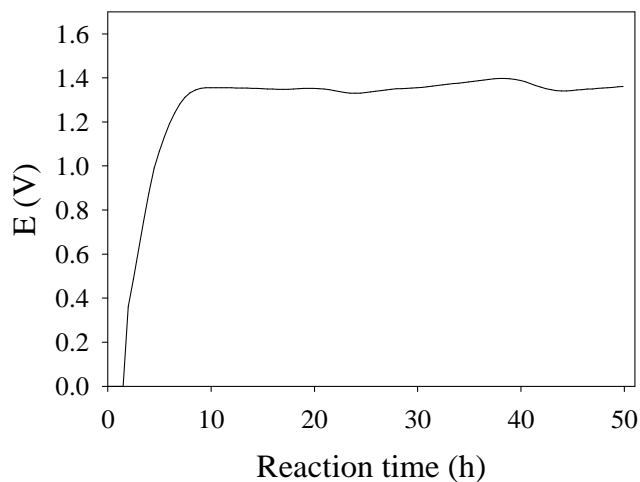


Figure A.2.11 Potential-time curve for the fed-batch coupled HLADH catalyzed oxidation of Cbz-amino propanol and electrochemical regeneration of NAD^+ obtained by electrolysis using a filter press microreactor on a microstructured gold made anode $S= 18 \text{ cm}^2$. Anolyte: Reaction mixture (18.7 mM Cbz- β -amino propanol in 100 mM sodium pyrophosphate buffer pH 8.7, 37.4 mM NAD^+ and 100 U/mL HLADH in a volume of 10 mL with 5 mM Cbz- β -amino propanol pulses added at 4 and 26 h). Catholyte: 100 mM sodium pyrophosphate buffer pH 8.7. Electrolysis time: 48 h at 0.5 mA. $T=25^\circ\text{C}$; $Q_{\text{anolyte}}= Q_{\text{catholyte}}=1 \text{ mL/min}$.